

POLYCARBONATE BASED ZEOLITE 4A FILLED MIXED MATRIX  
MEMBRANES: PREPARATION, CHARACTERIZATION AND  
GAS SEPARATION PERFORMANCES

A THESIS SUBMITTED TO  
THE GRADUATE SCHOOL OF NATURAL AND APPLIED SCIENCES  
OF  
MIDDLE EAST TECHNICAL UNIVERSITY

BY

DEĞER ŞEN

IN PARTIAL FULFILLMENT OF THE REQUIREMENTS  
FOR  
THE DEGREE OF DOCTOR OF PHILOSOPHY  
IN  
CHEMICAL ENGINEERING

FEBRUARY 2008

Approval of the thesis:

**POLYCARBONATE BASED ZEOLITE 4A FILLED MIXED MATRIX  
MEMBRANES: PREPARATION, CHARACTERIZATION AND GAS  
SEPARATION PERFORMANCES**

submitted by **DEĞER ŞEN** in partial fulfillment of the requirements for the degree  
of **Doctor of Philosophy in Chemical Engineering Department, Middle East  
Technical University** by,

Prof. Dr. Canan Özgen  
Dean, Graduate School of **Natural and Applied Sciences** \_\_\_\_\_

Prof. Dr. Gürkan Karakaş  
Head of Department, **Chemical Engineering** \_\_\_\_\_

Prof. Dr. Levent Yılmaz  
Supervisor, **Chemical Engineering Dept., METU** \_\_\_\_\_

Assoc. Prof. Dr. Halil Kalıpçılar  
Co-supervisor, **Chemical Engineering Dept., METU** \_\_\_\_\_

**Examining Committee Members:**

Prof. Dr. Ali Çulfaz  
Chemical Engineering Dept., METU \_\_\_\_\_

Prof. Dr. Levent Yılmaz  
Chemical Engineering Dept., METU \_\_\_\_\_

Prof. Dr. Levent Toppare  
Chemistry Dept., METU \_\_\_\_\_

Prof. Dr. Birgül Tantekin-Ersolmaz  
Chemical Engineering Dept., ITU \_\_\_\_\_

Assoc. Prof. Dr. Yusuf Uludağ  
Chemical Engineering Dept., METU \_\_\_\_\_

**Date:** 22.02.2008

**I hereby declare that all information in this document has been obtained and presented in accordance with academic rules and ethical conduct. I also declare that, as required by these rules and conduct, I have fully cited and referenced all material and results that are not original to this work.**

Name, Last name : Deđer Ően

Signature :

## **ABSTRACT**

### **POLYCARBONATE BASED ZEOLITE 4A FILLED MIXED MATRIX MEMBRANES: PREPARATION, CHARACTERIZATION AND GAS SEPARATION PERFORMANCES**

Şen, Değer

Ph.D., Department of Chemical Engineering

Supervisor : Prof. Dr. Levent Yılmaz

Co-supervisor : Assoc. Prof. Dr. Halil Kalıpçılar

February 2008, 183 pages

Developing new membrane morphologies and modifying the existing membrane materials are required to obtain membranes with improved gas separation performances. The incorporation of zeolites and low molecular-weight additives (LMWA) into polymers are investigated as alternatives to modify the permselective properties of polymer membranes. In this study, these two alternatives were applied together to improve the separation performance of a polymeric membrane. The polycarbonate (PC) chain characteristics was altered by incorporating *p*-nitroaniline (pNA) as a LMWA and the PC membrane morphology was modified by introducing zeolite 4A particles as fillers. For this purpose, pure PC and PC/pNA dense homogenous membranes, and PC/zeolite 4A and PC/pNA/zeolite 4A mixed matrix membranes (MMM) were prepared by solvent-evaporation method using dichloromethane as the solvent. The pNA and zeolite 4A concentrations in the

casting solutions were changed between 1-5% (w/w) and 5-30% (w/w), respectively. Membranes were characterized by SEM, DSC, and single gas permeability measurements of N<sub>2</sub>, H<sub>2</sub>, O<sub>2</sub>, CH<sub>4</sub> and CO<sub>2</sub>. They were also tested for their binary gas separation performances with CO<sub>2</sub>/CH<sub>4</sub>, CO<sub>2</sub>/N<sub>2</sub> and H<sub>2</sub>/CH<sub>4</sub> mixtures at different feed gas compositions.

DSC analysis of the membranes showed that, incorporation of zeolite 4A particles into PC/pNA increased the glass transition temperatures, T<sub>g</sub>, but incorporation of them to pure PC had no effect on the T<sub>g</sub>, suggesting that pNA was a necessary agent for interaction between zeolite 4A and PC matrix.

The ideal selectivities increased in the order of pure PC, PC/zeolite 4A MMMs and PC/pNA/zeolite 4A MMMs despite a loss in the permeabilities with respect to pure PC. A significant improvement was achieved in selectivities when the PC/pNA/zeolite 4A MMMs were prepared with pNA concentrations of 1 % and 2 % (w/w) and with a zeolite loading of 20 % (w/w). The H<sub>2</sub>/CH<sub>4</sub> and CO<sub>2</sub>/CH<sub>4</sub> selectivities of PC/pNA (1%)/zeolite 4A (20%) membrane were 121.3 and 51.8, respectively, which were three times higher than those of pure PC membrane.

Binary gas separation performance of the membranes showed that separation selectivities of pure PC and PC/pNA homogenous membranes were nearly the same as the ideal selectivities regardless of the feed gas composition. On the other hand, for PC/zeolite 4A and PC/pNA/zeolite 4A MMMs, the separation selectivities were always lower than the respective ideal selectivities for all binary gas mixtures, and demonstrated a strong feed composition dependency indicating the importance of gas-membrane matrix interactions in MMMs. For CO<sub>2</sub>/CH<sub>4</sub> binary gas mixture, when the CO<sub>2</sub> concentration in the feed increased to 50 %, the selectivities decreased from 31.9 to 23.2 and 48.5 to 22.2 for PC/zeolite 4A (20%) and PC/pNA (2%)/zeolite 4A (20%) MMMs, respectively.

In conclusion, high performance PC based MMMs were prepared by blending PC with small amounts of pNA and introducing zeolite 4A particles. The

prepared membranes showed promising results to separate industrially important gas mixtures depending on the feed gas compositions.

Keywords: Gas Separation, Mixed Matrix Membrane, Polycarbonate, Zeolite 4A, *p*-nitroaniline, Feed Composition.

## ÖZ

### POLİKARBONAT-ZEOLİT 4A KARIŞIK MATRİSLİ MEMBRANLARIN HAZIRLANMASI, KARAKTERİZASYONU VE GAZ AYIRIM PERFORMANSI

Şen, Değer

Doktora, Kimya Mühendisliği Bölümü

Tez Yöneticisi : Prof. Dr. Levent Yılmaz

Ortak Tez Yöneticisi : Doç. Dr. Halil Kalıpçılar

Şubat 2008, 183 sayfa

Yüksek gaz ayırım performans özelliklerine sahip membranlara olan gereksinim, araştırmaları yeni membran morfolojilerinin ve membran malzemelerinin geliştirilmesi yönünde yoğunlaştırmıştır. Bu kapsamda, polimerik membranların seçici-geçirgen özelliklerini değiştirmek amacıyla, polimere zeolit dolgu maddesinin katılması, polimerin düşük molekül ağırlıklı katkı maddeleri (LMWA) ile karıştırılması yaygın uygulanan yöntemler olmuştur. Bu çalışmada, polimerik membranların gaz ayırım performansını arttırmak için bu iki yöntem birlikte uygulanmıştır. Polikarbonat (PC) polimer zincir yapısı bir tür LMWA olan *p*-nitroanilin (pNA) katılmasıyla, PC membran morfolojisi de dolgu maddesi olan zeolit 4A taneciklerinin katılmasıyla değiştirilmiştir. Bu amaçla, yoğun homojen yapıları saf PC ve PC/pNA membranları ile karışık matrisli PC/zeolit 4A ve PC/pNA/zeolit 4A membranları çözücü-buharlaştırma yöntemiyle, diklorometan çözücüsüyle hazırlanmıştır.

Membran döküm çözeltilerinde pNA derişimi % (ağırlıkça) 1-5, zeolit 4A derişimi % (ağırlıkça) 5-30 arasında deęiştirilmiştir. Membranlar tarama elektron mikroskobu (SEM), fark taramalı kalorimetre (DSC) ve H<sub>2</sub>, CO<sub>2</sub>, O<sub>2</sub>, N<sub>2</sub> ve CH<sub>4</sub> gazlarının tek gaz geçirgenlik ölçümleri ile karakterize edilmiştir. Ayrıca membranların CO<sub>2</sub>/CH<sub>4</sub>, CO<sub>2</sub>/N<sub>2</sub> ve H<sub>2</sub>/CH<sub>4</sub> gaz karışımlarını ayırma performansları farklı besleme gaz kompozisyonları için test edilmiştir.

Membranların DSC analizleri PC/pNA membranların camsı geçiş sıcaklığının, T<sub>g</sub>, zeolit 4A ilavesiyle arttığını, saf PC membrana zeolit 4A ilavesinin ise T<sub>g</sub>' da bir deęişime neden olmadığını göstermiştir. Bu gözlem, pNA ilavesiyle PC matrisi ve zeolit 4A kristalleri arasında bir etkileşimin varlığını göstermiştir.

Membranların ideal seçicilikleri PC, PC/zeolit 4A, PC/pNA/zeolit 4A sırasıyla artarken, saf PC membrana kıyasla geçirgenlikleri azalmıştır. Ağırlıkça % 1-2 pNA ve % 20 zeolit 4A içeren karışık matrisli membranların ideal seçiciliklerinde önemli düzeyde artış gözlenmiştir. PC/pNA (1%)/zeolite 4A (20%) membranının H<sub>2</sub>/CH<sub>4</sub> ve CO<sub>2</sub>/CH<sub>4</sub> seçicilikleri sırasıyla 121.3 ve 51.8 olup, saf PC membranın seçicilik değerlerine kıyasla üç kat artış sağlanmıştır.

Membranların ikili gaz ayırım performansları, yoğun homojen yapılı saf PC ve PC/pNA membranları için farklı besleme gaz kompozisyonlarının membranların ayırım performansını etkilemediğini ve ideal performans değerleriyle aynı düzeyde olduğunu göstermiştir. Buna karşılık, PC/zeolite 4A ve PC/pNA/zeolite 4A karışık matrisli gaz ayırım membranlarında performansın gaz kompozisyonuna bağlı olarak deęiştiiği ve ikili gaz ayırım performans değerlerinin ideal performans değerlerinden düşük olduğu gözlenmiştir. Karışık matrisli membranların performansının gaz kompozisyonuna baęlılığı, membran morfolojisinde gerçekleştirilen deęişimin gaz-membran etkileşimini deęiştirmesi şeklinde yorumlanmıştır. PC/zeolit 4A (20%) ve PC/pNA (2%)/zeolit 4A (20%) membranlarının CO<sub>2</sub>/CH<sub>4</sub> ideal seçicilikleri sırasıyla 31.9 ve 48.5 iken, 50 % CO<sub>2</sub> içeren CO<sub>2</sub>/CH<sub>4</sub> besleme karışımını ayırma seçicilikleri 23.2 ve 22.2' ye düşmüştür.

Sonuç olarak, PC membran morfolojisinin ve zincir yapısının zeolit 4A ve çok küçük derişimlerde pNA katılmasıyla deęiştirilmesi PC membranın gaz ayırım performansını arttırmıştır. Ayrıca, geliştirilen membranların endüstriyel öneme



sahip gazların ayırımında kullanımlarının, besleme gaz kompozisyonunun etkisi dikkate alındığında yararları olacağı anlaşılmıştır.

Anahtar sözcükler: Gaz Ayırımı, Karışık Matrisli Membran, Polikarbonat, Zeolit 4A, *p*-nitroanilin, Besleme Kompozisyonu.

*To my father Ersin Şen and my mother Yurdağül Şen*

## **ACKNOWLEDGEMENTS**

When I look back over the years that have passed during my PhD, I would like to thank many people. First of all, I would like to express my sincere gratitude to my supervisor Prof. Dr. Levent Yılmaz for his guidance, interest and suggestions throughout this study. I would also like to thank my co-supervisor Assoc. Prof. Dr. Halil Kalıpçılar for his suggestions, criticisms and helps during each step of my research.

I would like to extend my thanks to Prof. Dr. Ali Çulfaz and Prof. Dr. Levent Toppare for their valuable comments and discussions during the progress of this study.

I would like to thank to thermal analysis specialists Doç. Dr. Necati Özkan and Elif Tarhan Bor for their helps in Differential Scanning Calorimetric analysis. I wish to thank specialist Cengiz Tan for his helps in Scanning Electron Microscopic analysis. I would like to thank Machine Shop for their help in constructing various set-up components and their availability to every call for help. I am also thankful to all staff of Department of Chemical Engineering for their helps throughout the study.

I would like to thank my colleagues Ceren Oktar Doğanay, Belma Soydaş and Alp Yürüm for their helps, suggestions and solutions to my problems. Thanks also to all my lab mates for their helpful and enjoyable friendships throughout this study.

Last, but not the least, I would like to thank my parents whose love, support and understanding have allowed me to achieve so much.

## TABLE OF CONTENTS

ABSTRACT .....	iv
ÖZ .....	vii
ACKNOWLEDGEMENTS .....	xi
TABLE OF CONTENTS .....	xii
LIST OF TABLES .....	xv
LIST OF FIGURES .....	xx
LIST OF SYMBOLS .....	xxvi
CHAPTER	
1. INTRODUCTION .....	1
2. LITERATURE SURVEY .....	8
2.1 Polymeric Gas Separation Membranes.....	8
2.2 Mixed Matrix Membranes.....	14
2.3 Zeolite Filled Mixed Matrix Membranes.....	15
2.4 Polymer/LMWA Blend Membranes .....	25
2.5 Separation of Binary Gas Mixtures with Polymeric Membranes ...	29
3. EXPERIMENTAL.....	36
3.1 Synthesis of Zeolite 4A Crystals .....	36
3.2 Preparation of Membranes.....	37
3.2.1 Materials.....	37
3.2.2 Membrane Preparation Methodology.....	38
3.3 Membrane Characterization .....	40
3.3.1 Thermal Characterization .....	40
3.3.2 Scanning Electron Microscopy (SEM) Characterization.....	41
3.4 Gas Permeability Measurements.....	41
3.4.1 Single Gas Permeability Measurements.....	41
3.4.2 Single Gas Permeability Calculations .....	43
3.4.3 Separation of Binary Gas Mixtures .....	45

3.4.3.1	Experimental Set-up.....	45
3.4.3.2	Experimental Procedure .....	47
3.4.3.3	Analysis with GC .....	48
3.4.3.4	Permeability and Selectivity Calculations .....	49
4.	MEMBRANE PREPARATION AND CHARACTERIZATION .....	51
4.1	Selection of Membrane Preparation Materials.....	51
4.2	Development of Membrane Preparation Methodology .....	53
4.3	Thermal Characterization of Membranes.....	55
4.3.1	TGA Experiments .....	55
4.3.2	DSC Experiments .....	56
4.4	Morphological Characterization of Membranes.....	62
5.	SINGLE GAS PERMEATION STUDIES.....	68
5.1	Single Gas Permeability Measurements .....	68
5.2	Reproducibility in Permeability Measurements and Membrane Preparation .....	69
5.3	Single Gas Permeability Results of the PC Based Membranes .....	71
5.3.1	PC/pNA Blend Membranes.....	71
5.3.2	PC/Zeolite 4A Mixed Matrix Membranes .....	73
5.3.3	PC/pNA/Zeolite 4A Mixed Matrix Membranes .....	79
6.	BINARY GAS PERMEATION STUDIES.....	86
6.1	Binary Gas Permeation Measurements .....	86
6.2	Evaluation of Pressure-Time Data for Permeability Calculations in Binary Gas Permeation.....	88
6.3	Evaluation of Permeate and Feed Side Compositions for Selectivity Calculations in Binary Gas Permeation .....	89
6.4	Reproducibility in Permeabilities and Selectivities .....	90
6.5	Binary Gas Permeation Studies .....	93
6.5.1	Binary Gas Permeation Studies through Dense Homogenous PC and PC/pNA Membranes .....	93
6.5.2	Binary Gas Permeation Studies through PC/4A and PC/pNA/4A Mixed Matrix Membranes.....	97
6.5.3	General Performance Evaluation of Membranes.....	106
7.	CONCLUSIONS .....	110
8.	RECOMMENDATIONS .....	113
	REFERENCES.....	115

APPENDICES .....	129
A. XRD PATTERN OF SYNTHESIZED ZEOLITE 4A POWDER .....	129
B. CALCULATION OF SINGLE GAS PERMEABILITIES .....	130
C. DETERMINATION OF DEAD VOLUME.....	132
D. CALIBRATION OF GC AND TYPICAL GAS CHROMATOGRAMS FOR DIFFERENT BINARY GAS PAIRS .....	134
D.1 Calibration of GC .....	134
D.2 Typical Gas Chromatograms.....	137
E. A SAMPLE CALCULATION FOR THE DETERMINATION OF PERMEABILITIES AND SELECTIVITIES OF BINARY GAS MIXTURES..	139
F. THERMAL GRAVIMETRY ANALYSIS GRAPHS.....	145
G. SAMPLE DSC THERMOGRAMS OF THE PREPARED MEMBRANES.....	149
H. DETERMINATION OF ADJUSTABLE PARAMETER K FOR PC/pNA BLEND MEMBRANES WITH GORDON TAYLOR ANTIPLASTICIZATION MODEL EQUATION .....	156
I. REPRODUCIBILITY EXPERIMENTS FOR SINGLE GAS PERMEABILITY MEASUREMENTS.....	159
J. SEPARATION SELECTIVITY DATA CALCULATED FROM SEMI-EMPIRICAL CURVE FITTING METHOD.....	169
K. REPRODUCIBILITY EXPERIMENTS FOR BINARY GAS PERMEABILITY MEASUREMENTS.....	171
K.1 Reproducibility Data for CO <sub>2</sub> /CH <sub>4</sub> Separation through pure PC Membrane .....	171
K.2 Reproducibility Data for CO <sub>2</sub> /CH <sub>4</sub> Separation through PC/pNA (2%) Blend Membrane.....	172
K.3 Reproducibility Data for CO <sub>2</sub> /CH <sub>4</sub> Separation through PC/4A MMMs .....	173
K.4 Reproducibility Data for CO <sub>2</sub> /CH <sub>4</sub> Separation through PC/pNA/4A MMMs .....	176
K.5 Reproducibility Data for H <sub>2</sub> /CH <sub>4</sub> Separation through PC/4A and PC/pNA/4A MMMs .....	177
K.6 Reproducibility Data for CO <sub>2</sub> /N <sub>2</sub> Separation through PC/4A and PC/pNA/4A MMMs .....	178
CURRICULUM VITAE.....	179

## LIST OF TABLES

Table 2.1	Single gas permeabilities and ideal selectivities of zeolite filled glassy polymer mixed matrix membranes .....19
Table 2.2	Void elimination methods in zeolite filled glassy polymer MMMs.....22
Table 2.3	CO <sub>2</sub> /CH <sub>4</sub> binary gas separation performances of different polymeric membrane morphologies.....31
Table 2.4	Binary gas separation performances of different polymeric membranes for different binary gas pairs .....33
Table 3.1	Operating conditions of gas chromatograph .....49
Table 4.1	Reproducibility results in T <sub>g</sub> measurements of different type of PC based membranes .....58
Table 5.1	The effect of aging on single gas permeabilities and ideal selectivities of the mixed matrix membranes.....70
Table 5.2	Single gas permeabilities of PC/pNA blend membranes at different pNA weight percentages, measured at room temperature, feed side pressure was 3.7 bar .....72
Table 5.3	Ideal selectivities of PC/pNA blend membranes at different pNA weight percentages .....72
Table 5.4	Permeabilities of PC/zeolite 4A mixed matrix membranes at different zeolite 4A weight percentages, measured at room temperature, feed side pressure was 3.7 bar.....74

Table 5.5	Ideal selectivities of PC/zeolite 4A mixed matrix membranes at different zeolite 4A weight percentages.....	74
Table 5.6	Single gas permeabilities of gases through PC/pNA/zeolite 4A MMMs at different pNA and zeolite 4A concentrations, measured at room temperature, feed side pressure 3.7 bar .....	80
Table 5.7	Ideal selectivities of PC/pNA/zeolite 4A MMMs at different pNA and zeolite 4A concentrations, measured at room temperature.....	82
Table 6.1	The pNA and zeolite 4A compositions of the PC based membranes used in the separation of binary gas mixtures and their CO <sub>2</sub> /CH <sub>4</sub> ideal selectivities .....	87
Table 6.2	Reproducibility experiments and relative standard deviations in permeabilities and selectivities.....	92
Table 6.3	Effect of feed composition on permeabilities and selectivities of CO <sub>2</sub> /CH <sub>4</sub> binary gas mixture through pure PC membrane (measured at room temperature, feed side pressure was 3.0 bar).....	95
Table 6.4	Effect of feed composition on permeabilities and selectivities of CO <sub>2</sub> /CH <sub>4</sub> binary gas mixture through PC/pNA (2%) membrane (measured at room temperature, feed side pressure was 3.0 bar) .....	95
Table 6.5	Effect of feed composition on permeabilities and selectivities of CO <sub>2</sub> /N <sub>2</sub> binary gas mixture through PC/4A (20%) and PC/pNA (2%)/4A(20%) MMMs (measured at room temperature, feed side pressure was 3.0 bar) .....	102
Table 6.6	Effect of feed composition on permeabilities and selectivities of H <sub>2</sub> /CH <sub>4</sub> binary gas mixture through PC/4A (20%) and PC/pNA (2%)/4A (20%) MMMs (measured at room	



	temperature, feed side pressure was 3.0 bar) .....	103
Table E.1	Feed and permeate side pressures and compositions.....	142
Table H.1	Experimental $T_g$ values of PC/pNA blend membranes with respect to weight fraction of additive pNA .....	157
Table H.2	Matlab nonlinear regression program to determine the "K" value.....	157
Table H.3	Comparison of calculated $T_g$ values of PC/pNA blend membranes with experimental $T_g$ values.....	158
Table I.1	Reproducibility data for pure PC membrane .....	159
Table I.2	Reproducibility data for PC/pNA blend membranes.....	160
Table I.3	Reproducibility data for PC/zeolite 4A (5%) MMM.....	160
Table I.4	Reproducibility data for PC/zeolite 4A (10%) MMM.....	161
Table I.5	Reproducibility data for PC/zeolite 4A (20%) MMM.....	161
Table I.6	Reproducibility data for PC/zeolite 4A (30%) MMM.....	162
Table I.7	Reproducibility data for PC/pNA (1%)/zeolite 4A (5%) MMM .....	163
Table I.8	Reproducibility data for PC/pNA (1%)/zeolite 4A (10%) MMM .....	163
Table I.9	Reproducibility data for PC/pNA (1%)/zeolite 4A (20%) MMM .....	164
Table I.10	Reproducibility data for PC/pNA (1%)/zeolite 4A (30%) MMM .....	164
Table I.11	Reproducibility data for PC/pNA (2%)/zeolite 4A (5%) MMM .....	165

Table I.12	Reproducibility data for PC/pNA (2%)/zeolite 4A (10%) MMM .....	165
Table I.13	Reproducibility data for PC/pNA (2%)/zeolite 4A (20%) MMM .....	166
Table I.14	Reproducibility data for PC/pNA (2%)/zeolite 4A (30%) MMM .....	166
Table I.15	Reproducibility data for PC/pNA (5%)/zeolite 4A (5%) MMM .....	167
Table I.16	Reproducibility data for PC/pNA (5%)/zeolite 4A (10%) MMM .....	167
Table I.17	Reproducibility data for PC/pNA (5%)/zeolite 4A (20%) MMM .....	168
Table I.18	Reproducibility data for PC/pNA (5%)/zeolite 4A (30%) MMM .....	168
Table J.1	Comparison of calculated and experimental data for permeate side compositions and separation selectivities of CO <sub>2</sub> /CH <sub>4</sub> binary gas mixture through PC/zeolite 4A (20%) MMMs.....	170
Table K.1.1	Reproducibility data for CO <sub>2</sub> /CH <sub>4</sub> mixture permeabilities through pure PC membrane .....	171
Table K.1.2	Reproducibility data for CO <sub>2</sub> /CH <sub>4</sub> selectivities of pure PC membrane .....	172
Table K.2.1	Reproducibility data for CO <sub>2</sub> /CH <sub>4</sub> mixture permeabilities and selectivities of PC/pNA (2%) blend membrane.....	172
Table K.3.1	Reproducibility data for CO <sub>2</sub> /CH <sub>4</sub> mixture permeabilities through PC/zeolite 4A (20%) MMM .....	173
Table K.3.2	Reproducibility data for CO <sub>2</sub> /CH <sub>4</sub> selectivities of PC/zeolite 4A (20%) MMM .....	174

Table K.3.3	Reproducibility data for CO <sub>2</sub> /CH <sub>4</sub> mixture permeabilities through PC/zeolite 4A (30%) MMM .....	175
Table K.3.4	Reproducibility data for CO <sub>2</sub> /CH <sub>4</sub> mixture selectivities through PC/zeolite 4A (30%) MMM .....	175
Table K.4.1	Reproducibility data for CO <sub>2</sub> /CH <sub>4</sub> mixture permeabilities and selectivities of PC/pNA (2%)/zeolite 4A (20%) MMM ....	176
Table K.4.2	Reproducibility data for CO <sub>2</sub> /CH <sub>4</sub> mixture permeabilities and selectivities of PC/pNA (2%)/zeolite 4A (30%) MMM ....	176
Table K.5.1	Reproducibility data for H <sub>2</sub> /CH <sub>4</sub> mixture permeabilities and selectivities of PC/zeolite 4A (20%) MMM .....	177
Table K.5.2	Reproducibility data for H <sub>2</sub> /CH <sub>4</sub> mixture permeabilities and selectivities of PC/pNA (2%)/zeolite 4A (20%) MMM ....	177
Table K.6.1	Reproducibility data for CO <sub>2</sub> /N <sub>2</sub> mixture permeabilities and selectivities of PC/zeolite 4A (20%) MMM .....	178
Table K.6.2	Reproducibility data for CO <sub>2</sub> /N <sub>2</sub> mixture permeabilities and selectivities of PC/pNA (2%)/zeolite 4A (20%) MMM ....	178

## LIST OF FIGURES

Figure 2.1	Movement of a gas molecule through the cavities of a polymeric membrane .....	10
Figure 2.2	Upper bound trade-off curves (Robeson plot 1991) for the (a) oxygen-nitrogen and (b) carbon dioxide-methane gas pairs. Also shown are the performance properties of the filler and polymer material used in this work .....	12
Figure 2.3	Schematic drawing of a mixed matrix membrane.....	14
Figure 2.4	CO <sub>2</sub> /CH <sub>4</sub> performance properties of MMMs based on rubbery polymer matrices. The unfilled shapes denote pure rubbery polymer matrices, and the filled shapes denote zeolite filled rubbery polymer MMMs. The zeolite loading, %(w/w) is noted next to each data point.....	18
Figure 2.5	(a) Cross sectional SEM image of a polysulfone-zeolite 4A MMM, "sieve in-a-cage" morphology; (b) Schematic representation of an undesirable void between the polymer matrix and zeolite .....	21
Figure 3.1	The repeating unit of poly(bisphenol-A-)carbonate (a), and the structure of <i>p</i> -nitroaniline (b) .....	38
Figure 3.2	Flowchart of the preparation methodology of PC/pNA/zeolite 4A membranes .....	39
Figure 3.3	Schematic drawing of the single gas permeability measurement set-up.....	42

Figure 3.4	Schematic representation of a home-made membrane cell....	42
Figure 3.5	Schematic drawing of the binary gas permeation set-up .....	46
Figure 3.6	Procedure for injecting gas samples into the GC using the six-port injection valve .....	48
Figure 4.1	Comparison of TGA graphs of pure PC, PC/pNA (2%), PC/4A (20%) and PC/pNA (2%)/4A (20%) membranes .....	56
Figure 4.2	DSC graphs of different type of PC based membranes .....	59
Figure 4.3	Effect of pNA concentration (Panel a) and zeolite 4A loading (Panel b) on the glass transition temperature of PC based membranes. The filled symbols represent PC/pNA blend membranes with increasing concentration of pNA.....	61
Figure 4.4	Cross-sectional SEM images of (a) pure PC, (b) PC/pNA (1%), (c) PC/pNA (2%) and (c) PC/pNA (5%) membranes.....	63
Figure 4.5	Cross-sectional SEM images of PC/zeolite 4A MMMs with respect to increasing zeolite 4A loading (a) 5% (w/w), (b) 10% (w/w), (c) 20% (w/w), (d) 30% (w/w), (e) 35% (w/w) and (f) 40% (w/w).....	64
Figure 4.6	Cross-sectional SEM images of PC/zeolite 4A MMMs at higher magnifications (a) PC/zeolite 4A (20%) MMM and (b) PC/zeolite 4A (30%) MMM .....	65
Figure 4.7	Cross-sectional SEM images of PC/pNA (x%)/zeolite 4A (20%) MMMs (a) x= 1%, (b) x= 2% and (c) x= 5% .....	66
Figure 5.1	Permeate side pressure-time data for pure PC membrane.....	69
Figure 5.2	H <sub>2</sub> /CH <sub>4</sub> selectivity and H <sub>2</sub> permeability of PC/zeolite 4A MMMs on a Robeson's upper bound trade-off curve .....	77
Figure 5.3	CO <sub>2</sub> /CH <sub>4</sub> selectivity and CO <sub>2</sub> permeability of PC/zeolite 4A MMMs	

	on a Robeson's upper bound trade-off curve .....	77
Figure 5.4	H <sub>2</sub> /N <sub>2</sub> selectivity and H <sub>2</sub> permeability of PC/zeolite 4A MMMs on a Robeson's upper bound trade-off curve .....	78
Figure 5.5	O <sub>2</sub> /N <sub>2</sub> selectivity and O <sub>2</sub> permeability of PC/zeolite 4A MMMs on a Robeson's upper bound trade-off curve .....	78
Figure 5.6	Effect of zeolite 4A loading on the N <sub>2</sub> permeability of PC/zeolite 4A and PC/pNA/zeolite 4A MMMs .....	81
Figure 5.7	Effect of zeolite 4A loading on the H <sub>2</sub> permeability of PC/zeolite 4A and PC/pNA/zeolite 4A MMMs .....	81
Figure 5.8	Comparing the permeability and selectivity of PC/pNA/zeolite 4A MMMs with PC/pNA blend membranes .....	85
Figure 6.1	Permeate side pressure-time data of CO <sub>2</sub> /CH <sub>4</sub> binary gas mixture through pure PC membrane, and pressure-time data splitting technique based on the permeate compositions of CO <sub>2</sub> and CH <sub>4</sub> .....	89
Figure 6.2	Semi-empirical curve fitting method (Panel a) and comparison of calculated separation selectivities with experimental data (Panel b) for the separation of CO <sub>2</sub> /CH <sub>4</sub> binary gas mixture through PC/4A (20%) MMM.....	91
Figure 6.3	Effect of feed composition on permeability and selectivity for CO <sub>2</sub> /CH <sub>4</sub> through pure PC membrane (Panel a) and PC/pNA membrane (Panel b).....	96
Figure 6.4	Effect of feed composition on the CO <sub>2</sub> /CH <sub>4</sub> binary gas mixture permeabilities through PC/4A and PC/pNA/4A MMMs.....	98
Figure 6.5	Effect of feed composition on the selectivity of CO <sub>2</sub> /CH <sub>4</sub> through PC/4A (20%) MMMs (Panel a) and PC/4A (30%) MMMs (Panel b) .....	99

Figure 6.6	Effect of feed composition on the selectivity of CO <sub>2</sub> /CH <sub>4</sub> through PC/pNA (2%)/4A (20%) MMMs (Panel a) and PC/pNA (2%)/4A (30%) MMMs (Panel b) .....	100
Figure 6.7	CO <sub>2</sub> /CH <sub>4</sub> selectivity and CO <sub>2</sub> permeability of different type of PC based membranes on a Robeson's upper bound trade-off curve .....	107
Figure 6.8	CO <sub>2</sub> /N <sub>2</sub> selectivity and CO <sub>2</sub> permeability of different type of PC based membranes on a Robeson's upper bound trade-off curve .....	107
Figure 6.9	H <sub>2</sub> /CH <sub>4</sub> selectivity and H <sub>2</sub> permeability of different type of PC based membranes on a Robeson's upper bound trade-off curve .....	108
Figure A.1	XRD patterns of zeolite 4A crystals: (1) commercial zeolite 4A (Acros), (2) synthesized zeolite 4A. The marked peaks are the characteristics peaks of zeolite 4A .....	129
Figure B.1	Algorithm for single gas permeability calculation.....	131
Figure D.1.1	Calibration plot of carbon dioxide for GC analysis.....	135
Figure D.1.2	Calibration plot of methane for GC analysis.....	135
Figure D.1.3	Calibration plot of nitrogen for GC analysis .....	136
Figure D.1.4	Calibration plot of hydrogen for GC analysis.....	136
Figure D.2.1	Sample GC output for carbon dioxide-methane mixture. First peak (retention time is 1.559 min) corresponds to methane and the second peak (retention time is 2.279 min) corresponds to carbon dioxide.....	137
Figure D.2.2	Sample GC output for hydrogen-methane mixture. First peak (retention time is 1.548 min) corresponds to hydrogen and the second peak (retention time is 2.198 min) corresponds to methane.....	137

Figure D.2.3	Sample GC output for hydrogen-carbon dioxide mixture. First peak (retention time is 1.636 min) corresponds to hydrogen and the second peak (retention time is 2.335 min) corresponds to carbon dioxide .....	138
Figure D.2.4	Sample GC output for nitrogen-carbon dioxide mixture. First peak (retention time is 1.254 min) corresponds to nitrogen and the second peak (retention time is 2.335 min) corresponds to carbon dioxide .....	138
Figure E.1	Pressure difference vs. time graph for CO <sub>2</sub> -CH <sub>4</sub> binary gas mixture through PC/pNA (2%) blend membrane.....	142
Figure F.1	The TGA graph for PC/pNA (5%) blend membrane.....	145
Figure F.2	The TGA graph for PC/zeolite 4A (10%) MMM.....	146
Figure F.3	The TGA graph for PC/zeolite 4A (30%) MMM.....	146
Figure F.4	The TGA graph for PC/pNA (2%)/zeolite 4A (30%) MMM .....	147
Figure F.5	The TGA graph for PC/pNA (5%)/zeolite 4A (20%) MMM .....	147
Figure F.6	The TGA graph for PC/pNA (5%)/zeolite 4A (30%) MMM .....	148
Figure G.1	The DSC graph of PC/pNA (2%) membrane blend (2 <sup>nd</sup> scan) .....	149
Figure G.2	The DSC graph of PC/pNA (5%) membrane blend (2 <sup>nd</sup> scan) .....	150
Figure G.3	The DSC graph of PC/4A (10%) MMM (2 <sup>nd</sup> scan).....	150
Figure G.4	The DSC graph of PC/4A (30%) MMM (2 <sup>nd</sup> scan).....	151
Figure G.5	The DSC graph of PC/pNA (1%)/4A (20%) MMM (2 <sup>nd</sup> scan)..	151
Figure G.6	The DSC graph of PC/pNA (1%)/4A (30%) MMM (2 <sup>nd</sup> scan)..	152
Figure G.7	The DSC graph of PC/pNA (2%)/4A (20%) MMM (2 <sup>nd</sup> scan)..	152



Figure G.8	The DSC graph of PC/pNA (2%)/4A (30%) MMM (2 <sup>nd</sup> scan) ..	153
Figure G.9	The DSC graph of PC/pNA (5%)/4A (10%) MMM (2 <sup>nd</sup> scan) ..	153
Figure G.10	The DSC graph of PC/pNA (5%)/4A (20%) MMM (2 <sup>nd</sup> scan) ..	154
Figure G.11	The DSC graph of PC/pNA (5%)/4A (20%) MMM (2 <sup>nd</sup> scan-reproducibility) .....	154
Figure G.12	The DSC graph of PC/pNA (5%)/4A (30%) MMM (2 <sup>nd</sup> scan) ..	155
Figure G.13	The DSC graph of PC/pNA (5%)/4A (30%) MMM (2 <sup>nd</sup> scan-reproducibility) .....	155

## LIST OF SYMBOLS

A	: Effective membrane area (cm <sup>2</sup> )
dn/dt	: Molar flow rate (mol/s)
dp/dt	: Pressure increase
J	: Flux (cm <sup>3</sup> /cm <sup>2</sup> .s)
K	: adjustable parameter
M	: Molecular weight of the gas
P	: Permeability (Barrer)
p <sub>f</sub>	: Feed side pressure (cmHg)
p <sub>p</sub>	: Permeate side pressure (cmHg)
R	: Ideal gas constant
T	: Temperature (°C)
T <sub>g</sub>	: Glass transition temperature (°C)
T <sub>ga</sub> and T <sub>gp</sub>	: Glass transition temperatures of additive and polymer
V <sub>d</sub>	: Dead volume (cm <sup>3</sup> )
w <sub>a</sub> and w <sub>p</sub>	: Weight fractions of additive and polymer
x <sub>i</sub>	: Mole fraction of gas component i in the feed side
y <sub>i</sub>	: Mole fraction of gas component i in the permeate side

### *Greek Letters*

δ	: Membrane thickness (μm)
α	: Selectivity
β and λ	: Empirical parameters
ρ	: Density of the gas
v	: Volumetric flow rate (cm <sup>3</sup> /s)
Δp	: Transmembrane pressure difference (cmHg)

### *Abbreviations*

ANP	: 4-amino 3-nitro phenol
CA	: Cellulose acetate
CMS	: Carbon molecular sieve
DBP	: Di-butyl phythalate
DCM	: Dichloromethane
DHM	: Dense homogenous membrane
DSC	: Differential scanning calorimetry
EPDM	: Ethylene-propylene rubber
FTIR	: Fourier transform infrared
GC	: Gas chromatograph
HBP	: 4-hydroxy benzophenone
HMA	: 2-hydroxy 5-methyl aniline
HPA	: Heteropolyacid
LMWA	: Low molecular-weight additive
MMM	: Mixed matrix membrane
NBR	: Nitrile-butadiene rubber
PC	: Polycarbonate
PDMS	: Poly(dimethylsiloxane)
PEI	: Polyetherimide
PEI/BMI	: Polyetherimide-bismaleimide
PES	: Polyethersulfone
PI	: Polyimide
pNA	: <i>p</i> -nitroaniline
PPO	: Poly(phenyleneoxide)
PSF	: Polysulfone
PVAc	: Poly(vinylacetate)
SEM	: Scanning electron microscopy
Semi-IPN	: Semi-interpenetrating polymer matrix
STP	: Standard temperature and pressure
TAP	: 2,4,6-triamino pyrimidine
TCD	: Thermal conductivity detector
TGA	: Thermal gravimetric analyzer
XRD	: X-Ray diffractometer

## **CHAPTER 1**

### **INTRODUCTION**

Membrane based gas separation has become an important process in chemical industry and competes with cryogenic separations, and pressure swing adsorption [1-4]. The main advantages of membrane based gas separation technology are; low energy consumption, adjustable membrane properties, simple operation, separation under mild conditions, low maintenance requirements, easy combination with other separation processes and easy to scale-up [3, 4]. Many research groups have therefore concentrated on the development of membranes with better gas separation performances as well as understanding the gas transport through membranes [5-9].

A membrane is a semipermeable barrier between two phases. It allows the passage of some molecules, called permeate, and reject the others, called retentate with the aid of a driving force such as pressure or concentration difference [3, 4]. The membrane performance depends on the physical and chemical properties of the membrane material and the permeating components. The permeability or flux through a membrane and the selectivity of the membrane to a component over another are the key parameters to evaluate the performance of a membrane [3, 4].

Membranes can be categorized regarding their material of construction, morphology and structure; for instance, biological vs. synthetic, organic vs. inorganic, homogenous vs. composite, symmetric vs. asymmetric and porous

vs. non-porous membranes. In gas separation applications attention has been focused on non-porous membranes [10-12]. Polymers are the commonly used membrane materials. Cellulose acetates, polysulfones, polycarbonates and polyimides are the most important conventional polymers for gas separation membranes [3, 10-12].

The polymeric membranes made of conventional polymers are known to have a trade-off between permeability and selectivity as shown in upper bound curves developed by Robeson [12]. Theoretical studies have also showed that permeability-selectivity trade-off is unlikely to be surpassed by further improvements of chemistries of conventional membrane polymers [13, 14]. Developing new membrane morphologies [15-18], and blending with low molecular-weight additives [8, 19, 20] may be promising alternatives to increase the polymeric membrane performances.

Membrane morphology may determine the transport mechanism and therefore, affects the separation performance strongly [3, 4]. The membranes usually have three types of morphologies: dense, asymmetric and composite. Dense membranes are homogenous films of a single polymer layer, whereas the asymmetric and composite membranes consist of a dense top layer supported by a porous sublayer [3]. In composite membranes, both layers may originate from different materials.

Mixed matrix membranes (MMM) have recently emerged as a promising alternative morphology to overcome the performance limitation of conventional polymeric membranes for gas separation. They are obtained by embedding a filler material, such as zeolites [15, 16, 21, 22], silica [23], carbon molecular sieves [15, 24] or conductive polymers [17, 25] into a polymer matrix. MMMs are expected to combine the processability and separation property of polymers with the high separation property of fillers to obtain membranes with better separation performances than pure polymeric membranes. A significant effort has been devoted to prepare MMMs using zeolites as filler due to their molecular sieving properties and glassy polymers as the polymer matrix due to their rigidities and higher intrinsic selectivities [26-32]. The separation performance of zeolite filled MMMs strongly depends

on the polymer and zeolite types, and concentration of zeolite in the membrane.

Nevertheless, most MMMs were reported to suffer from poor interaction between zeolite particles and glassy polymer chains, which may cause non-selective voids at the polymer-zeolite interface and be the reason for insufficient improvement of membrane performance [21, 22, 26-32]. A number of methods have been investigated to improve the interaction between polymer and zeolite. These methods can be categorized in two classes; first one is to promote flexibility of polymer during membrane formation, and the other one is to improve the compatibility between zeolite and polymer. The flexibility promotion in the matrix polymer during membrane formation was achieved either by annealing the membrane above the glass transition temperature of polymer [22, 28, 29] or by adding a plasticizer into membrane formulation [28]. It was thought that polymer chains may cover zeolite crystals more compactly during flexibility promotion. However, MMMs prepared with these methods generally showed lower gas separation performances in comparison to their pure polymer counterparts [22, 29]. Yet, it was also difficult to find an appropriate polymer-solvent-plasticizer system for these methods [28].

External surface of zeolite crystals was modified by silane-coupling agents to make them more compatible with the organic polymer phase [7, 22, 33, 34]. A little gain in performance properties of MMMs were observed despite indications of good compatibility between silylated zeolite crystals and polymer chains with SEM micrographs [22, 33]. This may be due to the difficulty in selecting a suitable silane-coupling agent, which can completely modify the external surface of zeolites. It is also possible that most of the zeolite pores may be blocked by the use of coupling agents [22]. As an alternative to silane-coupling agents, use of low molecular-weight additives (LMWA) with multifunctional groups were suggested [27]. These compounds are expected to interact both with polymer and zeolite, thus, they act as a compatibilizer between polymer and zeolite. Although it is also difficult to find such an additive in MMM preparation, the incorporation of these compounds

into membrane matrices are expected to eliminate the interfacial voids and improve the performance of MMMs.

The low molecular-weight additives were also used to prepare high performance glassy polymer/LMWA blend membranes in the absence of zeolites [19, 20, 35, 36]. Achieving an improved combination of permeability and selectivity in polymer/LMWA blend membranes hinges on the optimal selection of the additive and the polymer to be modified. A polymer/LMWA blend membrane is desired to have a homogenous morphology with non-porous and dense structure. In other words, LMWA should be miscible with the polymer matrix to investigate the effect of type and concentration of LMWA on permselective properties of different polymers [8, 19, 35]. In addition to provision of miscibility of additive and polymer, interaction capability of additives with polymers should also be considered for compatibility between selected compounds [19, 36]. Therefore, systematic evaluation of the additive should be carried out to find an appropriate polymer-additive system.

A number of studies have been conducted to investigate the effects of different additives on the structure and performance of polymeric membranes. Long aliphatic and polyaromatic based compounds containing polar atoms, rigid and planar structure are usually used as LMWAs [19, 35, 36]. The incorporation of these additives at high concentrations (10-30% w/w) into the membrane decreased the gas permeabilities and increased the selectivities [8, 19, 35]. The influence of LMWAs on membrane performances was explained by antiplasticization of polymer matrix, which was described as the increasing stiffness of the polymer matrix due to reduced rate of segmental motions in polymer chains [19, 20, 35, 36]. Thus, antiplasticization effect of such additives has been examined as a route to obtain better trade-off between permeability and selectivity of polymeric membranes. Additives with multifunctional groups that are capable of interacting with polymer can be more efficient to improve performance of polymeric membranes. Multifunctionality of the additives may allow them to be introduced at small concentrations into membrane blends, and this may lead them to be real additives instead of being a major component of the membrane [20].

The low molecular-weight additives can therefore be assessed as potential modifiers to change the structure and performance properties of polymeric membranes, and to improve the compatibility between polymer chains and zeolite particles in MMMs, if they can be efficient at small concentrations and have functional groups that may interact both with polymer and zeolite. Yet, this entails understanding of the influence of those additives on the structural and performance properties of zeolite filled MMMs. The focus of this work is to develop such mixed matrix gas separation membranes by introducing zeolite as filler and low molecular-weight compound as additive into glassy polymer matrix to obtain MMMs with high separation performances.

Several families of glassy polymers have attracted considerable interest for application as gas separation membranes. Certain polyimides, polyesters, polysulfones and polyamides have been shown to offer high permeabilities and selectivities. Among these polymers, polycarbonates constitute an important group used in gas permeation measurements. Poly(bisphenol-A)carbonate (PC) is generally chosen in the permeability measurements since it is commercially available and provides the necessary backbone rigidity for good thermal resistance and mechanical behavior while allowing relatively fast gas permeation rates [20, 25, 37-42]. It has a glass transition temperature of 150 °C and is thus a glassy polymer at preparation and application temperatures. Several groups worked on the gas permeation characteristics of PC, and they showed that PC is an efficient membrane material for gas separation since its high permeabilities and selectivities in comparison to many glassy polymer membranes [37-42]. The effect of membrane preparation parameters, such as polymer concentration in solvent, type of solvent, conditions of solvent evaporation and annealing, on the gas separation performance of PC membranes were examined in detail [42]. In addition, it was used to prepare MMMs with polypyrrole (PPy) as filler [17, 25], and found as an appropriate polymer for preparing MMMs. It was reported that the incorporation of PPy fillers into PC matrix remarkably improved the O<sub>2</sub>/N<sub>2</sub> and H<sub>2</sub>/N<sub>2</sub> selectivities of PC membrane. PC was also used to prepare blend membranes with different LMWAs [20]. The additives with functional groups were selected to increase the probability of interaction between PC and the additive. In their selection the main factor was their



possession of amine-, nitro-, and hydroxyl- functional groups. Since PC has strong hydrogen bonding capability through its carbonyl groups, selected LMWAs can interact with PC through their functional groups. Those additives were catechol, *p*-nitroaniline (pNA), 4-amino 3-nitro phenol (ANP) and 2-hydroxy 5-methyl aniline (HMA) and their concentrations in the membrane were changed between 1 and 10 % (w/w). The blend membranes prepared with PC and very small amount of LMWAs showed lower permeabilities for H<sub>2</sub>, N<sub>2</sub>, O<sub>2</sub>, CO<sub>2</sub> but higher selectivities than pure PC membranes since LMWAs antiplasticized the PC membranes. Among them, pNA was the most effective antiplasticizing additive, which provided the highest selectivity.

In this study, high performance engineering thermoplastic PC was used as the membrane polymer, and the preparation of PC/zeolite 4A and PC/pNA/zeolite 4A mixed matrix membranes was proposed as new gas separation membranes. The effects of pNA and zeolite 4A concentrations on the structure and gas permeation properties of membranes were investigated. For this purpose, pure PC, PC/pNA, PC/zeolite 4A and PC/pNA/zeolite 4A membranes were prepared and characterized by scanning electron microscopy (SEM) and differential scanning calorimetry (DSC). The gas permeation properties of those membranes were compared by measuring single gas permeabilities of H<sub>2</sub>, CO<sub>2</sub>, O<sub>2</sub>, N<sub>2</sub> and CH<sub>4</sub>.

The majority of literature on zeolite filled MMMs is based on the permeability studies with single gases, a comprehensive study with multicomponent gas mixtures is lacking. However, it was found that the performance of gas separation membranes can be severely affected by the presence of other components, and this may cause unanticipated changes in the performance of membranes [9, 43, 44]. The possible reasons for the performance changes are the competition in sorption and diffusion among the penetrants [9, 45], the plasticization induced by some components which can strongly interact with membrane matrix such as CO<sub>2</sub> and/or organic vapors [46], the concentration polarization [47] and the non-ideal gas behavior [45]. Therefore, the multicomponent gas permeability measurements are highly recommended to obtain true membrane separation performance in industrial

applications and to choose a correct membrane type in a certain industrial gas separation application.

Especially with the widespread usage of the natural gas as a primary energy source throughout the world, the membrane based gas separation studies have mainly focused on natural gas purification [44-47, 48]. Although the composition of natural gas varies from one location to another, it mainly contains methane, carbon dioxide, nitrogen, higher hydrocarbons, and small amounts of hydrogen sulfide, helium, oxygen, argon and water vapor [48]. Most commonly, carbon dioxide is the major component that must be removed from natural gas, since it can form carbonic acid, leading to corrosion of pipelines. Therefore, the membrane based gas separation studies have mainly focused on separation of CO<sub>2</sub>/CH<sub>4</sub> binary gas mixtures. In addition to natural gas purification, gas separation membranes have also been used in the production of oxygen enriched air [1, 49-51], purification of H<sub>2</sub> [52], separation of CO<sub>2</sub> from flue gases [43, 53] and recovery of vapours from vent gases [1, 51].

In this study, the membranes, which have showed the highest ideal selectivities in single gas permeation measurements were also used to separate binary gas mixtures of CO<sub>2</sub>/CH<sub>4</sub>, H<sub>2</sub>/CH<sub>4</sub> and CO<sub>2</sub>/N<sub>2</sub>. The effect of feed composition on permeability and selectivity of the membranes was investigated in detail. Therefore, both the applicability of these membranes for the separation of industrially important gas pairs could be determined, and the transport mechanism through each membrane type could be enlightened by mechanistic explanations on deviations from single gas permeability measurements of the membranes.

## CHAPTER 2

### LITERATURE SURVEY

#### 2.1 Polymeric Gas Separation Membranes

Membranes are selective barriers between two phases and allow the preferential transport of certain molecules under the influence of a gradient in pressure or concentration [3, 4]. The molecules which transport faster through the membrane is called the permeate, whereas the molecules which transport slower is called the retentate. The physical and chemical properties of both the membrane material and the permeating components determine the membrane performance. The performance of a membrane is determined by two parameters, permeability and selectivity [3, 4].

For gas separation membranes, permeability is defined as the flux of a permeate gas through a membrane per unit transmembrane driving force multiplied by membrane thickness and is expressed as,

$$P = \frac{J \cdot \delta}{p_f - p_p} \quad (2.1)$$

where  $J$  is flux of gas through the membrane,  $p_f$  and  $p_p$  are the partial pressures of the gas on the feed and permeate side, respectively; and  $\delta$  is the thickness of the membrane. The conventional unit for expressing

permeability,  $P$ , is Barrers, where 1 Barrer is equal to  $10^{-10} \text{ cm}^3 \text{ (STP).cm} / \text{cm}^2 \cdot \text{s} \cdot \text{cm-Hg}$ .

Selectivity is a measurement of a membrane's ability to separate the components of a mixture. Ideal selectivity is the ratio of permeabilities of single gases and is defined by the relation,

$$\alpha_{AB} = \frac{P_A}{P_B} \quad (2.2)$$

For binary gas mixtures, separation selectivity is defined by eqn. (2.3) [3, 4, 9],

$$\alpha_{A/B} = \frac{y_A / y_B}{x_A / x_B} \quad (2.3)$$

here,  $y_A$  and  $y_B$  are the mole fractions of components A and B in the gas mixture at the permeate side and  $x_A$  and  $x_B$  are the mole fractions of these components at the feed side of the membrane.

Polymers providing a broad range of properties are very common membrane materials [10-12]. They exhibit a good separation performance for many gas mixtures. They can be easily processed into membranes and easily implemented into the membrane modules because of their flexibility. They are usually cheaper than the alternative membrane materials such as ceramics, zeolites and palladium alloys.

Non-porous polymer membranes are usually applied in gas separation [1-4, 10-12]. The term non-porous is rather ambiguous because pores are present on a molecular level in order to allow transport even in such membranes. The existence of these "molecular pores" can be described in terms of free volume. The non-porous structure of the polymer is therefore related to the non-continuous gaps, called free volumes, present in the polymer chain

matrix [3, 10, 54, 55]. The diffusion of a penetrant is based on its movement through these gaps. Because of the movement of the polymer chains, a channel between gaps can be formed allowing gas molecules to “jump” from one gap to another (Figure 2.1) [55]. Through this jumping motion, gas molecules can effectively diffuse through the membrane structure. Large channels will allow faster diffusion of gases through a membrane at the cost of less selectivity between different gases; smaller channels will allow a much greater selectivity at the cost of lower permeabilities. The intrinsic properties of the polymeric material, the effects of penetrant activity (driving force) and operating conditions then play an important role in governing the gas transport rate of the membrane [54, 55].

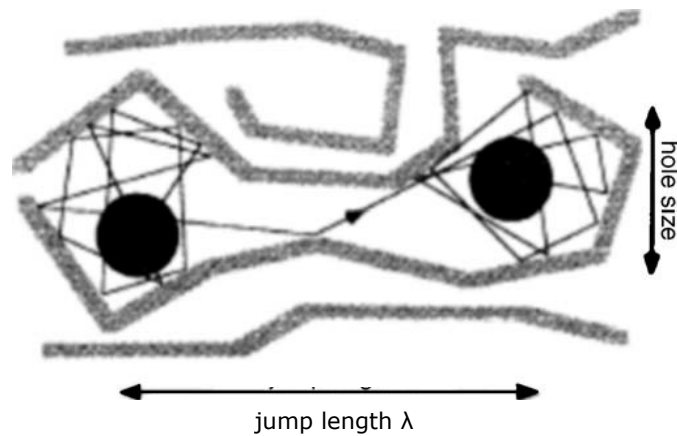


Figure 2.1 Movement of a gas molecule through the cavities of a polymeric membrane (from reference [55]).

A non-porous polymer with a high glass transition temperature ( $T_g$ ), high melting point, and/or high crystallinity is generally preferred as membrane material in gas separation applications [3, 10, 54]. Glassy polymers have stiffer backbones and/or more restricted segmental motions because of the strong binding forces between molecular segments of the polymer, and therefore have higher selectivities as compared to rubbery polymers [12-14, 17-29]. Due to their higher selectivities, glassy polymers are more commonly

used as gas separation membrane materials. Polycarbonates, polyesters, polysulfones, polyimides and polypyrrolones are some of the glassy polymers that are often used to prepare gas separation membranes [3, 4, 10].

Gas permeation through non-porous polymer membranes is explained by the solution-diffusion model. The solution-diffusion model involves three steps [3, 51, 54, 55]: (1) sorption of a molecule into the membrane, (2) diffusion across the membrane through the gaps (free volume) between the polymeric chains, and (3) desorption from the membrane. Both sorption/desorption and diffusion steps in solution-diffusion model depends on the characteristics of the membrane material and gases. This model can be expressed in terms of the sorption and diffusion coefficients for the individual polymer and gas, and the permeability coefficients can be defined as a product of a diffusion coefficient and a solubility coefficient.

A considerable amount of data has been available for many years on permeabilities and selectivities of large variety of polymeric membranes to different gases. A rather general trade-off relation has been recognized between permeability and selectivity. Polymeric membranes that are more permeable are generally less selective and the membranes that are more selective are less permeable. This relationship between the permeability and selectivity is presented in a well-known trade-off curve by plotting performance data of the polymeric membranes (Figure 2.2) [12].

Figures 2.2a and 2.2b present  $O_2/N_2$  selectivity versus  $O_2$  permeability and  $CO_2/CH_4$  selectivity versus  $CO_2$  permeability for many polymers on log-log scale. The same trade-off curve was drawn for different gas pairs like  $H_2/N_2$ ,  $CO_2/N_2$  and  $H_2/CH_4$ . Glassy polymers are generally concentrated near to upper bound line, whereas rubbery polymers are usually away from the upper bound line. Materials with the high permeability and selectivity combinations would be in the upper right hand corner of these curves (cross-hatched regions in figures). However, materials with permeability/selectivity combinations above and to the right of the line drawn in these figures are exceptionally rare. This line defines the so called upper-bound combinations of

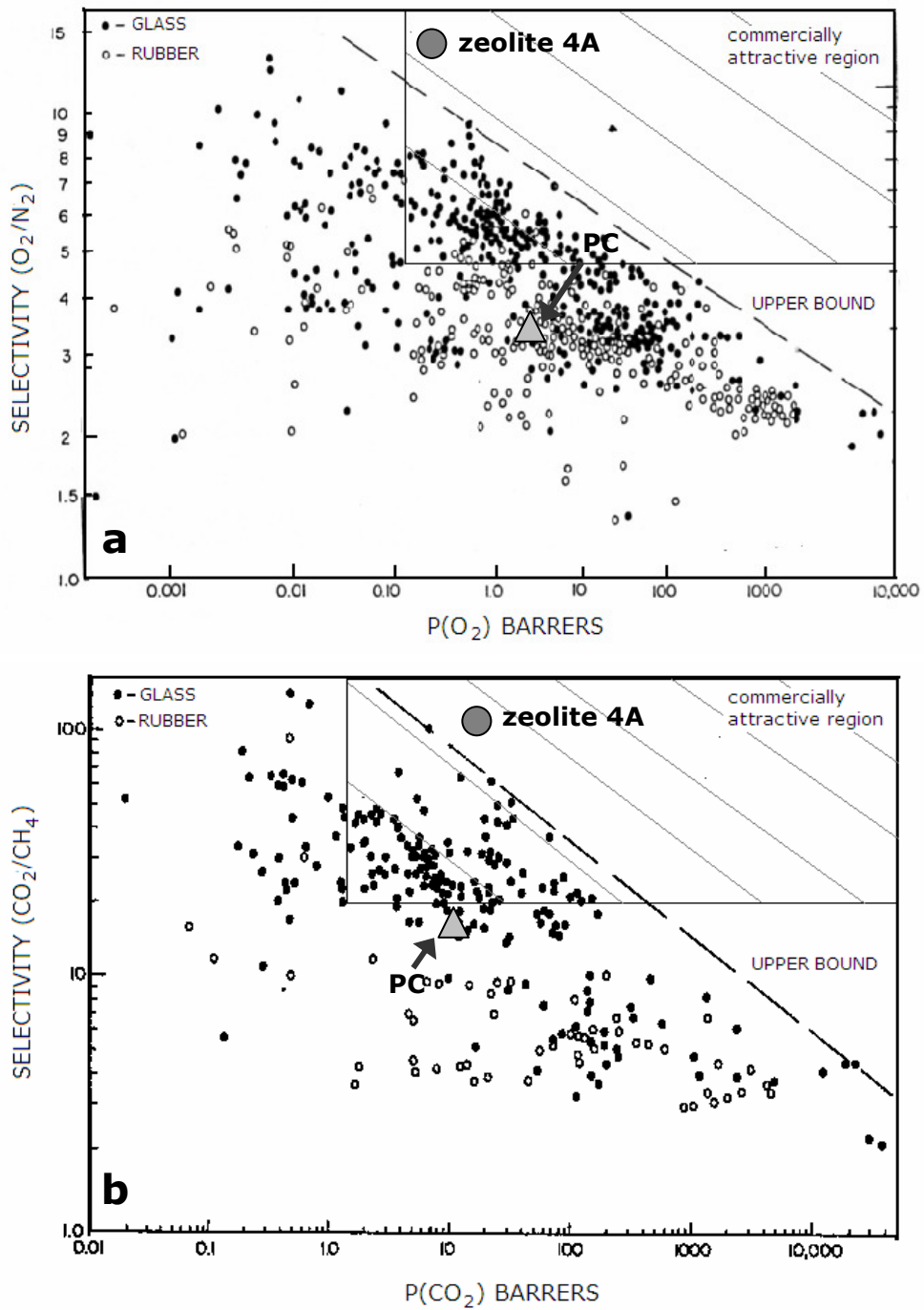


Figure 2.2 Upper bound trade-off curves (Robeson plot 1991) for the (a) oxygen-nitrogen and (b) carbon dioxide-methane gas pairs [12]. Also shown permeability and selectivity of polymeric membrane materials for a particular gas pair [12], are the performance properties of the filler and polymer material used in this work (see section 3.2).

permeability and selectivity of polymeric membrane materials for a particular gas pair [12].

The upper bound performance characteristics of polymeric membranes were described by the following equation in theoretical studies [13, 14]:

$$\ln \alpha_{A/B} = \ln \beta_{A/B} - \lambda_{A/B} \ln P_A \quad (2.4)$$

$P_A$  and  $\alpha_{A/B}$  are the permeability and selectivity of the polymeric membrane, respectively.  $\lambda_{A/B}$  is an empirical parameter depending on the size of gas molecule,  $\beta_{A/B}$  is also an empirical parameter depending on  $\lambda_{A/B}$  and solubility of the gas in polymer. The slope of the upper bound line,  $\lambda_{A/B}$ , is independent of the type and structure of polymer, it is constant for a given gas pair and a given polymer class (i.e. rubbery or glassy). On the other hand, the intercept,  $\beta_{A/B}$ , can be adjusted by manipulating the polymer structure. This implies that upper bound line cannot be exceeded by further improvements of chemistries of conventional membrane polymers [13, 14].

In recent studies introducing fillers such as zeolite, carbon molecular sieves and conducting polymers into polymer matrix has been shown as a promising way to exceed the upper bound curve [5, 49, 50]. The performance properties of these materials lie well above the upper bound line. Combining this property of these materials with easy processability and performance properties of polymers may increase the separation performance of polymeric membranes. This is the origin of mixed matrix membrane idea.

Another alternative to increase the gas separation performance of polymeric membranes is blending polymers with low molecular-weight additives (LMWAs). The incorporation of certain types of LMWAs at modest levels (10-30 weight % of polymer) into glassy polymers leads to an increase in stiffness because of the reduced rates of segmental motions in the polymer chain, and has been termed "antiplasticization" [8, 19, 20]. The extent of antiplasticization depends on some characteristics of the additives, such as



size, shape, stiffness and concentration in the polymer, and on the polymer's characteristics, as well as on the degree of interaction between the additive and the polymer [36]. In the membrane area, antiplasticization has been shown to provide a possible way to increase selectivities at the expense of permeabilities via a reduction in polymer free volume. The incorporation of LMWAs, like phthalates, sebacates, naphtylamines and fluorenes, into glassy polymers, like polysulfones, polyimides and polycarbonates, modifies the structural and performance characteristics of polymeric gas separation membranes, and results in better separation performances [8, 20, 35, 36]. Therefore, if the polymer-additive pair is selected judiciously, blending polymers with LMWAs can be examined as a route to tailor the permeability-selectivity balance of polymeric gas separation membranes.

## 2.2 Mixed Matrix Membranes

Mixed matrix membranes (MMM) are composed of two interpenetrating matrices of different materials as shown in Figure 2.3 [49, 50]. In MMMs the continuous phase can be a rubbery or glassy polymer, and the dispersed phase are fillers, such as zeolites, carbon molecular sieves (CMSs) and conductive polymers.

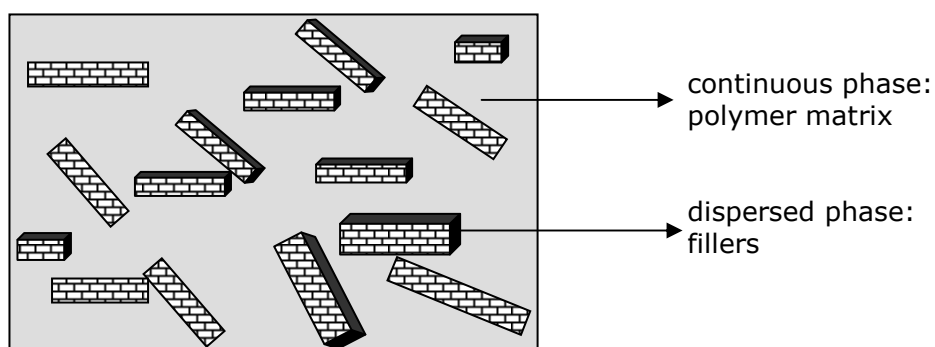


Figure 2.3 Schematic drawing of a mixed matrix membrane.

The fillers may provide higher selectivity to polymeric membranes due to their well defined pore size, specific sorption and shape selective properties. Therefore, MMMs are expected to combine the separation properties of polymers with those of fillers to obtain membranes with better separation performances than pure polymeric membranes.

In MMMs, two of the key challenges are selecting the suitable polymer–filler combination to separate a given gas pair [5, 26, 56] and overcoming problems occurring at polymer–filler interfaces within the membrane [26, 28, 30, 56]. Selecting appropriate polymer–filler combinations is complicated because the properties of each phase are potentially affected by the presence of the other and possibly by components of the feed gases. Tailoring interfacial morphology is a difficult problem frequently encountered in composite materials, but it is especially challenging for membranes since small changes in interfacial morphology can lead to dramatic changes in transport properties [26, 28, 30-32].

### **2.3 Zeolite Filled Mixed Matrix Membranes**

Most of the mixed matrix membrane studies in literature employ zeolites as the filler materials due to their well-defined pore size and their ability to discriminate between molecules of different sizes and shapes [15, 16, 26-32]. The size and shape selective property of the zeolites would be expected to generate precise molecular-sieving discrimination by permitting smaller-sized gas penetrants to diffuse at much higher rates than larger-sized penetrants. Therefore, the incorporation of zeolites into polymers may enhance the separation performance of the conventionally employed polymeric membranes due to their high selectivities in comparison to polymers. In addition, the facts that many different types of zeolites exist and the properties of a significant number of them may be adjusted (i.e. by changing Si/Al ratio, by ion-exchange) make the zeolites more preferable filler materials in MMMs [6, 15, 57, 58].

Early work with zeolite filled MMMs predominantly used elastomeric or rubbery polymers as the continuous matrix phase. Poly(dimethylsiloxane), PDMS, was

the commonly studied rubbery polymer matrix [15, 16, 59, 60]. Zeolite-filled rubbery polymer membranes were first introduced by Hennepe et al. for pervaporation and gas separation purposes [59, 60]. The pervaporation measurements with ethanol/water mixtures showed that the addition of silicalite-1, NaX and AgX type zeolites into PDMS increased both the ethanol permeability and selectivity of the PDMS membrane. The ethane and ethylene gas permeation results of the same membranes also showed an increase in permeability and selectivity of the membranes. They proposed that the increase in selectivity resulted from a longer pathway for the largest component around the zeolite particle and a shorter pathway for the smallest component through the zeolite pores. This effect was described as molecular-sieving property of zeolites.

Jia et al. [16] studied with silicalite-1 filled PDMS membranes. The permeabilities of He, H<sub>2</sub>, O<sub>2</sub> and CO<sub>2</sub> increased, while those of N<sub>2</sub>, CH<sub>4</sub> and C<sub>4</sub>H<sub>10</sub> decreased. They concluded that silicalite-1 behaved as a molecular sieve, and facilitated the permeation of smaller molecules, yet hindered the permeation of larger molecules. O<sub>2</sub>/N<sub>2</sub> and CO<sub>2</sub>/CH<sub>4</sub> selectivities increased from 2.15 to 2.50 and 3.45 to 5.67 for 50 % (w/w) silicalite addition, respectively.

Duval et al. [15] examined the effect of different zeolites (5A, silicalite, 13X and KY) and commercial carbon molecular sieves on the performance of a range of rubbery polymers (PDMS, ethylene-propylene rubber, EPDM, and nitrile-butadiene rubber, NBR). They observed significant improvement in CO<sub>2</sub>/CH<sub>4</sub> selectivity from 13.5 to 35 for a MMM prepared with NBR and 46 vol% zeolite KY. They also reported slight enhancement for O<sub>2</sub>/N<sub>2</sub> selectivity, such as from 3.0 to 4.7 for an EPDM rubber MMM with 53 vol% silicalite. However, they found no improvement with zeolite 5A filled MMMs, and they attributed this to either adsorbed water in the pores of zeolite 5A or strong adsorption in 5A such that permeation is very slow. They also showed that MMMs prepared from CMSs demonstrated no improvement in performance properties of rubbery polymers attributed to the dead end porous nature of CMSs.

Tantekin-Ersolmaz et al. [57] examined the permeabilities of various gases including, O<sub>2</sub>, N<sub>2</sub> and CO<sub>2</sub>, with the PDMS/silicalite MMMs and investigated the effect of zeolite particle size on the performance of MMMs. They observed that the permeability values corresponding to the PDMS/silicalite MMMs exceeded those pertaining to the pure PDMS polymer membrane and permeabilities increased with increasing particle size of the silicalite crystallites. They also reported slight enhancement in the CO<sub>2</sub>/N<sub>2</sub>, O<sub>2</sub>/N<sub>2</sub> and CO<sub>2</sub>/O<sub>2</sub> ideal selectivities with the incorporation of silicalite particles into PDMS matrix.

Above mentioned studies show that early work with MMMs in literature employ rubbery polymers as matrix polymers to combine easy processability and high permeabilities of rubbery polymers with high selectivities of zeolites and because of compatibility of rubbery polymers with zeolitic fillers. The results of these studies performed with MMMs, which used elastomeric and rubbery polymers as the continuous phase, were plotted in Figure 2.4 with reference to the CO<sub>2</sub>/CH<sub>4</sub> upper bound trade-off line.

It can be observed that some success has been achieved with the incorporation of zeolites into rubbery polymer matrices, increased permeabilities with slight increase in selectivities. However, the reported performance properties of those MMMs do not exhibit the anticipated performance enhancements necessary for commercial applications, because of the poor intrinsic separation performances of the pure rubbery polymer membranes. As compared to rubbery polymers, glassy polymer membranes offer enhanced separation performances due to the more restricted segmental motions in these polymers and hence their higher intrinsic selectivities [24-32]. Therefore, their usage as the matrix polymer in zeolite filled MMMs can be advantageous. For example, polyethersulfone (PES) and polycarbonate (PC) are glassy polymers and they have high separation performances. The CO<sub>2</sub>/CH<sub>4</sub> selectivities of PES and PC membranes are 50.0 and 26.7, respectively, and their CO<sub>2</sub> permeabilities are 3.4 and 10.0 Barrers, respectively [21, 29]. It is expected that MMMs prepared with the incorporation of zeolites into such glassy polymers can show higher gas separation performances than the MMMs prepared from rubbery polymers.

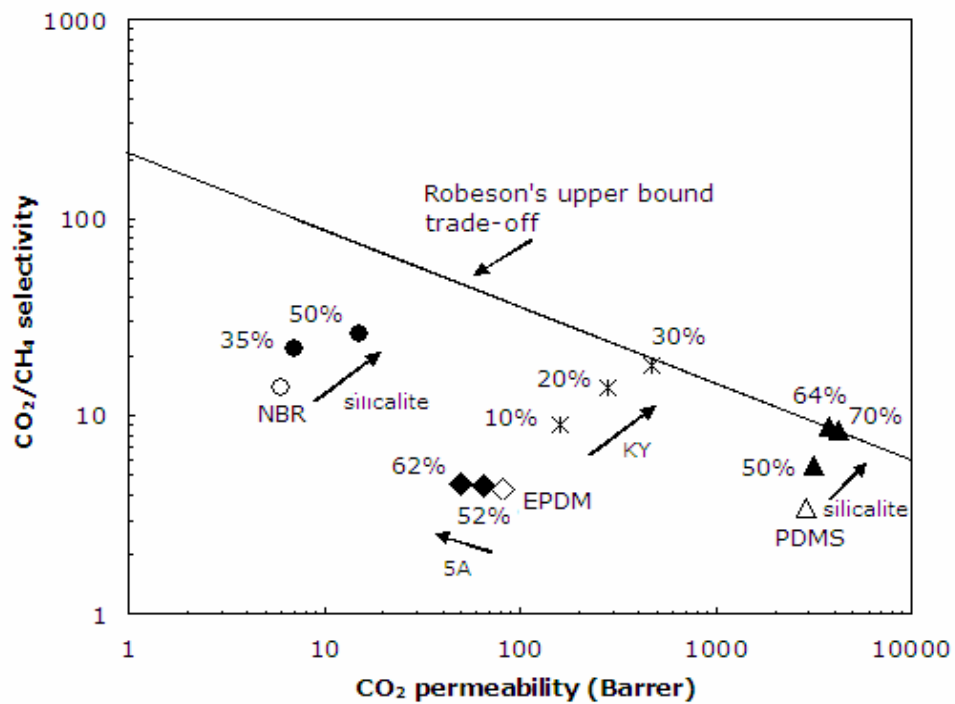


Figure 2.4 CO<sub>2</sub>/CH<sub>4</sub> performance properties of MMMs based on rubbery polymer matrices [adopted from reference 56]. The unfilled shapes denote pure rubbery polymer matrices, and the filled shapes denote zeolite filled rubbery polymer MMMs. The zeolite loading, %(w/w) is noted next to each data point.

Thus, the researchers have focused on a way to prepare zeolite filled MMMs with glassy polymers.

Table 2.1 summarizes the gas separation performances of zeolite filled glassy polymer based MMMs. The performances of pure polymeric membranes are also given for comparison with their MMMs. The effect of zeolite type and loading on membrane performance is the parameters investigated. Zeolite loading is usually changed in the range of 15 and 50 weight % of the polymer. When the zeolite content of the membranes was increased, the selectivities usually increased and permeabilities usually decreased regardless of the type of the glassy polymer. At high zeolite loadings, for instance, 50 % (w/w),

Table 2.1 Single gas permeabilities and ideal selectivities of zeolite filled glassy polymer MMMs.

Polymer*	Zeolite		Permeability (Barrer)				Ideal Selectivity		Ref.
	type	loading % (w/w)	N <sub>2</sub>	O <sub>2</sub>	CO <sub>2</sub>	O <sub>2</sub> /N <sub>2</sub>	CO <sub>2</sub> /CH <sub>4</sub>		
PES	13X	0.0	0.14	0.52	2.6	3.71	-	[21]	
		16.6	0.088	0.33	1.8	3.75	-		
		33.3	0.097	0.37	2.7	3.81	-		
		50.0	0.12	0.50	5.2	4.17	-		
		16.6	0.12	0.47	2.3	3.92	-		
PES	AgA	33.3	0.097	0.41	2.0	4.23	-		
		50.0	0.25	1.10	10.7	4.40	-		
		0.0	-	-	2.7	-	32.0	[6]	
PEI	silicalite-1	0.0	-	-	1.5	-	61.0	[22]	
		50.0	-	-	14.6	-	34.0		
PVAc	4A	0.0	0.080	0.50	-	5.90	-	[26]	
		15.0 (vol%)	0.060	0.45	-	7.30	-		
PI (Matrimid)	4A	0.0	0.18	1.32	-	7.20	-	[34]	
		20.0 (vol%)	0.56	4.00	-	7.20	-		
PI (Ulterm)	4A	0.0	0.049	0.38	-	7.80	-	[28]	
		15.0	0.039	0.38	-	9.70	-		
		35.0	0.022	0.28	-	12.90	-		

\* PES: polyethersulfone, PEI: polyetherimide, PVAc: poly(vinylacetate), PI: polyimide.

however, a loss in selectivities with an increase in permeabilities can be observed as in the case of PI/zeolite 4A (20 vol%) and PEI/silicalite (50 % w/w) membranes shown in Table 2.1. The separation performance of MMMs strongly depends on the type and concentration of the zeolite in the membrane.

In most of the studies with zeolite filled glassy polymer MMMs, examination of MMM morphology by SEM images revealed the presence of voids at the polymer-zeolite interface, which are likely to arise from the poor interaction between zeolite particles and glassy polymer chains. The term "sieve-in-a-cage" has been coined to describe polymer-zeolite morphologies with voids at the interface [30, 61]. Figure 2.5 shows a SEM image of a zeolite 4A filled polysulfone MMM, which has a sieve in-a-cage morphology [49]. This morphology is undesirable since the void can be much more permeable than zeolite. Especially, at high zeolite loadings these voids may combine in the matrix and they may form a channel network. This structure may lead to permeabilities greater than and selectivities lower than the matrix polymer. Therefore, the interfacial voids may decrease the separation performance of MMMs.

In addition to void formation, polymer matrix rigidification, which is described as the inhibition of polymer chain mobility near the polymer-zeolite interface, may occur at the interface [30, 31]. In such a case, the interface reduced the permeability of a MMM and lower permeabilities than pure glassy polymer membranes can be observed. The effect of a rigidified polymer region around zeolite particles on the performance properties of MMMs has been demonstrated in different systems, such as zeolite 4A dispersed in polyethersulfone (PES) [31] and in polyvinylacetate (PVAc) [56]. In these systems, increased glass transition temperatures was taken as a confirmation of rigidified polymeric regions in the membrane matrix. Li et al. [31] observed such a trend in PES-zeolite 4A MMM system. They reported an increment in  $T_g$  of PES with increasing zeolite 4A loading. The  $T_g$  of PES increased from 215 to 217°C and 219°C with the addition of 30 % and 50 % (w/w) zeolite 4A, respectively. They also reported a decrease in the  $H_2$ ,  $O_2$  and  $N_2$  permeabilities of PES membrane with the addition of zeolite 4A particles.

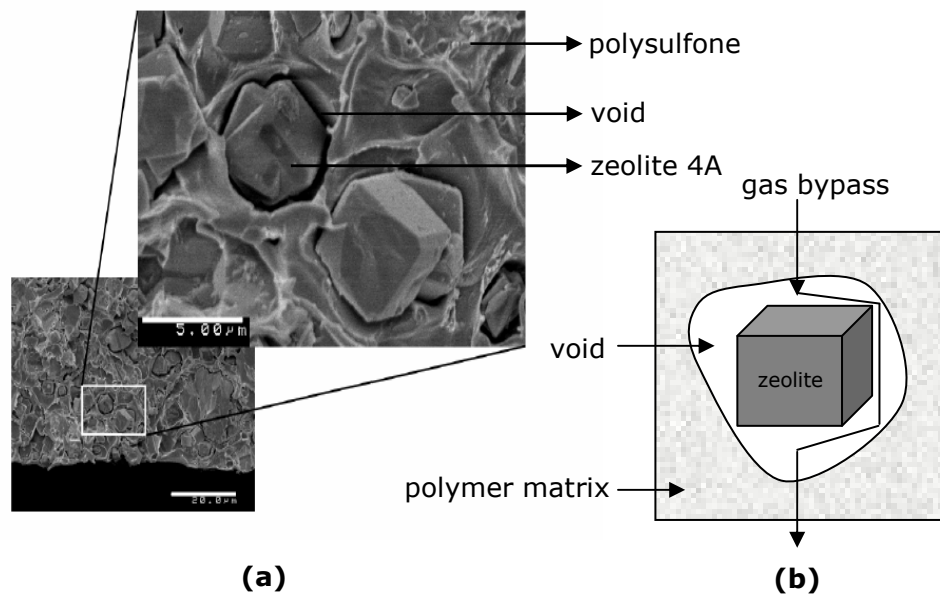


Figure 2.5 (a) Cross sectional SEM image of a polysulfone-zeolite 4A MMM, “sieve in-a-cage” morphology [56]; (b) Schematic representation of an undesirable void between the polymer matrix and zeolite [30, 49].

Therefore, changes in zeolite filled glassy polymer MMM performance are not only due to the intrinsic properties of zeolite particles and polymer matrix, but also depend on the final morphology of the polymer-zeolite MMMs, including the polymer-zeolite interface morphology. Several methods have been proposed to improve the performance characteristics of polymer-zeolite interface region. Table 2.2 summarizes these methods, which are used to improve the polymer-zeolite interaction hence to avoid non-selective voids, and their effect on the gas separation performance of MMMs.

Polymer chain flexibility was maintained during membrane preparation either by annealing the membranes above glass transition temperature of polymer or by adding a plasticizer into the membrane formulation so that polymer chains may cover zeolite crystals more compactly. In a study of Kulprathipanja et al. [32] zeolite 4A filled PES membranes were prepared by



Table 2.2 Void elimination methods in zeolite filled glassy polymer MMMs.

Method	Membrane*	Permeability		Selectivity		Ref.
		O <sub>2</sub>	CO <sub>2</sub>	O <sub>2</sub> /N <sub>2</sub>	CO <sub>2</sub> /CH <sub>4</sub>	
flexibility promotion by annealing the membrane above the T <sub>g</sub> of polymer	PES	0.77	-	5.99	-	[32]
	PES/zeolite 4A (20%)	0.34	-	5.91	-	
flexibility promotion by adding a plasticizer	PI	1.32	-	7.20	-	[28]
	PI/DBP (25%)	1.50	-	6.60	-	
	PI/DBP (25%)/4A (15%)	1.10	-	7.10	-	
external surface modification of zeolite by silane-coupling agent	PEI	-	1.50	-	61.0	[22]
	PEI/UM-silicalite (50%)	-	14.6	-	34.0	
	PEI/M-silicalite (50%)	-	8.00	-	30.0	
combination of external surface modification of zeolite and polymer chain flexibility promotion during membrane formation	PI	0.50	-	7.10	-	[29, 34]
	PI/M-zeolite 4A (20%)	0.47	-	9.40	-	
	PI/M-zeolite 4A (40%)	0.37	-	12.40	-	
reactive polymer usage	reactive fluorinated PI	22.00	-	4.20	-	[29, 34]
	PI/zeolite 4A (15%)	14.00	-	4.50	-	
nano-sized zeolite particles usage	PSF	1.30	-	5.90	-	[62]
	PSF/nano size-4A (25%)	1.80	-	7.70	-	
compatibilizer usage	PI	1.50	8.34	6.88	1.22	[27]
	PI/TAP (21%)	0.0346	0.194	15.4	84.0	
	PI/4A (43%)	1.91	9.36	4.20	2.23	
	PI/TAP (21%)/4A (43%)	0.0330	0.19	18.2	617.0	

\* PES: polyethersulfone, PI: polyimide, DBP: di-butyl phthalate, PEI: polyetherimide, PSF: polysulfone, TAP: 2,4,6-triaminopyrimidine, UM: unmodified zeolite, M: modified zeolite.

evaporating the solvent used to prepare polymer solutions above the  $T_g$  of PES during membrane formation. Although they observed an improvement in the contact between PES and zeolite 4A from SEM micrographs, selectivities for  $O_2/N_2$  decreased or remained unchanged. In another study, Mahajan et al. [28] added a plasticizer to decrease the  $T_g$  of polymer for maintaining polymer chain flexibility during membrane formation. Di-butyl phthalate (DBP) and 4-hydroxy benzophenone (HBP) were used as plasticizers with a plasticizer/polyimide ratio of 25/75 (w/w) in PI/zeolite 4A MMMs. Although this modification improved the adhesion between polymer and zeolite, separation performance was worse than the results obtained with the MMMs prepared without any modification (Table 2.2).

Another method to promote the adhesion between zeolite and glassy polymer is the modification of the external surface of zeolites with silane-coupling agents. Many MMM studies have been performed with this method, and aminopropylsilane is the commonly used silane-coupling agent in these studies [7, 18, 22, 33, 63]. Zeolite particles treated with a silane-coupling agents promoted the adhesion between zeolite and glassy polymer, however, membrane performances did not show any improvement. MMMs prepared with modified and unmodified zeolites had similar selectivities, and the selectivities of pure glassy polymeric membranes were generally higher than the selectivities of MMMs prepared by this modification method as shown in Table 2.2.

The methods, external surface modification of zeolite and polymer chain flexibility maintenance during membrane formation, were also combined to prepare high performance zeolite filled glassy polymer MMMs [29, 34]. Mahajan et al. [34] prepared such a membrane with polyimide and zeolite 4A. The resulting membranes had much higher  $O_2/N_2$  selectivity than pure polymeric membrane (Table 2.2).

In another study, a different strategy was used to improve polymer-zeolite contact. Mahajan et al. [29, 34] used polymer matrices with specific groups that react with the zeolites which were called reactive polymers. The polymer was a fluorinated polyimide with a reactive group of carboxylic acid, which

provided a hydrogen bonding or covalently bondable site for interaction with the zeolite surface. As shown in Table 2.2 that the O<sub>2</sub>/N<sub>2</sub> selectivity of pure reactive polymer increased from 4.2 to 4.5 with the addition of 15 % (w/w) zeolite 4A, whereas the O<sub>2</sub> permeability decreased from 22.0 to 14.0 Barrer.

The other method is to use of nano-sized zeolite particles in the preparation of MMMs. Wang et al. [62] reported that selectivity increased with the use of nanocrystals of zeolite 4A in polysulfone (Table 2.2), and they suggested that the nano-sized particles may alter the polymer chain packing in a different way compared to large zeolite particles, which in turn, may improve the permeability/selectivity properties of the MMMs without introducing interfacial voids.

Alternatively, Yong et al. [27] suggested adding a low molecular-weight organic compound, which is likely to link the polymer chain to the zeolite crystals, to the membrane formulation as a third component. These compounds may interact both with polymer and zeolite, thus, they act as "compatibilizer" between polymer and zeolite. They suggested 2,4,6-triaminopyrimidine (TAP) as a compatibilizer. The PI/zeolite 4A MMMs containing 21 % (w/w) TAP showed lower permeabilities but higher selectivities than PI/zeolite 4A MMMs as shown in Table 2.2. They concluded that TAP enhanced the contact between the zeolite particles and polymer chains presumably by forming hydrogen bonding between them and increased the separation performance of MMMs. However, the TAP concentration in the membrane matrix was so high that TAP was indeed one of the main components in the membrane rather than an additive and decreased the permeabilities considerably.

The aforementioned studies imply that zeolite filled glassy polymer MMMs can be appreciated as a favorable way to prepare high permeability and high selectivity gas separation membranes. However, the poor interaction between glassy polymers and zeolite particles is a continuing problem to obtain high performance MMMs.

## 2.4 Polymer/LMWA Blend Membranes

The incorporation of low molecular-weight additives (LMWA) into polymer matrices has also been examined as a promising way to modify the structure and performance properties of polymeric gas separation membranes. The addition of certain types of LMWAs into glassy polymers causes an increase in stiffness because of the reduced rates of segmental motions in the polymer chains. This phenomenon is known as antiplasticization and the LMWAs which cause this phenomenon are known as antiplasticizers in the polymer literature [64-67]. These additives also decrease the glass transition temperatures of the antiplasticised polymers because of their low glass transition temperatures,  $T_g$ , in comparison to polymers [35, 36, 64-67], but the magnitude of these  $T_g$  depressions generated by antiplasticizers is much smaller than those generated by neutral compounds or by plasticizers [3, 35, 36]. In the membrane area, this antiplasticization effect has been shown to appear by a decrease in the permeability of gases and by an increase in the selectivity of a membrane [19, 20, 68].

The LMWAs are expected to be miscible and to interact with the polymer matrix to modify the polymer chain characteristics [8, 19, 69]. Therefore, a polymer/LMWA blend membrane is desired to have a homogenous morphology with non-porous and dense structure to investigate the effect of type and concentration of LMWA on the structure and performance properties of different polymeric membranes [8, 19, 69]. Several studies have been performed to investigate the effects of different additives on the structure and performance of polymeric membranes. Usually long aliphatic and polyaromatic based compounds are incorporated into glassy polymers to prepare high performance blend membranes [8, 19, 35, 36, 68-70]. These additives generally have a rigid and planar structure and they contain polar atoms such as halogens, nitrogen and oxygen [8, 65].

Robeson [68] evaluated the effects of the addition of 4,4'-dichlorodiphenylsulfone (DDS) as a LMWA on the glass transition temperature and carbon dioxide permeability of polysulfone membrane. He found that the permeability value of CO<sub>2</sub> decreased from 5.76 to 2.16 with the addition of

10 % (w/w) DDS into PSF matrix. He suggested that DDS filled the free volume of polymer and reduced permeability. He also measured only a 5 °C decrease in the  $T_g$  of PSF membrane with DDS addition. These changes in membrane performance and structure was explained by antiplasticization effect of DDS on PSF matrix.

Maeda and Paul [35] prepared dense and homogenous polysulfone (PSF), and poly(phenyleneoxide) (PPO) membranes by introducing sebacate-, phthalate-, phosphate-, amine- and sulfone- based compounds as additives. Their concentrations in the membrane ranged between 10 and 30 % by weight. Although additives decreased the permeabilities of all gases studied, He, CO<sub>2</sub> and CH<sub>4</sub>, the selectivities of membranes for He/CH<sub>4</sub> and He/CO<sub>2</sub> increased significantly. The change in membrane performance was explained by antiplasticization effect of additives on polymer matrices. N-phenyl-2-naphthylamine was the most effective antiplasticizing additive, which provided the highest selectivity for PSF membranes. They concluded that achieving an improved combination of selectivity and permeability depended on the type of additive and the polymer to be modified. They also measured  $T_g$  of these blends and observed a decrease in  $T_g$ s. For PSF, this reduction was from 185 °C to 50 °C with the addition of 30 % (w/w) additive as antiplasticizer. They claimed that there was a relation between reduction in  $T_g$  and antiplasticization effect.

Ruiz-Treviño and Paul [8, 19] examined the effect of various naphthalene-, bisphenol-, and fluorine-, based additives on performance properties of the membranes with bisphenol A polysulfone. The additives were selected based on their interaction capability with the PSF through their functional groups. They speculated that the compounds which have hydroxyl groups and polar atoms in their structure showed strong interactions with PSF and this led to reduction in free volume by bringing the polymer chains closer, which in turn restricted the diffusion of gas molecules through modified PSF membranes, called antiplasticization effect. These additives increased selectivity and reduced permeability of PSF membrane when incorporated at the concentration range of 10-30 % (w/w). They observed that the highest increase in selectivities was caused by the additives that cause the highest

reductions in free volume of the polymer. They also concluded that the decrease in permeabilities, caused by antiplasticization, in polysulfone was quantitatively well correlated with the polymers' decreased free volume following the incorporation of additives.

Ruiz-Treviño and Paul also measured the  $T_g$ s of the PSF/LMWA blend membranes. They found that all additives decreased the  $T_g$ , and the magnitude of  $T_g$  decrease changed with the amount and type of additive. They used the Gordon-Taylor equation to determine the  $T_g$  of polymer/additive blends and to relate the extent of  $T_g$  depression by the additive content and the  $T_g$ s' of additives. Gordon-Taylor equation is a model relating the  $T_g$  of a blend to the weight fractions and  $T_g$ s of pure components when antiplasticization occurs (eqn. 2.5) [8, 19].

$$T_g = \frac{w_a T_{ga} + K w_p T_{gp}}{w_a + K w_p} \quad (2.5)$$

In this equation, the subscripts a and p stand for LMWA and polymer, respectively, and w is the weight fraction of the species in the membrane. K is an adjustable parameter that depends on the types of the polymer and LMWA and the extent of interaction between them. According to this equation compounds with low  $T_g$  decreases the glass transition temperature of polymer depending on the extent of interaction between polymer and additive. Ruiz-Treviño and Paul found that the measured  $T_g$ s of PSF/LMWA membranes fitted well with the Gordon-Taylor antiplasticization model equation.

Larocca and Pessan [36] prepared polyetherimide (PEI) membranes containing 5 to 40 % by mol halogen containing polyaromatic additives. They chose the additives according to some important characteristics that are assumed to strongly affect the degree of antiplasticization, namely, the size and stiffness of the additive molecule, and its level of interaction with the PEI chains. They evaluated the interaction between polymer and additives by a solubility parameter based approach. They claimed that as the difference between solubility parameters of PEI and additive decreased the level of interaction between polymer and additive or in other words the level of

antiplasticization of polymer increased. They observed the antiplasticization effect of those additives, which decreased gas permeabilities of the polymer. The incorporation of those additives at 20 % by mol into PEI matrix resulted only in a 10 to 20°C decrease in  $T_g$  of pure PEI. The additives decreased the permeabilities of oxygen and carbon dioxide by 50-60 %. They concluded that the extent of antiplasticization depended on the degree of interaction between the additive and the polymer as well as the concentration of additive in the matrix.

Pant et al. [70] studied the antiplasticization effect of a liquid-crystalline azo compound on polystyrene membranes at low concentrations changing from 1 to 10 % by weight. The additive decreased the permeabilities of nitrogen and carbon dioxide by 30-40 %, indicating that antiplasticization can be achieved at low concentrations of additive as well.

Sen et al. [20] prepared polycarbonate (PC)/LMWA blend membranes to examine the effect of different LMWAs with functional groups on the structure and performance of pure PC membrane. The additives with functional groups were selected to increase the probability of interaction between PC and the additive. In their selection the main factor was their possession of amine-, nitro-, and hydroxyl- functional groups, through which they could interact with PC matrix. Those additives were catechol, *p*-nitroaniline (pNA), 4-amino 3-nitro phenol (ANP) and 2-hydroxy 5-methyl aniline (HMA) and their concentrations in the membrane were changed between 1 and 10 % (w/w), which was significantly low as opposed to the LMWA concentration applied in the above mentioned studies. The blend membranes showed lower permeabilities for  $H_2$ ,  $N_2$ ,  $O_2$ ,  $CO_2$  but higher selectivities than pure PC membranes since LMWAs antiplasticized the membranes. In addition to that, all LMWAs decreased the  $T_g$  of PC membranes. The largest shift from the  $T_g$  of pure PC was observed for PC/catechol blend membrane, where the  $T_g$  of PC decreased from 146 °C to 130 °C, despite catechol had the highest pure substance  $T_g$  of -54 °C. On the other hand, ANP, with the lowest pure substance  $T_g$  of -93 °C, gave rise to the smallest shift in  $T_g$  of PC. These results indicated that the extent of shift from the  $T_g$  of pure PC depended on both the  $T_g$  of pure LMWA and the degree of interaction between LMWA and

PC. The interaction between PC chains and LMWAs was apparent in FTIR spectra of membranes. Among the LMWAs, pNA was the most effective antiplasticizing additive, which provided the highest selectivity and lowest  $T_g$  reduction.

The above mentioned studies imply that the incorporation of additives into a polymer may improve the permeability-selectivity properties of gas separation membranes if polymer-additive pair is selected judiciously. Moderately high molecular-weight additives are generally introduced to modify the polymer at concentrations of 10-30 % by weight. The interaction between polymer and additive seems to be an important factor in the preparation of high performance blend membranes. Additives with multifunctional groups that are capable of interacting with polymer were found to be more efficient to improve performance of polymeric membranes. Multifunctionality of the additives allowed them to be introduced at small concentrations into blend membranes, and led them to be real additives instead of being a major component of the membrane. It can be concluded that the introduction of LMWAs with multifunctional groups into glassy polymers can be used as a tool to tailor the structure and performance properties of the polymeric membranes. In addition, such additives can be used to prepare better performing zeolite filled mixed matrix membranes by improving the interaction between polymer and zeolite.

## **2.5 Separation of Binary Gas Mixtures with Polymeric Membranes**

Polymeric membranes have been successfully used in many industrial gas separation applications because of their low energy consumption, ease of installation and operation, low maintenance requirements and high process flexibility [48, 51-53, 55]. Understanding the transport behavior of the target gases through polymeric membranes is thus of fundamental and practical interest for effective separation of gaseous mixture and selecting the appropriate feed conditions.

A great deal of experimental data and basic knowledge have been collected on membrane based gas separation, and almost all is obtained from single gas



permeability measurements of the membranes [12, 51-53, 55]. Single gas permeability measurement is a commonly used technique to provide an indication of possible performance of membranes under ideal conditions. However, the use of single gas permeation data to estimate the performance properties of membranes for a gas mixture may lead to erroneous results. The transport behavior of a component in gas mixture through membrane can be affected by the presence of other penetrants so that it may deviate from that of the single gas [9, 43, 44, 71]. This, in turn, may affect the correct choice of membrane for a certain industrial gas separation application. Thus, in recent studies, the requirement of multicomponent gas mixture permeation measurements are commonly emphasized, which can also be helpful to acquire a better understanding on transport mechanism of penetrants through membranes in molecular level.

The multicomponent gas mixture permeation measurement studies are mostly concentrated on the CO<sub>2</sub>/CH<sub>4</sub> binary gas mixture because of the importance of removal of CO<sub>2</sub> from natural gas [9, 41, 45, 72-78]. Table 2.3 shows the CO<sub>2</sub>/CH<sub>4</sub> binary gas separation performances of different types of polymeric membranes, and compares the differences between binary and single gas separation performances of the membranes. The comparison was based on the typical membrane matrix because of its polarizable nature, is highly soluble and/or preferentially sorped in most of the membranes [9, 72, 75]. This interactive nature of CO<sub>2</sub> generally leads to differences in the gas permeability and membrane selectivity when its binary gas mixture and single gas permeation measurements are compared. Especially in MMMs, which contain fillers with specific sorption properties, like zeolite 4A in PES/zeolite 4A membranes [75], the sorption of CO<sub>2</sub> in the membrane matrix increases due to the availability of more sorption sites in the membrane matrices for interaction with the CO<sub>2</sub>, and this in turn may give rise in deviation between binary and single gas permeability measurements. On the other hand, for PDMS [9], PI (Matrimid) [46] and PES [75] membranes the competition in sorption among CO<sub>2</sub> and CH<sub>4</sub> may not be effective to change the separation performances for CO<sub>2</sub>/CH<sub>4</sub> binary gas mixture. Apparently, the type of polymer matrix and the membrane

Table 2.3 CO<sub>2</sub>/CH<sub>4</sub> binary gas separation performances of different polymeric membrane morphologies<sup>a</sup>.

Membrane Morphology	Membrane Materials <sup>b</sup>	Feed composition % CO <sub>2</sub>	Permeability <sup>c</sup> (Barrer) <sup>d</sup>			Selectivity <sup>c</sup> (CO <sub>2</sub> /CH <sub>4</sub> )		Ref		
			Single gas	Binary gas		Ideal	Binary			
			CO <sub>2</sub>	CH <sub>4</sub>	CO <sub>2</sub>	CH <sub>4</sub>	mixture			
DHRM	PDMS	5, 25, 50, 75	3.0	1.00	3.2	0.88	-	3.0	3.6	[9]
DHGM	PI-TPI	5, 25, 50, 75	13.8	0.38	16.1	0.26	-	36.0	62.0	[9]
	PI-Matrimid	50	10.0	-	9.0	0.22	5.7	-	44.0	[46]
	PI-crosslinked	50	4.5	-	5.0	0.10	3.0	-	50.0	[74]
	PC	50	$P_{(CO_2)single} > P_{(CO_2)binary}$						$\alpha_{(ideal)} > \alpha_{(binary)}$	[77]
	PES	0 to 100	$P_{(CH_4)single} > P_{(CH_4)binary}$							[75]
	PPO/HPA	5 to 40	2.61	0.109	-	-	0.540	23.9	25.0	[75]
DHBM	PPO/HPA	5 to 40	28.2	1.36	-	-	-	20.6	8.8	[73]
Asymmetric	CA	2.04, 30.6, 70.6	$P_{(CO_2)single} > P_{(CO_2)binary}$						$\alpha_{(ideal)} > \alpha_{(binary)}$	[76]
MMM	PES/zeolite 4A	0 to 100	4.07	0.11	-	-	1.40	37.0	25.0	[75]

<sup>a</sup> DHRM: dense homogeneous rubbery polymer membrane, DHGM: dense homogeneous glassy polymer membrane, DHBM: dense homogeneous blend membrane, MMM: mixed matrix membrane.

<sup>b</sup> PDMS: poly(dimethylsiloxane), PI: polyimide, PC: polycarbonate, PES: poly(ethersulfone), CA: cellulose acetate, PPO/HPA: poly(phenyleneoxide)/heteropolyacid.

<sup>c</sup> Permeability (P) and selectivity ( $\alpha$ ) data are given for 50 % nominal feed gas compositions and at low feed pressures.

<sup>d</sup> 1 Barrer=  $1 \times 10^{-10}$  cm<sup>3</sup>(STP).cm/cm<sup>2</sup>.cmHg.s.

morphology are the most important factors that influence in deviation between binary and single gas permeation measurements.

The effect of feed gas composition and pressure on the CO<sub>2</sub>/CH<sub>4</sub> binary gas mixture permeabilities and selectivities of the above mentioned membranes were also investigated. At low feed pressures, an increase in CO<sub>2</sub> feed concentration generally leads to an increase in permeabilities, while the selectivities may decrease, increase or stay constant depending on the interaction strength between CO<sub>2</sub> and membrane matrix [9, 73, 75]. At high feed pressures and/or at high CO<sub>2</sub> feed concentrations, the plasticization effect of CO<sub>2</sub>, which refers to the situation where the permeabilities of the penetrants are accelerated because of the swelling of the polymer matrix due to the strong interaction of CO<sub>2</sub> with polymers, greatly influences the permeation through membranes and leads to a decrease in separation performance of the membranes [74, 76, 77]. Therefore, operating parameters can substantially alter the membrane performance and different type of membranes may have better performance characteristics at different feed compositions and pressures.

Table 2.4 summarizes the binary gas separation performances of different type of polymeric membranes for different binary gas pairs and gives some explanations about permeation mechanisms. When none of the gas components has a possibility of strong interaction with the membrane matrix, as in the case of H<sub>2</sub>/CH<sub>4</sub>, He/CH<sub>4</sub> and N<sub>2</sub>/CH<sub>4</sub> binaries, the permeation mechanism across the membranes is related to the molecular size difference of gas components, called competitive diffusion [75, 79-81]. If the molecular size difference is high (H<sub>2</sub>/CH<sub>4</sub> and He/CH<sub>4</sub>), increasing concentration of the smallest gas molecule in the feed and increasing temperature result in increase in selectivities and permeabilities, while if this difference is small (N<sub>2</sub>/CH<sub>4</sub>) separation performances generally decreases. Battal et al. [75] reported that, for the H<sub>2</sub>/CH<sub>4</sub> binary gas mixtures, higher H<sub>2</sub> concentration in the feed caused higher selectivity values which were below the ideal selectivity of PES/zeolite 4A MMM. For example, the H<sub>2</sub>/CH<sub>4</sub> separation selectivity of the MMMs increased from 46.0 to 95.0 as the H<sub>2</sub> concentration in the feed increased from 10 % to 70 % (mol/mol). This means that,

Table 2.4 Binary gas separation performances of different polymeric membranes for different binary gas pairs.

Binary Gas	Membrane Type*	Parameters	Results	Proposed Possible Mechanism	Ref
CO <sub>2</sub> /CH <sub>4</sub>	PES/zeolite 4A	Feed composition	Decrease in CO <sub>2</sub> /CH <sub>4</sub> and CO <sub>2</sub> /Ar selectivities with CO <sub>2</sub> concentration	Gas component-membrane matrix interactions.	[75]
CO <sub>2</sub> /Ar	MMM			High solubility of CO <sub>2</sub> in membrane matrix.	
H <sub>2</sub> /CH <sub>4</sub>			Increase in H <sub>2</sub> /CH <sub>4</sub> selectivity with H <sub>2</sub> concentration.	Molecular size difference of gas components. Fast diffusion of H <sub>2</sub> through membrane matrix.	[75]
CO <sub>2</sub> /CH <sub>4</sub>	PEI/BMI semi-IPN	Feed composition	Increase in CO <sub>2</sub> /CH <sub>4</sub> and CO <sub>2</sub> /N <sub>2</sub> selectivity with CO <sub>2</sub> concentration.	Gas component-membrane matrix interactions.	[72]
CO <sub>2</sub> /N <sub>2</sub>	asymmetric mem.			Strong interaction of CO <sub>2</sub> with membrane.	
He/CH <sub>4</sub>	Polyphosphazene DHGM	Temperature	Increase in He/CH <sub>4</sub> selectivity with temperature.	Molecular size difference of gas components. Fast diffusion of He through membrane matrix.	[79]
SO <sub>2</sub> /N <sub>2</sub>			Decrease in SO <sub>2</sub> /N <sub>2</sub> , CO <sub>2</sub> /CH <sub>4</sub>	Gas component-membrane matrix interactions.	[80]
CO <sub>2</sub> /CH <sub>4</sub>			And H <sub>2</sub> S/CH <sub>4</sub> selectivities with temperature.	Decrease in sorption of more polar gases (SO <sub>2</sub> , H <sub>2</sub> S and CO <sub>2</sub> ) with temperature.	
H <sub>2</sub> S/CH <sub>4</sub>					
CO <sub>2</sub> /CH <sub>4</sub>	Polyimides		Low separation performances for N <sub>2</sub> /CH <sub>4</sub> .	Smaller molecular size difference of gas components decrease the performance.	[81]
CO <sub>2</sub> /N <sub>2</sub>	DHGM				
N <sub>2</sub> /CH <sub>4</sub>			Low and/or high separation performances for CO <sub>2</sub> /CH <sub>4</sub> and CO <sub>2</sub> /N <sub>2</sub> .	Specific interaction of a gas component with membrane may increase or decrease the separation performance.	

\* PES: polyethersulfone, PEI/BMI semi-IPN: polyetherimide-bismaleimide semi-interpenetrating polymer networks.

approximately 50 % increase in selectivity was observed in comparison to the lowest CO<sub>2</sub> concentration in the feed. Peterson et al. [79] also showed that the He/CH<sub>4</sub> separation selectivity of the dense homogenous polyphosphazene membranes increased from 3.1 to 3.8 with an increase in temperature from 50 to 100 °C for the feed mixtures containing 34 % (mol/mol) He.

On the other hand, the presence of an interactive type gas component, such as CO<sub>2</sub>, SO<sub>2</sub> and/or H<sub>2</sub>S, in the gas mixture, leads permeation mechanism to deviate from the permeability-size correlation. In such a case, the sorption of gas components becomes an important factor in the transport of gas mixtures, called competitive sorption [72, 75, 80, 81]. Depending on the interaction strength between gas component and membrane matrix, the separation performance of a membrane may increase or decrease. Sridhar et al. [73] investigated the separation of CO<sub>2</sub>/CH<sub>4</sub> binary gas mixtures through poly(phenylene oxide) (PPO)/heteropolyacid (HPA) blend membranes by varying the CO<sub>2</sub> feed concentration between 5 and 40 mol % at a constant pressure. They observed that the permeability and selectivity data obtained for the binary gas mixtures were lower than those obtained with single gases, which was explained by the reduced partial pressure of each gaseous component in the mixture. They also observed an increase in separation selectivity with an increase in CO<sub>2</sub> concentration due to the increasing sorption of the CO<sub>2</sub> gas in the membrane matrix. The CO<sub>2</sub>/CH<sub>4</sub> separation selectivity of PPO/HPA membrane increased from 2.1 to 5.8 as the CO<sub>2</sub> concentration in the feed increased from 5 to 40 mol %. On the contrary, Battal et al. [75] reported a decrease in the CO<sub>2</sub>/CH<sub>4</sub> separation selectivity of PES/zeolite 4A MMMs with CO<sub>2</sub> feed concentration. They observed approximately 50 % decrease in CO<sub>2</sub>/CH<sub>4</sub> selectivities of PES/zeolite 4A MMMs, when the CO<sub>2</sub> concentration in the feed was increased from 10 % to 60 % (mol/mol).

The studies mentioned in Table 2.3 and Table 2.4 imply that single gas permeability measurements and ideal selectivities may not be enough to evaluate the separation performance of a membrane. There may be some differences between single and binary gas permeation properties of the

membranes, and this is especially true for MMMs at which more deviation from their ideal performance is observed. The properties of the gas components and membrane, gas-membrane matrix and gas-gas-membrane matrix interactions as well as the feed conditions seem to be important factors that affect the separation performance of a membrane for a gas mixture. It is also important to note that, most of the studies about dependence of separation performance of membranes to operating parameters were done by changing the temperature and pressure. Whereas the composition dependence of permeability and selectivity has not been substantially studied. Therefore, increasing the number of studies on this subject can be helpful to determine at which feed gas composition the prepared membranes are best performing in industrial gas separation applications, and at the same time more mechanistic information can be gathered on permeation through membranes.

## CHAPTER 3

### EXPERIMENTAL

#### 3.1 Synthesis of Zeolite 4A Crystals

Zeolite 4A crystals were synthesized hydrothermally from a hydrogel with a molar composition of  $2.5\text{Na}_2\text{O}:\text{Al}_2\text{O}_3:1.7\text{SiO}_2:150\text{H}_2\text{O}$  [82]. The materials used to prepare synthesis gel were sodium silicate solution (7.5-8.5%  $\text{Na}_2\text{O}$ , 25.5-28.5%  $\text{SiO}_2$ , 63-67%  $\text{H}_2\text{O}$ , Merck), aluminum hydroxide ( $\text{Al}(\text{OH})_3$ , Merck), sodium hydroxide (97%  $\text{NaOH}$ , Merck) and distilled water.

The synthesis gel was formed by mixing sodium silicate and sodium aluminate solutions which were prepared separately in polypropylene cups. Sodium silicate solution was diluted with the half of the total distilled water required for crystallization. Sodium aluminate solution was prepared by the addition of  $\text{Al}(\text{OH})_3$  to sodium hydroxide solution, and it was heated with stirring until a clear solution was obtained. The amount of water lost during heating was added to the solution. Then, the sodium silicate solution was added on the sodium aluminate solution to form a hydrogel, and the hydrogel was stirred vigorously for 24 h on a magnetic stirrer at room temperature for homogeneity.

The synthesis gel was transferred to stainless steel autoclaves with PTFE inserts, and the crystallization was carried out at 80 °C for 24 h. The solid product was recovered by filtration and washed with distilled water till the pH

of filtrate reduced nearly to 8. The solid product was then dried at 80 °C for 24 h and powdered in a ceramic mortar.

The powder was analyzed with Philips PW 1840 X-Ray diffractometer (XRD) using Cu-K $\alpha$  tube with Ni filter at a voltage of 30 kV and a current of 24 mA. The XRD patterns were taken between 5<sup>o</sup> and 40<sup>o</sup> Bragg angles with a speed of 0.1 °/s. A commercial zeolite 4A (Acros) was used as an external standard. Existence of zeolite 4A was checked by comparing the positions of peaks of sample with those of standard. A typical XRD pattern of synthesized zeolite 4A powder and that of external standard were shown in Appendix A. The XRD patterns showed that the synthesized samples were highly crystalline zeolite 4A.

The shape of the crystals and their average particle size were determined with an optical microscope. The crystals were in a cubic shape with a particle size of less than 5  $\mu$ m.

## **3.2 Preparation of Membranes**

### **3.2.1 Materials**

The polymeric material used for membrane preparation was analytical grade poly(bisphenol-A-carbonate), PC, which was purchased from Aldrich. The polymer has a weight-averaged molecular weight of 64,000 and glass transition temperature,  $T_g$ , of about 150 °C. Figure 3.1a shows the repeating unit of the poly(bisphenol-A-carbonate).

Analytical grade dichloromethane, DCM, (Aldrich) was used as solvent. It has the chemical formula of CH<sub>2</sub>Cl<sub>2</sub> and the boiling point of 40 °C.

The filler material was home-made zeolite 4A crystals. They were dried at 300 °C for 20 h before using in membrane preparation.

The low molecular weight-additive was *p*-nitroaniline, pNA, (Acros,  $M_w$ = 138.1) with a chemical formula of C<sub>6</sub>H<sub>4</sub>(NH<sub>2</sub>)(NO<sub>2</sub>), which has -amine and



-nitro functional groups. The solubility of pNA in DCM is 2 % (w/v) [20, 83], and its melting point is 148.5 °C [84]. Figure 3.1b shows the chemical structure of *p*-nitroaniline.

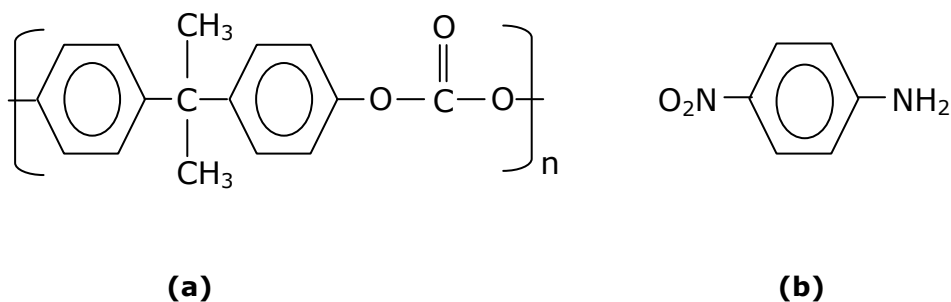


Figure 3.1 The repeating unit of poly(bisphenol-A)-carbonate (a), and the structure of *p*-nitroaniline (b).

### 3.2.2 Membrane Preparation Methodology

Membranes were prepared by solvent-evaporation method [17, 20, 25]. The flowchart of the membrane preparation methodology of PC/pNA/zeolite 4A membranes was shown in Figure 3.2. pNA was dissolved in DCM, and then zeolite 4A was added into this solution. The mixture was ultrasonicated (Branson 2510, 40 kHz) for 40 min to improve the dispersion of zeolite particles in the mixture. Zeolite 4A particles were then primed by adding approximately 15 w % of total amount of PC, which was suggested to increase the compatibility between zeolite and polymer, and to minimize the aggregation of zeolite particles [24, 85, 86].

The mixture was stirred overnight on a magnetic stirrer and ultrasonicated for 40 min more to enhance the homogeneity. The remaining PC was added, and the final mixture was mixed for 4 h and then ultrasonicated for 40 min. The concentration of PC in DCM was 12 % (w/v). The concentrations of pNA in PC

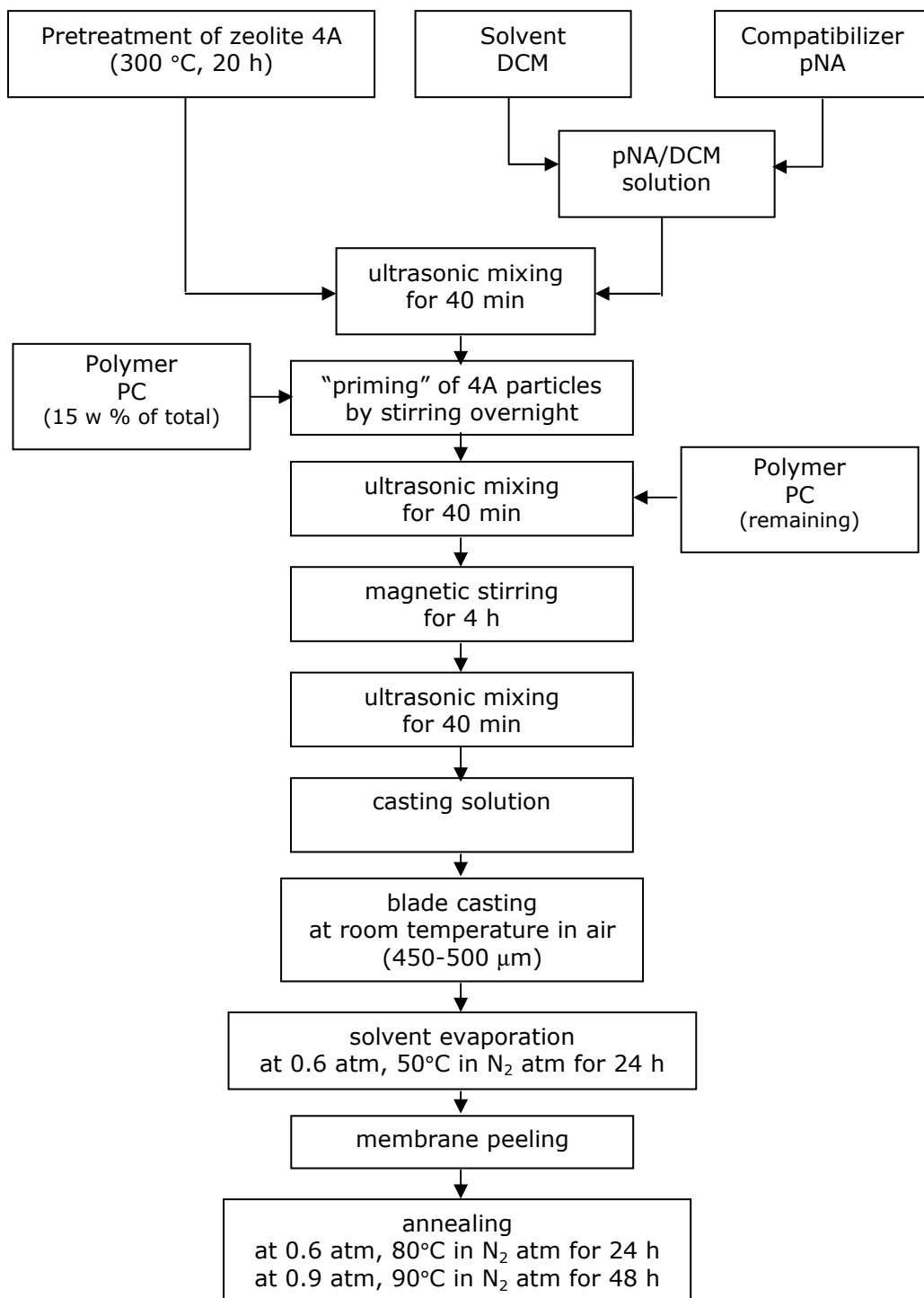


Figure 3.2 Flowchart of the preparation methodology of PC/pNA/zeolite 4A membranes.

and the zeolite 4A in PC were varied between 1-5 % (w/w) and 5-30 % (w/w) on solvent-free basis, respectively.

The mixture was blade cast on a glass plate at room temperature in air using a stainless steel film applicator (Automatic Film Applicator, Sheen 1133) with a casting knife of 500  $\mu\text{m}$  clearness. The film was dried at 50°C and 0.6 bar for 24 h in nitrogen. The membrane that was detached from the glass plate was annealed for 24 h at 80°C and then for 48 h at 90°C in nitrogen at 0.9 bar to remove the residual solvent.

The same procedure was also applied to prepare pure PC, PC/pNA and PC/zeolite 4A membranes. All type of membranes were tested with gas permeation as soon as after their preparation and they were kept in vacuum desiccator for later use.

The thicknesses of all membranes were measured with a micrometer and those of several membranes were measured from SEM micrographs. The thicknesses were in the range of 35-95  $\mu\text{m}$ .

### **3.3 Membrane Characterization**

#### **3.3.1 Thermal Characterization**

Membranes were analyzed to determine the glass transition temperatures by Perkin-Elmer Diamond Differential Scanning Calorimeter (DSC). A small piece of membrane was heated at a heating rate of 10 °C/min from 20 to 200 °C in nitrogen with a flow rate of 20 ml/min. The sample was then cooled down to 20 °C and heated again to 200 °C with the same procedure for a second scan. The second scan thermogram was used to determine the glass transition temperature ( $T_g$ ) of the membrane.

Membranes were also analyzed by a Perkin Elmer Pyris Thermal Gravimetry Analyzer and Fourier Transform Infrared Spectrometry (TGA-FTIR). The samples were heated at a rate of 5 °C/min in  $\text{N}_2$  atmosphere. The nitrogen flow rate was 70 ml/min.

### **3.3.2 Scanning Electron Microscopy (SEM) Characterization**

Membrane morphology was determined by Scanning Electron Microscopy (SEM) on a JEOL JSM-6400. Membranes were fractured in liquid nitrogen to obtain a clean break and a smooth section for micrography. The samples were then stuck vertically on to a circular aluminum sample holder to observe the cross sectional morphology. The samples were coated with gold in order to provide an electrically conductive layer, to minimize radiation damage, and to increase electron emission [87]. After coating, the membranes were analyzed at a magnification of 1500x, 5000x and 10,000x.

### **3.4 Gas Permeability Measurements**

#### **3.4.1 Single Gas Permeability Measurements**

Figure 3.3 shows the schematic drawing of the experimental set-up used to measure single gas permeabilities. It was previously designated and used by our research group [83, 88, 89]. The set-up consists of a home-made membrane cell, a pressure transducer, a gas tank and a vacuum pump. The membrane cell was located in a constant temperature silicone oil bath.

The membrane cell consists of two horizontal stainless steel flanges which are 10 cm in diameter and 1.5 cm thick (Figure 3.4). Circular depressions were machined in each flange, so that a cylindrical cavity was formed when the flanges were superimposed with the depression facing one another. The membrane that was placed in the membrane cell was supported by several sheets of filter paper (Whatman 41, 125 mm Dia, No: 144125) and clamped between two flanges by means of six equally spaced bolts. Filter papers were cut to fit the circular depressions in the lower and upper flanges. Synthetic rubber gaskets were used to ensure a pressure-tight seal between the membrane and flanges. The effective membrane area was 19.6 cm<sup>2</sup>. The dead volume of the set-up, which is described as the volume between permeate side of the membrane cell and the pressure transducer, was measured as 6 cm<sup>3</sup> [83, 88, 89].

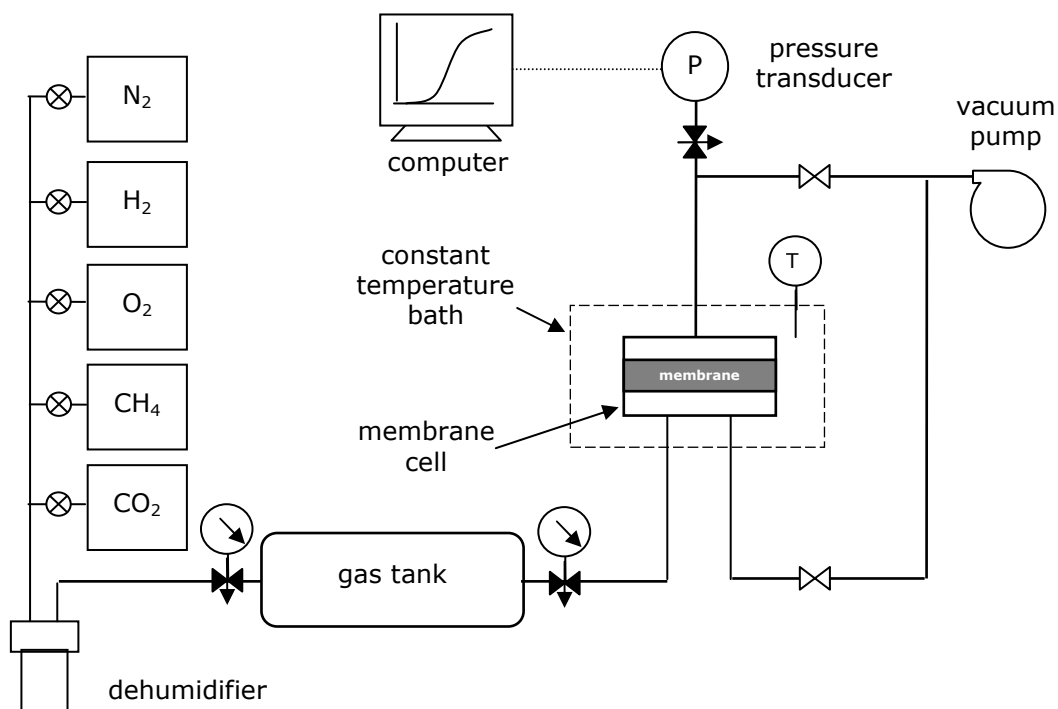


Figure 3.3 Schematic drawing of the single gas permeability measurement set-up.

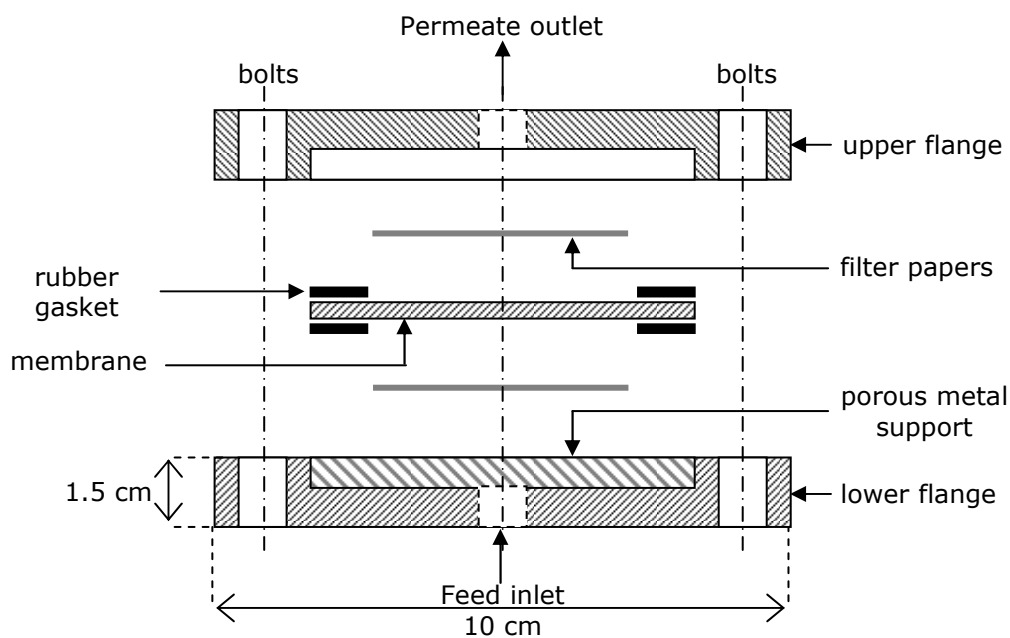


Figure 3.4 Schematic representation of the home-made membrane cell.

Single gas permeabilities of nitrogen, methane, hydrogen, oxygen and carbon dioxide were measured at room temperature. The gases were purchased from local companies (Oksan) and their purities were higher than 99%. The measurements always began with N<sub>2</sub> and ended up with CO<sub>2</sub> as a precaution for the possibility of plasticization of membrane by carbon dioxide.

Before each permeation measurement, both sides of the membrane were evacuated to less than 0.1 bar by a 2-stage mechanical vacuum pump (Model E2M5, Edwards High Vacuum Pump). The membrane was kept in vacuum for 1.5-2 h between two runs carried out with the same gas, and for 2-2.5 h before switching to another gas.

The experimental measurements were performed by constant volume-variable pressure technique at room temperature as described previously in detail [21, 88-90]. The penetrant gas was sent to the gas tank after passing through the dehumidifier, which was filled with zeolite 4A. The pressure was 3.7 bar in the gas chamber. Then, the gas was fed to the permeation cell at this pressure (the feed side). The initial transmembrane pressure difference was 2.8 bar.

Since this is a dead-end system with no outlet for the feed except through the membrane, the pressure rise at the other side of the membrane (the permeate side) was monitored to calculate the permeability. The pressure was measured by a pressure transducer (Data Instruments, Model SA, 0–100 psia pressure range) with a sensitivity of 0.01 psia. The permeability of each gas through a membrane was measured at least twice.

### **3.4.2 Single Gas Permeability Calculations**

Permeability of a single gas through a membrane can be calculated from Equation 3.1,

$$P = \frac{v \cdot \delta}{\Delta p \cdot A} \quad (3.1)$$

where,

$P$  = permeability (Barrer), 1Barrer =  $10^{-10}$  cm<sup>3</sup> (STP).cm / cm<sup>2</sup>.s.cmHg

$v$  = volumetric flow rate of the permeate gas through the membrane (cm<sup>3</sup>/s)

$A$  = effective membrane area (cm<sup>2</sup>)

$\delta$  = thickness of the membrane (cm)

$\Delta p$  = transmembrane pressure difference (cmHg)

The volumetric flow rate of the permeate gas can be found by,

$$v = \left( \frac{dn}{dt} \right) M \cdot \left( \frac{1}{\rho} \right) \quad (3.2)$$

where  $dn/dt$  is the molar flow rate of the permeate gas,  $\rho$  is the density of the permeate gas and  $M$  is the molecular weight of the gas. Density of permeate gas is calculated by assuming ideal gas law (eqn. 3.3).

$$\rho = \frac{pM}{RT} \quad (3.3)$$

where  $p$  is taken as the average of initial and final pressures at the permeate side.

By using the ideal gas law, the molar flow rate of the gas can be expressed as;

$$\frac{dn}{dt} = \left( \frac{dp}{dt} \right) \left( \frac{V_d}{RT} \right) \quad (3.4)$$

In this equation  $dp/dt$  is the slope of pressure versus time graph. The slope was taken on the region, where the pressure rises steadily in the permeate side.  $V_d$  is the dead volume and  $T$  is the absolute temperature. Pressure vs. time data points were fit to a straight line by linear regression method. The slope of this line ( $dp/dt$ ) was used for calculation of permeabilities. The algorithm for single gas permeability calculations was given in Appendix B.

The ideal selectivity of a membrane for a gas over another was defined as the ratio of single gas permeabilities, which can be expressed as;

$$\alpha_{ij} = P_i / P_j \quad (3.5)$$

### **3.4.3 Separation of Binary Gas Mixtures**

#### **3.4.3.1 Experimental Set-up**

A new gas permeation set-up which was used to separate binary gas mixtures was constructed. It was connected on-line to gas chromatograph to provide a leak proof way of transferring binary gas mixtures for concentration analysis. The schematic diagram of the set-up for separation of binary gas mixtures is shown in Figure 3.5.

Besides allowing binary gas permeation experiments, the same set-up can be used to carry out single gas permeation experiments. The basic infrastructure of the set-up is similar to the single gas permeability measurement set-up described in Section 3.4.1. The differences are in (1) the type of membrane cell used, (2) the type of pressure transducer used, (3) the valves and fittings used, (4) the ability to measure permeability in high vacuum, and (5) the ability to analyze feed and permeate side gas streams with a gas chromatograph. The set-up was constructed with 316 stainless steel tubings, Swagelok ultra-torr vacuum fittings and vacuum sealed valves.

The membrane cell was a stainless steel Millipore filter holder (Millipore, part no. XX45 047 00) with a double Viton O-ring seal. The membrane that was placed in the membrane cell was supported by a filter paper on the top of a porous metal screen. The effective membrane area was 9.6 cm<sup>2</sup>. The dead volume of the set-up, which is the volume occupied by the permeate gas from permeate side of the membrane cell to pressure transducer and gas chromatograph, was measured as 22 cm<sup>3</sup>. Measurement of dead volume of the set-up was given in detail in Appendix C.



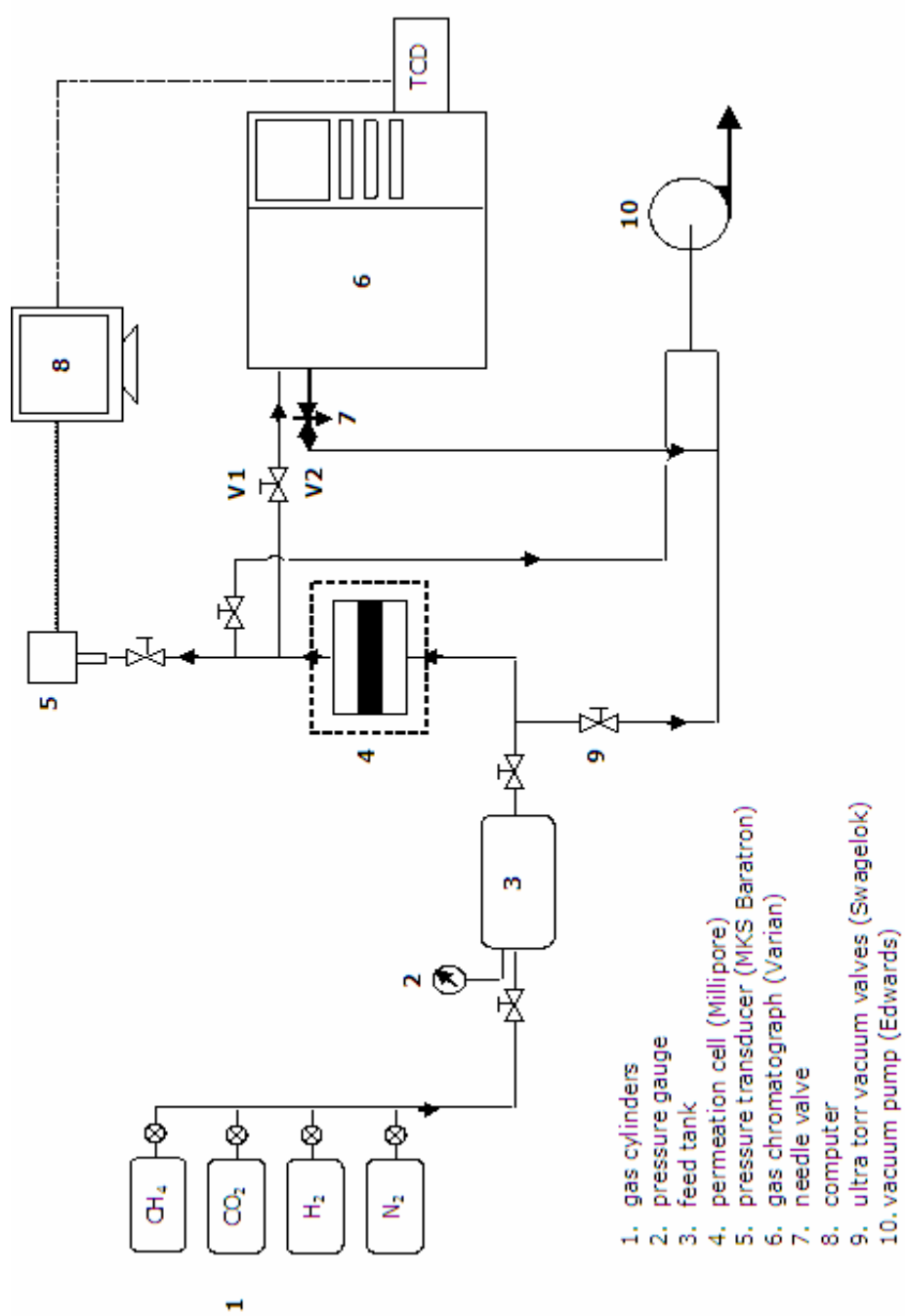


Figure 3.5 Schematic drawing of the binary gas permeation set-up.

A pressure transducer (MKS Baratron, 0-100 Torr) with a sensitivity of 0.1 Torr was used to monitor the pressure increase at the permeate side of the permeation cell. The feed and permeate gas streams were analyzed by an online gas chromatograph (GC, Varian CP-3800) equipped with a Chromosorp 102 column (80-100 mesh) and a thermal conductivity detector (TCD). The GC was connected to the permeate section of the permeation cell and the vacuum pump through the six-port injection valve. The sample inlet and outlet to the six-port valve was controlled by valves V1 and V2, respectively. The sample loop of GC has a total volume of 100  $\mu\text{l}$  ( $0.1 \text{ cm}^3$ ).

### **3.4.3.2 Experimental Procedure**

The membranes were evaluated by their separation performances of  $\text{CO}_2/\text{CH}_4$ ,  $\text{H}_2/\text{CH}_4$  and  $\text{CO}_2/\text{N}_2$  binary gas mixtures. For  $\text{CO}_2/\text{CH}_4$  binary, the feed gas mixture composition was changed between 5-95 % (mol/mol)  $\text{CO}_2$ . For  $\text{CO}_2/\text{N}_2$  and  $\text{H}_2/\text{CH}_4$  binaries, three different feed gas mixture compositions, 20, 50 and 80 % (mol/mol)  $\text{CO}_2$  and/or  $\text{H}_2$  were studied, respectively. Measurements were performed by constant volume-variable pressure technique at room temperature.

The experimental measurements were conducted in two consecutive steps. In the first step, a binary gas mixture was prepared in the feed tank by using the pressure gauge at the inlet, and kept at 3 bar. To obtain the desired proportion, one of the gases is fed to the tank up to the corresponding pressure and the other is allowed to the tank to final pressure. Then, this mixture was fed to the membrane cell, while the permeate side was held at vacuum ( $1.32 \times 10^{-5}$  bar). The pressure rise at the permeate side of the membrane was monitored to calculate the permeability of mixture. In the second step, after the permeation was terminated, the permeate gas stream was analyzed online by GC. The feed gas stream was also analyzed by GC before and after gas permeation experiment to be sure that the feed side gas composition remained constant during permeation. Permeate and feed gas stream compositions were used to calculate the selectivity of a membrane.

After the permeation of any gas mixture through a membrane, both feed and permeate sides of the membrane were evacuated to  $1.32 \times 10^{-5}$  bar and kept in vacuum for 2 h in order to return the membrane material to its original state. The permeability of a gas mixture through a membrane was measured at least twice for reproducibility.

### 3.4.3.3 Analysis with GC

Various steps involved during analyzing the permeate and feed gas concentrations by GC (Figure 3.6). Starting with a completely degassed sample loop of GC, the GC outlet valve, V2, was closed and the GC inlet valve, V1, opened for 3 s to introduce a sample of the permeate or feed gas mixture into the sample loop.

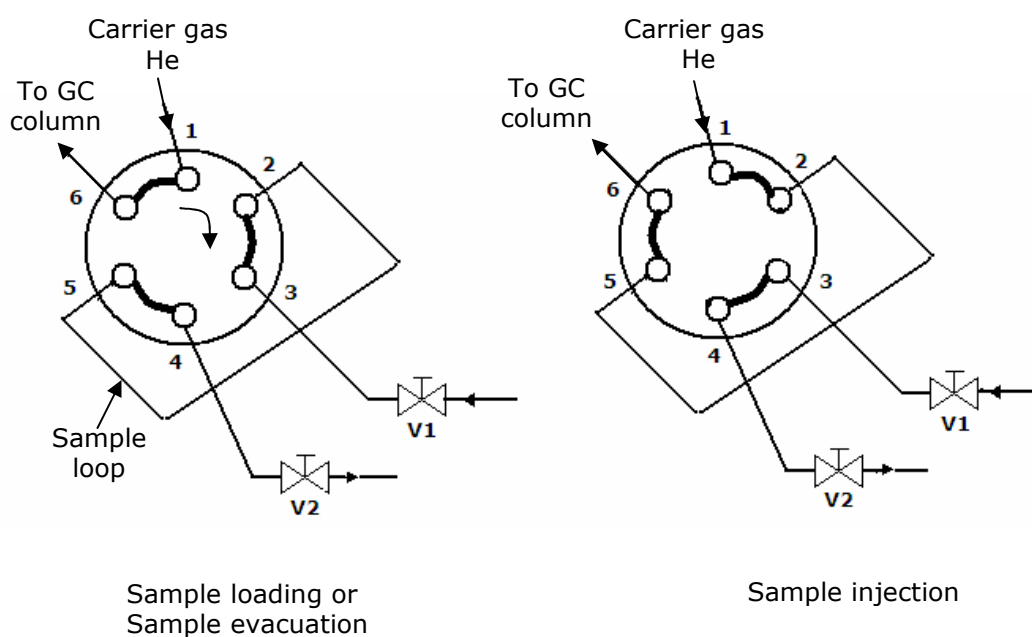


Figure 3.6 Procedure for injecting gas samples into the GC using the six-port injection valve.

Valve V1 was then closed and the sample was automatically injected into the GC column. When the injection sequence of the six-port valve was completed, V2 was opened to degas the sample loop. Thus, the cyclic procedure was reinitialized for another sampling, with the whole procedure repeated at least two times to confirm permeate and feed gas concentrations.

For the quantitative analysis of feed and permeate gas mixtures, GC was calibrated with the CO<sub>2</sub>, CH<sub>4</sub>, H<sub>2</sub> and N<sub>2</sub> gases, separately. For each gas, a calibration curve was constructed by relating the chromatographic peak area to the measured amount of a gas, under fixed operating conditions of GC. The same operating conditions (Table 3.1) were then maintained during the binary gas permeation experiment, and the amount of each gas in the binary gas mixtures was determined from the chromatogram since for each single gas area corresponding to a known amount was previously determined. The calibration curves for GC were given in Appendix D.

Table 3.1 Operating conditions of gas chromatograph.

Column	Chromosorp 102, 80-100 mesh
Column temperature	80 °C
Valve temperature	80 °C
Detector	TCD
Detector temperature	100 °C
Sample flow rate	50 ml/min
Reference gas and flow rate	He, 30 ml/min
Column pressure	50 psi

#### 3.4.3.4 Permeability and Selectivity Calculations

The permeability of a binary gas mixture through a membrane was calculated similar to the single gas permeability calculations given in Section 3.4.2. On

the other hand, the permeability of each component in the binary gas mixture was calculated based on the feed and permeate gas stream concentrations as follows,

$$P_i = \frac{v \cdot y_i \cdot \delta}{(p_{feed} \cdot x_i - p_{permeate} \cdot y_i) \cdot A} \quad (3.6)$$

where,

$P_i$  = permeability of component i in the binary gas mixture (Barrer),

$x_i, y_i$  = mol fraction of component i in the feed and permeate sides, respectively,

$p_{feed}, p_{permeate}$  = pressures of feed and permeate sides, respectively (cmHg).

The separation selectivity was defined as the ratio of mol fractions of components in the permeate and feed side. It can be expressed as,

$$\alpha_{ij} = \frac{(y_i / y_j)_{permeate}}{(x_i / x_j)_{feed}} \quad (3.7)$$

The calculation of the permeability of each component in the binary gas mixture and the separation selectivity is shown in more detail in Appendix E.

## CHAPTER 4

### MEMBRANE PREPARATION AND CHARACTERIZATION

#### 4.1 Selection of Membrane Preparation Materials

Polymer/zeolite mixed matrix membranes and polymer/additive blend membranes have potential for efficient separation of gas mixtures. In this study, the incorporation of zeolites, blending with multifunctional low molecular-weight additives and their combination were investigated as alternatives for modifying the permeability and selectivity properties of a polymeric membrane.

A glassy polymer with high glass transition temperature poly(bisphenol-A)carbonate, PC, was used as the polymer matrix. PC is an attractive commercially available polymer to prepare gas separation membranes since it allows fast gas permeation rates with reasonable selectivities [17, 25, 37-42, 91-93]. The permeability and selectivity values of PC near the upper bound line on the middle region of Robeson's plot, which is usually applied to evaluate the performance of polymeric membranes. For example, it shows H<sub>2</sub> and CO<sub>2</sub> permeabilities of 12.0 and 7.5 Barrer, respectively, with H<sub>2</sub>/CH<sub>4</sub> and CO<sub>2</sub>/CH<sub>4</sub> selectivities of 37.5 and 23.4. PC was also used to prepare MMMs with polypyrrole as filler and to prepare blend membranes with different low molecular-weight additives [17, 20, 25]. It was found that PC could be an appropriate polymer to prepare both MMMs and blend membranes. In addition to these, the effect of membrane preparation parameters, such as polymer concentration, type of solvent, conditions of solvent evaporation and

annealing, on the gas separation performance of pure PC membranes was investigated in detail [42]. Due to these reasons, PC was selected as the matrix polymer in this study.

Hacarlıoğlu et al. [42] studied the effect of type of solvent and the conditions of solvent evaporation and annealing on the gas separation performance of dense homogenous PC membranes. They found that the solvent dichloromethane, DCM, can be easily removed from the PC matrix, and the PC membranes prepared with DCM exhibit good separation performances. Therefore, DCM was used as the solvent.

Şen et al. [20] used PC to prepare blend membranes with different low molecular-weight additives. The following criteria were taken into account in the selection of additives: have multifunctional groups capable of interacting both with polymer and zeolite, be soluble in DCM which is used to make polymer solution, have high melting point to produce stable membrane structures, and have low molecular-weight to interact simultaneously with polymer and zeolite. According to these criteria, catechol, *p*-nitroaniline (pNA), 4-amino 3-nitro phenol (ANP) and 2-hydroxy 5-methyl aniline (HMA) were selected as additives. Their concentrations in the membrane were changed between 1 % and 10 % (w/w). The blend membranes showed lower permeabilities for H<sub>2</sub>, O<sub>2</sub>, CO<sub>2</sub>, N<sub>2</sub> but higher selectivities than pure PC membranes since the additives antiplasticized the membranes. Among them, pNA, was the most effective antiplasticizing additive, which provided the highest selectivity. Therefore, pNA was used as additive in the preparation of zeolite filled PC based MMMs.

Zeolite 4A was used as the filler in the preparation of MMMs. It is the most frequently used commercially available zeolite in the preparation of mixed matrix gas separation membranes [18, 21, 27]. It can be synthesized easily with a narrow particle size distribution, since its synthesis is widely studied and therefore well-known [82, 94]. The pore size of zeolite 4A is comparable with the kinetic diameter of industrially important gases, and the test gases used in this study. In addition, the three-dimensional pore structure of zeolite 4A is ideally suited to the MMMs, since it is unnecessary to orient the pores to

achieve enhanced transport properties [56]. Because of these reasons, zeolite 4A was selected as a filler in this study.

#### **4.2 Development of Membrane Preparation Methodology**

The solvent-evaporation method was used to prepare PC based dense homogenous membranes and zeolite 4A filled MMMs. Basic steps of the membrane preparation procedure are, i) preparation of casting solution, ii) casting the film and evaporating the solvent, iii) annealing the membrane. The major difficulties in the preparation of MMMs are incompatibility between zeolite and the polymeric material, and the non-homogenous dispersion of zeolite crystals in the polymer matrix. Therefore, in order to solve these difficulties, solvent-evaporation method was modified and adopted to our polymer-zeolite system in the following main steps:

##### *1. Preparation of zeolite 4A crystals*

Commercial zeolite 4A crystals when used as received in the preparation of membranes led to formation of large agglomerates in the PC membrane matrix. These agglomerates prevented the homogenous dispersion of zeolite crystals in the membrane matrix and increased the incompatibility between zeolite and the polymer matrix. The SEM images of these MMMs showed large voids around the zeolite agglomerates which is undesirable in gas separation applications since such a structure may cause lower selectivities relative to the pure polymeric membrane. These agglomerates also led to formation of pinholes in films that prevents their function as permselective membranes and meaningful permeability measurements cannot be carried out. Therefore, in order to eliminate the agglomerate formation in MMMs and to obtain permselective self-supporting membranes, home-made zeolite 4A crystals were used as filler in the preparation of membranes. It was supposed that synthesizing zeolite 4A crystals in laboratory under strict control of preparation conditions can produce crystals with more uniform particle size distribution and the membranes prepared from these zeolite 4A crystals may not contain large agglomerates.



## *2. Preparation of casting mixture*

The membranes were prepared from casting solutions with a PC concentration of 12 % (w/v). In our previous study, casting solutions with a PC concentration of 7 % (w/v) was used when PC/LMWA blend membranes were prepared by drop casting method [20]. It was observed that blade casting method was not a suitable method for the PC concentrations of lower than 12 % (w/v) due to the less viscous behavior of the casting solution. At lower PC concentrations, the solution spread over the glass plate so rapidly that there was no time to apply blade casting to the casting solution. Therefore, the concentration of PC in DCM was increased to 12 % (w/v) so as to increase the viscosity of casting solution that makes blade casting easier and more efficient in the casting of zeolite filled MMMs.

After initial dispersion of synthesized zeolite 4A crystals in DCM by ultrasonic mixing, adding the entire polymer to the mixture made the resulting mixture very viscous and difficult to mix with the ultrasonic bath. Therefore, approximately 15 wt% of total amount of PC was first added into the zeolite 4A-DCM mixture. Mixing the zeolite suspension with a small amount of polymer was likely to increase the compatibility between zeolite and polymer, and minimize the aggregation of zeolite particles.

## *3. Casting the film*

Membranes were cast by blade-casting method at a speed of 5 cm/s. In this method, since a shear is applied on the casting solution by a blade zeolite particles can be dispersed uniformly through the film without settling and more uniform MMM structures can be obtained.

## *4. Solvent evaporation and annealing*

Solvent evaporation and membrane annealing steps were carried out for long duration times at temperatures below the  $T_g$  of PC in order to remove any residual solvent in the membrane matrix and to produce stable membrane structures.

## 4.3 Thermal Characterization of Membranes

### 4.3.1 TGA Experiments

A solvent residue in the resulting membrane matrix is not desired since it may interact with the membrane matrix and affect the gas separation performance of the membranes [42, 95-97]. Low levels of residual solvents can reduce the mobility of polymer chains, which is known as antiplasticization effect of solvents on polymer matrices [56, 97]. The antiplasticization effect of residual solvent on the membrane matrix typically results in lower permeabilities and higher selectivities than the membranes without residual solvents. On the other hand, in the presence of higher solvent concentrations, the membrane may plasticize as the polymer chains loosen, allowing faster permeation and lower selectivities [28, 97]. Therefore, in order to investigate whether or not any solvent remained in the membrane after evaporation and annealing periods of the membranes, TGA measurements were performed for several membranes.

Thermograms of the samples were taken in the temperature range of 30-200 °C in N<sub>2</sub> atmosphere at a heating rate of 5 °C/min. Thermograms of four different type of PC based membranes, namely, pure PC, PC/pNA (2%), PC/zeolite 4A (20%) and PC/pNA (2%)/zeolite 4A (20%), were compared in Figure 4.1.

No weight loss was observed in pure PC and PC/pNA (2%) membranes in the examined temperature range. In PC/zeolite 4A (20%) and PC/pNA (2%)/zeolite 4A (20%) MMMs, the samples lost 3.4% and 4.2% of their weight approximately between 80-180 °C. The solvent used in this study was dichloromethane and it has a boiling point of 40 °C. Therefore, there was no solvent loss in the MMM samples in the examined temperature range. This implies that our samples can be considered as solvent free. Since most of the weight loss occurred in between 80-180 °C, water may be trapped in the membrane matrix during the membrane preparation period and water vapor may be evolved during TGA measurements. It is also probable that after 160 °C, the additive pNA may leave the membrane matrix, since its melting

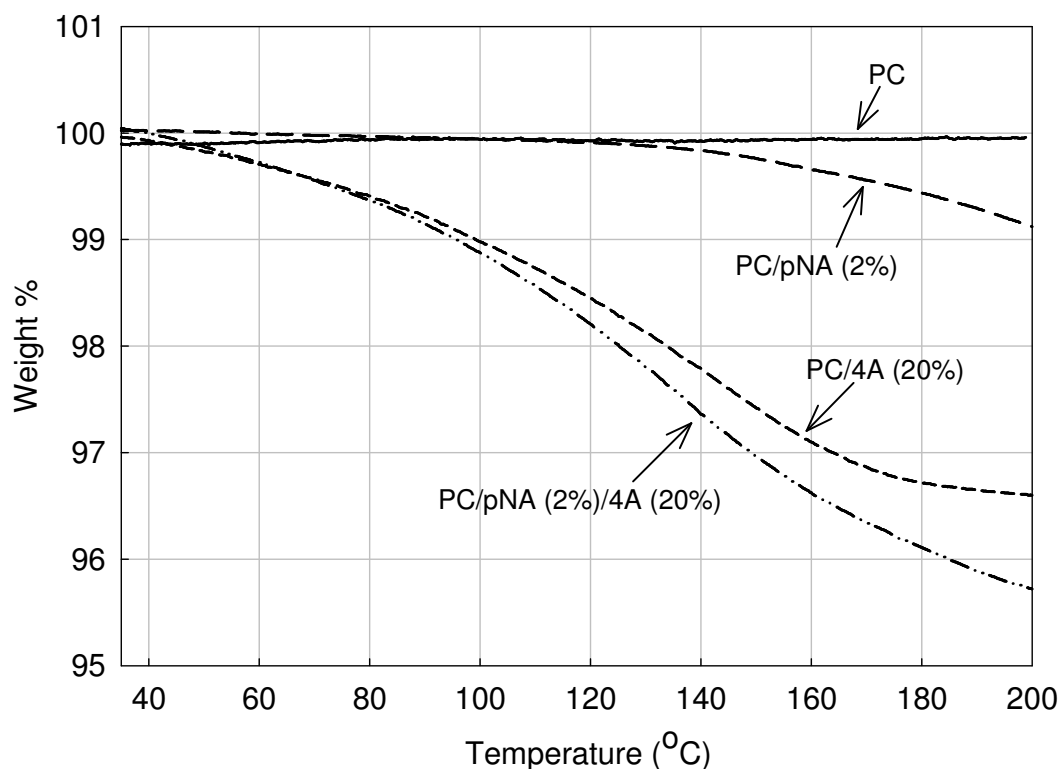


Figure 4.1 Comparison of TGA graphs of pure PC, PC/pNA (2%), PC/4A (20%) and PC/pNA (2%)/4A (20%) membranes.

point,  $\sim 150^{\circ}\text{C}$ , would have been exceeded during TGA measurements, and the membranes may start to decompose after that temperature. These situations could not be a problem during gas permeation measurements through membranes, since the measurements were performed at room temperature which was well below the melting temperature of pNA. The TGA thermograms of the other membranes are given in Appendix F.

#### 4.3.2 DSC Experiments

One of the most important properties of a polymeric material is its glass transition temperature. The glass transition temperature ( $T_g$ ) provides an indirect measurement of the degree of flexibility and/or rigidity of polymeric

materials at room temperature; the lower the  $T_g$ , the more flexible the material and the higher the  $T_g$  the more rigid the material [28]. Therefore,  $T_g$  measurement was very useful to compare the polymer chain rigidity of pure polymeric membranes with those of blend membranes at different additive types and amounts, and with mixed matrix membranes at different zeolite types and loadings. It can also be used to analyze the strength of interaction between phases in the membrane matrix [30, 75, 98].

In this study, pure PC, PC/pNA dense homogenous membranes and PC/zeolite 4A, PC/pNA/zeolite 4A MMMs were prepared, and the glass transition temperatures of them were determined from the second scan DSC thermograms of the membranes. In the membranes, the concentrations of zeolite 4A and pNA were changed between 5 % and 30 % (w/w), and 1 % and 5 % (w/w), respectively. For a particular membrane formulation, two membranes cast from two different casting solutions were analyzed by DSC. Therefore, reproducibility in the preparation and analyzing of membranes with complex heterogenous structures could be determined.

Table 4.1 lists the reproducibility results of  $T_g$ 's of different type of membranes. For all type of membranes, whether homogenous or mixed matrix membrane, the relative standard deviation between  $T_g$  measurements changed between 0.7-1.4 %, which is in the sensitivity range of DSC,  $\pm 1-2$  °C, used in the experiments. These results are similar to the standard deviations reported in DSC analysis of the membranes [30, 31] and confirm that the membrane preparation and analyzing methods are reproducible. Table 4.1 also lists the average  $T_g$  values of the membranes. All interpretations and the discussions in the text were made based on the average  $T_g$  values of the membranes.

Typical second scan DSC thermograms of pure PC, PC/pNA membranes, and PC/zeolite 4A and PC/pNA/zeolite 4A MMMs are depicted in Figure 4.2. For all type of membranes, in the studied concentration ranges, a distinctive single  $T_g$  was observed, indicating the existence of a single homogenous polymer phase in the membranes [3, 20, 69, 99]. The second scan DSC thermograms of some of the membranes were given in Appendix G.

Table 4.1 Reproducibility results in  $T_g$  measurements of different type of PC based membranes.

Membrane type	PC/pNA (x%)/4A (y%)		Membrane #1 <sup>a</sup>		Membrane #2 <sup>a</sup>		Average $T_{g,avg.}$ (°C)
	x	y	$T_{g1}$ (°C) <sup>b</sup>	$T_{g2}$ (°C) <sup>b</sup>	$T_{g1}$ (°C) <sup>b</sup>	$T_{g2}$ (°C) <sup>b</sup>	
pure PC	-	-	146	145	146	145	146
PC/pNA	1	-	138	138	138	138	138
	2	-	128	-	128	-	128
	5	-	116	-	116	-	116
PC/4A	-	10	146	-	146	-	146
	-	20	145	-	145	-	145
	-	30	146	-	146	-	146
PC/pNA/4A	1	5	138	136	138	136	137
		10	141	139	141	139	140
		20	137	137	137	137	137
	2	30	139	141	139	141	140
		5	133	132	133	132	133
		10	133	134	133	134	134
	5	20	135	134	135	134	135
		30	135	137	135	137	136
		1	120	119	120	119	120
	5	5	121	125	121	125	123
		10	123	122	123	122	123
		20	127	126	127	126	127
	30	123	124	123	124	124	

<sup>a</sup> Membrane #1 and Membrane #2 indicate the membranes with same formulation and cast from different casting solutions.

<sup>b</sup>  $T_{g1}$  and  $T_{g2}$  are the glass transition temperatures calculated from second scan thermograms.

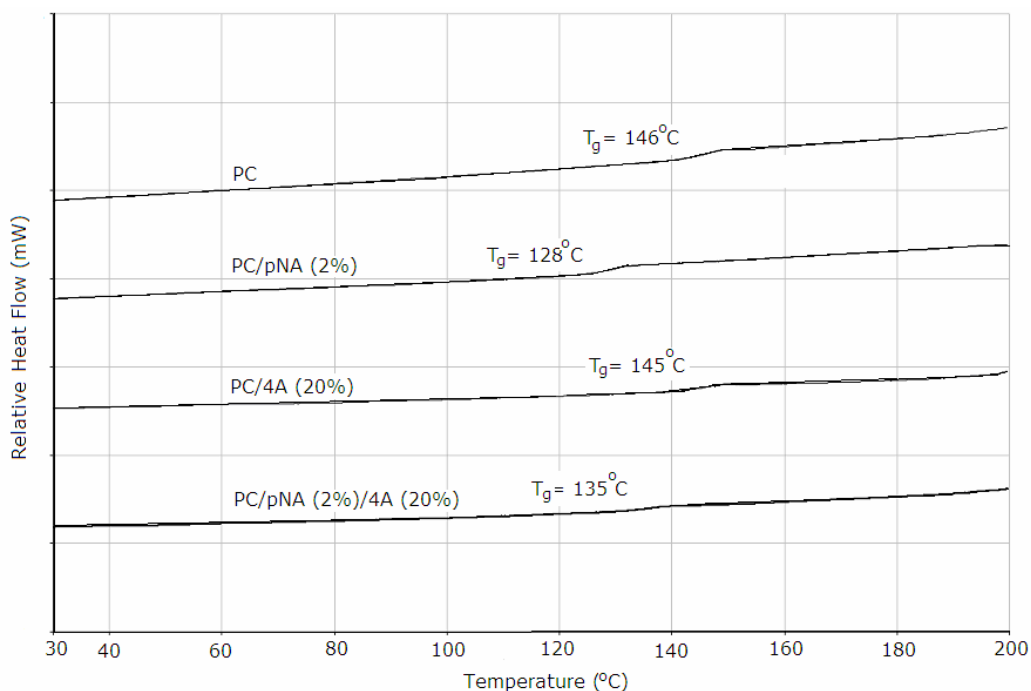


Figure 4.2 DSC graphs of different type of PC based membranes.

Figure 4.3a and b show the effects of pNA and zeolite 4A contents on the  $T_g$  of membranes, respectively. The  $T_g$  of PC/pNA membranes decreased as the pNA concentration of the membranes increased, and they were related to the pNA content by Gordon-Taylor model equation [8, 19, 20]. Gordon-Taylor equation is a model relating the  $T_g$  of a blend to the weight fractions and  $T_g$ s of pure components when antiplasticization occurs [19, 20, 36]. As it fits well with the measured  $T_g$ s of PC/pNA membranes, we may speculate that an antiplasticization type interaction occurs between pNA and PC.

The Gordon-Taylor equation was applied to our PC/pNA system to determine the adjustable parameter  $K$  in the equation. For this purpose, the  $T_g$ s of PC/pNA blend membranes at different pNA contents and the  $T_g$ s of additive pNA, which was measured as  $-72^\circ\text{C}$  [20], were used. The value of  $K$  for PC/pNA membranes was found as 0.28 by nonlinear regression analysis (Appendix H), which is similar to the  $K$  values reported for polysulfone (PSF)/naphthalene membranes, where PSF matrix was antiplasticized by

naphthalene [19]. Therefore, it can be concluded that the effect of pNA on  $T_g$  of PC membrane is similar to the effect of antiplasticizers on glassy polymers. That means, pNA acted as an antiplasticizer in the PC membrane matrix. It is also important to note that, the  $T_g$  was altered using pNA at very low concentrations, such as 1-5 % in the membranes, unlike many blend membranes reported in literature, in which similar effects were observed with additive concentrations of greater than 10 % (w/w) [19, 35, 36].

No change on the  $T_g$  was seen with increasing zeolite content of the membranes in the absence of pNA (Figure 4.3), suggesting that there is no significant interaction between PC chains and zeolite 4A particles. A similar conclusion was also reached previously for zeolite 4A filled polyethersulfone (PES) MMMs [75]. On the other hand, Moore and Koros [30] reported an increase in  $T_g$  of polyimide (PI) membranes with the addition of zeolite 4A particles. This observation was explained as the restricted segmental motion of the polymer chain because of PI-zeolite 4A interactions. Apparently, one of the factors that influence in the interaction between the polymer matrix and the zeolite is the type of polymer matrix.

The PC/pNA/zeolite 4A membranes had lower glass transition temperatures with respect to PC/zeolite 4A membranes but higher glass transition temperatures with respect to PC/pNA blend membranes. The increment in the  $T_g$  of PC/pNA blends with the incorporation of zeolite 4A particles is likely to be resulted from the polymer chain rigidification, which was often attributed to an interaction between the filler material like zeolites and the polymer matrix [24 30, 61, 100, 101] .

Therefore, higher  $T_g$  of PC/pNA/zeolite 4A membranes with reference to PC/pNA membranes indicates an interaction between the PC chains and the zeolite particles in the presence of pNA [102]. The pNA acts as a facilitator to provide the interaction and is essential in order zeolite to affect the PC matrix. The extent of shift from the  $T_g$  of PC/pNA blends can also be related to the degree of interaction between the polymer chain and zeolite 4A particles, so that the higher the shift in  $T_g$  is, the stronger the interaction between phases.

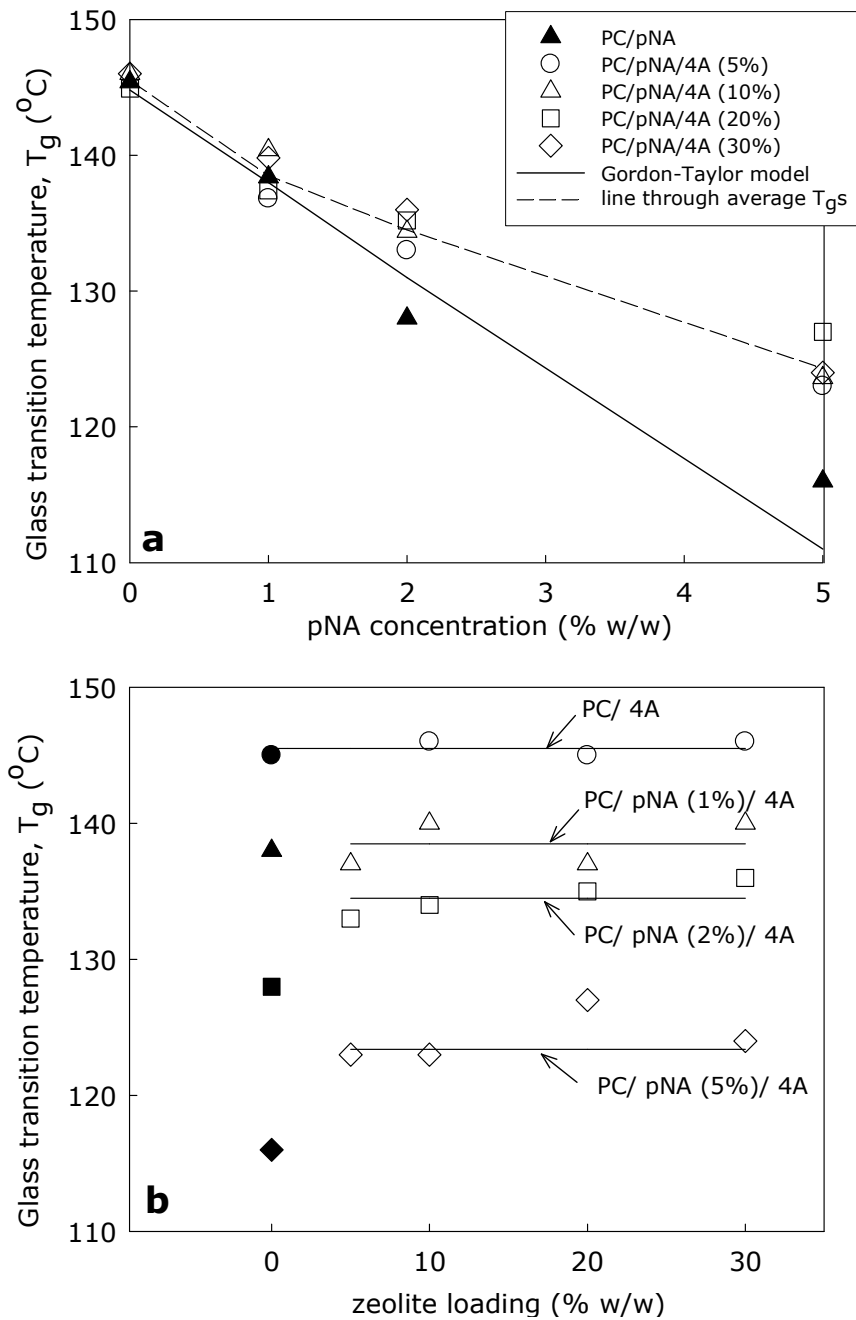


Figure 4.3 Effect of pNA concentration (Panel a) and zeolite 4A loading (Panel b) on the glass transition temperature of PC based membranes. The filled symbols represent PC/pNA blend membranes with increasing concentration of pNA.



On the other hand, after a certain amount of zeolite incorporation glass transition temperature of PC/pNA/zeolite 4A membranes did not increase with further increases of zeolite amount, demonstrating that due to heterogenous nature of mixed matrix membrane morphology, only a limited amount of zeolite particles may act as chain rigidification agents [101].

#### **4.4 Morphological Characterization of Membranes**

The SEM images of the cross-sections of pure PC membrane and PC/pNA blend membranes with respect to increasing pNA concentration are shown in Figure 4.4. The membranes have dense and homogenous structures, and no pores were observed at these magnifications. Additive pNA formed homogenous compatible blends with PC polymer matrix at all pNA concentrations investigated. Membrane thicknesses increased with pNA content, and they were in the range of 30-65  $\mu\text{m}$ .

In contrast to the pure PC and PC/pNA membranes, the PC/zeolite 4A MMMs have heterogenous structures, where the cubic particles are zeolite 4A crystals, and the continuous phase is PC (Figure 4.5). Zeolite 4A particles homogeneously distributed in the PC membrane matrix without forming large agglomerates except the membrane with zeolite 4A loading of 5 % (w/w). At this loading, zeolite particles could not be distributed uniformly (Figure 4.5a). Therefore, this percentage was taken as the lower limit in PC/zeolite 4A MMM preparation. On the other hand, at zeolite 4A loadings of higher than 30 % (w/w), workable membranes could not be prepared due to the lack of mechanical stability of the membranes. Therefore, the maximum zeolite 4A loading in PC/zeolite 4A MMMs was taken as 30 % (w/w). Membrane thicknesses increased with zeolite 4A loading, and they were in the range of 30-90  $\mu\text{m}$ .

The cross-sectional SEM images of the PC/zeolite 4A MMMs were illustrated in Figure 4.6 at higher magnification ( $\times 3500$  and  $\times 10,000$ ). As can be seen from the figures, the dark area between the zeolite 4A crystals and PC matrix is considered as an empty space (interfacial void). The voids appeared around

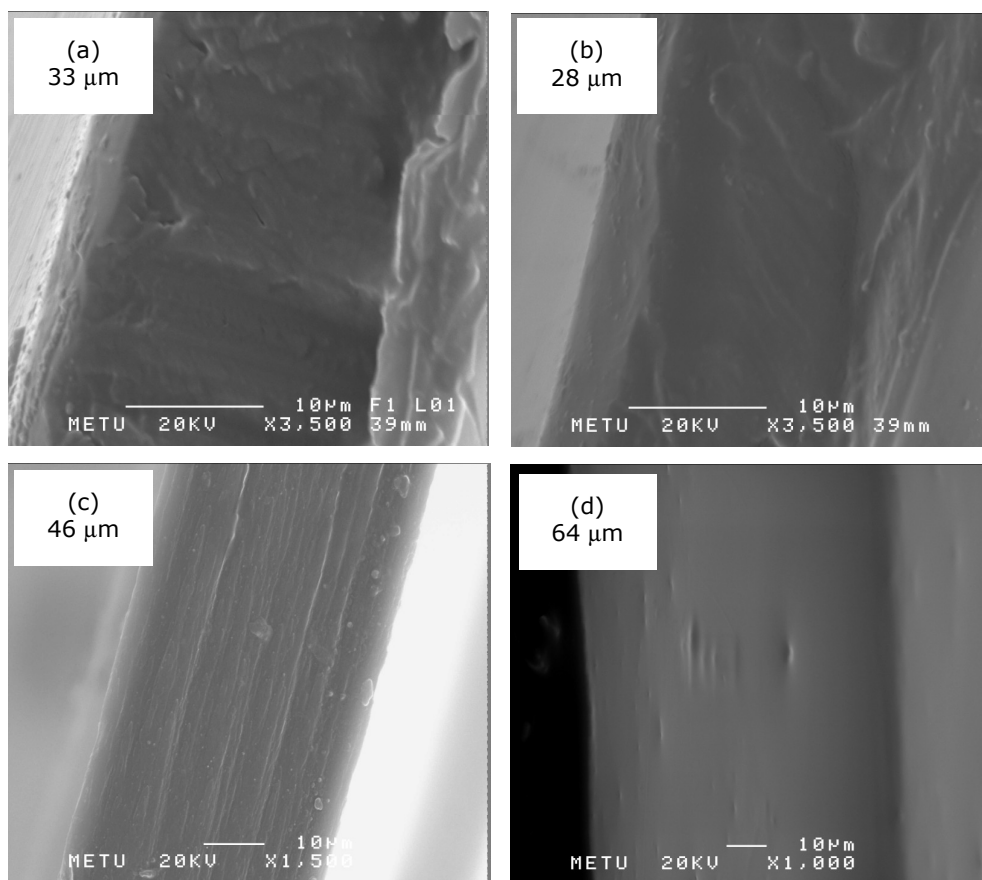


Figure 4.4 Cross-sectional SEM images of (a) pure PC, (b) PC/pNA (1%), (c) PC/pNA (2%) and (c) PC/pNA (5%) membranes. (PC/DCM= 12% w/v).

zeolite 4A crystals were probably formed because of low adhesion between the glassy polymer matrix and zeolite crystals [18, 21, 27-32]. This is undesirable since such a structure may cause lower selectivities relative to pure polymeric membranes [18, 21]. As the zeolite content increases, the void spaces that are formed around the zeolite crystals may combine to give a channel network, this may increase the permeabilities and decrease the selectivities [21]. On the other hand, the increase of the free volume at the zeolitic locations with the increase in the zeolite content may cause an increase in the packing density of the polymer at the polymer-zeolite

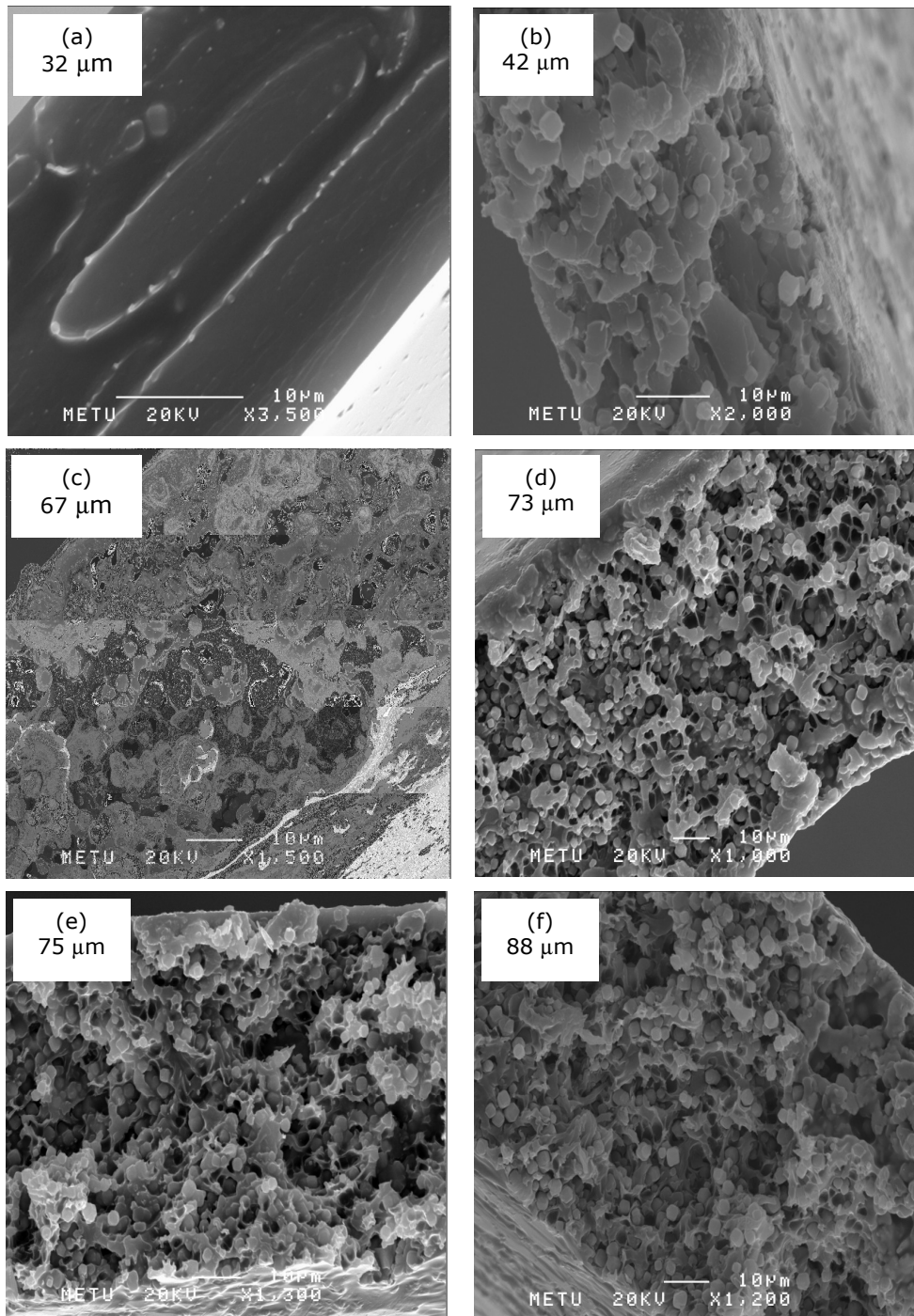


Figure 4.5 Cross-sectional SEM images of PC/zeolite 4A MMMs with respect to increasing zeolite 4A loading (a) 5 % (w/w), (b) 10 % (w/w), (c) 20 % (w/w), (d) 30 % (w/w), (e) 35 % (w/w) and (f) 40 % (w/w). (PC/DCM= 12 % w/v).

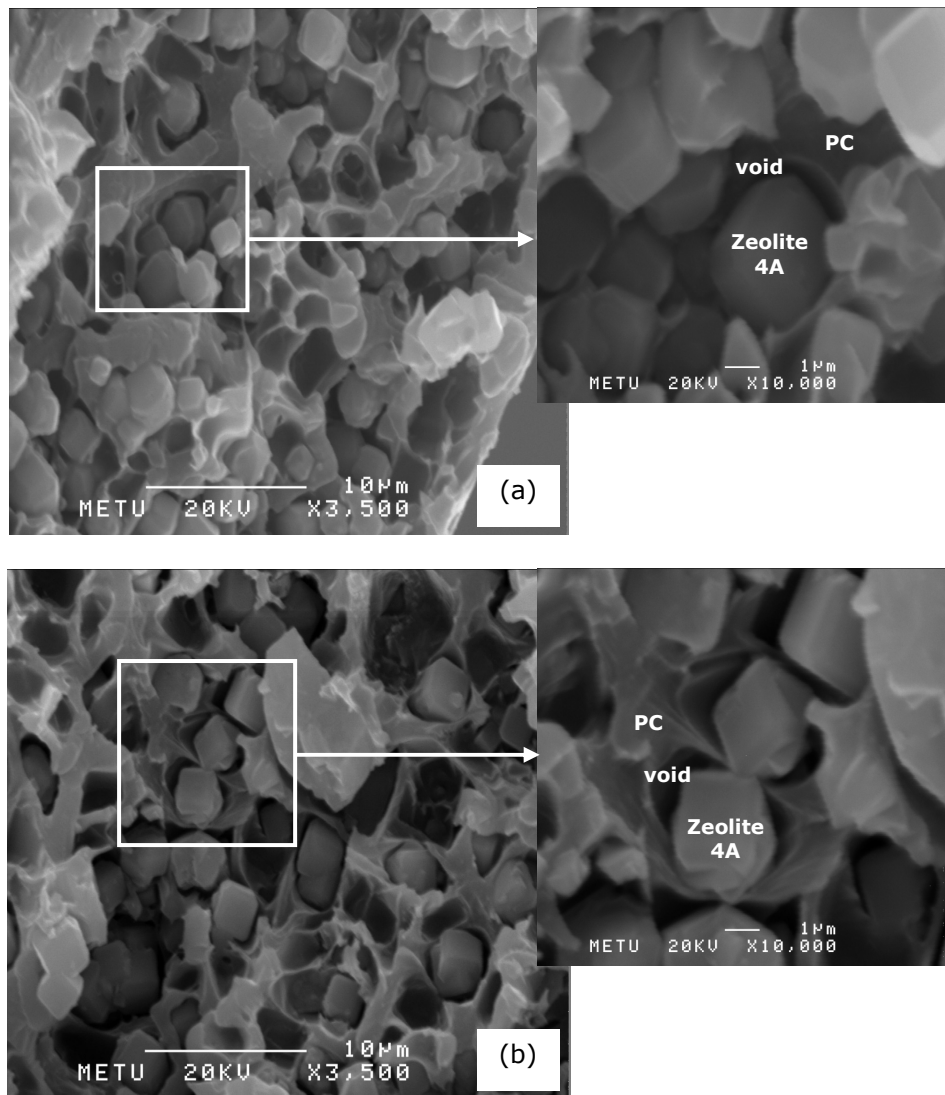


Figure 4.6 Cross-sectional SEM images of PC/zeolite 4A MMMs at higher magnifications x3500 (a) PC/zeolite 4A (20%) MMM and (b) PC/zeolite 4A (30%) MMM.

interface, called “polymer chain rigidification”, and this may restrict the diffusion of gases and lower the permeabilities [30, 31]. Therefore, the final morphology of the zeolite filled mixed matrix membranes has an important effect on the separation performance of MMMs. Figure 4.7 shows the cross-sectional SEM images of PC/pNA/zeolite 4A MMMs at a constant zeolite 4A

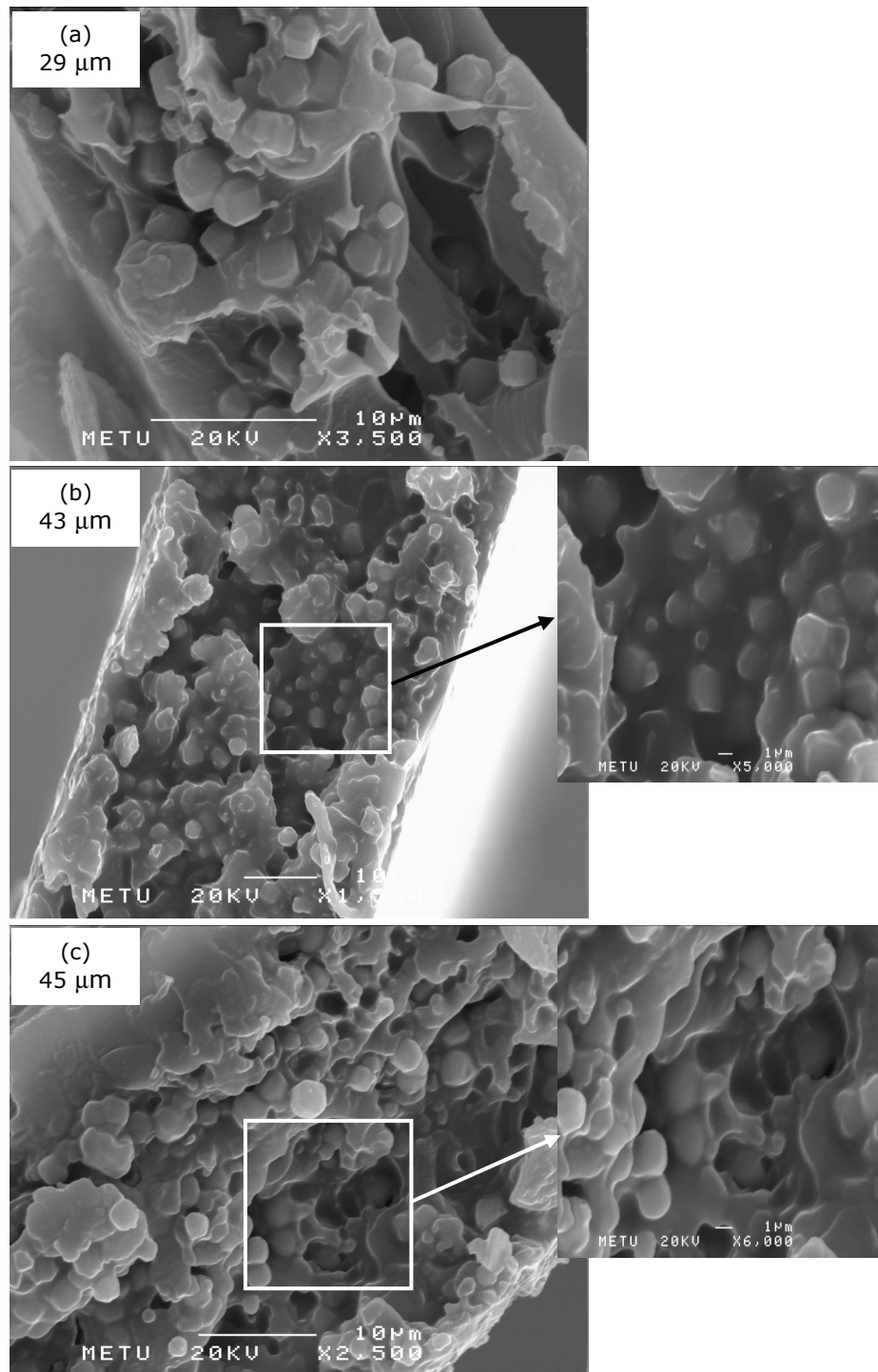


Figure 4.7 Cross-sectional SEM images of PC/pNA (x%)/zeolite 4A (20%) MMMs (a) x= 1%, (b) x= 2% and (c) x= 5%.

loading of 20 % (w/w) with respect to increasing pNA concentration. Zeolite 4A particles were distributed uniformly throughout the membrane matrix as in the case of pNA free PC/zeolite 4A MMMs. However, a somewhat different morphology compared to PC/zeolite 4A MMMs was observed when the pNA was introduced to the PC/zeolite 4A matrix. Although the interfacial voids could not be eliminated completely, the PC/zeolite 4A structure was slightly intensified and fewer voids remained with the addition of pNA. Therefore, LMWAs like pNA can enhance the compatibility between zeolite 4A particles and PC chains, and this can be achieved with the incorporation of very small amount of LMWAs into PC matrix.

## CHAPTER 5

### SINGLE GAS PERMEATION STUDIES

#### 5.1 Single Gas Permeability Measurements

The PC based membranes prepared at different pNA and zeolite 4A concentrations were tested by measuring the single gas permeabilities of H<sub>2</sub>, O<sub>2</sub>, CO<sub>2</sub>, N<sub>2</sub> and CH<sub>4</sub> in a dead-end system described in Section 3.4.1 at room temperature. The feed side pressure was always kept at 3.7 bar, and the permeate side pressure was initially at atmospheric pressure (~ 0.9 bar). The pressure rise at the permeate side with time was shown in Figure 5.1 for pure PC membrane.

Permeability measurements always began with hydrogen and ended with carbon dioxide as a precaution for the possibility of plasticization of PC membranes by carbon dioxide [103, 104]. The permeate side pressure increased steadily for all gases. For pure PC and PC/zeolite 4A membranes, the pressure reached 0.98 bar in approximately 15 min during the hydrogen permeation, in 45 min during the carbon dioxide permeation, and in 160 min during the oxygen permeation, however, this period was 620 min and 1800 min for methane and nitrogen, respectively. On the other hand, for PC/pNA and PC/pNA/zeolite 4A membranes methane permeation period was longer than the nitrogen permeation period.

Permeabilities were calculated by fitting all pressure-time data on a straight line by linear regression method. The slope of this line was used to find

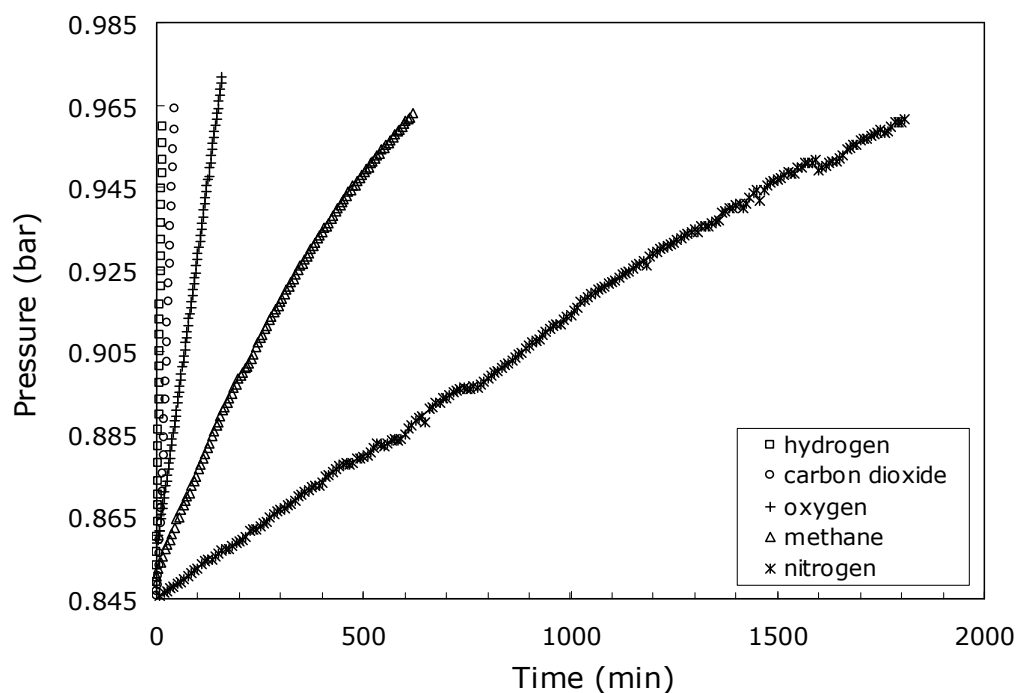


Figure 5.1 Permeate side pressure-time data for pure PC membrane.

membrane's permeability as described in Section 3.4.2 and shown in Appendix B.

## 5.2 Reproducibility in Permeability Measurements and Membrane Preparation

Reproducibility is a substantial issue in the preparation and testing of membranes with complex heterogenous structures, since it shows the robustness of the membrane preparation methodology [17, 20, 21, 31]. Therefore, a series of reproducibility experiments were carried out with the prepared membranes. For a particular membrane formulation, at least two membranes, which were prepared in different times with similar conditions, were tested by gas permeation measurements. For some of the membranes, two membranes from the same film were also tested. The permeability of each gas through a given membrane was measured at least twice. Therefore, both the repeatability of permeability measurements and the reproducibility of



membrane preparation were examined. The reproducibility experiment results of the membranes were tabulated in Appendix I. The averages of all permeability measurements for each gas and membrane were reported in the text.

The relative standard deviation was found as 7.0% for CH<sub>4</sub> and 6.5% for N<sub>2</sub>, which are the slowly permeating gases, 4.6% for O<sub>2</sub>, 3.3% for CO<sub>2</sub> and 2.6% for H<sub>2</sub>, which are the fast permeating gases. These results are similar to the standard deviations reported in the membrane literature [17, 20, 21, 31], and confirm that the membrane preparation and testing methods are reproducible.

The permeabilities through some of the membranes were measured again 1 year after their preparation to investigate the effect of aging. During this period of time, membranes were kept in vacuum at room temperature. Table 5.1 compares the CO<sub>2</sub> and CH<sub>4</sub> single gas permeabilities and CO<sub>2</sub>/CH<sub>4</sub> ideal selectivities of dense homogenous membranes and some of the MMMs.

Table 5.1 The effect of aging on single gas permeabilities and ideal selectivities of the membranes.

Membrane type	P(CO <sub>2</sub> ) (Barrer)		P(CH <sub>4</sub> ) (Barrer)		Selectivity CO <sub>2</sub> /CH <sub>4</sub>	
	fresh*	old*	fresh	old	fresh	old
PC	9.25	9.02	0.374	0.321	24.8	28.1
PC/4A (20%)	7.66	8.51	0.232	0.280	33.0	30.4
PC/4A (30%)	6.86	7.09	0.195	0.200	35.2	35.5
PC/pNA (2%)/4A (20%)	3.97	4.24	0.078	0.091	50.9	46.6
PC/PNA (2%)/4A (30%)	4.38	5.13	0.104	0.125	42.1	41.0

\* fresh: right after preparation, old: 1 year later.

The single gas permeability and ideal selectivity values of the membranes, which were tested right after preparation, were slightly different from the ones that were tested 1 year later. For pure PC membranes, slight decrease in permeabilities and increase in ideal selectivities were observed. On the other hand, for MMMs, an increase in permeabilities (up to 20%) was observed with a slight decrease in selectivities (up to 9%). The changes in performance properties of membranes with aging were not significant in comparison to the performance changes reported in the membrane literature, indicating that the membranes have preserved their structure.

### **5.3 Single Gas Permeability Results of the PC Based Membranes**

#### **5.3.1 PC/pNA Blend Membranes**

Membrane preparation parameters; such as solvent type, polymer composition, the surface on which the membrane is cast (glass, steel, Teflon etc.), the casting techniques (drop casting, blade casting), the casting temperature, evaporation and annealing conditions were stated to be important factors that may affect the membrane morphology and separation performance [42, 95, 105]. These parameters were fixed in the preparation of PC based dense homogenous membranes and zeolite filled mixed matrix membranes throughout this study for comparison purposes.

Şen et al. [20] prepared PC membranes by drop-casting method from solutions with a PC concentration of 7 % (w/v), and showed that it is an appropriate concentration to prepare workable and permselective PC and PC/pNA membranes [17, 20, 25]. In this study, the concentration of PC was increased to 12 % (w/v) to increase the viscosity of the casting solution that makes blade casting easier and more efficient, and to obtain workable membranes. Tables 5.2 and 5.3 show the single gas permeability and ideal selectivity results of pure PC and PC/pNA membranes prepared with that higher polymer concentration.

Table 5.2 Single gas permeabilities of PC/pNA blend membranes at different pNA weight percentages, measured at room temperature, feed side pressure was 3.7 bar.

% weight of pNA	Permeability (Barrer)				
	H <sub>2</sub>	CO <sub>2</sub>	O <sub>2</sub>	N <sub>2</sub>	CH <sub>4</sub>
0	15.3	8.8	1.81	0.267	0.374
1	10.0	4.2	1.31	0.147	0.104
2	9.3	4.0	1.00	0.128	0.077
5	7.2	3.9	0.85	0.079	0.073

Table 5.3 Ideal selectivities of PC/pNA blend membranes at different pNA weight percentages.

% weight of pNA	Ideal Selectivity				
	H <sub>2</sub> /N <sub>2</sub>	O <sub>2</sub> /N <sub>2</sub>	CO <sub>2</sub> /N <sub>2</sub>	H <sub>2</sub> /CH <sub>4</sub>	CO <sub>2</sub> /CH <sub>4</sub>
0	57.2	6.8	33.00	40.9	23.6
1	68.0	8.9	28.40	96.2	40.1
2	72.5	7.9	31.30	120.5	51.9
5	91.1	10.8	49.40	98.6	53.4

The permeabilities of all gases decreased with increasing pNA concentration. The largest decrease was observed in CH<sub>4</sub> and N<sub>2</sub> permeabilities. In contrast, the smallest decrease was observed in H<sub>2</sub> and O<sub>2</sub> permeabilities. As opposed to the permeabilities, ideal selectivities of PC/pNA blend membranes, calculated relative to the slow gases like N<sub>2</sub> and CH<sub>4</sub>, were higher than the selectivities of pure PC membranes. The highest increase was observed for H<sub>2</sub>/CH<sub>4</sub> and CO<sub>2</sub>/CH<sub>4</sub> selectivities. The increase in H<sub>2</sub>/N<sub>2</sub> selectivity follows these pairs and the lowest increase was observed for O<sub>2</sub>/N<sub>2</sub> and CO<sub>2</sub>/N<sub>2</sub> gas pairs. The increase in the selectivities were very fast up to 2 % (w/w) pNA for H<sub>2</sub>/CH<sub>4</sub> and CO<sub>2</sub>/CH<sub>4</sub> selectivities, above that concentration the rate of increase in selectivities was slow for these pairs. In contrast, the selectivity

increase was gradual up to 2 % (w/w) pNA concentration, and sharp at 5 % (w/w) pNA concentration for H<sub>2</sub>/N<sub>2</sub>, O<sub>2</sub>/N<sub>2</sub> and CO<sub>2</sub>/N<sub>2</sub> gas pairs.

These trends of permeabilities and selectivities were very similar to the trends observed with the membranes prepared with a PC concentration of 7 % (w/v), which was reported by Şen et al. [20], and the effect of pNA on PC matrix was explained as antiplasticization. Antiplasticization is defined as decreasing flexibility (or increasing stiffening) of polymers with the addition of a low molecular-weight compound due to reduced rates of segmental motions in the polymer chain and hence reduced the free volume in the polymer [64-70]. This effect has been shown to appear by a decrease in permeabilities of gases and increase in selectivities [35, 36]. The pNA caused the gas permeabilities to decrease, as antiplasticizers do, therefore, it can be concluded that pNA acted as an antiplasticizer in the PC membrane matrix. It is important to note that, this antiplasticization effect of pNA was found to be effective at very small amounts of pNA in the membrane matrix.

### **5.3.2 PC/Zeolite 4A Mixed Matrix Membranes**

Effect of zeolite loading on the performance of PC/zeolite 4A membranes were investigated in detail by preparing membranes with broadly varying zeolite amounts. The single gas permeabilities and ideal selectivities of PC/zeolite 4A MMMs were presented in Tables 5.4 and 5.5. Highest loading at which a self-supporting pinhole free permselective MMM can be produced was 30 % (w/w).

The permeabilities through PC/zeolite 4A MMMs were lower than those through pure PC membrane, except O<sub>2</sub>, which remained nearly the same until the zeolite 4A loading was increased to 30%. The most noticeable decrease was in the permeability of CH<sub>4</sub>, whereas the smallest decrease was observed in the H<sub>2</sub> permeability. Permeabilities also decreased with zeolite loading.

The decreasing trend of permeabilities with the addition of zeolites into glassy polymer matrices has been similarly reported in many studies [21, 26-32]. In

Table 5.4 Permeabilities of PC/zeolite 4A mixed matrix membranes at different zeolite 4A weight percentages, measured at room temperature, feed side pressure was 3.7 bar.

% weight of zeolite 4A	Permeability (Barrer)				
	H <sub>2</sub>	CO <sub>2</sub>	O <sub>2</sub>	N <sub>2</sub>	CH <sub>4</sub>
0	15.3	8.80	1.81	0.267	0.374
5	14.1	8.40	1.77	0.249	0.266
10	13.6	8.20	1.79	0.211	0.250
20	13.4	7.80	1.77	0.202	0.240
30	13.1	7.00	1.55	0.179	0.186

Table 5.5 Ideal selectivities of PC/zeolite 4A mixed matrix membranes at different zeolite 4A weight percentages.

% weight of zeolite 4A	Selectivity				
	H <sub>2</sub> /N <sub>2</sub>	O <sub>2</sub> /N <sub>2</sub>	CO <sub>2</sub> /N <sub>2</sub>	H <sub>2</sub> /CH <sub>4</sub>	CO <sub>2</sub> /CH <sub>4</sub>
0	57.2	6.8	33.0	40.9	23.6
5	56.6	7.1	33.7	53.0	31.6
10	64.5	8.5	38.9	54.4	32.8
20	66.3	8.8	38.6	55.8	32.5
30	73.2	8.7	39.1	70.4	37.6

most of these studies the maximum zeolite loading at which a workable MMM can be produced was 20 % (w/w). In the study of Sürer et al. [21], who prepared zeolite 4A filled polyethersulfone (PES) mixed matrix membranes, the maximum zeolite loading employed in MMMs was 50 % (w/w). This concentration is very high compared to the maximum zeolite 4A concentration examined in this study. They reported that the permeabilities of N<sub>2</sub>, O<sub>2</sub>, H<sub>2</sub> and CO<sub>2</sub> through PES/zeolite 4A MMMs decreased up to a zeolite loading of 33.3 % (w/w), which was similarly observed with PC/zeolite 4A MMMs in this study. They also reported an increase in permeabilities above 33.3 % (w/w)

zeolite 4A loading which was continued up to 50 % (w/w) zeolite 4A loading. They claimed that as the percentage of zeolite in the matrix increases, the interfacial voids around the zeolites may connect and provide alternate path for gas molecules, and this may lead to increases in the permeation rates of gas molecules. Apparently, the matrix polymer type and the amount of zeolite are the most important factors that influence in the gas separation performance of zeolite filled MMMs.

As opposed to the permeabilities, selectivities of PC/zeolite 4A MMMs, calculated relative to the slow gases like  $N_2$  and  $CH_4$ , were higher than the selectivities of pure PC membranes (Table 5.5). The improvement in the selectivities with the addition of zeolites into the glassy polymer membranes had also been previously reported [6, 18, 28]. In these studies, the zeolite loading was usually 20 % or 30 %. Similarly, our membranes showed a significant improvement in the selectivities by adding 30 % (w/w) zeolite 4A into the membrane formulation. Moreover, the selectivities in this study were reasonably raised even at low zeolite loadings such as 5 % and 10 % (w/w).

The decreasing behavior of permeabilities and the increasing behavior of selectivities of PC membranes with the addition of zeolite 4A particles can be explained by different mechanistic speculations; the zeolite particles can act as molecular sieves altering the permeability and selectivity in relation to molecular size of the penetrants, the zeolite particles can disrupt the polymer matrix resulting in microcavities and hence change the permeabilities and selectivities, or they can extend the diffusion pathways of the penetrants through the membrane and reduce the permeability. Therefore, it can be concluded that the zeolites that are of molecular sieving properties decrease the permeabilities and increase the selectivities of PC membrane either because of their intrinsic properties or by modifying the membrane morphology.

Similar conclusions were also reached previously for different glassy polymer-zeolite MMM systems. Huang et al. [32] stated that enhancement in selectivities of polymeric membranes with the incorporation of zeolites might be due to the molecular-sieving effects of zeolite crystals. On the other hand,

Süer et al. [21] claimed that improvement in selectivities might not only be due to the molecular sieving effect of zeolite crystals, but also depend on the complex heterogenous micromorphology of the MMMs, including lack or presence of voids around zeolite crystals in the membrane matrix.

Several other studies have also considered different possible hypotheses for the change in performance properties of polymeric membranes with zeolite addition. One of them is the inhibition of the polymer chain mobility near the polymer-zeolite interface; in other words, the presence of zeolite seems to rigidify polymeric chains, which in turn leads to reduced permeabilities and increased glass transition temperatures [30, 31]. This hypothesis might not be true for our PC/zeolite 4A MMMs, since the glass transition temperature of PC did not change with zeolite 4A addition. The other hypothesis is the partial pore blockage of zeolites by polymer chains [31]. Even though polymer chains can hardly enter into the zeolite pores, they may obstruct a part of pores, hindering gas permeation [31]. The combined effect of polymer chain rigidification and partial pore blockage of zeolites, is also considered [31]. Therefore, depending on the resulting performance of zeolite filled MMMs different possible mechanisms can be considered as reasons for the changes in polymeric membrane performances with the inclusion of zeolite particles.

Permeability and selectivity results clearly showed that successful mixed matrix membranes were obtained with the addition of zeolite 4A into PC membrane matrix. The separation performances of PC/zeolite 4A MMMs were shown in Figures 5.2 to 5.5 with reference to the upper bound lines for  $H_2/CH_4$ ,  $CO_2/CH_4$ ,  $H_2/N_2$  and  $O_2/N_2$ , respectively. The region of improved permeability-selectivity trade-off was defined as the above or to the right of the upper bound lines [12]. General trend observed is in agreement with the literature [30, 52]. Selectivity improvement was especially remarkable for  $H_2/CH_4$  pair. Since the kinetic diameter of  $H_2$  was much smaller than that of  $CH_4$ , its permeability might be influenced to a lesser extent from the incorporation of zeolite particles into the PC matrix. The membrane performance approached the upper bound line with increasing amount of zeolite 4A. Even for  $O_2/N_2$  pair, PC/zeolite 4A MMMs showed the permeation characteristics located over the upper bound line. Although the performance

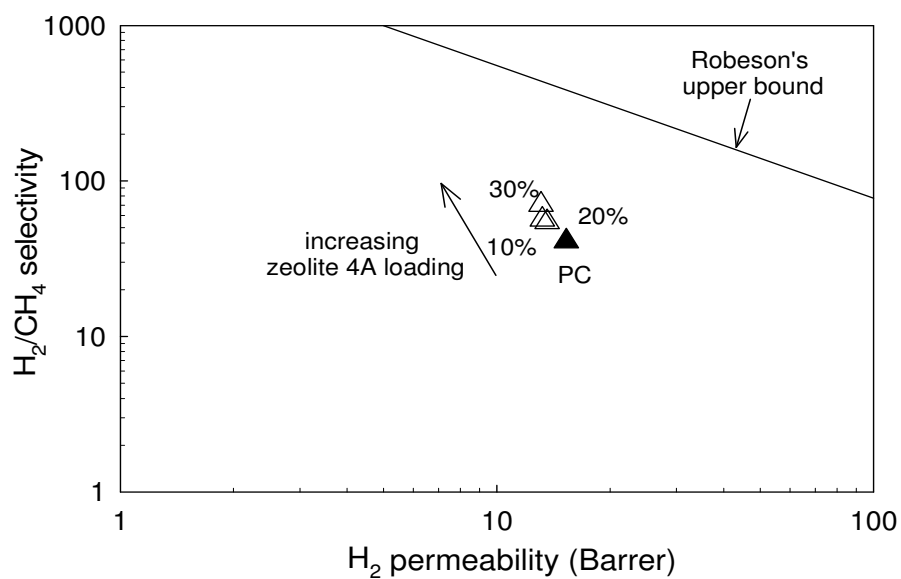


Figure 5.2  $H_2/CH_4$  selectivity and  $H_2$  permeability of PC/zeolite 4A MMMs on a Robeson's upper bound trade-off curve.

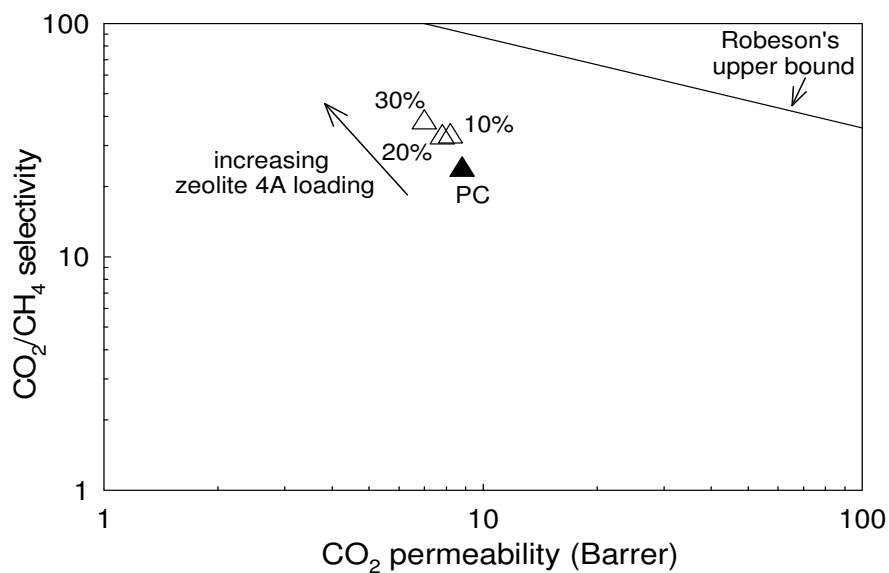


Figure 5.3  $CO_2/CH_4$  selectivity and  $CO_2$  permeability of PC/zeolite 4A MMMs on a Robeson's upper bound trade-off curve.



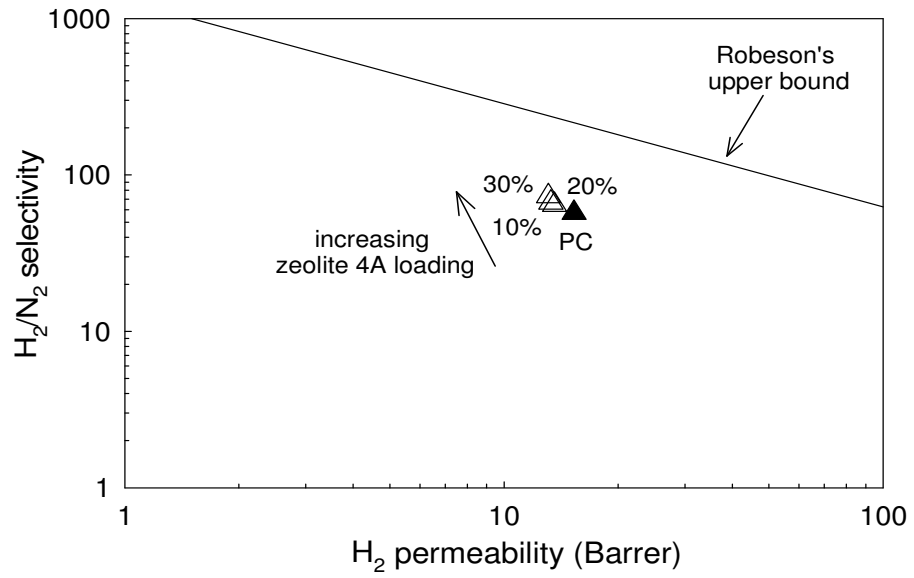


Figure 5.4  $H_2/N_2$  selectivity and  $H_2$  permeability of PC/zeolite 4A MMMs on a Robeson's upper bound trade-off curve.

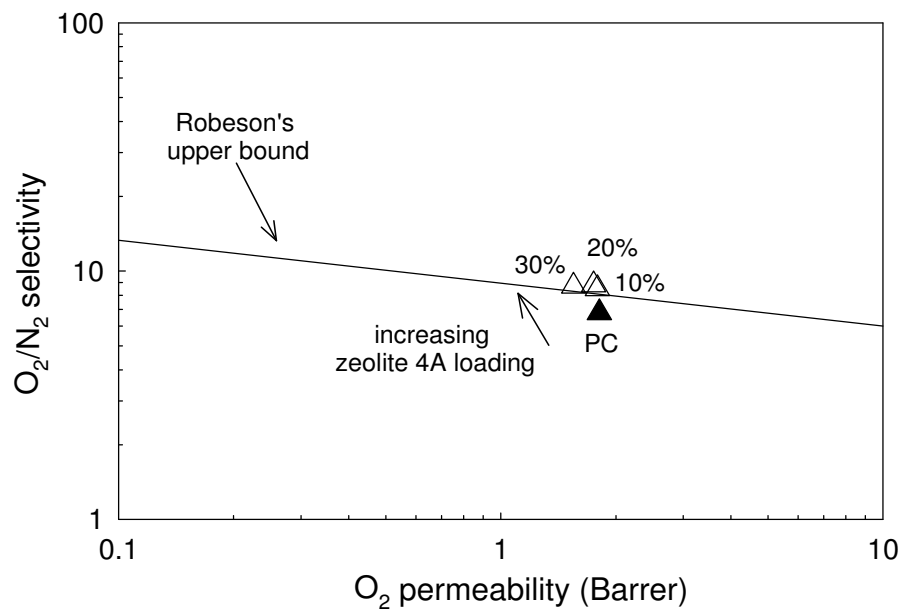


Figure 5.5  $O_2/N_2$  selectivity and  $O_2$  permeability of PC/zeolite 4A MMMs on a Robeson's upper bound trade-off curve.

values for PC/zeolite 4A MMMs were still under the Robeson's upper bound for H<sub>2</sub>/CH<sub>4</sub>, CO<sub>2</sub>/CH<sub>4</sub> and H<sub>2</sub>/N<sub>2</sub> gas pairs, the addition of zeolite 4A produced steeper slopes, therefore, a better trade-off between permeability and selectivity than the pure PC membrane, indicating the potential of mixed matrix membranes. The performance of PC/zeolite 4A membranes can be further developed by blending with a low molecular-weight additive, which has also potential to increase the separation performance of PC membranes.

### **5.3.3 PC/pNA/Zeolite 4A Mixed Matrix Membranes**

The permeabilities of H<sub>2</sub>, CO<sub>2</sub>, O<sub>2</sub>, N<sub>2</sub> and CH<sub>4</sub> gases through PC/pNA/zeolite 4A MMMs were presented in Table 5.6. The permeabilities of all gases through PC/pNA/zeolite 4A MMMs were lower than those through pure PC membrane. As the pNA concentration was increased for a given zeolite content, the extent of decrease in permeabilities increased. Similarly, when the zeolite content was increased at a constant pNA concentration, the extent of decrease in the permeabilities increased. The changes in permeabilities can be correlated with the kinetic diameter of the permeating gas. The largest decrease was in the permeability of CH<sub>4</sub>, and the lowest decreases were in the permeabilities of O<sub>2</sub> and H<sub>2</sub>.

In Figures 5.6 and 5.7, the N<sub>2</sub> and H<sub>2</sub> single gas permeabilities through PC/zeolite 4A and PC/pNA/zeolite 4A MMMs were compared. The permeabilities through PC/zeolite 4A membranes exhibited a continuous decrease with zeolite loading whereas the permeabilities through PC/pNA/zeolite 4A membranes showed a maximum at approximately 5-10 % (w/w) zeolite 4A loadings. Similar trends were also observed for other gases tested. This shows that the existence of pNA as a low molecular-weight antiplasticizer, alters strongly the character of polymer matrix in zeolite filled MMMs.

Table 5.7 shows the selectivities of PC/pNA/zeolite 4A membranes for industrially important gas pairs. The selectivities increased with increasing pNA and zeolite 4A concentrations in the membrane formulation. A significant improvement was achieved in selectivities when the PC/pNA/zeolite 4A MMMs

Table 5.6 Single gas permeabilities of gases through PC/pNA/zeolite 4A MMMs at different pNA and zeolite 4A concentrations, measured at room temperature, feed side pressure 3.7 bar.

PC/x% pNA/y% 4A membrane		Permeability (Barrer) <sup>b</sup>				
x	y	H <sub>2</sub> (0.289 nm) <sup>a</sup>	CO <sub>2</sub> (0.330 nm)	O <sub>2</sub> (0.346 nm)	N <sub>2</sub> (0.364 nm)	CH <sub>4</sub> (0.380 nm)
0	0	15.3	8.80	1.81	0.267	0.374
1	5	11.8	6.03	1.55	0.213	0.144
	10	10.3	4.89	1.33	0.198	0.111
	20	10.8	4.61	1.06	0.141	0.089
2	30	8.7	3.64	0.81	0.139	0.081
	5	10.6	5.17	1.35	0.164	0.129
	10	9.5	4.21	1.11	0.180	0.123
5	20	10.5	3.97	1.09	0.144	0.078
	30	9.0	4.38	0.96	0.130	0.104
	5	9.6	4.14	0.99	0.151	0.121
10	10	8.6	3.82	0.94	0.145	0.116
	20	8.1	4.11	0.92	0.125	0.111
	30	8.2	3.23	0.80	0.115	0.074

<sup>a</sup> Kinetic diameters of the studied gases.

<sup>b</sup> 1 Barrer= 10<sup>-10</sup> cm<sup>3</sup>(STP)cm/cm<sup>2</sup> s cmHg.

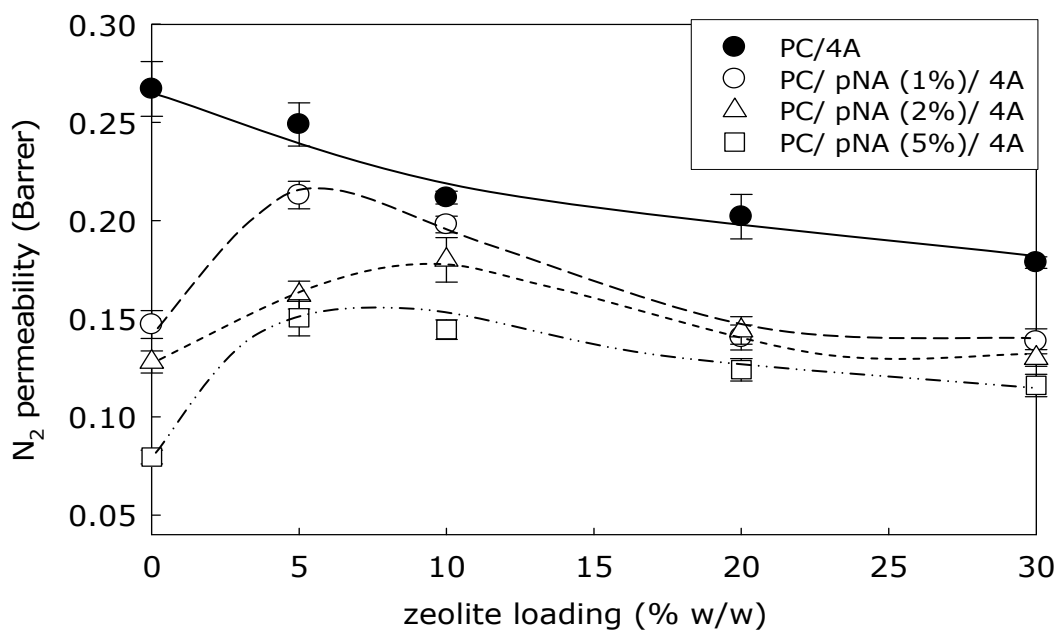


Figure 5.6 Effect of zeolite 4A loading on the N<sub>2</sub> permeability of PC/zeolite 4A and PC/pNA/zeolite 4A MMMs.

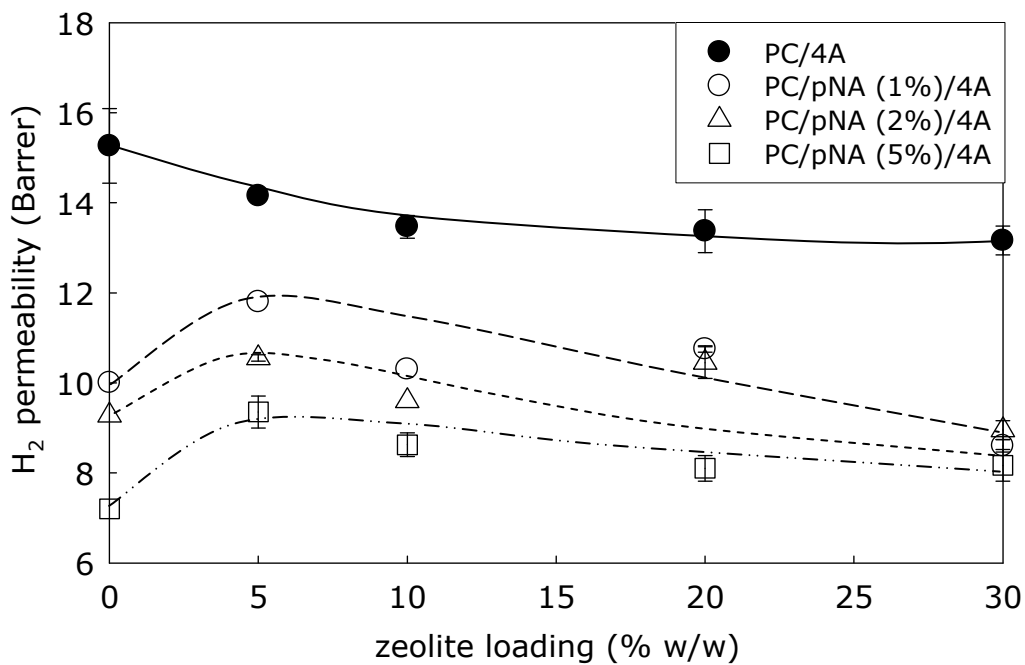


Figure 5.7 Effect of zeolite 4A loading on the H<sub>2</sub> permeability of PC/zeolite 4A and PC/pNA/zeolite 4A MMMs.

Table 5.7 Ideal selectivities of PC/pNA/zeolite 4A MMMs at different pNA and zeolite 4A concentrations, measured at room temperature.

PC/x% pNA/y% 4A membrane		Selectivity				
x	y	H <sub>2</sub> /N <sub>2</sub>	O <sub>2</sub> /N <sub>2</sub>	H <sub>2</sub> /CH <sub>4</sub>	CO <sub>2</sub> /CH <sub>4</sub>	N <sub>2</sub> /CH <sub>4</sub>
0	0	57.2	6.80	40.9	23.6	0.71
1	5	55.4	7.30	81.9	41.9	1.48
	10	52.0	6.70	92.8	44.1	1.78
	20	76.6	7.50	121.3	51.8	1.58
	30	62.6	5.80	107.4	44.9	1.72
2	5	64.6	8.20	82.2	40.1	1.27
	10	52.9	6.20	77.5	34.2	1.46
	20	72.8	7.60	135.0	51.3	1.85
	30	69.1	7.40	86.3	42.2	1.25
5	5	63.5	6.60	79.3	34.2	1.25
	10	59.5	6.50	74.4	32.9	1.25
	20	65.1	7.40	73.3	37.2	1.13
	30	70.8	6.90	111.3	44.0	1.55

were prepared with pNA concentrations of 1 % and 2 % (w/w) and with a zeolite loading of 20 % (w/w). The  $H_2/CH_4$  selectivity of PC/pNA (1%)/zeolite 4A (20%) membrane was 121.3 which is three times higher than that of pure PC membrane and twice as high as that of PC/zeolite 4A (20%) membrane. Similarly, the  $CO_2/CH_4$  selectivity of PC/pNA (1%)/zeolite 4A (20%) membrane was twice as high as the one for pure PC. The  $N_2/CH_4$  selectivities for all membranes were lower than two. The pure PC and PC/zeolite 4A membranes were selective for  $CH_4$  over  $N_2$ , interestingly, the membranes became  $N_2$  selective with the integration of pNA.

The comparison of permeabilities and selectivities of pure PC, PC/pNA, PC/zeolite 4A and PC/pNA/zeolite 4A membranes indicates the strong effect of pNA on the membrane matrix, and suggests that the use of zeolite 4A and pNA together in the PC membrane has more contribution to the membrane performance than their individual use in the membranes. The complex micro morphological structure of the PC/pNA/zeolite 4A MMMs, which is expected to have different characteristics than PC and PC/zeolite 4A membranes, can therefore strongly influence the membrane performance.

Besides, Yong et al. [27] compared the performance of polyimide (PI) membranes containing 43 % (w/w) zeolite 4A and 21 % (w/w) 2,4,6-triaminopyrimidine (TAP) with the performance of pure polyimide membranes. The permeabilities of  $CO_2$  and  $CH_4$  through PI/TAP/zeolite 4A membranes were lower but the selectivity for  $CO_2$  over  $CH_4$  was higher than pure PI membrane. The changes in membrane performance were attributed to the elimination of interfacial voids due to the improvement in the adhesion between the polymer and zeolite. A similar conclusion was made based on SEM micrographs by Pechar et al. [7] and Mahajan and Koros [18, 28], who prepared polyimide membranes using zeolites where silane-coupling agents were used to enhance the adhesion between polymer and zeolite phases. The pNA may have similar effect even at very small concentrations as suggested by gas permeation results and the changes in glass transition temperatures. Because of the functional groups that the pNA has, it may induce an interaction between zeolite particles and PC chains in this ternary compound membrane system besides modifying the polymer matrix itself. In addition,

the presence of pNA may lead to a polymer chain rigidification since the  $T_g$  of PC/pNA/4A MMMs were higher than PC/pNA membranes.

The permeabilities and selectivities of  $H_2/CH_4$  and  $CO_2/CH_4$  gas pairs are shown in Figure 5.8 for PC/pNA and PC/pNA/zeolite 4A membranes. The selectivities for both gas pairs and the permeabilities of fast permeating gases,  $H_2$  and  $CO_2$ , increased but the permeability of slowly permeating gas,  $CH_4$ , decreased with the addition of zeolite 4A. These results suggest that, as opposed to the general inversely proportional relationship between permeability and selectivity, both the selectivity and permeability of desired gases can be increased by proper formulation of ternary component membranes, which may enable the production of much better performing membranes.

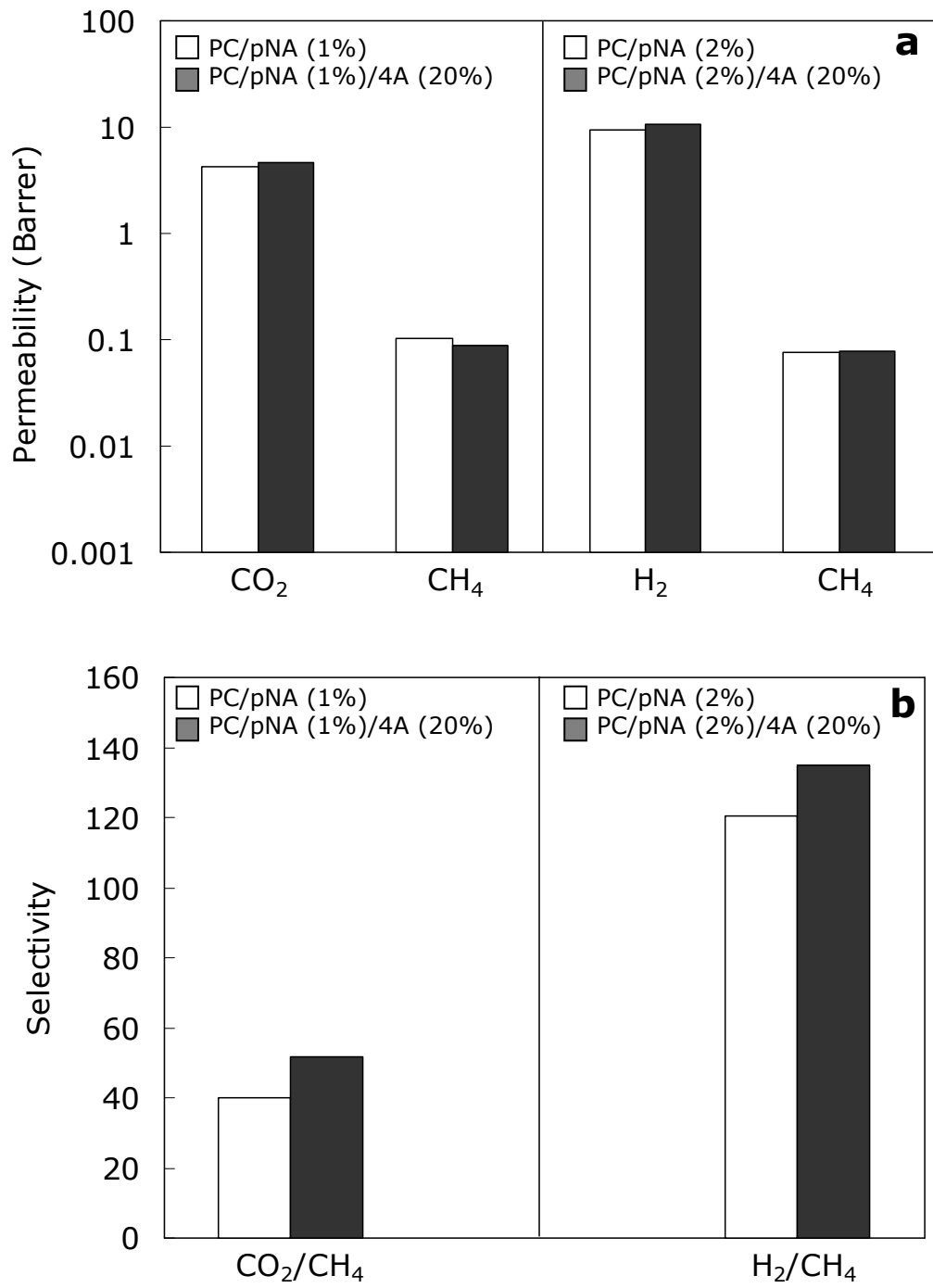


Figure 5.8 Comparing the permeability (Panel a) and selectivity (Panel b) of PC/pNA/zeolite 4A MMMs with PC/pNA blend membranes.



## CHAPTER 6

### BINARY GAS PERMEATION STUDIES

#### 6.1 Binary Gas Permeation Measurements

The pNA and zeolite 4A compositions of the membranes used in the separation of binary gas mixtures were listed in Table 6.1 with their membrane codes and CO<sub>2</sub>/CH<sub>4</sub> ideal selectivities. These membranes, which exhibited highest ideal selectivities of its own type, were selected for the separation of CO<sub>2</sub>/CH<sub>4</sub>, H<sub>2</sub>/CH<sub>4</sub> and CO<sub>2</sub>/N<sub>2</sub> binary gas mixtures. The effect of feed gas composition on the separation performance of these membranes was also investigated in detail. For CO<sub>2</sub>/CH<sub>4</sub> binary, CO<sub>2</sub> feed gas composition range as wide as possible, 5-95%, was studied. For other binary gas pairs, three different feed gas compositions, namely, 20%, 50% and 80% CO<sub>2</sub> and/or H<sub>2</sub> were studied.

The binary gas permeation experiments have a similar operational procedure as the single gas permeation experiments described in Section 5.1. The permeabilities of the binary gas mixtures through the membranes were measured by using a constant volume-variable pressure technique at room temperature. The feed side pressure was kept at 3.0 bar and the permeate side was initially at high vacuum, 0.01 Torr ( $1.33 \times 10^{-5}$  bar). Therefore, the total transmembrane pressure difference in the separation of binary gas mixtures was initially the same as the transmembrane pressure difference in single gas permeability measurements. The pressure increase in the

Table 6.1 The pNA and zeolite 4A compositions of the PC based membranes used in the separation of binary gas mixtures and their CO<sub>2</sub>/CH<sub>4</sub> ideal selectivities.

Membrane code	Composition (w/w)% of the PC		CO <sub>2</sub> /CH <sub>4</sub> ideal selectivity
	pNA/PC	zeolite 4A/PC	
PC	-	-	23.6
PC/pNA (2%)	2	-	51.9
PC/4A (20%)	-	20	32.5
PC/4A (30%)	-	30	37.6
PC/pNA (2%)/4A (20%)	2	20	51.3
PC/pNA (2%)/4A (30%)	2	30	42.2

permeate side at constant volume was recorded by a pressure transducer (MKS Baratron, 0-100 Torr), and plotted as a function of time for permeability calculations. Prior to binary gas permeation experiments, feed gases were analyzed online at least two times in the gas chromatograph. After the permeation was completed, the permeate and feed side gas streams were analyzed online by the same way. During these measurements, it was observed that, the feed side gas compositions remained constant throughout the permeation.

Binary gas permeation experiments showed that, the analysis of the permeate gas stream by GC during permeation at different time intervals disturbed our composition and permeation measurements probably because of the changing pressure differences and possible air leaks to the permeate side. In addition, it was difficult to quantitatively measure the gas composition from the gas chromatogram at the beginning of the permeation process, since the permeate concentration at the start of any permeation experiment was very low. Therefore, it was decided that permeate analysis with GC should be done

after the permeation was terminated when the amount of gas in the permeate side of the membrane reached to a measurable level. The duration of the permeation experiment, which was needed to obtain a measurable level, changed with the type of membrane, gas pairs, and their compositions. Generally, the permeation measurement times for CO<sub>2</sub>/CH<sub>4</sub>, H<sub>2</sub>/CH<sub>4</sub> and CO<sub>2</sub>/N<sub>2</sub> binary gas mixtures were between 8 to 12 hours.

## **6.2 Evaluation of Pressure-Time Data for Permeability Calculations in Binary Gas Permeation**

Binary gas permeabilities were calculated by fitting the pressure-time data on a straight line by linear regression method as in the case of single gas permeability calculations described in Section 3.4.2 and Appendix B. Only the dead-end volume of the system, which is 22 cm<sup>3</sup>, and the effective membrane area, which is 9.6 cm<sup>2</sup>, were different in the calculations.

The data were also used to calculate the individual permeabilities of component gases. Figure 6.1 shows the pressure-time data of CO<sub>2</sub>/CH<sub>4</sub> binary gas mixture through a pure PC membrane. This data was split into individual gas pressure-time data based on the permeate concentration of the gas mixture. Each data point was multiplied by the mole fractions of each gas in the permeate side, and the obtained pressure-time data were drawn for each gaseous component separately. With the knowledge of partial feed pressure of the gases and the pressure-time data of each gas, the curve fitting method was then used to estimate the permeabilities of individual gases.

In Figure 6.1, for a feed composition of 25% CO<sub>2</sub>-75%CH<sub>4</sub>, the permeability of CO<sub>2</sub>/CH<sub>4</sub> binary gas mixture was calculated as 2.02 Barrer, and the permeabilities of CO<sub>2</sub> and CH<sub>4</sub> in the binary gas mixture were found as, 7.50 and 0.311 Barrer, respectively. Thus, the mixture permeability were lower than the permeability of CO<sub>2</sub>, and higher than the permeability of CH<sub>4</sub>. It could not be calculated by summing the individual permeabilities of each gaseous component in the mixture. This might be attributed to the different partial pressures of each gaseous component in the permeate and feed side, and in turn different driving forces applied for each gaseous component in the

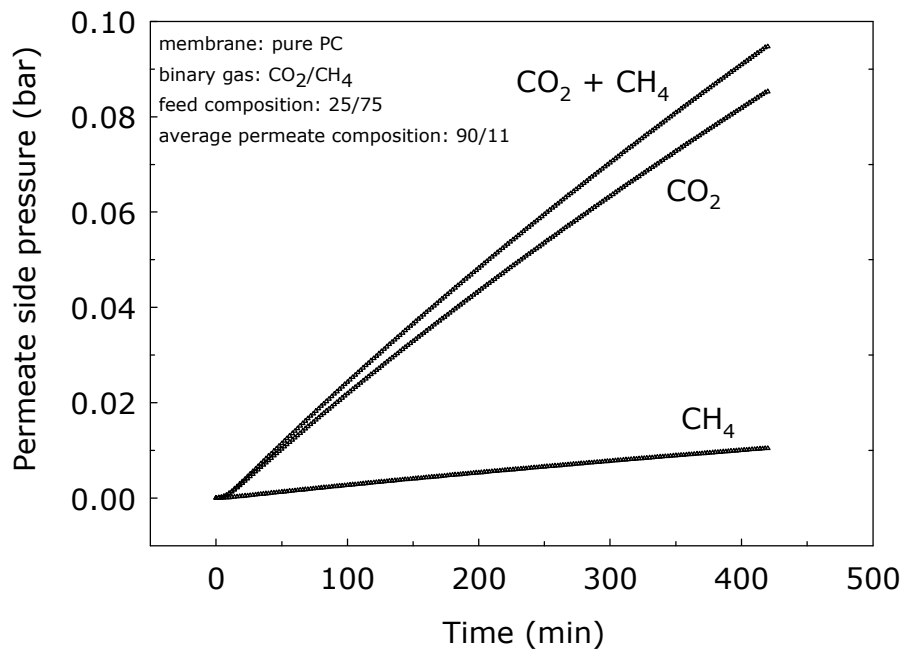


Figure 6.1 Permeate side pressure-time data of CO<sub>2</sub>/CH<sub>4</sub> binary gas mixture through pure PC membrane, and pressure-time data splitting technique based on the permeate compositions of CO<sub>2</sub> and CH<sub>4</sub>.

mixture. A sample calculation for the individual permeabilities of gas components in a gas mixture was given in Appendix E.

### 6.3 Evaluation of Permeate and Feed Side Compositions for Selectivity Calculations in Binary Gas Permeation

The separation selectivities of the membranes were calculated from the ratio of permeate and feed side compositions of the binary gas mixtures as described in Section 3.4.3.4 and Appendix E. Feed side and permeate side gas stream compositions were measured by gas chromatograph connected on-line to the gas permeation set-up.

In the case of CH<sub>4</sub> and/or N<sub>2</sub> containing binary gas mixtures, the analysis of gas mixtures with GC at low CH<sub>4</sub> and/or N<sub>2</sub> concentrations, i.e. smaller than

1%, may cause difficulties because of low sensitivity of TCD of GC in He carrier gas. As an illustration, in the case of 80 % (mol/mol) or higher CO<sub>2</sub> containing feed gas mixtures, the final CO<sub>2</sub> permeate gas concentration is generally 99% (mol/mol) and higher independent from the type of membrane used in permeation experiments. Such high concentration of CO<sub>2</sub> in the permeate may limit the accuracy of CH<sub>4</sub> concentration measurements because of the limitations in detection sensitivity. These limitations may then affect the separation selectivity calculations. In order to check the separation selectivities calculated from the analysis of each gaseous component in GC, a semi-empirical curve fitting method was developed. This method could also be used as an extrapolation technique to find the permeate gas compositions and separation selectivities of the membranes at feed compositions which are difficult to prepare. The application of this method was explained in detail for CO<sub>2</sub>/CH<sub>4</sub> binary gas mixture in two consecutive steps as follows.

In the first step, experimentally measured feed and permeate side CO<sub>2</sub> concentrations were plotted and the best fit curve was passed through the points (Figure 6.2a). The fitted equation was then used to calculate the permeate side CO<sub>2</sub> and CH<sub>4</sub> concentrations ( $= 1 - y_{(CO_2)}$ ) for small constant feed gas composition intervals. Calculated data was given in Appendix J. In the second step, based on the calculated permeate concentrations, separation selectivities were recalculated and plotted against to CO<sub>2</sub> feed concentration (Figure 6.2b). Separation selectivity data calculated from experimentally determined permeate compositions were also plotted on the same graph for comparison. It was found that the separation selectivities calculated from experimental data were in agreement with the separation selectivity calculations based on semi-empirical curve fitting method. Thus, this method can be used safely to calculate the separation selectivities of membranes at extreme feed gas compositions and at feed gas compositions which are difficult to prepare.

#### **6.4 Reproducibility in Permeabilities and Selectivities**

In order to obtain reliable results, reproducibility in permeability measurements and selectivities have a great importance. Therefore, a series

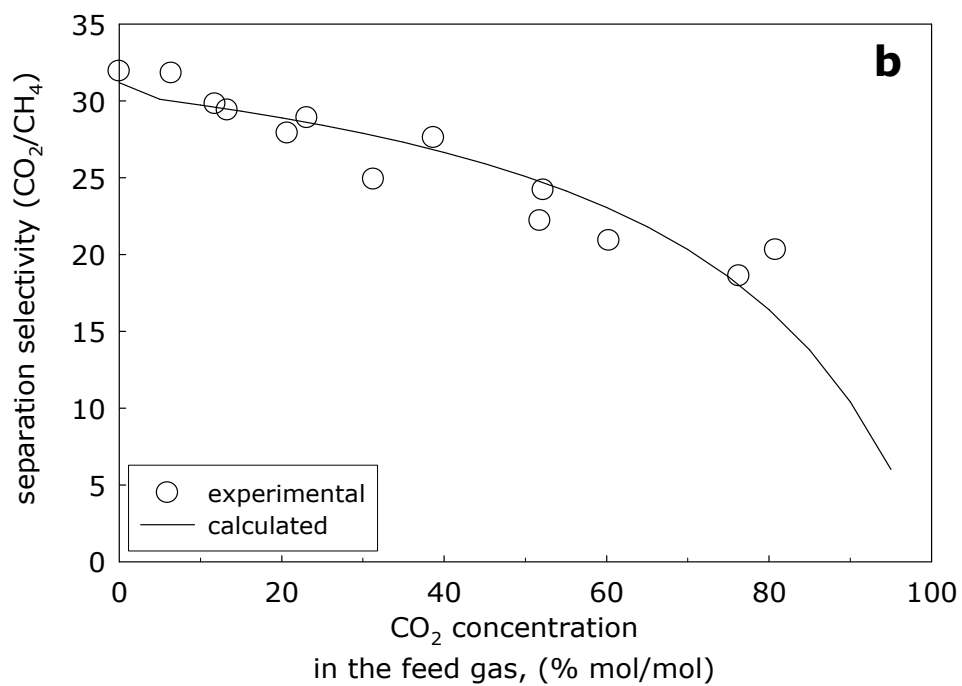
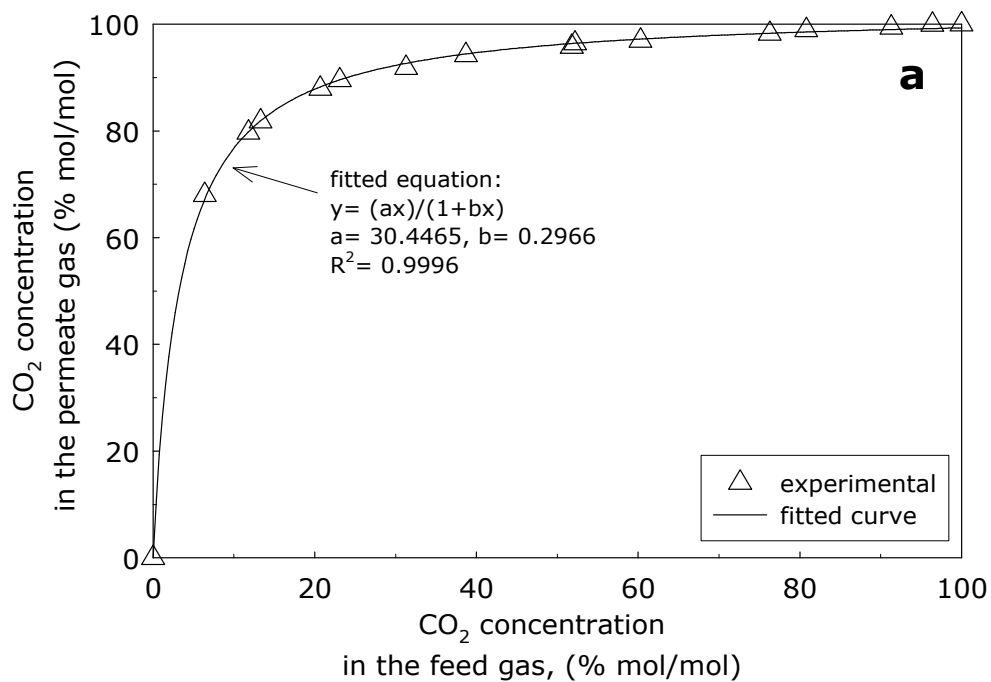


Figure 6.2 Semi-empirical curve fitting method (Panel a) and comparison of calculated separation selectivities with experimental data (Panel b) for the separation of CO<sub>2</sub>/CH<sub>4</sub> binary gas mixture through PC/4A (20%) MMM.

of reproducibility experiments were carried out in binary gas permeation measurements of the membranes. The permeability of each gas mixture through a particular membrane was measured at least two times, called reproducibility between runs. Additionally, for a particular membrane formulation, two membranes from the same film, and two membranes from two casting solutions were also tested by binary gas permeation experiments. Thus, the reproducibility in permeability measurements and membrane preparation were examined for different membranes in a same cast (reproducibility between the parts of the same membrane), and for different membrane in a different cast (reproducibility between membranes prepared at different times). The relative standard deviations between the results of reproducibility measurements were summarized in Table 6.2. The reproducibility experiment results of the membranes were tabulated in Appendix K. The averages of all permeabilities, selectivities, feed and permeate side compositions for each gas mixture were reported in the text.

Table 6.2 Reproducibility experiments and relative standard deviations in permeabilities and selectivities.

Reproducibility experiment	Relative standard deviations, %	
	in permeabilities	in selectivities
between runs	% 2.0 – 3.2	% 2.4 - 6.1
between parts of the same membrane	% 4.0 - % 5.6	% 4.1 - % 16.9
between membranes prepared at different times	% 3.4 - 8.6	% 7.3 - % 22.9

Table 6.2 shows that the reproducibility in binary gas permeability measurements and membrane preparation was very high. The higher standard deviations for selectivities may be the result of lower precision of

GC measurements at very low and high concentrations of gaseous components in the binary mixtures.

Based on these results, it can be concluded that the binary gas permeation system and methodology to measure permeabilities and selectivities were reliable. The results also showed that the procedure developed to prepare membranes is successful and yields reproducible membranes, which had also been confirmed by single gas permeability measurements.

## **6.5 Binary Gas Permeation Studies**

In literature, most of the studies about the separation performance of homogenous and mixed matrix membranes were restricted to single gas permeability measurements. Ideal selectivities were reported as selectivities assuming that the presence of a more than one gaseous component and composition variations of gas mixtures will not affect the separation performance of the membranes. However, these factors may have a primary importance since the interactions between components in the feed stream and the membrane can substantially alter the membrane performance. Selection of the proper membranes for gas separations requires the consideration of these alterations.

The membrane literature lacks studies about the effect of feed composition on the separation performance of membranes. Especially for MMMs very few studies investigated the effect of feed composition on membrane performances. Therefore, in this part of the study, binary gas studies were planned in order to verify the improved single gas performance results of the newly developed membranes, and to observe the effect of feed composition on the separation performance of membranes.

### **6.5.1 Binary Gas Permeation Studies through Dense Homogenous PC and PC/pNA Membranes**

Effect of feed gas composition on the separation performance of dense homogenous PC membranes and PC/pNA blend membranes were investigated



with CO<sub>2</sub>/CH<sub>4</sub> binary gas mixture for a feed gas composition changing between 5 and 95 % (mol/mol) CO<sub>2</sub>. Tables 6.3-6.4 and Figure 6.3 show the CO<sub>2</sub>/CH<sub>4</sub> binary gas permeabilities and separation selectivities of pure PC and PC/pNA membranes. The single gas permeabilities and ideal selectivities of the membranes are also presented.

The mixture permeabilities were always between the permeabilities of pure CO<sub>2</sub> and CH<sub>4</sub>. With increasing concentration of CO<sub>2</sub> in the feed, the mixture permeability increased linearly (Figure 6.3). On the other hand, the CO<sub>2</sub>/CH<sub>4</sub> separation selectivities of the membranes, which remained nearly constant, was around the ideal selectivity of each membrane. Thus, the presence of a second component did not change the separation performance of the PC and PC/pNA membranes.

The independent behavior of the selectivities of pure PC and PC/pNA membranes on feed gas composition may point to the non-interactive nature of gas permeation through these membranes. That means, the gas phase non-idealities and competition in sorption and diffusion among CO<sub>2</sub> and CH<sub>4</sub> in the membrane matrix (solubility and diffusion coupling) because of the gas- membrane matrix and gas-gas-membrane matrix interactions cannot affect the gas permeation through PC and PC/pNA membranes appreciably, and leave the selectivities unaffected.

Similar conclusions were also made previously for membranes made from a glassy polymer of polyethersulfone (PES) [75] and from a rubbery polymer of poly(dimethylsiloxane) (PDMS) [9]. In these studies, the absence of deviation between separation selectivities and ideal selectivities were explained by the dense homogenous morphologies of the membranes. Dense homogenous membrane morphologies were stated as a reason of the absence of gas-membrane matrix and gas-gas-membrane matrix interactions through the membranes. On the other hand, Dhingra et al. [9] reported an increase in the CO<sub>2</sub>/CH<sub>4</sub> separation selectivities of dense homogenous pure polyimide (PI) membranes with increasing concentration of CO<sub>2</sub> in the feed mixture. This observation was explained as the presence of gas component-membrane matrix interactions in the PI matrix. Apparently, the type of the polymer

Table 6.3 Effect of feed composition on permeabilities and selectivities of CO<sub>2</sub>/CH<sub>4</sub> binary gas mixture through pure PC membrane\* (measured at room temperature, feed side pressure was 3.0 bar).

	CO <sub>2</sub> concentration in the feed (% mol/mol)												
	0	6	10.5	15.3	25.0	40.2	50.1	60.4	75.3	80.0	89.1	95.7	100
Permeability (Barrer)	0.341	0.558	0.812	1.20	2.01	3.13	4.12	5.12	6.17	6.73	7.61	7.81	9.14
Selectivity (CO <sub>2</sub> /CH <sub>4</sub> )	-	23.2	19.3	20.6	24.8	29.1	29.7	28.8	27.8	26.8	24	25.1	-

\* CO<sub>2</sub>/CH<sub>4</sub> ideal selectivity is 26.8.

Table 6.4 Effect of feed composition on permeabilities and selectivities of CO<sub>2</sub>/CH<sub>4</sub> binary gas mixture through PC/pNA (2%) membrane\* (measured at room temperature, feed side pressure was 3.0 bar).

	CO <sub>2</sub> concentration in the feed (% mol/mol)									
	0	12.1	21.5	28.3	53.2	61.8	78.9	100		
Permeability (Barrer)	0.083	1.18	1.33	1.54	2.09	2.37	3.43	4.01		
Selectivity (CO <sub>2</sub> /CH <sub>4</sub> )	-	55.1	53.5	53.6	47.7	49.6	49.4	-		

\* CO<sub>2</sub>/CH<sub>4</sub> ideal selectivity is 48.3.

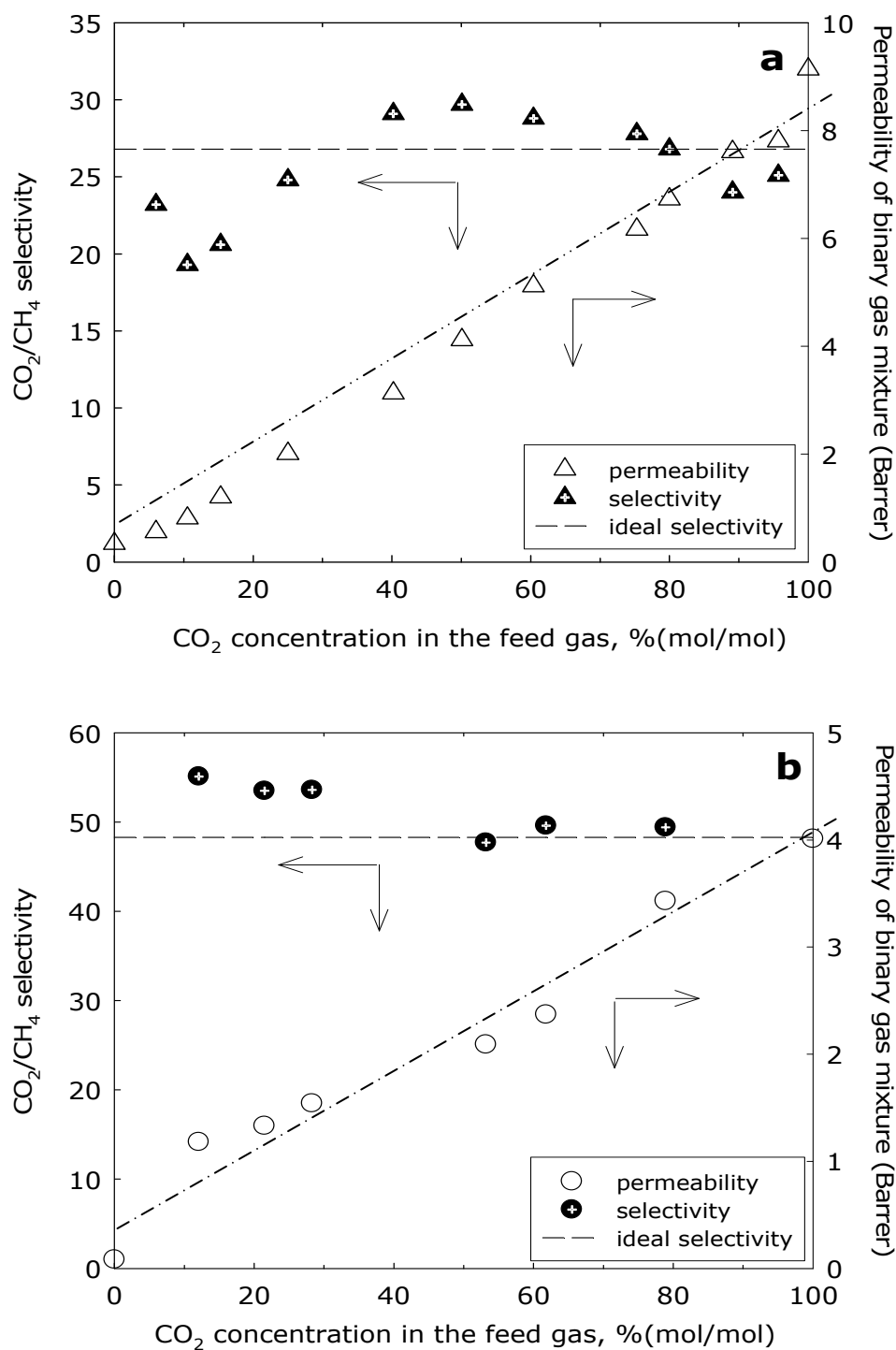


Figure 6.3 Effect of feed composition on permeability and selectivity for CO<sub>2</sub>/CH<sub>4</sub> binary gas mixture through pure PC membrane (Panel a) and PC/pNA blend membrane (Panel b).

matrix has high influence on the separation of binary gas mixtures and depending on the matrix polymer type the separation performances of dense homogenous polymer membranes may be either affected from the feed gas compositions or not.

The constant selectivity observation with feed composition is especially important for PC/pNA blend membranes, since the incorporation of pNA changed the structure and performance properties of the PC membranes due to its antiplasticization effect on PC matrix as demonstrated with single gas permeability and  $T_g$  measurement results [20]. The explanation of composition independency of selectivities for PC/pNA membranes may be based on the dense homogenous morphology of these membranes. They may behave as if a newly developed single pure polymer membranes for binary gas mixture separations.

### **6.5.2 Binary Gas Permeation Studies through PC/4A and PC/pNA/4A Mixed Matrix Membranes**

Effect of feed gas composition on the permeabilities and selectivities of the PC/4A and PC/pNA/4A MMMs were also investigated by using CO<sub>2</sub>/CH<sub>4</sub> binary gas mixture. Figure 6.4 shows the influence of CO<sub>2</sub> feed concentration on CO<sub>2</sub>/CH<sub>4</sub> mixture permeabilities through MMMs prepared at different zeolite 4A loadings. As in the case of homogenous PC and PC/pNA membranes, with the increase of CO<sub>2</sub> feed concentration, the permeability of CO<sub>2</sub>/CH<sub>4</sub> binary mixture through MMMs increased and the permeability values located between those of each single gas (CO<sub>2</sub> and CH<sub>4</sub>).

The increase in permeability with CO<sub>2</sub> feed concentration was almost linear for PC/4A MMMs. The slope of this line decreased with increasing zeolite 4A content of the membranes and the presence of pNA in the membrane matrix. For PC/pNA/4A MMMs, the increase in permeability with CO<sub>2</sub> feed concentration was not linear, the presence of pNA gave a slight curvature in PC/pNA (2%)/4A (30%) MMMs, while this curvature became apparent in PC/pNA (2%)/4A (20%) MMMs. This may show that the existence of pNA as a low molecular-weight antiplasticizer, alters the character of PC matrix in

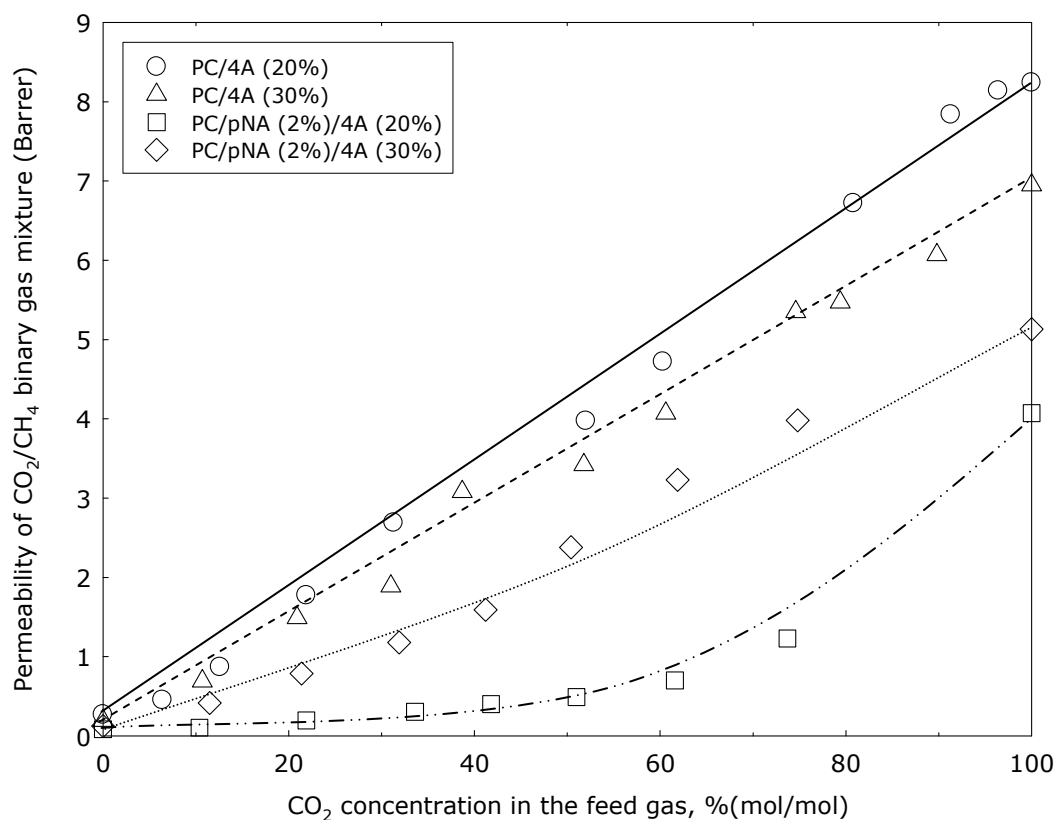


Figure 6.4 Effect of feed composition on the CO<sub>2</sub>/CH<sub>4</sub> binary gas mixture permeabilities through PC/4A and PC/pNA/4A MMMs.

zeolite filled MMMs, and influences the gas transport across the membrane in a different way compared to dense homogenous PC based membranes and PC/zeolite 4A MMMs.

Figures 6.5 and 6.6 show the CO<sub>2</sub>/CH<sub>4</sub> selectivities of PC/4A and PC/pNA/4A MMMs with respect to increasing CO<sub>2</sub> concentration in the feed gas. As opposed to the selectivities of pure PC and PC/pNA membranes, selectivities of MMMs indicated a strong feed concentration dependency as shown in figures. Higher CO<sub>2</sub> concentrations in the feed caused appreciably lower selectivity values which are below the ideal selectivity values of the MMMs. The selectivity decrease was gradual with increasing CO<sub>2</sub> (selectively permeating component) feed concentration for PC/4A MMMs, whereas

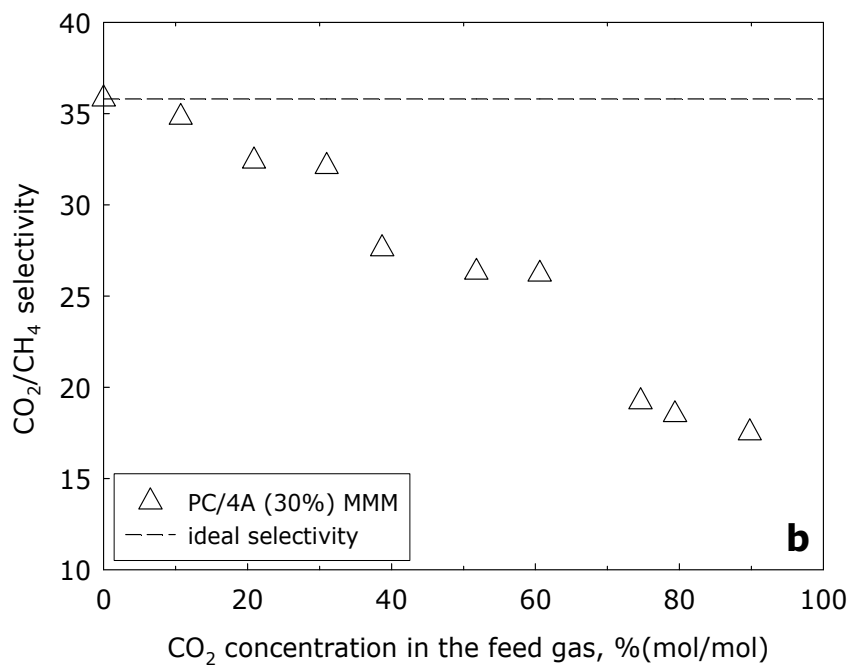
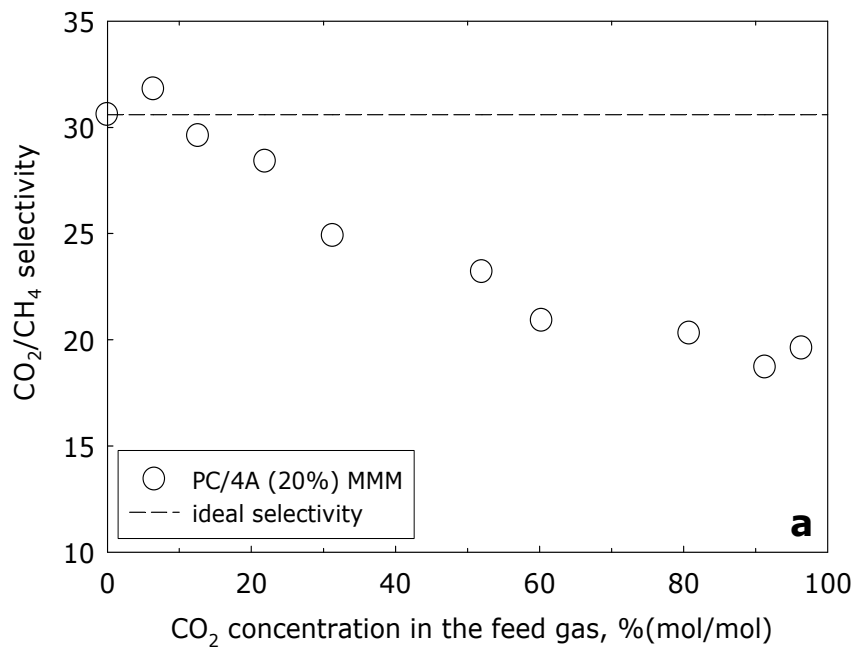


Figure 6.5 Effect of feed composition on the selectivity of CO<sub>2</sub>/CH<sub>4</sub> through PC/4A (20%) MMMs (Panel a) and PC/4A (30%) MMMs (Panel b).

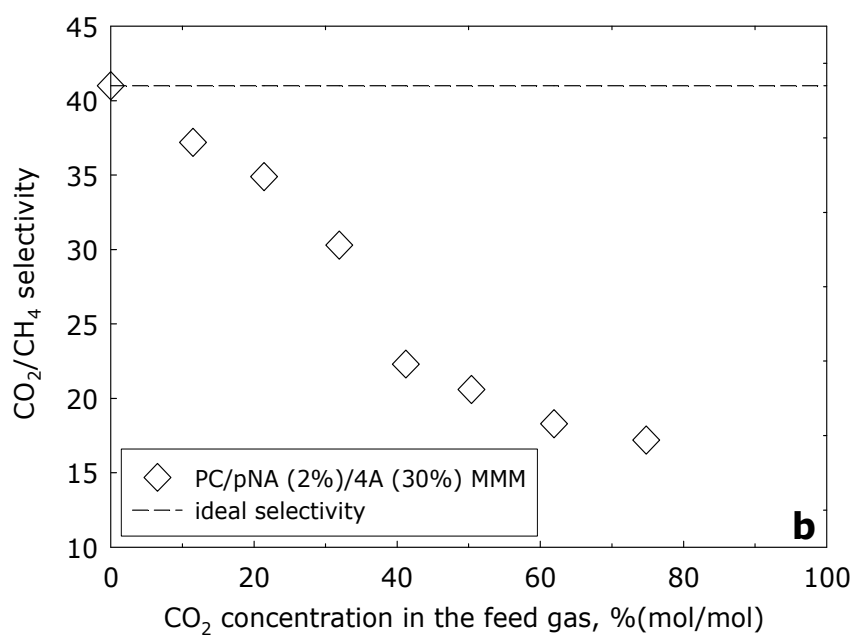
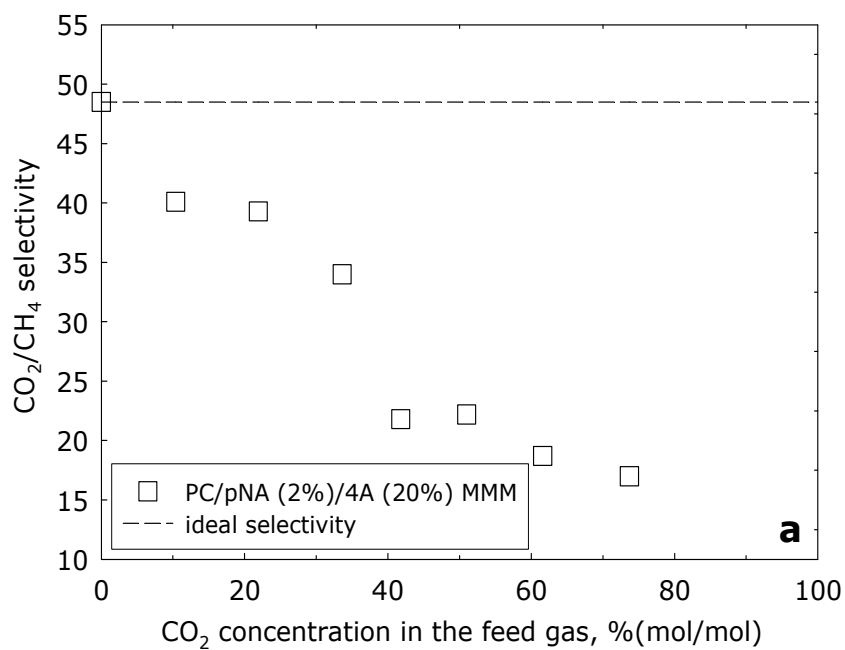


Figure 6.6 Effect of feed composition on the selectivity of CO<sub>2</sub>/CH<sub>4</sub> through PC/pNA (2%)/4A (20%) MMMs (Panel a) and PC/pNA (2%)/4A (30%) MMMs (Panel b).

there was a sharper decrease in the selectivity of PC/pNA/4A MMMs. For example, when the CO<sub>2</sub> concentration in the feed increased to 50 % (mol/mol), approximately 20% and 50% decrease in selectivities were observed in comparison to the ideal selectivities of the PC/4A (20%) and PC/pNA (2%)/4A (20%) MMMs, respectively. In addition to these, when the zeolite content of the PC/4A MMMs was increased from 20 % to 30 % (w/w), the extent of decrease in selectivities with feed gas composition increased. On the other hand, this trend was not observed for PC/pNA/4A MMMs. As the zeolite concentration of the PC/pNA/4A MMMs was increased for a given pNA content, the extent of decrease in selectivities with feed gas composition did not change much. That means, the presence of pNA might change the effect of zeolite 4A on the performance of MMMs.

In order to investigate the effect of different gas systems on the performance of zeolite filled PC based MMMs, the separation of CO<sub>2</sub>/N<sub>2</sub> and H<sub>2</sub>/CH<sub>4</sub> binary gas systems were also studied at different feed gas compositions. Tables 6.5 and 6.6 show the effects of CO<sub>2</sub> and/or H<sub>2</sub> feed concentration on the CO<sub>2</sub>/N<sub>2</sub> and H<sub>2</sub>/CH<sub>4</sub> permeabilities and selectivities for PC/4A and PC/pNA/4A MMMs. For the CO<sub>2</sub>/N<sub>2</sub> binary gas mixture, the behavior of the MMMs was similar to CO<sub>2</sub>/CH<sub>4</sub> mixture separation. With increasing concentration of CO<sub>2</sub> in the feed, which is the selectively permeating component in CO<sub>2</sub>/N<sub>2</sub> separation, the permeability of the CO<sub>2</sub>/N<sub>2</sub> mixture through the membranes increased while the CO<sub>2</sub>/N<sub>2</sub> selectivity of the membranes decreased. The percent reduction in CO<sub>2</sub>/N<sub>2</sub> selectivities with feed gas composition was close to that of CO<sub>2</sub>/CH<sub>4</sub> selectivities.

In the case of H<sub>2</sub>/CH<sub>4</sub> mixture, similar to the cases with CO<sub>2</sub>/CH<sub>4</sub> and CO<sub>2</sub>/N<sub>2</sub> binary gas mixtures, the separation selectivities of the MMMs were lower than the respective ideal selectivities at each feed gas composition. However, in this case, as opposed to the cases with CO<sub>2</sub>/CH<sub>4</sub> and CO<sub>2</sub>/N<sub>2</sub>, increasing the concentration of the selectively permeating component, which is H<sub>2</sub>, in the feed gas mixture increased the H<sub>2</sub>/CH<sub>4</sub> separation selectivities of MMMs and the selectivity values approached the ideal selectivity values of the MMMs. When the H<sub>2</sub> concentration in the feed increased from 15 % to 85 % (mol/mol), the H<sub>2</sub>/CH<sub>4</sub> separation selectivities of PC/4A and PC/pNA/4A MMMs



Table 6.5 Effect of feed composition on permeabilities and selectivities of CO<sub>2</sub>/N<sub>2</sub> binary gas mixture through PC/4A (20%) and PC/pNA (2%)/4A(20%) MMMs (measured at room temperature, feed side pressure was 3.0 bar).

Membrane: PC/4A (20%) MMM <sup>a</sup>					
	CO <sub>2</sub> concentration in the feed (% mol/mol)				
	0	21.3	52.5	83.9	100
Permeability (Barrer)	0.261	0.899	3.33	5.96	8.24
Selectivity (CO <sub>2</sub> /N <sub>2</sub> )	-	29.6	23.2	15.8	-
Membrane: PC/pNA (2%)/4A (20%) MMM <sup>b</sup>					
	CO <sub>2</sub> concentration in the feed (% mol/mol)				
	0	20.9	52.5	82.7	100
Permeability (Barrer)	0.132	0.8	1.84	2.8	4.07
Selectivity (CO <sub>2</sub> /N <sub>2</sub> )	-	25.9	20.5	13.4	-

<sup>a</sup> CO<sub>2</sub>/N<sub>2</sub> ideal selectivity is 31.6.

<sup>b</sup> CO<sub>2</sub>/N<sub>2</sub> ideal selectivity is 30.8.

increased from 26.1 to 60.8 and 24.1 to 94.2, respectively (Table 6.6). Thus, approximately 60% and 80% increase in selectivities were observed in comparison to the selectivities at the lowest H<sub>2</sub> concentration in the feed for PC/4A and PC/pNA/4A MMMs, respectively.

Apparently, the permeabilities and selectivities of zeolite filled PC based MMMs were changed significantly in binary gas permeation experiments. The feed gas composition had a strong effect on their gas separation performances. The strong concentration dependency of permeabilities and selectivities was observed and discussed previously in many studies with different type of membranes [43-47, 71-81]. For instance, in a study of Battal et al. [75] zeolite 4A filled polyethersulfone MMMs were prepared and the binary gas permeation results of the MMMs indicated similar changes in membrane performances as in PC/4A and PC/pNA/4A MMMs with feed gas composition. The changes in membrane performances with feed gas composition was

Table 6.6 Effect of feed composition on permeabilities and selectivities of H<sub>2</sub>/CH<sub>4</sub> binary gas mixture through PC/4A (20%) and PC/pNA (2%)/4A (20%) MMMs (measured at room temperature, feed side pressure was 3.0 bar).

Membrane: PC/4A (20%) MMM <sup>a</sup>					
H <sub>2</sub> concentration in the feed (% mol/mol)					
	0	17.8	51.8	84.3	100
Permeability (Barrer)	0.245	2.2	7.7	11.8	15
Selectivity (H <sub>2</sub> /CH <sub>4</sub> )	-	26.1	37.9	60.8	-

Membrane: PC/pNA (2%)/4A (20%) MMM <sup>b</sup>					
H <sub>2</sub> concentration in the feed (% mol/mol)					
	0	16.8	51.3	84.3	100
Permeability (Barrer)	0.084	2.08	6.48	9.05	11.8
Selectivity (H <sub>2</sub> /CH <sub>4</sub> )	-	24.1	47.6	94.2	-

<sup>a</sup> H<sub>2</sub>/CH<sub>4</sub> ideal selectivity is 61.4.

<sup>b</sup> H<sub>2</sub>/CH<sub>4</sub> ideal selectivity is 140.5.

explained by the competition of penetrants for the sorption sites and the associated diffusion pathways in the membrane matrices. It was claimed that any speculation about the composition dependency of separation performances should consider the membrane morphology since the competition of penetrants because of interaction of gas molecules with the membrane matrix is strongly affected by the membrane morphology. Therefore, for zeolite filled MMMs the change in separation performances with feed gas composition can be explained with the complex heterogenous morphology of the membranes.

Previous SEM studies with zeolite filled MMMs showed that the addition of zeolite particles induce a porous structure in membrane matrix because of the interfacial voids appear around zeolite particles [29, 31-33]. In this morphology, different alternative transport pathways for gas molecules may exist; they may pass through the polymer matrix, they may flow through

the interfacial voids formed around zeolite crystals, and they may be transported through zeolitic surfaces by interacting with it [21, 29, 31, 32]. The availability and dominance of one of these pathways for a gas may mainly depend on its size, polarity and interaction potential with the membrane matrix (in other words affinity of a gas to membrane). However, in the case of gas mixtures the existence of another gaseous component may strongly affect the transport behavior of one component through membrane. Therefore, some arguments about the change in selectivities of the PC/4A and PC/pNA/4A MMMs can be made based on this morphology of MMMs.

For CO<sub>2</sub> containing binary gas mixtures, the CO<sub>2</sub> molecules may saturate the sorption sites of PC and the active sites of zeolite 4A crystals more quickly than the CH<sub>4</sub> and/or N<sub>2</sub> molecules, since the CO<sub>2</sub> gas has higher affinity toward zeolite 4A crystals and PC matrix than the CH<sub>4</sub> and/or N<sub>2</sub> due to its higher heat of adsorption on zeolite 4A and higher solubility in PC matrix [37, 94, 103-107]. With increasing CO<sub>2</sub> feed concentration, the interaction potential of CO<sub>2</sub> with the membrane matrix may be reduced because the sorption sites in the membrane matrix may not be sufficient for interaction with the more number of CO<sub>2</sub> molecules. This may lead to self-inhibition of CO<sub>2</sub> and the priority for CO<sub>2</sub> to permeate through the membrane may no longer be effective. Thus, the CO<sub>2</sub>/CH<sub>4</sub> and CO<sub>2</sub>/N<sub>2</sub> selectivities are decreased.

It may be concluded that, when the faster permeating component of a mixture has a strong interaction possibility with the membrane matrix (CO<sub>2</sub>), selectivities decrease with increasing concentration of this component independent from the type of the relatively less-interactive component (CH<sub>4</sub> and/or N<sub>2</sub>) in the mixture, indicating the importance of competitive sorption among penetrants. A similar conclusion was also reached previously in the examination of CO<sub>2</sub>/CH<sub>4</sub> and CO<sub>2</sub>/Ar separation performance properties of PES/zeolite 4A MMMs [75]. On the other hand, Sridhar et al. [73] reported an increase in CO<sub>2</sub>/CH<sub>4</sub> selectivities of poly(phenyleneoxide) (PPO)/heteropolyacid (HPA) blend membranes with CO<sub>2</sub> concentration. They claimed that the permeation of CH<sub>4</sub> may be impeded due to increasing polarization of CO<sub>2</sub> molecules near the membrane surface, and this may increase the selectivities at high CO<sub>2</sub> concentrations. Therefore, depending on

the gas-membrane matrix interactions binary gas separation performance of the membranes can show different behaviors with feed composition.

For H<sub>2</sub>/CH<sub>4</sub> binary gas system, since none of the gas components has strong interaction potential with the membrane matrix as in the case of CO<sub>2</sub>, the molecular size difference of gas components may be considered to explain the selectivity dependence to the feed composition. CH<sub>4</sub> as a relatively larger molecule may hinder the permeation of small molecule H<sub>2</sub> by blocking and/or occupying the narrow regions and voids in the membrane matrix, resulting in lower selectivity values for CH<sub>4</sub> rich feed mixtures. Similar arguments were also reported by Battal et al. [75] and Krystal et al. [108, 109] based on the H<sub>2</sub>/CH<sub>4</sub> separation performances of PES/zeolite 4A MMMs and heterogenous zeolite-based membranes with polymeric binder. They concluded that when the component with a high permeability transport faster because of its size, selectivities decrease with increasing composition of larger component.

The comparison of the effect of feed gas composition on the permeabilities and selectivities of PC/4A and PC/pNA/4A membranes indicated that the feed gas composition has pronounced effect on the separation performances of PC/pNA/4A MMMs. The decrease in selectivities with an increase in CO<sub>2</sub> feed concentration, and the increase in selectivities with an increase in H<sub>2</sub> feed concentration were higher for PC/pNA/4A MMMs. This suggests that the use of zeolite 4A and pNA together in the PC membrane has a different contribution to the membrane separation performance than their individual use in the membranes. This different behavior of PC/pNA/4A MMMs compared to PC/4A MMMs was observed previously in their SEM, DSC characterization and single gas permeability measurement results [102]. The additive pNA decreased the free volume of PC and restricts the diffusion of gas molecules through the membrane due to its antiplasticization effect on PC matrix [20]. In addition, pNA enhanced the compatibility between zeolite crystals and PC matrix by inducing an interaction between polymer chains and zeolite particles, and this may also decrease the permeation of gas molecules. Thus, the pNA modified the MMM morphology, and changed the interaction potential of gas molecules with the membrane matrix. This may lead to sharp changes in separation performances of PC/pNA/4A MMMs with feed concentration.

### 6.5.3 General Performance Evaluation of Membranes

The CO<sub>2</sub>/CH<sub>4</sub> separation performance of different type of PC based membranes demonstrated that the permeability and selectivity of membranes depend strongly on membrane morphology and feed composition. Additionally, the CO<sub>2</sub>/N<sub>2</sub> and H<sub>2</sub>/CH<sub>4</sub> separation performance of the MMMs indicated that the dependence of performance properties on membrane morphology and feed composition can also change with the binary gas systems studied.

Previous single gas permeation studies of the membranes showed that the individual and combined addition of zeolite 4A and pNA into PC matrix improved the PC membrane performance and the performance values of the membranes approached to upper-bound line for industrially important gas pairs. However, in the case of binary gas permeation experiments of the membranes, it was observed that the gas separation performance of the PC/4A and PC/pNA/4A MMMs deviate from the respective ideal separation performances, and the permeability-selectivity trade-off relation of the membranes alters with feed gas composition. It was observed that the binary gas separation selectivities and the permeabilities of fast gases (CO<sub>2</sub> in CO<sub>2</sub>/CH<sub>4</sub> and CO<sub>2</sub>/N<sub>2</sub> binaries, H<sub>2</sub> in H<sub>2</sub>/CH<sub>4</sub> binary) in binary gas mixtures were always lower than ideal selectivities and single gas permeabilities of the MMMs. On the contrary, the binary gas separation performance of pure PC and PC/pNA membranes did not deviate from their ideal performance values with feed gas composition.

The CO<sub>2</sub>/CH<sub>4</sub>, CO<sub>2</sub>/N<sub>2</sub> and H<sub>2</sub>/CH<sub>4</sub> binary gas separation performances of dense homogenous PC membranes and zeolite 4A filled PC based MMMs were compared in Figures 6.7-6.9 with reference to their upper bound lines, respectively. This is the first report of making such a comparison between membrane performance on Robeson's upper bound trade-off graphs with respect to feed composition. Single gas permeability and ideal selectivity of the membranes were also shown on the graphs.

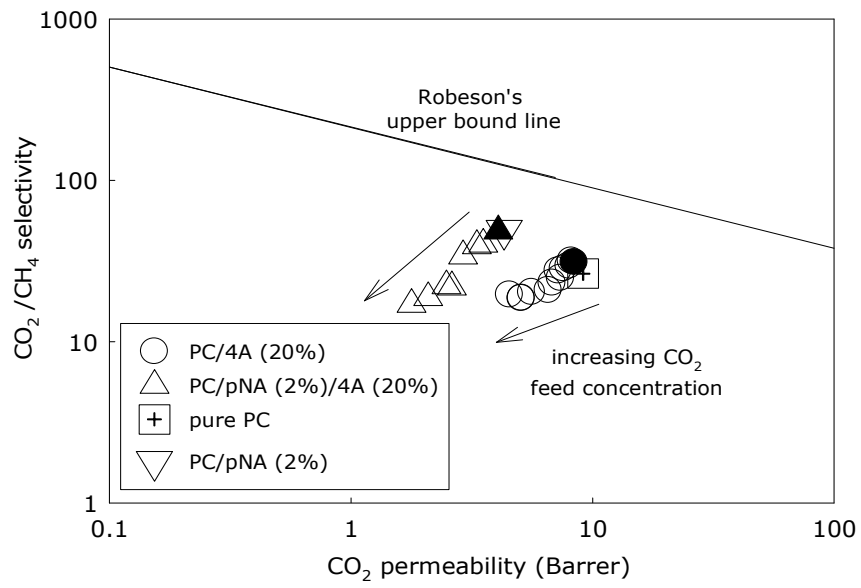


Figure 6.7  $\text{CO}_2/\text{CH}_4$  selectivity and  $\text{CO}_2$  permeability of different type of PC based membranes on a Robeson's upper bound trade-off curve. The symbols (▲) and (●) indicate ideal selectivity values of MMMs.

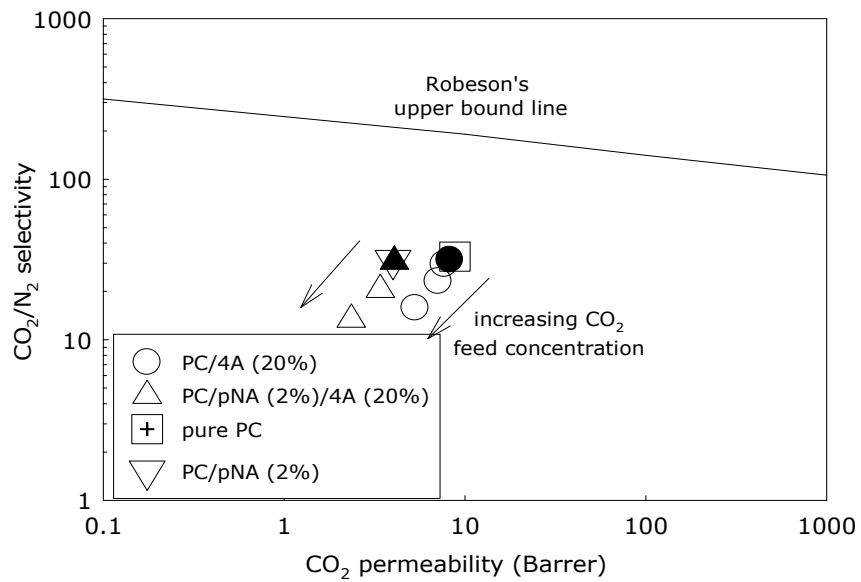


Figure 6.8  $\text{CO}_2/\text{CH}_4$  selectivity and  $\text{CO}_2$  permeability of different type of PC based membranes on a Robeson's upper bound trade-off curve. The symbols (▲) and (●) indicate ideal selectivity values of MMMs.

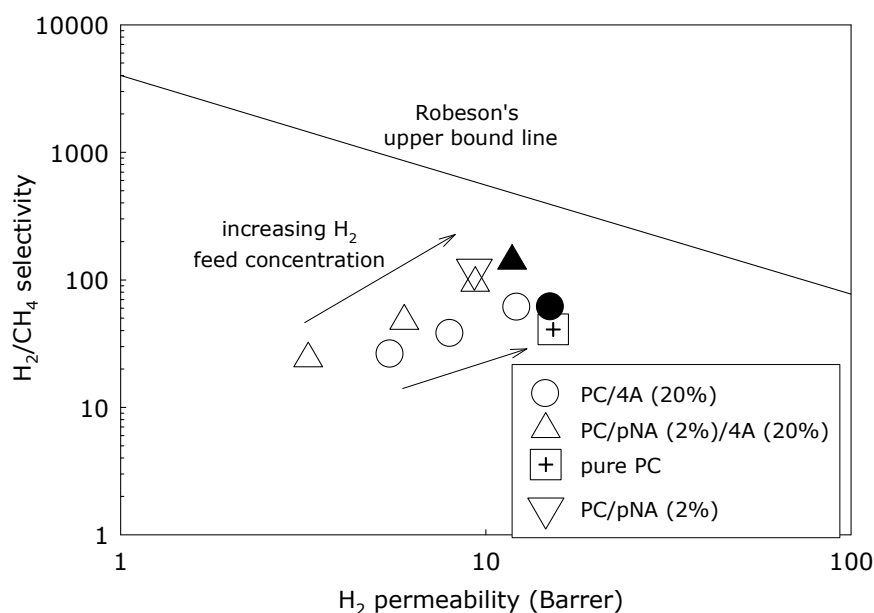


Figure 6.9  $\text{CO}_2/\text{CH}_4$  selectivity and  $\text{CO}_2$  permeability of different type of PC based membranes on a Robeson's upper bound trade-off curve. The symbols ( $\blacktriangle$ ) and ( $\bullet$ ) indicate ideal selectivity values of MMMs.

As can be seen from the figures, different type of PC based membranes results in a better trade-off relation between permeability and selectivity at different feed compositions for different gas pairs. For  $\text{CO}_2/\text{CH}_4$  and  $\text{CO}_2/\text{N}_2$  binary gas mixtures, PC/4A and PC/pNA/4A MMMs can be used to separate mixtures containing low  $\text{CO}_2$  concentrations, lower than 40%, while homogenous PC and PC/pNA membranes can be more suitable for  $\text{CO}_2$  rich mixtures, higher than 50%. In addition, for  $\text{H}_2/\text{CH}_4$  mixtures, PC/4A and PC/pNA/4A MMMs can show high separation performances at high  $\text{H}_2$  concentrations, higher than 50%, whereas homogenous PC and PC/pNA membranes can be used for  $\text{CH}_4$  rich mixtures.

Apparently, for  $\text{CO}_2$  containing binary gas mixtures, MMMs preserved their high performance characteristics at low feed concentrations, less than 40% (mol/mol), of selectively permeating component  $\text{CO}_2$ , whereas for  $\text{H}_2$  containing binary gas mixtures, MMMs showed high performance

characteristics at high feed concentrations, higher than 50 % (mol/mol), of selectively permeating component H<sub>2</sub>. These are important results because most of the industrially important gas separation studies, that remove CO<sub>2</sub> from natural gas or flue gas and recover H<sub>2</sub> from off-gases, use gas mixtures containing low CO<sub>2</sub> concentrations and/or high H<sub>2</sub> concentrations [52, 53, 72]. Therefore, the newly developed PC/4A and PC/pNA/4A MMMs can show promising results to separate CO<sub>2</sub> from natural gas or flue gas and to recover H<sub>2</sub> from off-gases at those feed composition ranges.

In conclusion, it can be said that in order to verify the improved separation performances of the developed membranes and to make a correct choice of membrane for a certain industrial gas separation application, the multicomponent gas mixture permeability measurements should be performed and the dependence of permeability and selectivity on feed gas compositions must be taken into account in designing and evaluating a membrane separation system.



## **CHAPTER 7**

### **CONCLUSIONS**

In this study, mixed matrix membranes for use in gas separation were prepared by blending polycarbonate with a multifunctional low molecular-weight additive, pNA, and incorporating zeolite 4A particles as filler. During the development of these membranes, PC and PC/pNA dense homogenous membranes and PC/zeolite 4A mixed matrix membranes were prepared at the intermediate stages. Thus, both the individual and combined effects of zeolite 4A and pNA on the structure and performance properties of polycarbonate gas separation membranes were investigated in detail.

The following conclusions were drawn from this study :

1. The characterization and gas separation performance results of the membranes showed that the methodology developed to prepare membranes reproducibly yields dense homogenous and mixed matrix PC based membranes. Self-supporting permselective membranes were obtained with a concentration of zeolite 4A between 5 % and 30 % (w/w) and of pNA between 1 % and 5 % (w/w).
2. Single gas permeability measurements of the membranes demonstrated that the PC/pNA/zeolite 4A MMMs showed generally higher ideal selectivities than the PC/zeolite 4A MMMs and those showed higher ideal selectivities than pure PC membranes despite a loss in the permeabilities with the addition of pNA and zeolite 4A into the membrane formulation. The ideal selectivities of

membranes increased because of modification of membrane morphology by zeolite 4A particles and pNA. pNA even at very small concentrations (1-2 % w/w) effectively changed the permselective properties of PC/zeolite 4A MMMs.

3. DSC analysis of the MMMs showed that, in the absence of pNA, incorporation of zeolite 4A particles into PC matrix has no effect on the  $T_g$  of PC, indicating the absence of interaction between phases. On the other hand, the addition of very small concentration of pNA changed the  $T_g$  of PC/zeolite 4A MMMs, which was considered as an indication of interaction between PC and zeolite 4A particles. Therefore, in order zeolite to affect PC membrane matrix the incorporation of pNA into membrane matrix is essential.

4. SEM images of the PC/zeolite 4A MMMs showed voids around the zeolite crystals, pointing the incompatibility between PC chains and zeolite 4A crystals. On the other hand, SEM images of the PC/pNA/zeolite 4A MMMs showed that the interfacial voids were partially eliminated and fewer voids remained with the addition of pNA, suggesting that low molecular-weight additives like pNA may improve the compatibility between the zeolite particles and PC matrix.

5. Characterization and single gas permeability results of the membranes indicated that pNA acts as a facilitator for provision of better interaction between rigid, glassy polymer PC and zeolite 4A particles, and consequently improved the separation performances. It was concluded that the incorporation of an additive with functional groups into zeolite filled MMMs can be used as a tool to tailor the structure and performance properties of the membranes.

6. Binary gas permeation results of the membranes demonstrated that for dense homogenous PC and PC/pNA membranes, separation selectivities remained nearly constant around the ideal selectivities of the membranes. The absence of deviation between separation selectivities and ideal selectivities of these membranes indicated that the penetrants competition due to different gas-membrane matrix and gas-gas-membrane matrix

interactions might not affect the gas permeation mechanism appreciably for these type of membranes.

7. For PC/zeolite 4A and PC/pNA/zeolite 4A MMMs, separation performances demonstrated a strong feed concentration dependency. Since the zeolite 4A and pNA acted as morphology modifiers in the PC matrix, the different morphologies of the MMMs compared to those of dense homogenous PC and PC/pNA membranes were considered as an important factor in composition dependency of separation performance of MMMs.

8. The dependence of separation performance on feed gas composition for the MMMs was found to change with different binary gas systems. Depending on the different molecular size of the gas molecules in the feed mixture and different interaction potential of gas molecules with the membrane matrix, MMMs demonstrated different trends in selectivity with feed composition. In the case of CO<sub>2</sub> containing binary gas mixtures, selectivities decreased with increasing CO<sub>2</sub> concentration in the feed because of its high sorption property in membrane matrices, whereas in the case of H<sub>2</sub>/CH<sub>4</sub> mixture, selectivities increased with increasing H<sub>2</sub> concentration in the feed because of its small size in comparison to CH<sub>4</sub>. For all binary gas mixtures, the separation selectivities of the MMMs were always lower than the respective ideal selectivities.

9. It was concluded that the change in separation performances with feed gas composition must be taken into account in designing and evaluating a membrane separation system, especially in the case of MMMs. Different type of membranes may have better performance characteristics at different feed concentration ranges. The observed variations between binary and single gas permeability measurements warrant the need for further studies with different gas pair-membrane systems to make a correct choice of membrane for a certain industrial gas separation application.

## CHAPTER 8

### RECOMMENDATIONS

1. For PC/zeolite 4A MMMs, highest zeolite loading at which a workable permselective MMMs can be produced was 30 % (w/w). High permeabilities and selectivities can be obtained at high zeolite loadings therefore, new polymers and zeolites should be searched and analyzed for the preparation of MMMs that would be workable at higher zeolite loadings.
2. The effect of zeolite type and particle size on the structure and performance of MMMs should be explored to understand the changes in polymer membrane morphology and performance with these parameters.
3. The effect of different type of low molecular-weight additives, that contain two or more functional groups and rigid structures, on the structure and performance of MMMs should be investigated.
4. The effect of membrane preparation parameters, such as casting solution preparation, evaporation and annealing temperatures, on the structure and performance properties of ternary compound polymer/additive/zeolite MMMs should be examined.
5. Studies which may ascertain our gas transport mechanism proposal through PC based homogenous and MMMs should be planned and performed. For example, sorption capacities of both homogenous and MMMs for different gases should be measured.

6. Separation studies of different gas mixtures, such as hydrogen/carbon dioxide, hydrocarbon/methane, should be studied. Strong emphasis can be given for the permeation and separation studies of gases such as  $\text{Cl}_2$ ,  $\text{H}_2\text{S}$ ,  $\text{SO}_2$ ,  $\text{CO}$ .

## REFERENCES

- [1] Baker, R.W., "Future directions of membrane gas separation technology", *Industrial Engineering and Chemistry Research*, 41, 2002, p. 1393-1402.
- [2] Meindersma, G.W., Kuczynski, M., "Implementing membrane technology in the process industry: problems and opportunities", *Journal of Membrane Science*, 113, 1996, p. 285-296.
- [3] Mulder, M., "Basic Principles of Membrane Technology", Kluwer Academic Publishers, Second edition, 1997, Dordrecht.
- [4] Nunes, S.P., Peinemann, K.V., "Membrane Technology in the Chemical Industry", Wiley-VCH, First edition, 2001, Weinheim.
- [5] Zimmerman, C.M., Singh, A., Koros, W.J., "Tailoring mixed matrix composite membranes for gas separation", *Journal of Membrane Science*, 137, 1997, p. 145-154.
- [6] Li, Y., Chung, T.S., Kulprathipanja, S., "Novel Ag<sup>+</sup>-zeolite/polymer mixed matrix membranes with a high CO<sub>2</sub>/CH<sub>4</sub> selectivity", *AICHE Journal*, 53 2007, p. 610-616.
- [7] Pechar, T.W., Tsapatsis, M., Marand, E., Davis, R., "Preparation and characterization of a glassy fluorinated polyimide zeolite mixed matrix membrane", *Desalination*, 146, 2002, p. 3-9.

- [8] Ruiz-Treviño, F.A., Paul, D.R., "Gas permselectivity properties of high free volume polymers modified by a low molecular weight additive", *Journal of Applied Polymer Science*, 68, 1998, p. 403-415.
- [9] Dhingra, S.S., Marand, E., "Mixed gas transport through polymeric membranes", *Journal of Membrane Science*, 141, 1998, p. 45-63.
- [10] Stern, S.A., "Polymer for gas separations: The next decade", *Journal of Membrane Science*, 94, 1994, p. 1-65.
- [11] Naylor, T.V., "Polymer Membranes- Materials, Structure and Separation Performance", *Rapra Review Reports*, Vol. 8, 1996, p. 21-30.
- [12] Robeson, L.M., "Correlation of separation factor versus permeability for polymeric membranes", *Journal of Membrane Science*, 62, 1991, p. 165-185.
- [13] Freeman, B.D., "Basis of permeability/selectivity tradeoff relations in polymeric gas separation membranes", *Macromolecules*, 32, 1999, p. 375-381.
- [14] Teplyakov, V., Meares, P., "Correlation aspects of the selective gas permeabilities of polymeric materials and membranes", *Gas Separation and Purification*, 4, 1990, p. 66-77.
- [15] Duval, J.M., Folkers, B., Mulder, M.H.V, Desgrandchamps, G., Smolders, C.A., "Adsorbent filled membranes for gas separation. Part 1. Improvement of the gas separation properties of polymeric membranes by incorporation of microporous adsorbents", *Journal of Membrane Science*, 80, 1993, p. 189-201.

- [16] Jia, M., Peinemann, K.V., Behling, R.D., "Molecular sieving effect of the zeolite-filled silicone rubber membranes in gas permeation", *Journal of Membrane Science*, 57, 1991, p. 289-300.
- [17] Hacıoğlu, P., Toppare, L., Yılmaz, L., "Polycarbonate-polypyrrole mixed matrix gas separation membranes", *Journal of Membrane Science*, 225, 2003, p. 51-62.
- [18] Mahajan, R., Koros, W.J., "Mixed matrix membrane materials with glassy polymers. Part I", *Polymer Engineering Science*, 42, 2002, p. 1420-1431.
- [19] Ruiz-Treviño, F.A., Paul, D.R., "Modification of polysulfone gas separation membranes by additives", *Journal of Applied Polymer Science*, 66, 1997, p. 1925-1941.
- [20] Şen, D., Kalıpçılar, H., Yılmaz, L., "Gas separation performance of polycarbonate membranes modified with multifunctional low molecular-weight additives", *Separation Science and Technology*, 41, 2006, p. 1813-1828.
- [21] Suer, M.G., Bac, N., Yılmaz, L., "Gas permeation characteristics of polymer-zeolite mixed matrix membranes", *Journal of Membrane Science*, 91, 1994, p. 77-86.
- [22] Duval, J.M., Kemperman, A.J.B., Folkers, B., Desgrandchamps, G., Smolders, C.A., "Preparation of zeolite filled glassy polymer membranes", *Journal of Applied Polymer Science*, 54, 1994, p. 409-418.
- [23] Moaddeb, M., Koros, W.J., "Gas transport properties of thin polymeric membranes in the presence of silicon dioxide particles", *Journal of Membrane Science*, 125, 1997, p. 143-163.



- [24] Vu, D.Q., Koros, W.J., Miller, S.J., "Mixed matrix membranes using carbon molecular sieves I. Preparation and experimental results", *Journal of Membrane Science*, 211, 2003, p. 311-334.
- [25] Gulsen, D., Hacıoğlu, P., Toppare, L., Yılmaz, L., "Effect of preparation parameters on the performance of conductive composite gas separation membranes", *Journal of Membrane Science*, 182, 2001, p. 29-39.
- [26] Mahajan, R., Koros, W.J., "Factors controlling successful formation of mixed-matrix gas separation materials", *Industrial Engineering and Chemistry Research*, 39, 2000, p. 2692-2696.
- [27] Yong, H.H., Park, H.C., Kang, Y.S., Wan, J., Kim, W.N., "Zeolite-filled polyimide membrane containing 2,4,6-triaminopyrimidine", *Journal of Membrane Science*, 188, 2001, p. 151-163.
- [28] Mahajan, R., Burns, R., Schaeffer, M., Koros, W.J., "Challenges in forming successful mixed matrix membranes with rigid polymeric materials", *Journal of Applied Polymer Science*, 86, 2002, p. 881-890.
- [29] Mahajan, R., Koros, W.J., "Mixed matrix membrane materials with glassy polymers. Part II", *Polymer Engineering and Science*, 42, 2002, p. 1432-1440.
- [30] Moore, T.T., Koros, W.J., "Non-ideal effects in organic-inorganic materials for gas separation membranes", *Journal of Molecular Structure*, 739, 2005, p. 87-98.
- [31] Li, Y., Chung, T., Cao, C., Kulprathipanja, S., "The effects of polymer chain rigidification, zeolite pore size and pore blockage on polyethersulfone (PES)-zeolite 4A mixed matrix membranes", *Journal of Membrane Science*, 260, 2005, p. 45-55.

- [32] Huang, Z., Li, Y., Wen, R., Teoh, M.M., Kulprathipanja, S., "Enhanced gas separation properties by using nanostructured PES-zeolite 4A mixed matrix membranes", *Journal of Applied Polymer Science*, 101, 2006, p. 3800-3805.
- [33] Hu, C.C., Liu, T.C., Lee, K.R., Ruan, R.C., Lai, J.Y., "Zeolite-filled PMMA composite membranes: influence of coupling agent addition on gas separation properties", *Desalination*, 193, 2006, p. 14-24.
- [34] Mahajan, R., Koros, W.J., "Mixed matrix membrane materials with glassy polymers. Part I", *Polymer Engineering and Science*, 42, 2002, p. 1420-1431.
- [35] Maeda, Y., Paul, D.R., "Effect of antiplasticization on selectivity and productivity of gas separation membranes", *Journal of Membrane Science*, 30, 1987, p. 1-9.
- [36] Larocca, N.M., Pessan, L.A., "Effect of antiplasticization on the volumetric, gas sorption and transport properties of polyetherimide", *Journal of Membrane Science*, 218, 2003, p. 69-92.
- [37] Barbari, T.A., Koros, W.J., Paul, D.R., "Gas transport in polymers based on bisphenol-A", *Journal of Polymer Science Part B: Polymer Physics*, 26, 1988, p. 709-727.
- [38] Haraya, K., Hwang, S.T., "Permeation of Oxygen, Argon, and Nitrogen through polymer membranes", *Journal of Membrane Science*, 71, 1992, p. 13-27.
- [39] Chen, S.H., Ruan, R.C., Lai, J.Y., "Sorption and transport mechanism of gases in polycarbonate membranes", *Journal of Membrane Science*, 134, 1997, p. 143-150.

- [40] Koros, W.J., Walker, D.R.B., "Gas separation membrane selection criteria: weakly and strongly interacting feed component situations", *Polymer Journal*, 23, 1991, p. 481-490.
- [41] Sridhar, S., Aminabhavi, T.M., Ramakrishna, M., "Separation of binary mixtures of carbon dioxide and methane through sulfonated polycarbonate membranes", *Journal of Applied Polymer Science*, 105, 2007, p. 1749-1756.
- [42] Hacıoğlu, P., Toppare, L., Yılmaz, L., "Effect of preparation parameters on performance of dense homogenous polycarbonate gas separation membranes", *Journal of Applied Polymer Science*, 90, 2003, p. 776-785.
- [43] Yeom, C.K., Lee, S.H., Lee, J.M., "Study of transport of pure and mixed CO<sub>2</sub>/N<sub>2</sub> gases through polymeric membranes", *Journal of Applied Polymer Science*, 78, 2000, p. 179-189.
- [44] Wu, F., Li, L., Xu, Z., Tan, S., Zhang, Z., "Transport study of pure and mixed gases through PDMS membrane", *Chemical Engineering Journal*, 117, 2006, p. 51-59.
- [45] Chern, R.T., Koros, W.J., Yui, B., Hoppenberg, H.B., Stannett, V.T., "Selective permeation of CO<sub>2</sub> and CH<sub>4</sub> through Kapton Polyimide: Effects of penetrant competition and gas phase non-ideality", *Journal of Polymer Science: Polymer Physics Edition*, 22, 1984, p. 1061-1084.
- [46] Bos, A., Pünt, I.G.M., Wessling, M., Strathmann, H., "Plasticization-resistant glassy polyimide membranes for CO<sub>2</sub>/CH<sub>4</sub> separations", *Separation and Purification Technology*, 14, 1998, p. 27-39.
- [47] Bhattacharya, S., Hwang, S.T., "Concentration polarization, separation factor, and Peclet number in membrane processes", *Journal of Membrane Science*, 132, 1997, p. 73-90.

- [48] Tabe-Mohammadi, A., "A review of the applications of membrane separation technology in natural gas treatment", *Separation Science and Technology*, 34, 1999, p. 2095-2111.
- [49] Mahajan, R., Koros, W.J., Thundiyil, M., "Mixed matrix membranes: Important and challenging", *Membrane Technology*, 105, p. 6-8.
- [50] Koros, W.J., Mahajan, R., "Pushing the limits on possibilities for large scale gas separation: which strategies?", *Journal of Membrane Science*, 175, 2000, p. 181-196.
- [51] Koros, W.J., Fleming, G.K., "Membrane based gas separation", *Journal of Membrane Science*, 83, 1993, p. 1-80.
- [52] Ritter, J.A., Ebner, A.D., "State-of-the-art adsorption and membrane separation processes for hydrogen production in the chemical and petrochemical industries", *Separation Science and Technology*, 42, 2007, p. 1123-1193.
- [53] Favre, E., "Carbon dioxide recovery from post-combustion processes: Can gas permeation membranes compete with absorption ?", *Journal of Membrane Science*, 294, 2007, p. 50-59.
- [54] Dhingra, S.S., "Mixed gas transport study through polymeric membranes: A novel technique", PhD Thesis, Virginia Polytechnic Institute and State University, June 1997.
- [55] Powell, C.E., Qiao, G.G., "Polymeric CO<sub>2</sub>/N<sub>2</sub> gas separation membranes for the capture of carbon dioxide from power plant flue gases", *Journal of Membrane Science*, 279, 2006, p. 1-49.
- [56] Moore, T.T., "Effects of Materials, Processing, And Operating Conditions On The Morphology And Gas Transport Properties Of Mixed

Matrix Membranes", PhD Thesis, The University of Texas, December 2004.

- [57] Tantekin-Ersolmaz, B., Atalay-Oral, Ç., Tatlier, M., Erdem-Şenatalar, A., Schoeman, B., Sterte, J., "Effect of zeolite particle size on the performance of polymer-zeolite mixed matrix membranes", *Journal of Membrane Science*, 175, 2000, p. 285-288.
- [58] Tatlier, M., Tantekin-Ersolmaz, B., Atalay-Oral, Ç., Erdem-Şenatalar, A., "Power-law scaling behavior of membranes", *Journal of Membrane Science*, 182, 2001, p. 183-193.
- [59] Hennepe, H.J.C., Bargeman, D., Mulder, M.H.V., Smolders, C.A., "Zeolite-filled silicone rubber membranes Part 1. Membrane preparation and pervaporation results", *Journal of Membrane Science*, 35, 1987, p. 39-55.
- [60] Boom, J.P., Bargeman, D., Strathmann, H., "Zeolite filled membranes for gas separation and pervaporation", *Studies in Surface Science and Catalysis*, 84, 1994, p. 1167-1174.
- [61] Moore, T.T., Mahajan, R., Vu, D., Koros, W., "Hybrid membrane materials comprising organic polymers with rigid dispersed phases", *AIChE Journal*, 50, 2004, p. 311-321.
- [62] Wang, H., Holmberg, B.A., Yan, Y., "Homogenous polymer-zeolite nanocomposite membranes by incorporating dispersible template-removed zeolite nanocrystals", *Journal of Materials Chemistry*, 12, 2002, p. 3640-3643.
- [63] Pechar, T.W., Kim, S., Vaughan, B., Marand, E., Baranauskos, V., Riffle, J., Jeong, H.K., Tsapatsis, M., "Preparation and characterization

of poly(imide-siloxane) and zeolite L mixed matrix membrane”, *Journal of Membrane Science*, 277, 2006, p. 210-218.

- [64] Jackson, W.J., Caldwell, J.R., “Antiplasticization. II. Characteristics of antiplasticizers”, *Journal of Applied Polymer Science*, 11, 1967, p. 211-226.
- [65] Jackson, W.J., Caldwell, J.R., “Antiplasticization. III. Characteristics of antiplasticizers”, *Journal of Applied Polymer Science*, 11, 1967, p. 227-244.
- [66] Vrentas, J.S., Duda, J.L., Ling, H.C., “Antiplasticization and volumetric behavior in glassy polymers”, *Macromolecules*, 21, 1988, p. 1470-1475.
- [67] Anderson, S.L., Grulke, E.A., DeLassus, P.T., Smith, P.B., Kocher, C.W., Landes, B.G., “A model for antiplasticization in polystyrene”, *Macromolecules*, 28, 1995, p. 2944-2954.
- [68] Robeson, L.M., “The effect of antiplasticization on secondary loss transitions and permeability of polymers”, *Polymer Engineering and Science*, 9, 1969, p. 277-281.
- [69] Garcia, A., Iriarte, M., Uriarte, C., Iruin, J.J., Etxeberria, A., Rio, J., “Antiplasticization of a polyamide: a positron annihilation lifetime spectroscopy study”, *Polymer*, 45, 2004, p. 2949-2957.
- [70] Pant, B.G., Kulkarni, S.S., Panse, D.G., Joshi, S.G., “Modification of polystyrene barrier properties”, *Polymer*, 35, 1994, p. 2549-2553.
- [71] H. Ettouney, U. Majeed, Permeability functions for pure and mixture gases in silicone rubber and polysulfone membranes: Dependence on pressure and composition, *J. Membr. Sci.* 135 (1997) 251-261.

- [72] Kurdi, J., Kumar, A., "Performance of PEI/BMI semi-IPN membranes for separations of various binary gaseous mixtures", *Separation and Purification Technology*, 53, 2007, p. 301-311.
- [73] Sridhar, S., Smitha, B., Ramakrishna, M., Aminabhavi, T.M., "Modified poly(phenylene oxide) membranes for the separation of carbon dioxide from methane", *Journal of Membrane Science*, 280, 2006, p. 202-209.
- [74] Staudt-Bickel, C., Koros, W.J., "Improvement of CO<sub>2</sub>/CH<sub>4</sub> separation characteristics of polyimides by chemical crosslinking", *Journal of Membrane Science*, 155, 1999, p. 145-154.
- [75] Battal, T., Baç, N., Yilmaz, L., "Effect of feed composition on the performance of polymer-zeolite mixed matrix gas separation membranes", *Separation Science and Technology*, 30, 1995, p. 2365-2384.
- [76] Donohue, M.D., Minhas, B.S., Lee, S.Y., "Permeation behavior of carbon dioxide-methane mixtures in cellulose acetate membranes", *Journal of Membrane Science*, 42, 1989, p. 197-214.
- [77] Jordan, S.M., Koros, W.J., Fleming, G.K., "The effects of CO<sub>2</sub> exposure on pure and mixed gas permeation behavior: comparison of glassy polycarbonate and silicone rubber", *Journal of Membrane Science*, 30, 1987, p. 191-212.
- [78] Minhas, B.S., Matsuura, T., Sourirajan, S., "Formation of asymmetric cellulose acetate membranes for the separation of carbon dioxide-methane gas mixtures", *Industrial and Engineering Chemistry Research*, 26, 1987, p. 2344-2348.
- [79] Peterson, E.S., Stone, M.L., "Helium separation properties of phosphazene polymer membranes", *Journal of Membrane Science*, 86, 1994, p. 57-65.

- [80] Peterson, E.S, Stone, M.L., McCaffrey, R.R., Cummings, D.G., "Mixed-gas separation properties of phosphazene polymer membranes", *Separation Science and Technology*, 28, 1993, p. 423-440.
- [81] Cecopieri-Gómez, M.L., Palacios-Alquisira, J., Domínguez, J.M., "On the limits of gas separation in CO<sub>2</sub>/CH<sub>4</sub>, N<sub>2</sub>/CH<sub>4</sub> and CO<sub>2</sub>/N<sub>2</sub> binary mixtures using polyimide membranes", *Journal of Membrane Science*, 293, 2007, p. 53-65.
- [82] Kalıpçılar, H., "Modification of morphology of zeolite A for use as phosphate replacement in detergents", MSc Thesis, METU, September 1995.
- [83] Şen, D., "Effect of compatibilizers on the gas separation performance of polycarbonate membranes", MSc Thesis, METU, September 2003.
- [84] Weast, R.C., "CRC Handbook of Chemistry and Physics", The Chemical Rubber Company, 53rd Edition, Weast, R.C. (ed.), 1972, Ohio.
- [85] Koros, W.J., Vu, D.Q., Mahajan, R.V., Miller, S.J., "Gas separations using mixed matrix membranes", U.S. Patent 6503295, Chevron U.S.A. Incorporation, The University of Texas System, September 2000.
- [86] Koros, W.J., Vu, D.Q., Mahajan, R., Miller, S.J., "Mixed matrix membranes and methods for making the same", U.S. Patent 6585802, Chevron U.S.A. Incorporation, The University of Texas System, April 2001.
- [87] Campbell, D., Pethrick, R.A., White, J.R., "Polymer Characterization Physical Techniques", Stanley Thornes, Second edition, 2000.
- [88] Battal, T., "Separation of binary gas mixtures with zeolite-polymer mixed matrix membranes", MSc Thesis, METU, August 1994.



- [89] Hacıoğlu, P., "Effect of preparation parameters on the performance of dense homogenous polycarbonate and polypyrrole-polycarbonate mixed matrix membranes", MSc Thesis, METU, July 2001.
- [90] Pye, D.G., Hoehn, H.H., Panar, M., "Measurement of gas permeability of polymers. I. Permeabilities in constant volume/variable pressure apparatus", *Journal of Applied Polymer Science*, 20, 1976, p. 287-301.
- [91] Aguillar-Vega, M., Paul, D.R., "Gas transport properties of polycarbonates and polysulfones with aromatic substitutions on the bisphenol connector group", *Journal of Polymer Science Part B: Polymer Physics*, 31, 1993, p. 1599-1610.
- [92] Billmeyer, F.W., "Textbook of Polymer Science", John Wiley and Sons, 1962, New York.
- [93] Rubin, I., "Handbook of Plastics Materials and Technology", Wiley Interscience, 1990.
- [94] Breck, D.W., "Zeolite Molecular Sieves", John Wiley & Sons Incorporation, 1974, Toronto.
- [95] Moe, M., Koros, W.J., Hoehn, H.H., Husk, G.R., "Effects of film history on gas transport in a fluorinated aromatic polyimide", *Journal of Applied Polymer Science*, 36, 1988, p. 1833-1846.
- [96] Recio, R., Palacio, L., Pr'adanos, P., Hern'andez, A., Lozano, A.E., Marcos, A., Campa, J.G., Abajo, J., "Gas separation of 6FDA-6FpDA membranes: Effect of the solvent on polymer surfaces and permselectivity", *Journal of Membrane Science*, 293, 2007, p. 22-28.
- [97] Jansen, J.C., Macchione, M., Drioli, E., "On the unusual solvent retention and the effect on the gas transport in perfluorinated Hyflon AD membranes", *Journal of Membrane Science*, 287, 2007, p. 132-137.

- [98] Tsujita, Y., "Membrane Science and Technology", Dekker, Osada Y. And Nakagawo T. (Eds.), 1992, New York, p. 3-57.
- [99] Queiroz, S.M., Machado, J.C., Porto, A.O., Silva, G.G., "Positron annihilation and differential scanning calorimetry studies of plasticized poly(ethylene oxide)", *Polymer*, 42, 2001, p. 3095-3101.
- [100] López-Martínez, E.I., Márquez-Lucero, A., Hernández-Escobar, C.A., Flores-Gallardo, S.G., Ibarra-Gómez, R., Yacamán, M.J., Zaragoza-Contreras, E.A., "Incorporation of silver/carbon nanoparticles into poly(methyl methacrylate) via in situ miniemulsion polymerization and its influence on the glass transition temperature", *Journal of Applied Polymer Science Part B: Polymer Physics*, 45, 2007, p. 511-518.
- [101] Qiao, X., Chung, T.S., Rajagopalan, R., "Zeolite filled P84 co-polyimide membranes for dehydration of isopropanol through pervaporation process", *Chemical Engineering Science*, 61, 2006, p. 6816-6827.
- [102] Şen, D., Kalıpçılar, H., Yılmaz, L., "Development of polycarbonate based zeolite 4A filled mixed matrix gas separation membranes", *Journal of Membrane Science*, 303, 2007, p. 194-203.
- [103] Chio, J.S., Paul, D.R., "Effects of CO<sub>2</sub> exposure on gas transport properties of glassy polymers", *Journal of Membrane Science*, 32, 1987, p. 195-201.
- [104] Wonders, A.G., Paul, D.R., "Effects of CO<sub>2</sub> exposure history on sorption and transport in polycarbonate", *Journal of Membrane Science*, 5, 1979, p. 63-71.
- [105] Joly, C., Cerf, D.L., Chappey, C., Langevin, D., Muller, G., "Residual solvent effect on the permeation properties of fluorinated polyimide films", *Separation and Purification Technology*, 16, 1999, p. 47-54.

- [106] Aoki, K., Kusakabe, K., Morooka, S., "Separation of gases with an A-type zeolite membrane", *Industrial and Engineering Chemistry Research*, 39, 2000, p. 2245-2251.
- [107] Zhu, W., Gora, L., Berg, A.W.C., Kapteijn, F., Jansen, J.C., Moulijn, J.A., "Water vapour separation from permanent gases by a zeolite-4A membrane", *Journal of Membrane Science*, 253, 2005, p. 57-66.
- [108] Hradil, J., Krystl, V., Hrabànek, P., Bernauer, B., Kočířík, M., "Heterogenous membranes based on polymeric adsorbents for separation of small molecules", *Reactive and Functional Polymers*, 61, 2004, p. 303-313.
- [109] Krystl, V., Hradil, J., Bernauer, B., Kočířík, M., "Heterogenous membranes based on zeolites for separation of small molecules", *Reactive and Functional Polymers*, 48, 2001, p.129-139.

## APPENDIX A

### XRD PATTERN OF SYNTHESIZED ZEOLITE 4A POWDER

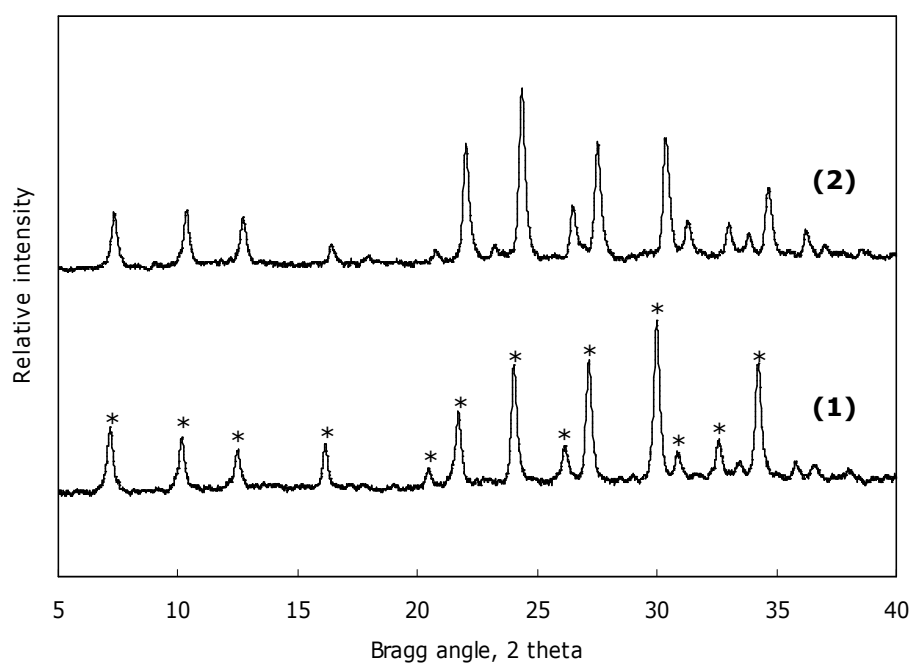


Figure A.1 XRD patterns of zeolite 4A crystals: (1) commercial zeolite 4A (Acros), (2) synthesized zeolite 4A. The marked peaks are the characteristics peaks of zeolite 4A.

## **APPENDIX B**

### **CALCULATION OF SINGLE GAS PERMEABILITIES**

Pressure change with respect to time data points were taken with certain time intervals. This time intervals were changed with respect to gases used. For fast gases, hydrogen, oxygen and carbon dioxide this interval was in the range of 15-200 minutes; for slow gases nitrogen and methane this interval was 1000-2000 minutes. From the slope of pressure versus time graphs permeabilities were calculated according to the algorithm given in Figure B.1.

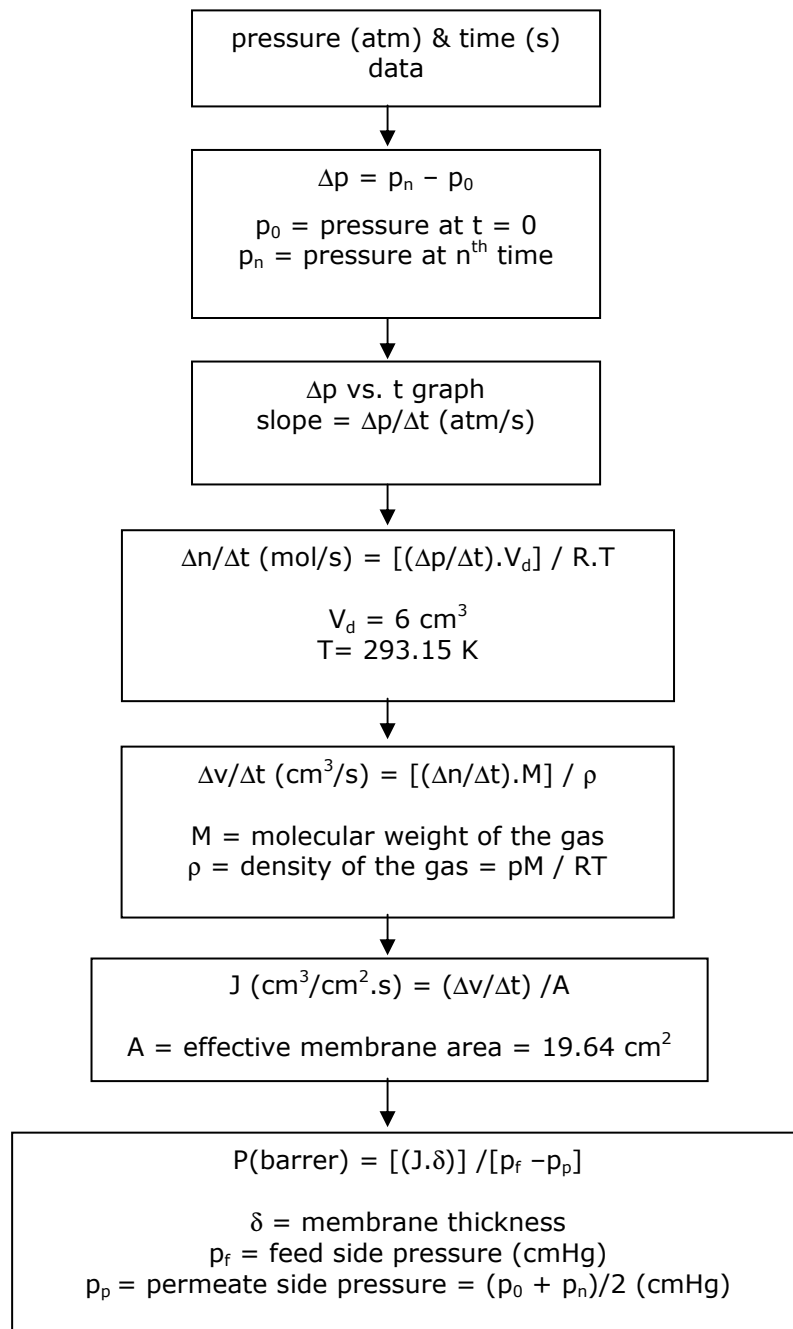


Figure B.1 Algorithm for single gas permeability calculation.

## APPENDIX C

### DETERMINATION OF DEAD VOLUME

Dead volume is the volume that the permeate gas stream occupies in the low pressure side of the membrane cell. It includes the volume of the permeate side of the membrane cell, and the volume of the tubings and valves up to gas chromatograph and pressure gauge in the permeate side. Since the calculated permeabilities are directly proportional to the dead volume,  $V_d$ , any error in its measurement affects all of the reported gas and/or gas mixture permeabilities. Therefore, its precise measurement is very important.

Dead volume of the set-up was first determined by measuring and calculating the volume of all parts, i.e. tubings and valves, of dead volume. Although the dead volume created by the membrane and filter paper in the membrane cell could not be included in this method, it gave an idea about the magnitude of dead volume. The measured dead volume was in the range of 20 – 25 cm<sup>3</sup>. Then, the measured values were confirmed by conducting single gas permeability experiments in the set-up with standard membranes of known permeabilities. Polycarbonate, PC, and polyethersulfone, PES, membranes were used as standard test membranes. Their single gas permeabilities for N<sub>2</sub>, CH<sub>4</sub>, O<sub>2</sub>, H<sub>2</sub> and CH<sub>4</sub>, were previously measured in our single gas permeation setup. By knowing the single gas permeability values of each gas through these membranes, pressure-time data of each gas was collected in the set-up and a reverse permeability calculation was performed to find the dead volume of the set-up. Dead volume was found as 21 cm<sup>3</sup> and 22 cm<sup>3</sup> during the permeability measurements with pure PC membrane and pure PES

membrane, respectively. Thus, the average of all measurements, which was 22 cm<sup>3</sup>, was taken as dead volume in permeability calculations.



## **APPENDIX D**

### **CALIBRATION OF GC AND TYPICAL GAS CHROMATOGRAMS FOR DIFFERENT BINARY GAS PAIRS**

#### **D.1 Calibration of GC**

As mentioned in the experimental section, for the analysis of gas composition, gas chromatograph was calibrated for CO<sub>2</sub>, CH<sub>4</sub>, N<sub>2</sub> and H<sub>2</sub> gases. For this purpose, each gas was fed to the GC separately at several pressures, which were varied between 0-100 Torr, and the corresponding area under the peaks were recorded. For each gas, pressure versus area counts graphs were plotted as pure gas calibration curves. From the chromatogram of the binary gas mixtures, areas corresponding to each gas component were used to find the partial pressures from these pure gas calibration curves. Pure gas calibration curves for CO<sub>2</sub>, CH<sub>4</sub>, N<sub>2</sub> and H<sub>2</sub> are shown in Figures D.1.1 to D.1.4.

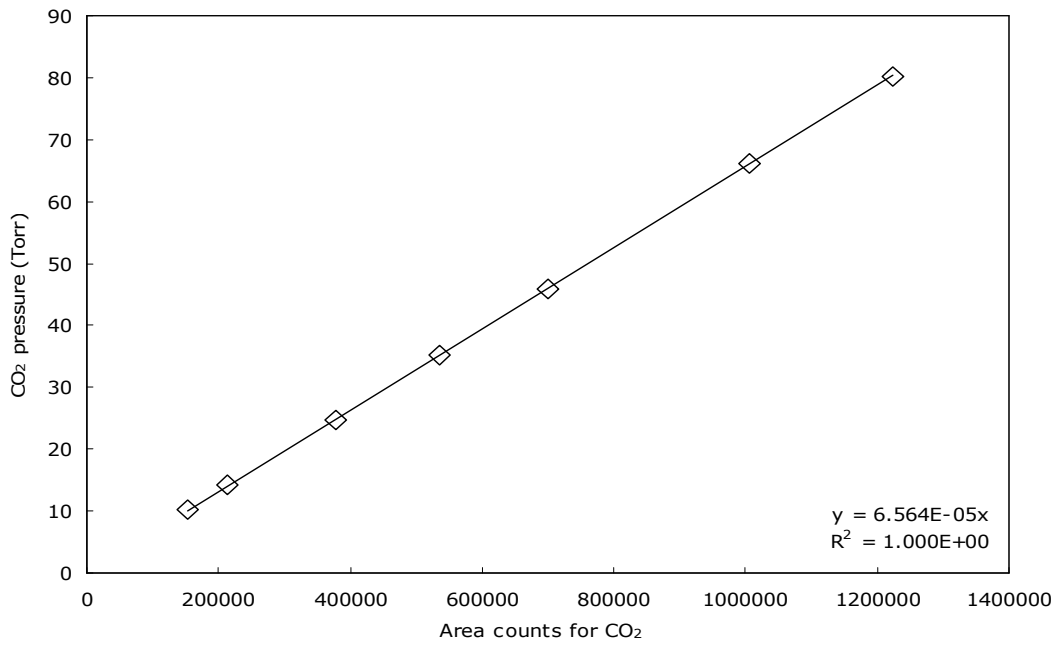


Figure D.1.1 Calibration plot of carbon dioxide for GC analysis.

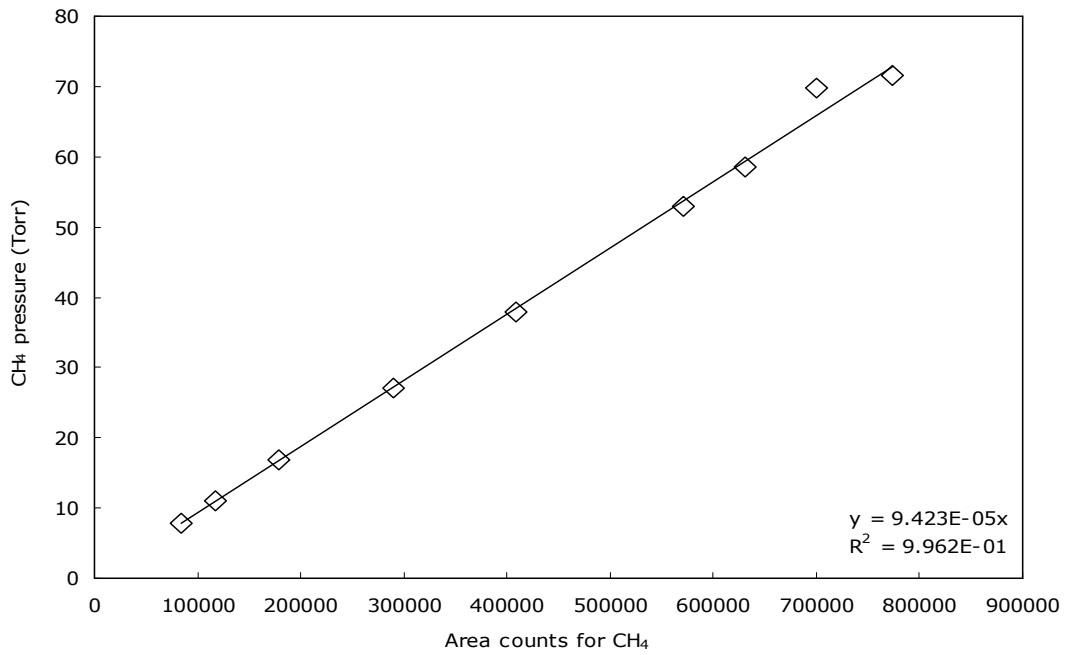


Figure D.1.2 Calibration plot of methane for GC analysis.

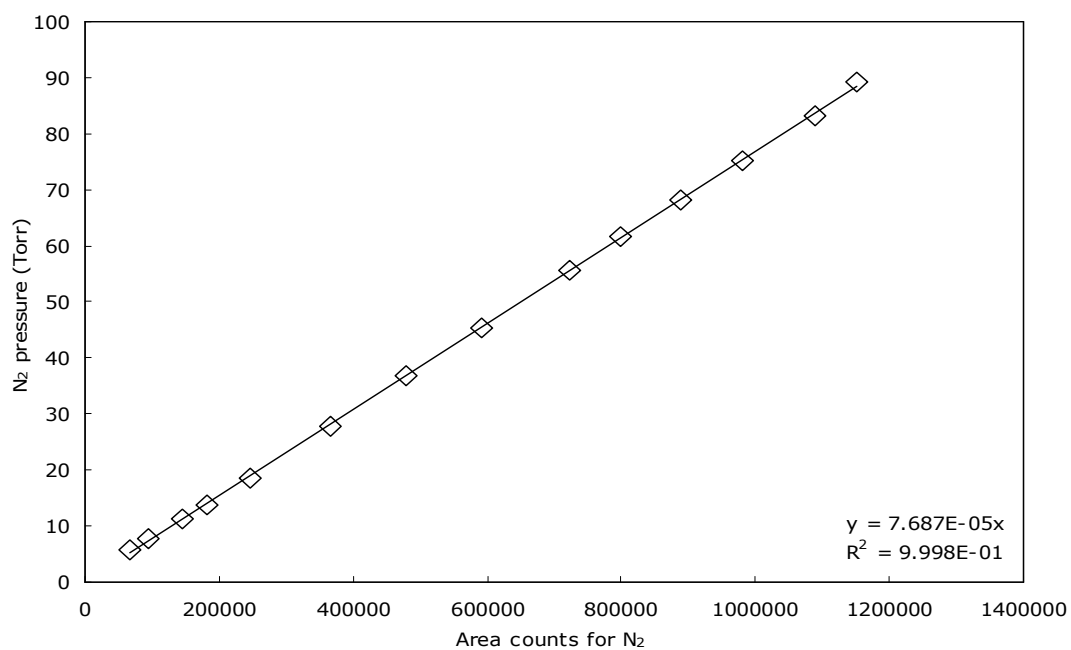


Figure D.1.3 Calibration plot of nitrogen for GC analysis.

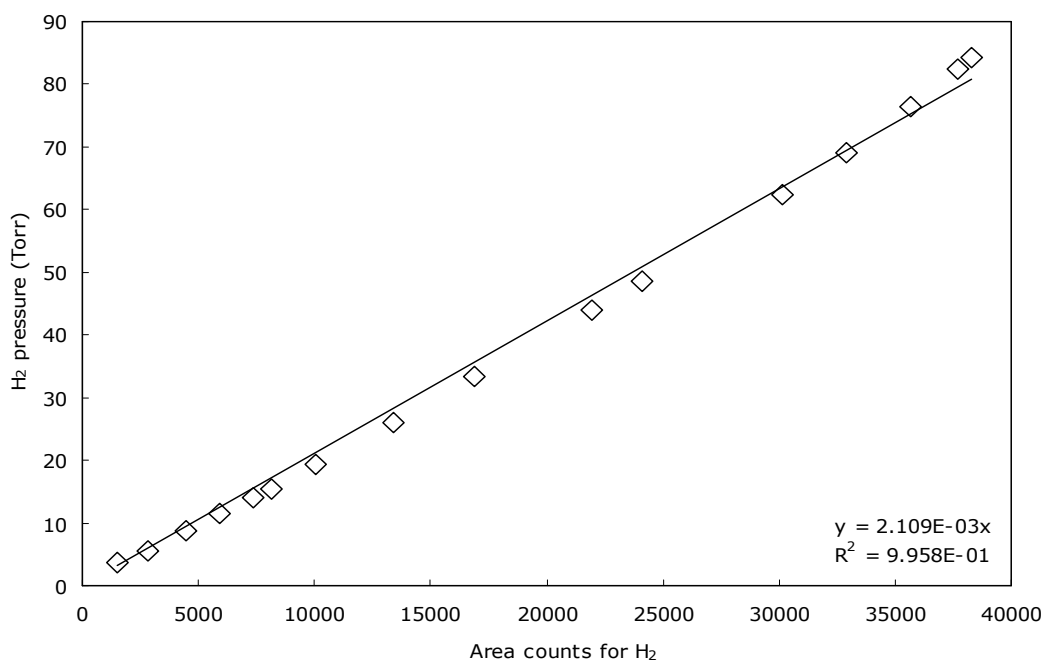


Figure D.1.4 Calibration plot of hydrogen for GC analysis.

## D.2 Typical Gas Chromatograms

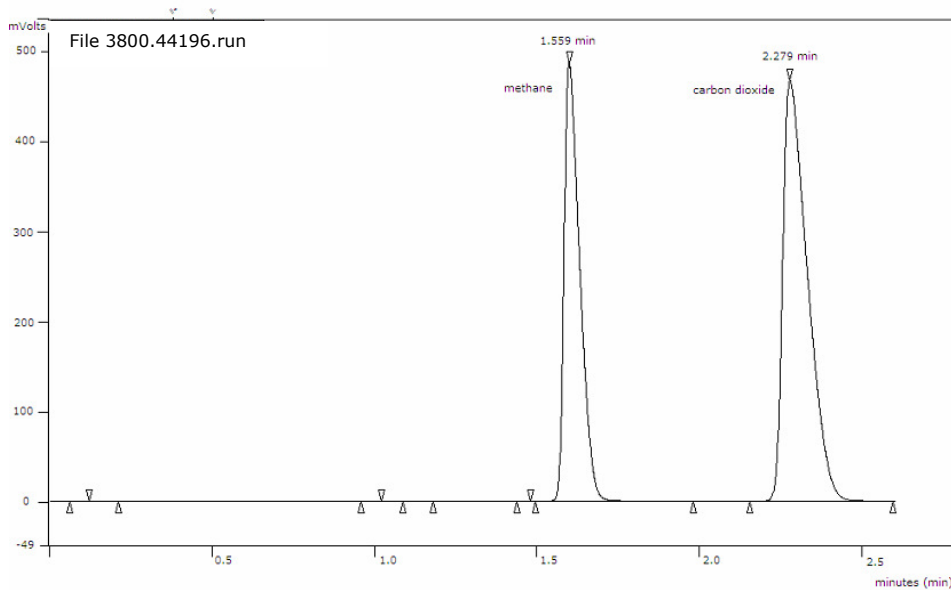


Figure D.2.1 Sample GC output for carbon dioxide-methane mixture. First peak (retention time is 1.559 min) corresponds to methane and the second peak (retention time is 2.279 min) corresponds to carbon dioxide.

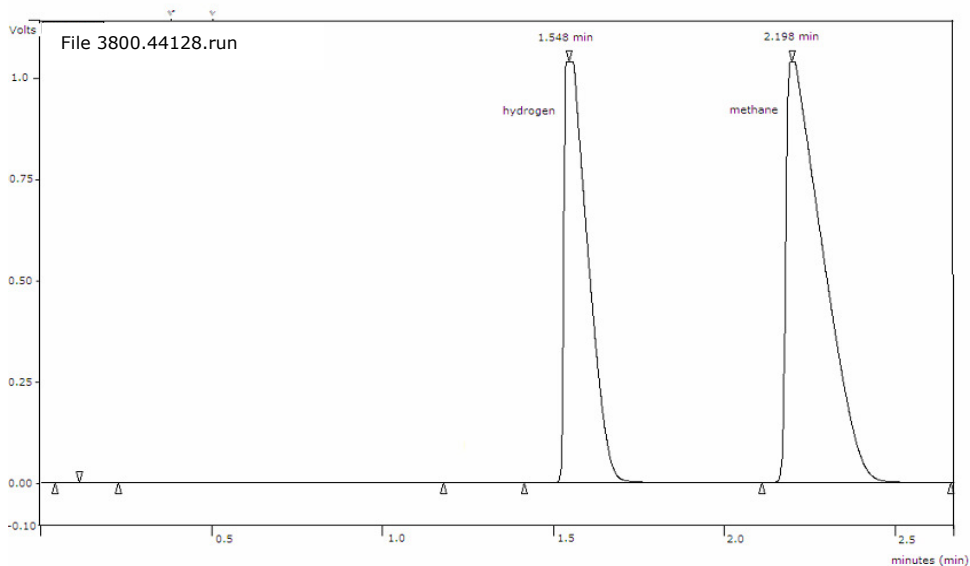


Figure D.2.2 Sample GC output for hydrogen-methane mixture. First peak (retention time is 1.548 min) corresponds to hydrogen and the second peak (retention time is 2.198 min) corresponds to methane.

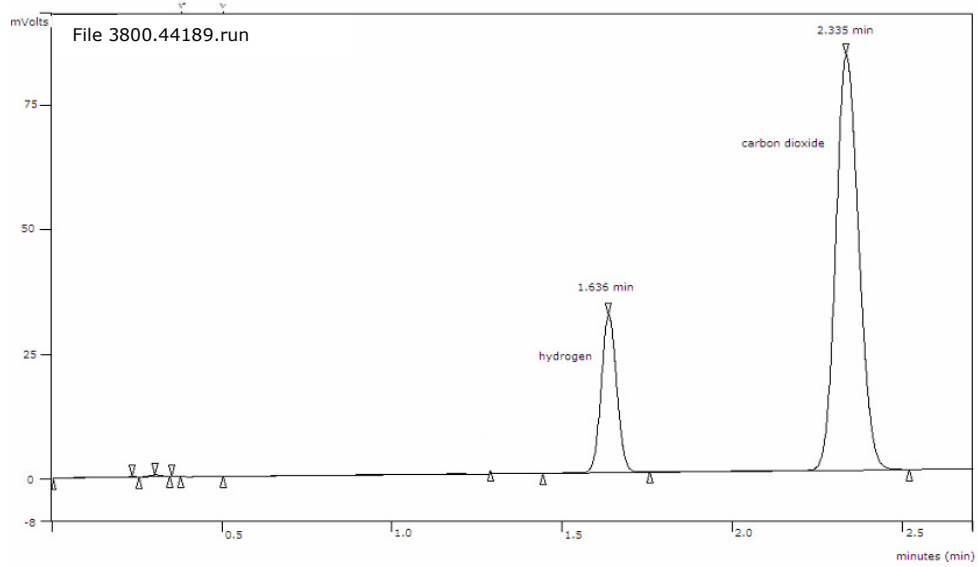


Figure D.2.3 Sample GC output for hydrogen-carbon dioxide mixture. First peak (retention time is 1.636 min) corresponds to hydrogen and the second peak (retention time is 2.335 min) corresponds to carbon dioxide.

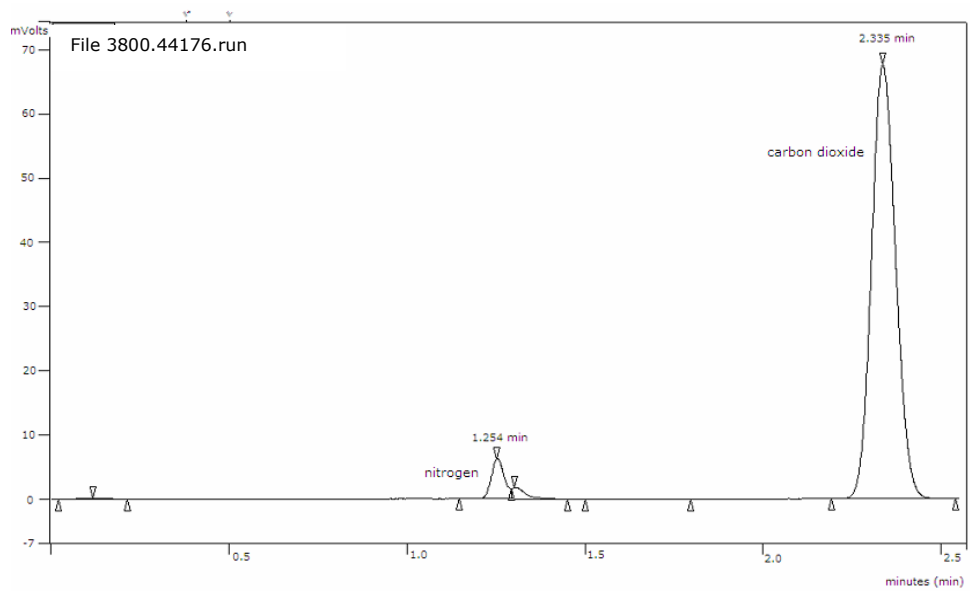


Figure D.2.4 Sample GC output for nitrogen-carbon dioxide mixture. First peak (retention time is 1.254 min) corresponds to nitrogen and the second peak (retention time is 2.335 min) corresponds to carbon dioxide.

## APPENDIX E

### A SAMPLE CALCULATION FOR THE DETERMINATION OF PERMEABILITIES AND SELECTIVITIES OF BINARY GAS MIXTURES

Membrane: PC/pNA (2%) blend membrane

Membrane thickness: 70  $\mu\text{m}$

Gas mixture:  $\text{CO}_2$ - $\text{CH}_4$  binary

Feed composition: 50/50

System temperature: 22  $^\circ\text{C}$

Feed side analysis at 2353 mbar (1765.19 Torr) – 1<sup>st</sup> analysis

GC outputs:

Area counts for  $\text{CH}_4$  = 8840805                      Retention time for  $\text{CH}_4$  = 1.493 min.

Area counts for  $\text{CO}_2$  = 14319726                      Retention time for  $\text{CO}_2$  = 2.112 min.

By using pure gas calibration curve equations;

Partial pressure of  $\text{CO}_2 = P_{\text{CO}_2, \text{feed}} = 0.00006509 * (\text{area counts of } \text{CO}_2)$

Partial pressure of  $\text{CH}_4 = P_{\text{CH}_4, \text{feed}} = 0.00009423 * (\text{area counts of } \text{CH}_4)$

$$P_{\text{CO}_2, \text{feed}} = 0.00006509 * (14319726) = 932.07 \text{ Torr} \quad (\text{E.1})$$

$$P_{\text{CH}_4, \text{feed}} = 0.00009423 * (8840805) = 833.07 \text{ Torr} \quad (\text{E.2})$$

$$x_{\text{CO}_2, \text{feed}} = (P_{\text{CO}_2, \text{feed}}) / (\text{feed pressure}) \quad (\text{E.3})$$

$$x_{\text{CH}_4, \text{feed}} = (P_{\text{CH}_4, \text{feed}}) / (\text{feed pressure}) \quad (\text{E.4})$$

$$x_{CO_2,feed} = 932.07 / 1765.19 = 0.528 \text{ (52.8 \%)} \quad (E.5)$$

$$x_{CH_4,feed} = 833.07 / 1765.19 = 0.472 \text{ (47.2 \%)} \quad (E.6)$$

Feed side analysis at 2309 mbar (1731.74 Torr) – 2<sup>nd</sup> analysis

GC outputs:

Area counts for CH<sub>4</sub>= 8675170                      Retention time for CH<sub>4</sub>= 1.485 min.

Area counts for CO<sub>2</sub>= 14045938                      Retention time for CO<sub>2</sub>= 2.112 min.

$$P_{CO_2,feed} = 0.00006509*(14045938) = 914.25 \text{ Torr} \quad (E.7)$$

$$P_{CH_4,feed} = 0.00009423*(8675170) = 817.46 \text{ Torr} \quad (E.8)$$

$$x_{CO_2,feed} = 914.25 / 1731.74 = 0.528 \text{ (52.8 \%)} \quad (E.9)$$

$$x_{CH_4,feed} = 817.46 / 1731.74 = 0.472 \text{ (47.2 \%)} \quad (E.10)$$

**Before permeation started,**

Feed composition                      : CO<sub>2</sub>= 52.8% , CH<sub>4</sub>= 47.2%

Feed side pressure                      : 2 barg (2.93 atm)

Permeate side pressure                      : high vacuum (0.02 Torr)

Permeate side analysis at 67.21 Torr – 1<sup>st</sup> analysis

GC outputs:

Area counts for CH<sub>4</sub>= 13951                      Retention time for CH<sub>4</sub>= 1.642 min.

Area counts for CO<sub>2</sub>= 1010747                      Retention time for CO<sub>2</sub>= 2.323 min.

$$P_{CO_2,permeate} = 0.00006509*(1010747) = 65.790 \text{ Torr} \quad (E.11)$$

$$P_{CH_4,permeate} = 0.00009423*(13951) = 1.315 \text{ Torr} \quad (E.12)$$

$$x_{CO_2,permeate} = 65.790 / 67.21 = 0.979 \text{ (97.9\%)} \quad (E.13)$$

$$x_{CH_4,permeate} = 1.315 / 67.21 = 0.019 \text{ (1.9\%)} \quad (E.14)$$

normalized %CO<sub>2</sub> in permeate = (97.9/99.8) \* 100 = 98.1%

normalized %CH<sub>4</sub> in permeate = (1.9/99.8) \* 100 = 1.9%

### Permeate side analysis at 56.91 Torr – 2<sup>nd</sup> analysis

GC outputs:

Area counts for CH<sub>4</sub>= 11777

Retention time for CH<sub>4</sub>= 1.641 min.

Area counts for CO<sub>2</sub>= 852650

Retention time for CO<sub>2</sub>= 2.327 min.

$$P_{CO_2\text{permeate}} = 0.00006509*(852650) = 55.499 \text{ Torr} \quad (\text{E.15})$$

$$P_{CH_4\text{permeate}} = 0.00009423*(11777) = 1.110 \text{ Torr} \quad (\text{E.16})$$

$$x_{CO_2\text{permeate}} = 55.499 / 56.91 = 0.975 \text{ (97.5\%)} \quad (\text{E.17})$$

$$x_{CH_4\text{permeate}} = 1.110 / 56.91 = 0.019 \text{ (1.9\%)} \quad (\text{E.18})$$

normalized %CO<sub>2</sub> in permeate = (97.5/99.4) \* 100 = 98.09%

normalized %CH<sub>4</sub> in permeate = (1.9/99.4) \* 100 = 1.91%

#### **After permeation (20 hours),**

Feed composition : CO<sub>2</sub>= 52.8% , CH<sub>4</sub>= 47.2%

Permeate composition : CO<sub>2</sub>= 98.1%, CH<sub>4</sub>= 1.9%

Feed side pressure : 2 barg (2.93 atm)

Permeate side pressure : 95 Torr

Separation selectivity is the ratio of mol fractions of gases in the permeate and feed side;

$$\alpha_{ij} = ((x_i / x_j)_{\text{permeate}} / (x_i / x_j)_{\text{feed}}) \quad (\text{E.19})$$

$$\alpha_{CO_2/CH_4} = [(0.981/0.019)/(0.528/0.472)] \quad (\text{E.20})$$

$$\alpha_{CO_2/CH_4} = 46.2 \quad (\text{E.21})$$

The permeability of each gas in binary gas mixture was calculated by using the pressure versus time data of binary gas mixture. The slope of this graph, dp/dt, was split into individual dp/dt data for each gas. In Figure E.1 pressure vs. time graph of CO<sub>2</sub>-CH<sub>4</sub> binary gas mixture through PC/pNA (2%) blend membrane was illustrated. Table E.1 listed the feed and permeate side conditions before and after permeation.



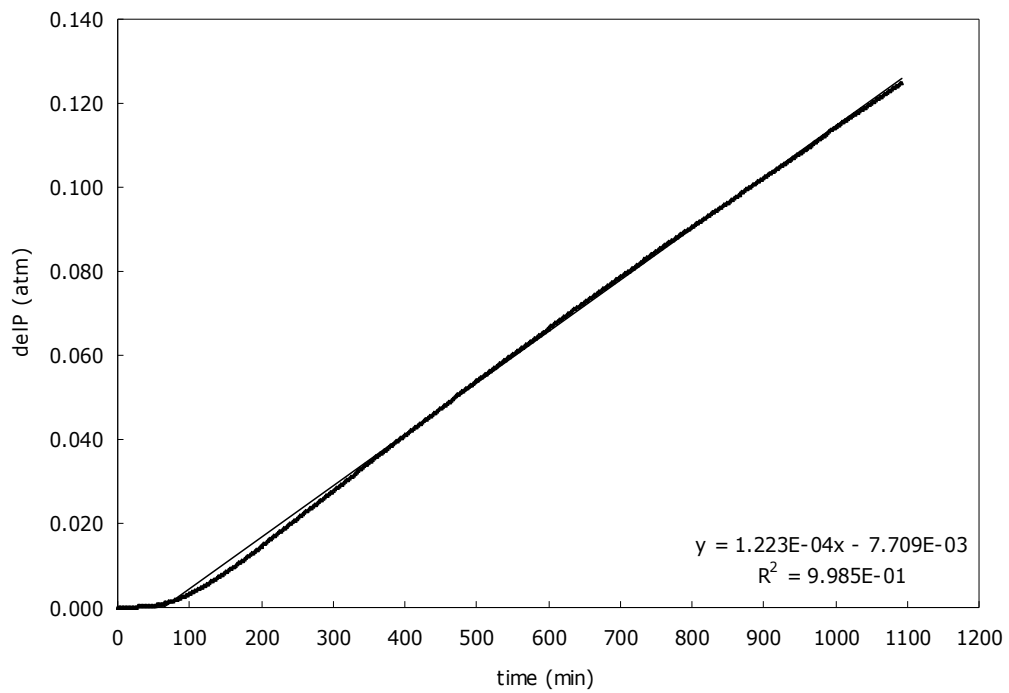


Figure E.1 Pressure difference vs. time graph for CO<sub>2</sub>-CH<sub>4</sub> binary gas mixture through PC/pNA (2%) blend membrane.

Table E.1 Feed and permeate side pressures and compositions.

	Before permeation	After permeation
Feed pressure	2 barg (2.91 atm)	2 barg (2.91 atm)
Permeate pressure	0.02 Torr ( $2.63 \times 10^{-5}$ atm)	95 Torr (0.125 atm)
Feed composition	$x_{CO_2} = 0.528$ $x_{CH_4} = 0.472$	$x_{CO_2} = 0.528$ $x_{CH_4} = 0.472$
Permeate composition	-	$y_{CO_2} = 0.981$ $y_{CH_4} = 0.019$

$$\left(\frac{dp}{dt}\right)_{CO_2-CH_4} = 1.223*10^{-4} \text{ atm/min} \quad (\text{E.22})$$

$$\left(\frac{dp}{dt}\right)_{CO_2} = \left(\frac{dp}{dt}\right)_{CO_2-CH_4} * y_{CO_2} = 1.199*10^{-4} \text{ atm/min} \quad (\text{E.23})$$

$$\left(\frac{dp}{dt}\right)_{CH_4} = \left(\frac{dp}{dt}\right)_{CO_2-CH_4} * y_{CH_4} = 2.324*10^{-6} \text{ atm/min} \quad (\text{E.24})$$

Partial pressures of each component in the feed and permeate side were also calculated;

$$P_{CO_2,feed} = P_{feed} * x_{CO_2} = 2.91 \text{ atm} * 0.528 = 1.536 \text{ atm} \quad (\text{E.25})$$

$$P_{CH_4,feed} = P_{feed} * x_{CH_4} = 2.91 \text{ atm} * 0.472 = 1.374 \text{ atm} \quad (\text{E.26})$$

$$P_{CO_2,permeate} = P_{permeate} * y_{CO_2} = 2.63*10^{-5} \text{ atm} * 0.981 = 2.58*10^{-5} \text{ atm (initial)}$$

$$P_{CO_2,permeate} = P_{permeate} * y_{CO_2} = 0.125 \text{ atm} * 0.981 = 0.123 \text{ atm (final)}$$

$$P_{CO_2,permeate-average} = (2.58*10^{-5} \text{ atm} + 0.123 \text{ atm})/2 = 0.0615 \text{ atm} \quad (\text{E.27})$$

$$P_{CH_4,permeate} = P_{permeate} * y_{CH_4} = 2.63*10^{-5} \text{ atm} * 0.019 = 4.99*10^{-7} \text{ atm (initial)}$$

$$P_{CH_4,permeate} = P_{permeate} * y_{CH_4} = 0.125 \text{ atm} * 0.019 = 2.375*10^{-3} \text{ atm (final)}$$

$$P_{CH_4,permeate-average} = (4.99*10^{-7} \text{ atm} + 2.375*10^{-3} \text{ atm})/2 = 1.188*10^{-3} \text{ atm}$$

After calculation of the individual dp/dt data for each gas and their partial pressures at the permeate and feed side, the permeability of each gas was calculated according to the algorithm given in Appendix 2. Only the dead-end volume of the system, which was measured as 22 cm<sup>3</sup>, and the effective membrane area, which was calculated as 9.6 cm<sup>2</sup>, were different in the algorithm.

At the last step permeability becomes,

$$P_{CO_2}(\text{Barrer}) = \left[ \frac{J_{CO_2} * \delta}{P_{CO_2,feed} - P_{CO_2,permeate-avg}} \right] \quad (\text{E.28})$$

$$P_{CH_4}(\text{Barrer}) = \left[ \frac{J_{CH_4} * \delta}{P_{CH_4 \text{ feed}} - P_{CH_4 \text{ permeate-avg}}} \right] \quad (\text{E.29})$$

$$P_{CO_2} = 2.84 \text{ Barrer} \quad (\text{E.30})$$

$$P_{CH_4} = 0.060 \text{ Barrer} \quad (\text{E.31})$$

## APPENDIX F

### THERMAL GRAVIMETRY ANALYSIS GRAPHS

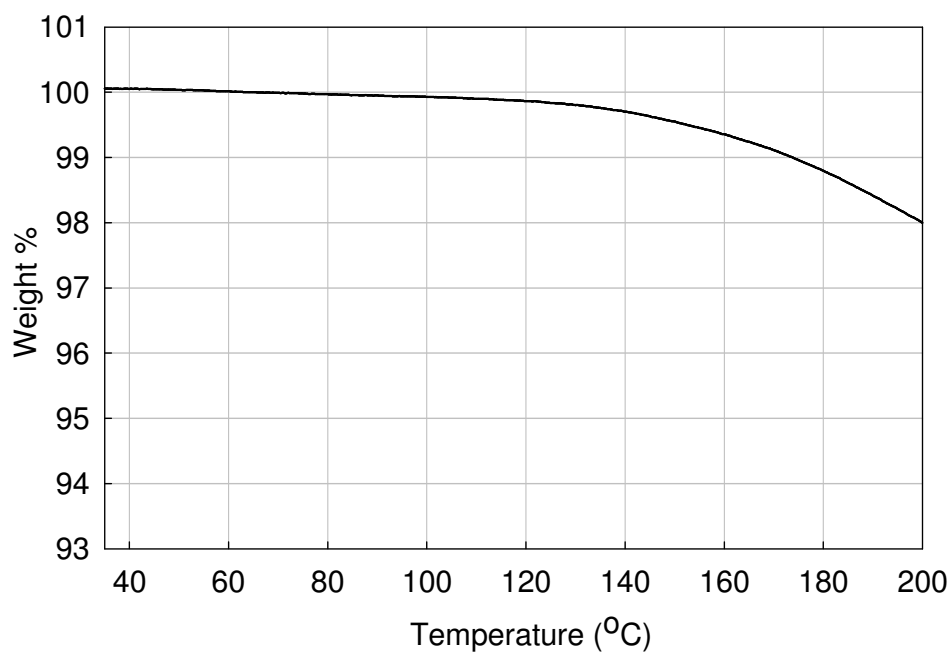


Figure F.1 The TGA graph for PC/pNA (5%) blend membrane.

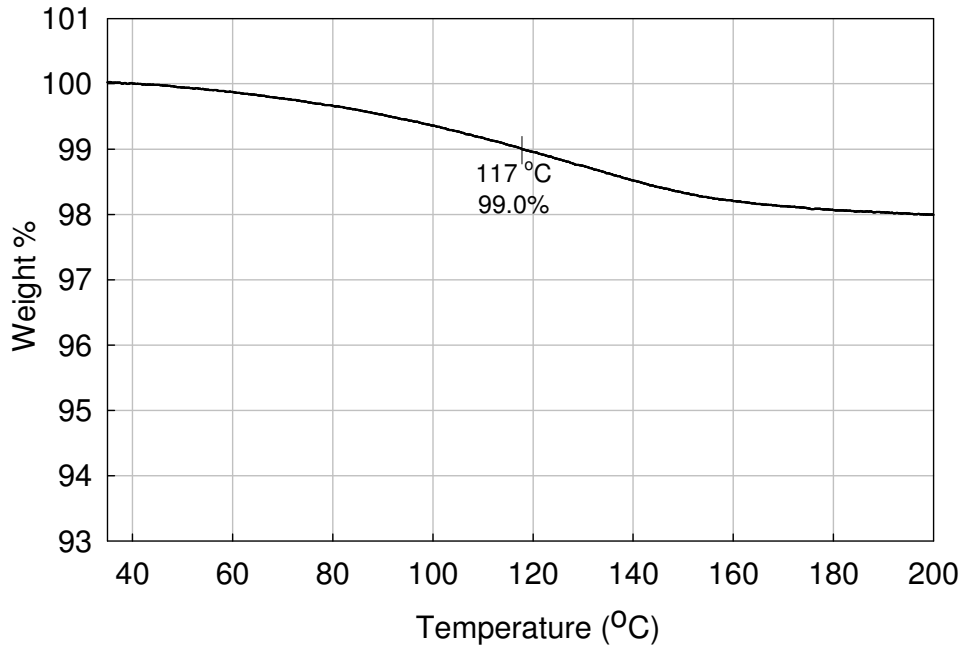


Figure F.2 The TGA graph for PC/zeolite 4A (10%) MMM.

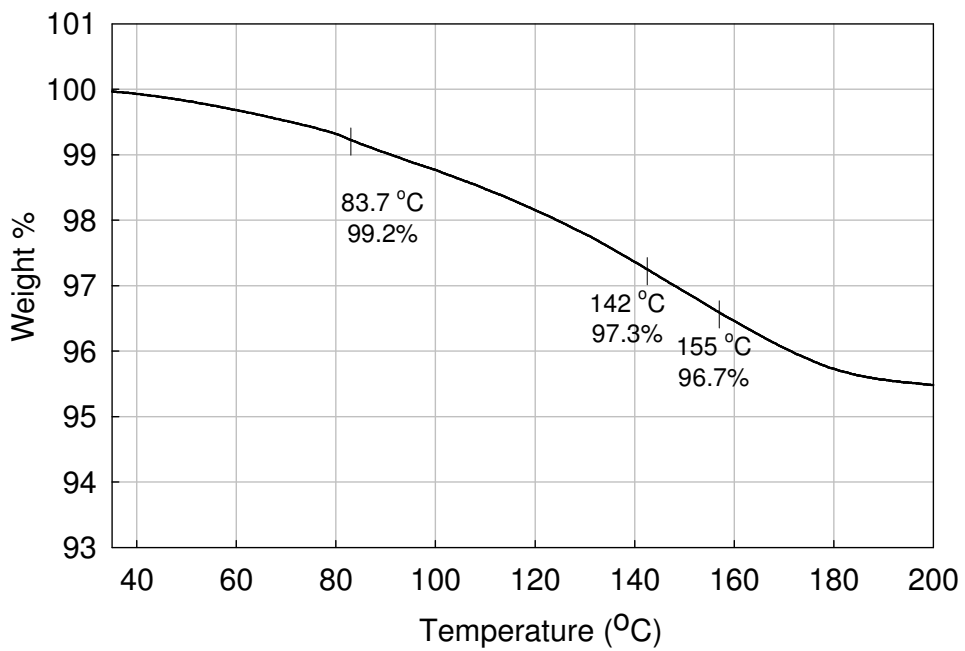


Figure F.3 The TGA graph for PC/zeolite 4A (30%) MMM.

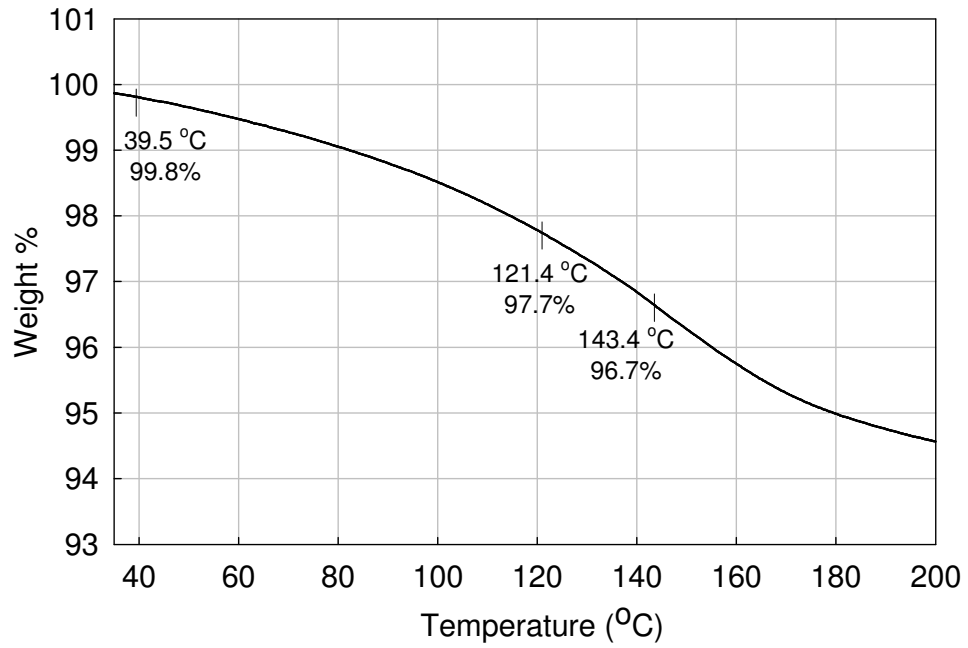


Figure F.4 The TGA graph for PC/pNA (2%)/zeolite 4A (30%) MMM.

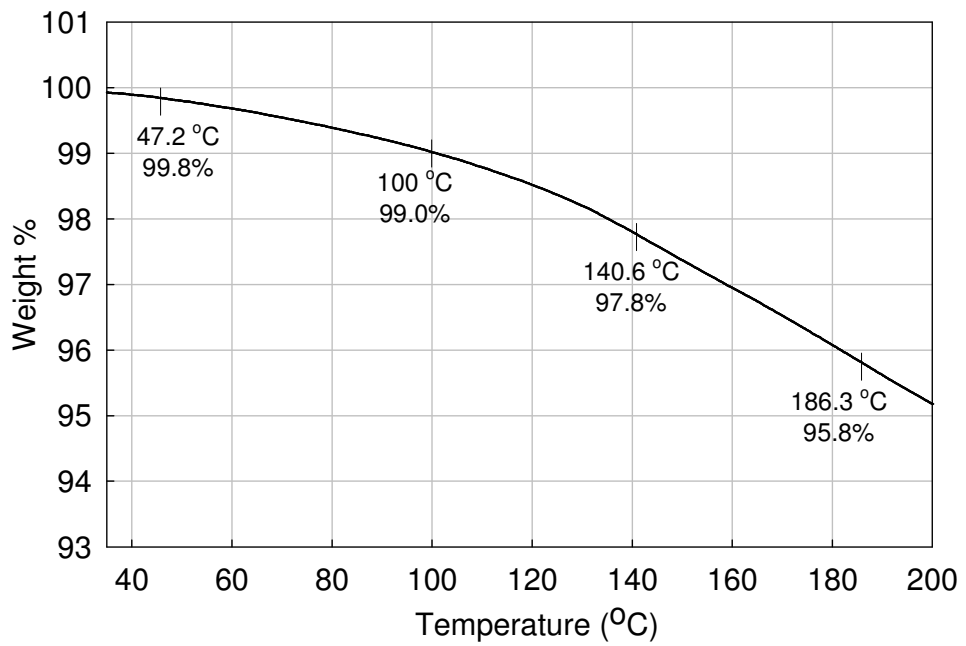


Figure F.5 The TGA graph for PC/pNA (5%)/zeolite 4A (20%) MMM.

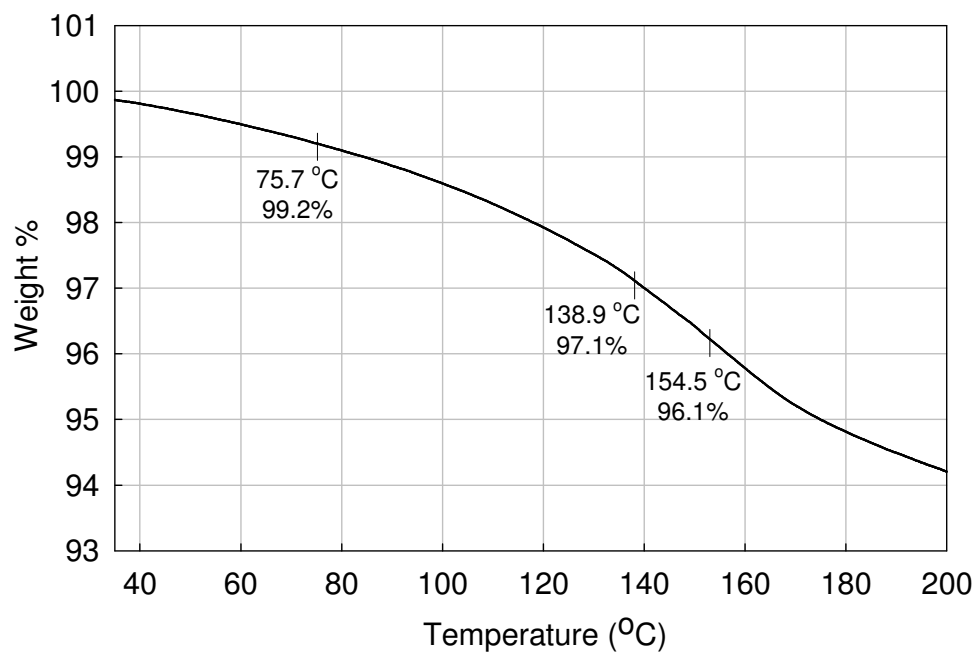


Figure F.6 The TGA graph for PC/pNA (5%)/zeolite 4A (30%) MMM.

## APPENDIX G

### SAMPLE DSC THERMOGRAMS OF THE PREPARED MEMBRANES

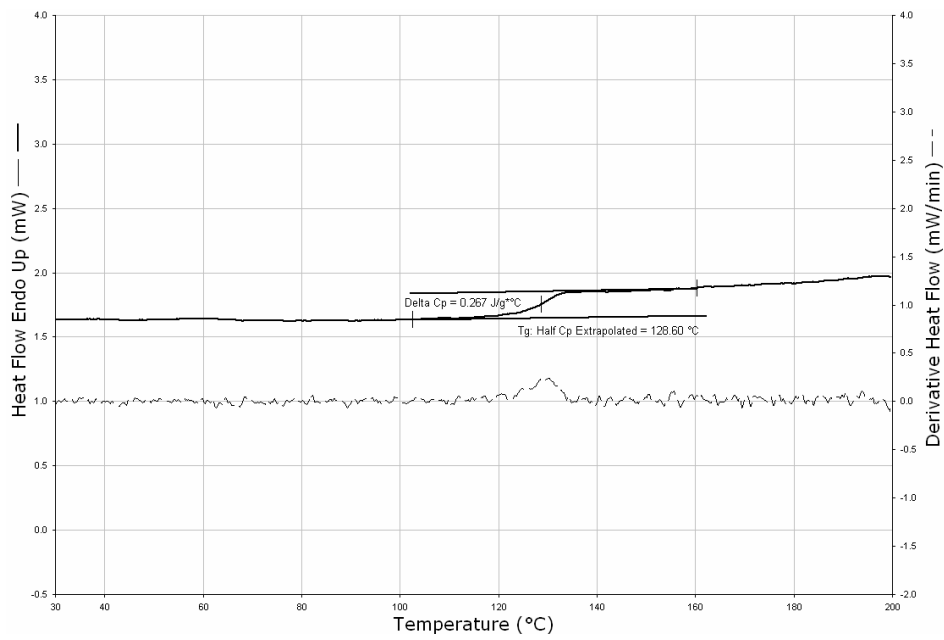


Figure G.1 The DSC graph of PC/pNA (2%) membrane blend (2<sup>nd</sup> scan).



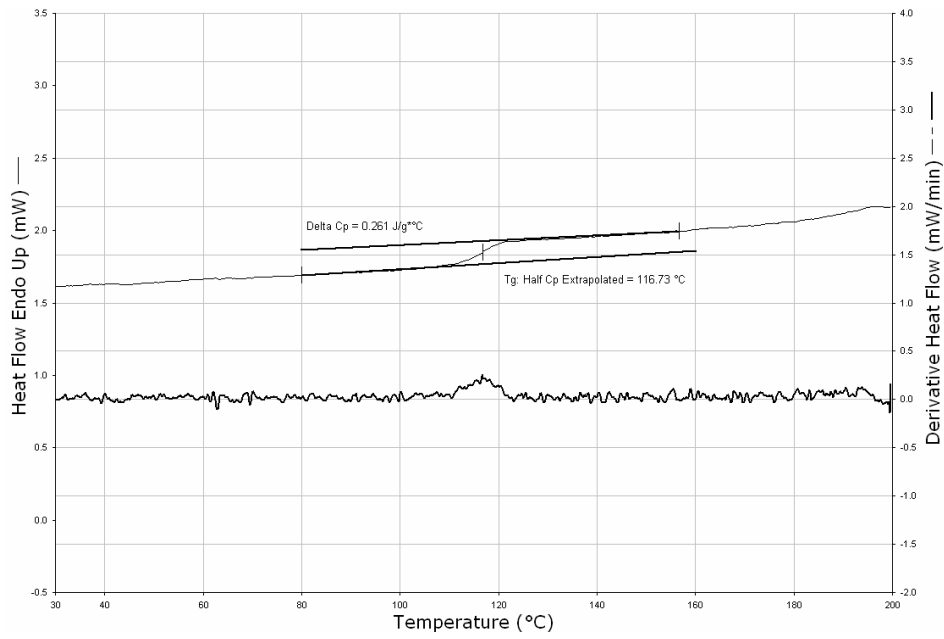


Figure G.2 The DSC graph of PC/pNA (5%) membrane blend (2<sup>nd</sup> scan).

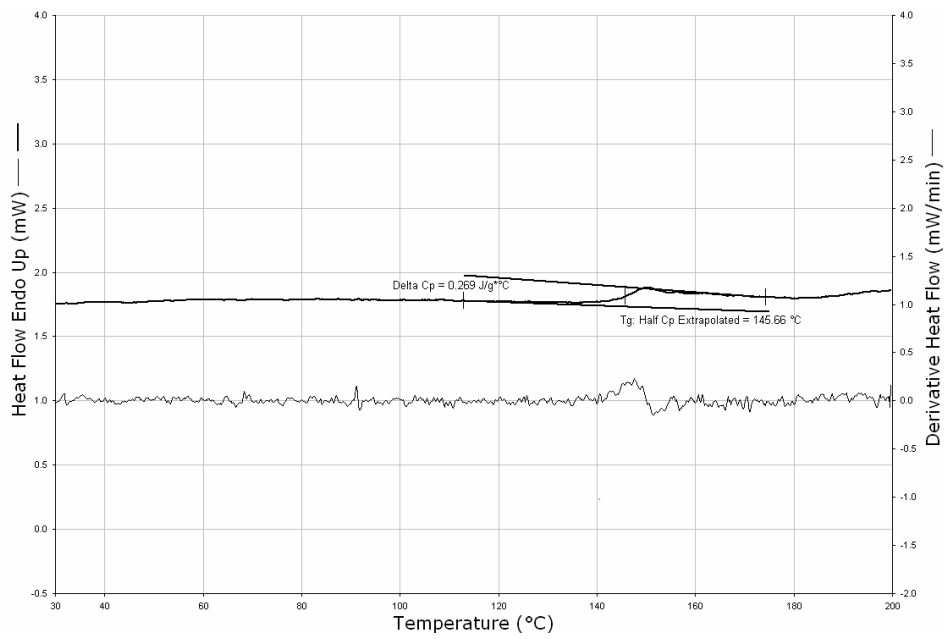


Figure G.3 The DSC graph of PC/4A (10%) MMM (2<sup>nd</sup> scan).

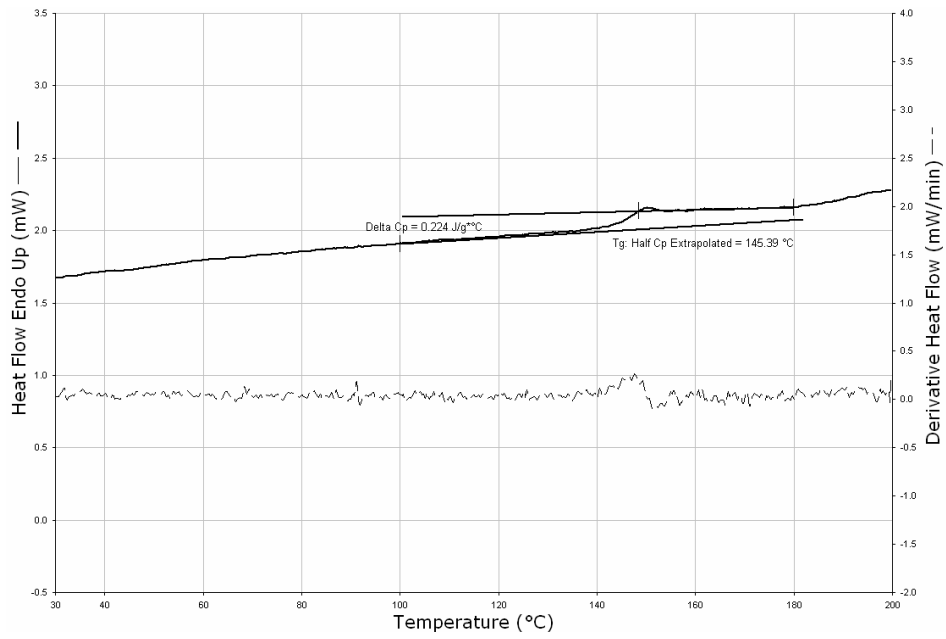


Figure G.4 The DSC graph of PC/4A (30%) MMM (2<sup>nd</sup> scan).

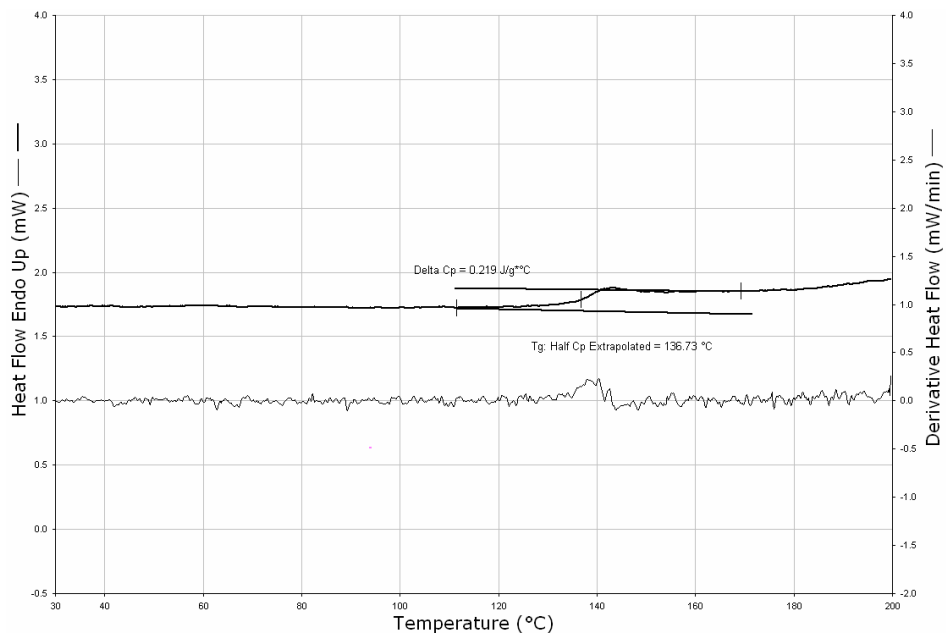


Figure G.5 The DSC graph of PC/pNA (1%)/4A (20%) MMM (2<sup>nd</sup> scan).

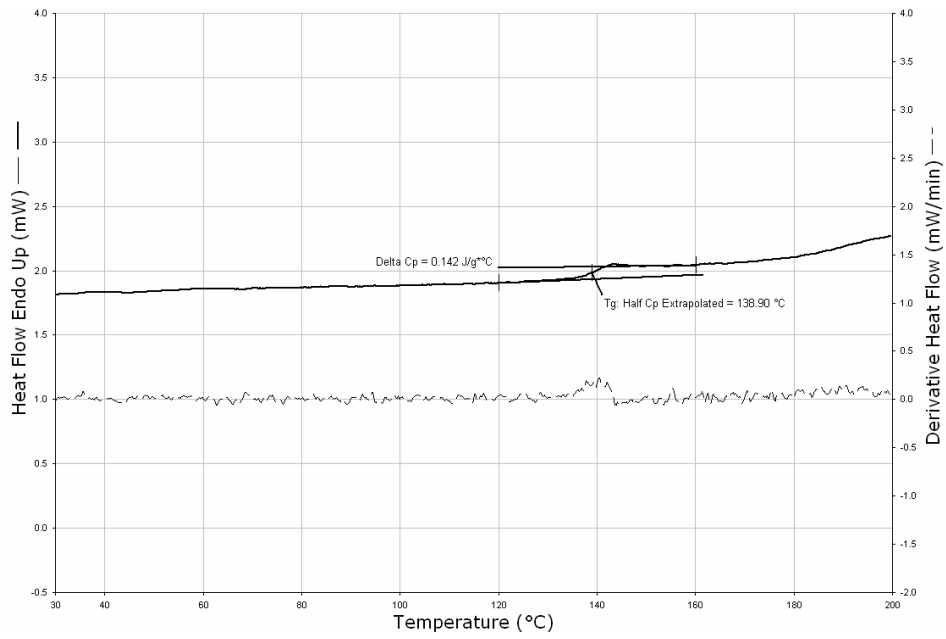


Figure G.6 The DSC graph of PC/pNA (1%)/4A (30%) MMM (2<sup>nd</sup> scan).

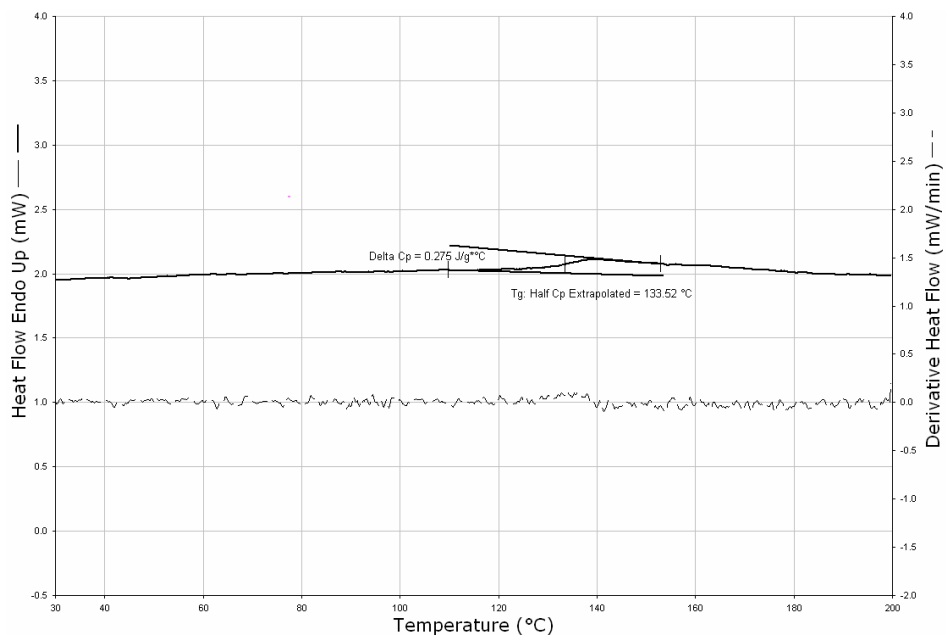


Figure G.7 The DSC graph of PC/pNA (2%)/4A (20%) MMM (2<sup>nd</sup> scan).

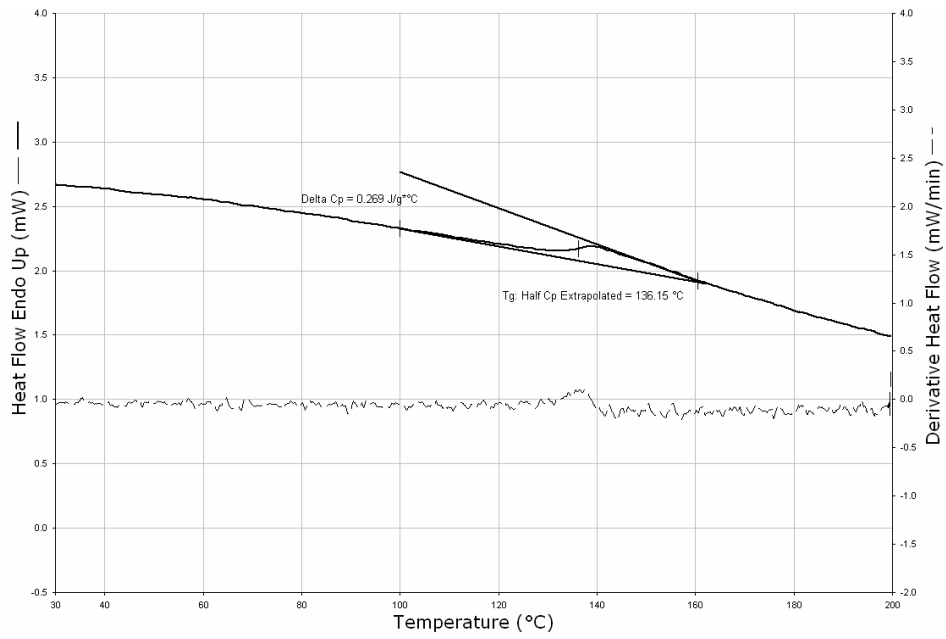


Figure G.8 The DSC graph of PC/pNA (2%)/4A (30%) MMM (2<sup>nd</sup> scan).

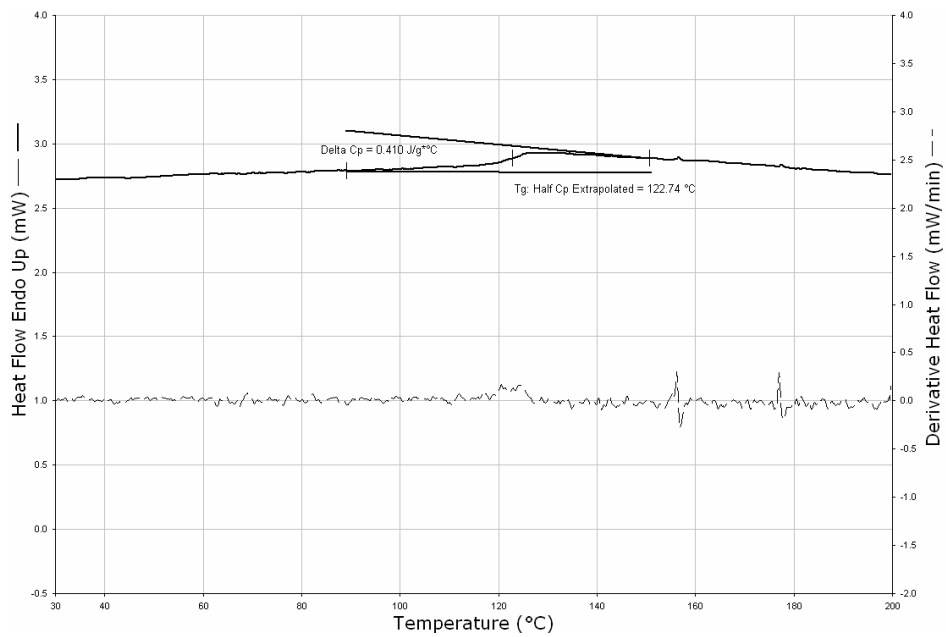


Figure G.9 The DSC graph of PC/pNA (5%)/4A (10%) MMM (2<sup>nd</sup> scan).

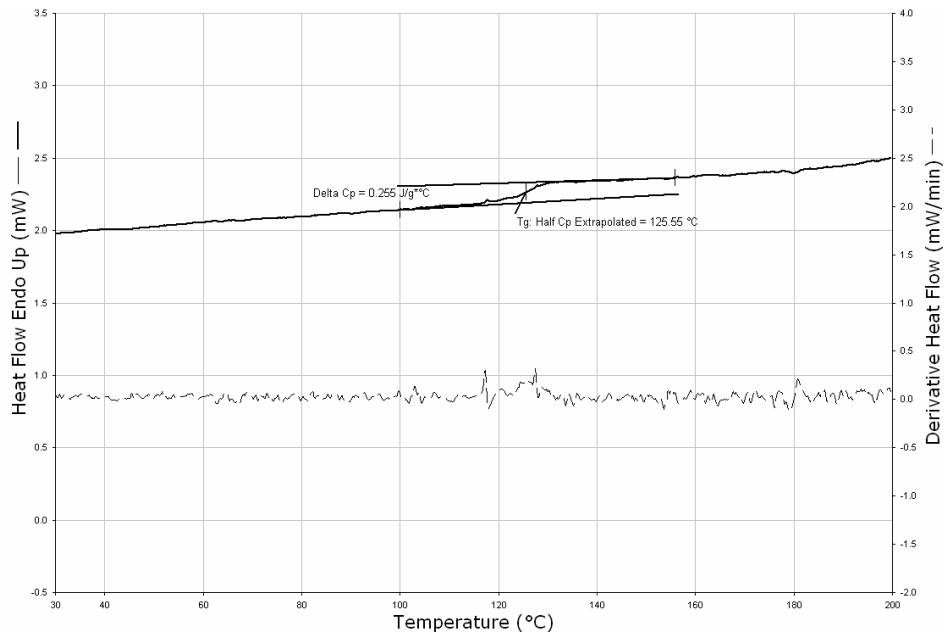


Figure G.10 The DSC graph of PC/pNA (5%)/4A (20%) MMM (2<sup>nd</sup> scan).

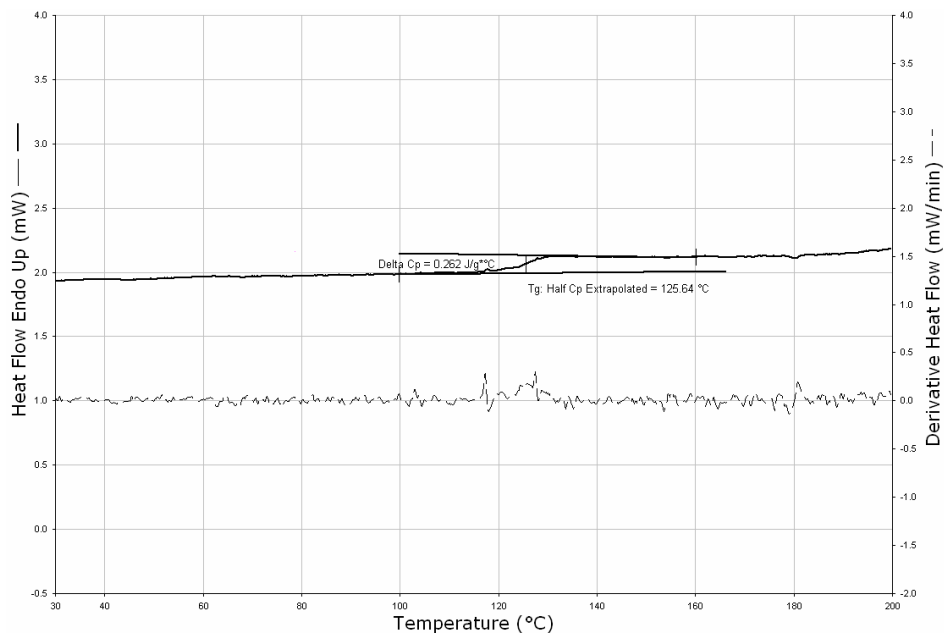


Figure G.11 The DSC graph of PC/pNA (5%)/4A (20%) MMM (2<sup>nd</sup> scan-reproducibility).

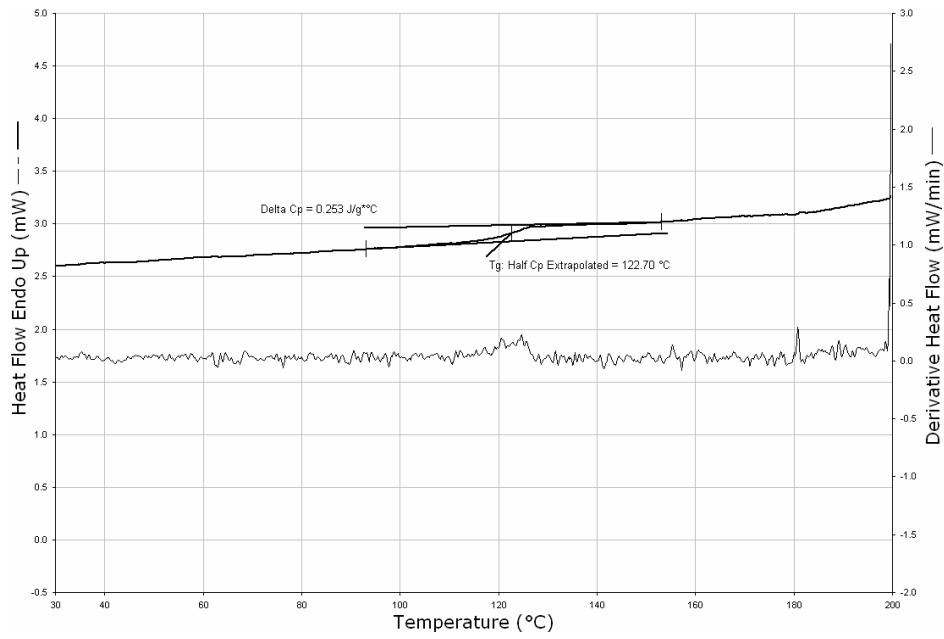


Figure G.12 The DSC graph of PC/pNA (5%)/4A (30%) MMM (2<sup>nd</sup> scan).

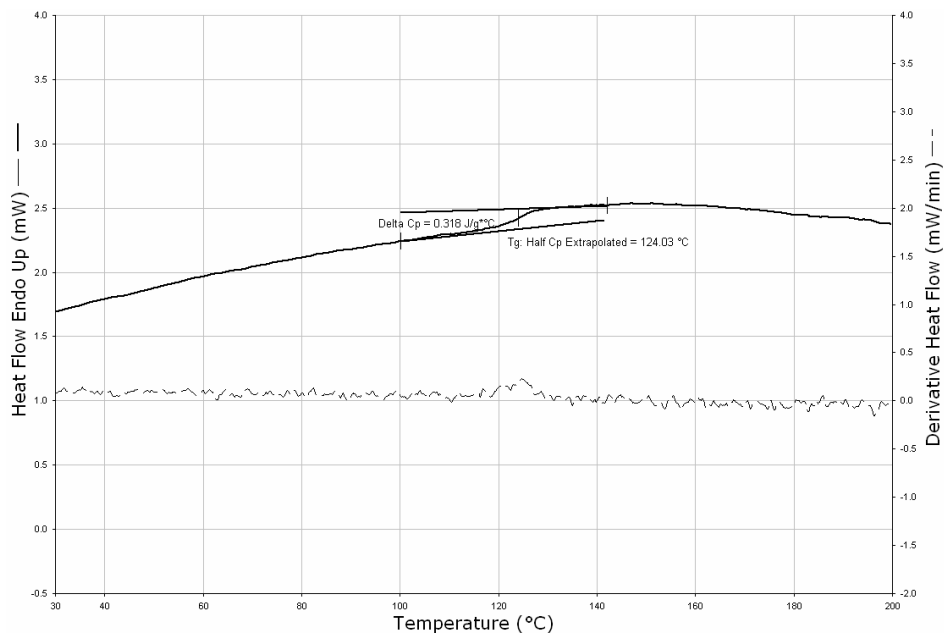


Figure G.13 The DSC graph of PC/pNA (5%)/4A (30%) MMM (2<sup>nd</sup> scan-reproducibility).

## APPENDIX H

### DETERMINATION OF ADJUSTABLE PARAMETER K FOR PC/pNA BLEND MEMBRANES WITH GORDON TAYLOR ANTIPLASTICIZATION MODEL EQUATION

Gordon-Taylor antiplasticization model equation was applied to PC/pNA blend membrane system in order to find adjustable parameter " K ". The equation describes the behavior of the  $T_g$  of a mixture with composition,

$$T_g = \frac{w_a T_{ga} + Kw_p T_{gp}}{w_d + Kw_p} \quad (\text{H.1})$$

$T_g$ : glass transition temperature of polymer-additive mixture ( $^{\circ}\text{C}$ ).

$T_{ga}$  and  $T_{gp}$ : glass transition temperatures of the additive and polymer, respectively ( $^{\circ}\text{C}$ ).

$w_a$  and  $w_p$ : weight fractions of the additive and polymer, respectively.

K: adjustable parameter.

In order to determine " K " for the PC/pNA blend membrane system the following  $T_g$  data and the Matlab nonlinear regression program were used:

Table H.1 Experimental  $T_g$  values of PC/pNA blend membranes with respect to weight fraction of additive pNA.

$w_a$ (%w/w)	$T_g$ (°C)
0.0 (pure PC)	146
0.01	138
0.02	128
0.05	116
1.00 (pure pNA)	-71

Table H.2 Matlab nonlinear regression program to determine the "K" value\*.

```
function difference= myfuc(coeff);
x=[0 0.01 0.02 0.05];
y=[146 138 128 116];
a1= -71;
a2=coeff(1);
ycalc=(a1*x+a2*(1-x)*146)./(x+a2*(1-x));
difference=(y-ycalc).*sqrt(x);

function nonlinreg;
clc;
x=[0 0.01 0.02 0.05];
y=[146 138 128 116];
cf=[0.221];
[rstl,resnorm]=lsqnonlin('myfuc',cf);
fprintf('initial K =%15.10f \n', cf(1));
fprintf('K =%15.10f \n', rstl(1));
fprintf('Normalised SSQ of error =%12.10f\n', resnorm);
xx=0:0.01:0.05
```



Table H.2 Matlab nonlinear regression program to determine the "K" value\* (cont'd).

```

plot(x,y,'+b',xx,ycalc,'-k');
legend('Experimental data','Nonlinear regression result') ;
xlabel('w_d') ;
ylabel('T_g') ;

Optimization terminated successfully :
Relative function value changing by less than OPTIONS.TolFun
Initial K= 0.22100000
K= 0.28320384
Normalised SSQ of error= 0.0008643357
    
```

\* x : weight fraction of pNA, y : T<sub>g</sub> of PC/pNA membranes at different pNA concentrations, a1: T<sub>g</sub> of pure pNA, ycalc: calculated T<sub>g</sub> of PC/pNA membranes by Gordon-Taylor model.

After finding "K" value, the T<sub>g</sub> of PC/pNA membranes were calculated by using Gordon-Taylor model equation. The calculated and experimental T<sub>g</sub> values were compared in Table H.3.

Table H.3 Comparison of calculated T<sub>g</sub> values of PC/pNA blend membranes with experimental T<sub>g</sub> values.

w <sub>a</sub> (%w/w)	T <sub>g</sub> (°C) experimental	T <sub>g</sub> (°C) calculated
0.00	146	146.0
0.01	138	138.4
0.02	128	131.0
0.05	116	112.7

## APPENDIX I

### REPRODUCIBILITY EXPERIMENTS FOR SINGLE GAS PERMEABILITY MEASUREMENTS

Table I.1 Reproducibility data for pure PC membrane.

Membrane Number	Run Number	Permeability (Barrer)					Selectivity	
		H <sub>2</sub>	CO <sub>2</sub>	O <sub>2</sub>	N <sub>2</sub>	CH <sub>4</sub>	H <sub>2</sub> /N <sub>2</sub>	O <sub>2</sub> /N <sub>2</sub>
M1 (45 μm)	1	16.5	8.70	1.88	0.255	-	64.0	7.3
	2	16.6	8.87	1.87	0.261	-		
	avg.	16.5	8.79	1.88	0.258	-		
M2 (50 μm)	1	14.7	-	-	0.251	-	58.8	-
	2	15.4	-	-	0.259	-		
	avg.	15.0	-	-	0.255	-		
M3 (40 μm)	1	15.2	8.29	1.72	0.269	-	51.0	5.7
	2	15.4	8.49	1.71	0.330	-		
	avg.	15.3	8.39	1.72	0.300	-		
M4 (40 μm)	1	14.2	9.70	1.84	0.258	0.395	54.6	7.1
	2	14.1	8.80	1.84	0.262	0.387		
	avg.	14.2	9.25	1.84	0.260	0.391		
M5 (33 μm)	1	15.7	-	-	0.268	0.369	58.2	-
	2	14.9	-	-	0.258	0.345		
	avg.	15.3	-	-	0.263	0.357		

Table I.2 Reproducibility data for PC/pNA blend membranes.

Membrane Type	Run Number	Permeability (Barrer)						Selectivity			
		H <sub>2</sub>	CO <sub>2</sub>	O <sub>2</sub>	N <sub>2</sub>	CH <sub>4</sub>	H <sub>2</sub> /N <sub>2</sub>	O <sub>2</sub> /N <sub>2</sub>	CO <sub>2</sub> /N <sub>2</sub>	CO <sub>2</sub> /CH <sub>4</sub>	N <sub>2</sub> /CH <sub>4</sub>
PC/pNA (28 μm)	1	10.0	4.13	1.29	0.144	0.098					
	2	9.90	4.20	1.33	0.150	0.110					
	avg.	10.0	4.17	1.31	0.147	0.104	68.0	8.9	28.4	96.2	40.1
PC/pNA (46 μm)	1	9.40	4.08	1.00	0.121	0.074					
	2	9.16	3.92	1.02	0.134	0.079					
	avg.	9.28	4.00	1.01	0.128	0.077	72.5	7.9	31.3	120.5	51.9
PC/pNA (64 μm)	1	7.0	3.92	0.84	0.082	0.074					
	2	7.3	3.88	0.85	0.076	0.071					
	avg.	7.2	3.90	0.85	0.079	0.073	91.1	10.8	49.4	98.6	53.4

Table I.3 Reproducibility data for PC/zeolite 4A (5%) MMM.

Membrane Number	Run Number	Permeability (Barrer)						Selectivity			
		H <sub>2</sub>	CO <sub>2</sub>	O <sub>2</sub>	N <sub>2</sub>	CH <sub>4</sub>	H <sub>2</sub> /N <sub>2</sub>	O <sub>2</sub> /N <sub>2</sub>	CO <sub>2</sub> /N <sub>2</sub>	CO <sub>2</sub> /CH <sub>4</sub>	N <sub>2</sub> /CH <sub>4</sub>
M1 (40 μm)	1	14.3	8.30	1.78	0.244	0.260					
	2	13.9	8.50	1.76	0.254	0.272					
	avg.	14.1	8.40	1.77	0.249	0.266	56.6	7.1	33.7	53.0	31.6
M2 (45 μm)	1	14.2	8.25	1.76	0.234	0.244					
	2	14.1	8.28	1.76	0.251	0.258					
	avg.	14.2	8.27	1.76	0.243	0.251	58.4	7.2	34.0	56.6	32.9

Table I.4 Reproducibility data for PC/zeolite 4A (10%) MMM.

Membrane Number	Run Number	Permeability (Barrer)				Selectivity					
		H <sub>2</sub>	CO <sub>2</sub>	O <sub>2</sub>	CH <sub>4</sub>	H <sub>2</sub> /N <sub>2</sub>	O <sub>2</sub> /N <sub>2</sub>	CO <sub>2</sub> /N <sub>2</sub>	H <sub>2</sub> /CH <sub>4</sub>	CO <sub>2</sub> /CH <sub>4</sub>	N <sub>2</sub> /CH <sub>4</sub>
M1-part 1 (60 μm)	1	13.8	8.32	1.79	0.213	0.264					
	2	13.6	8.26	1.77	0.203	0.276					
	avg.	13.7	8.29	1.78	0.208	0.270	65.9	8.6	39.9	50.7	30.7
M1-part 2 (65 μm)	1	13.6	7.93	1.80	0.216	0.220					
	2	13.4	8.28	1.78	0.210	0.240					
	avg.	13.5	8.11	1.79	0.213	0.230	63.4	8.4	38.1	58.7	35.3
M2 (55 μm)	1	13.3	8.12	1.77	0.214	0.242					
	2	13.0	8.04	1.78	0.205	0.246					
	avg.	13.2	8.08	1.78	0.210	0.244	62.9	8.5	38.5	54.1	33.1

Table I.5 Reproducibility data for PC/zeolite 4A (20%) MMM.

Membrane Number	Run Number	Permeability (Barrer)				Selectivity					
		H <sub>2</sub>	CO <sub>2</sub>	O <sub>2</sub>	CH <sub>4</sub>	H <sub>2</sub> /N <sub>2</sub>	O <sub>2</sub> /N <sub>2</sub>	CO <sub>2</sub> /N <sub>2</sub>	H <sub>2</sub> /CH <sub>4</sub>	CO <sub>2</sub> /CH <sub>4</sub>	N <sub>2</sub> /CH <sub>4</sub>
M1 (55 μm)	1	13.1	8.00	1.67	0.210	-					
	2	13.0	8.09	1.69	0.167	-					
	avg.	13.0	8.05	1.68	0.189	-	68.8	8.9	42.6	-	-
M2 (60 μm)	1	13.3	7.99	1.81	0.198	0.229					
	2	13.1	7.33	1.79	0.217	0.234					
	avg.	13.2	7.66	1.80	0.208	0.232	63.5	8.7	36.8	56.9	33.0
M3 (65 μm)	1	14.0	7.78	1.86	0.218	0.245					
	2	13.7	7.75	1.82	0.199	0.251					
	avg.	13.9	7.77	1.84	0.209	0.248	66.5	8.8	37.2	56.0	31.3

Table I.6 Reproducibility data for PC/zeolite 4A (30%) MMM.

Membrane Number	Run Number	Permeability (Barrer)					Selectivity					
		H <sub>2</sub>	CO <sub>2</sub>	O <sub>2</sub>	N <sub>2</sub>	CH <sub>4</sub>	H <sub>2</sub> /N <sub>2</sub>	O <sub>2</sub> /N <sub>2</sub>	CO <sub>2</sub> /N <sub>2</sub>	H <sub>2</sub> /CH <sub>4</sub>	CO <sub>2</sub> /CH <sub>4</sub>	N <sub>2</sub> /CH <sub>4</sub>
M1-part 1 (70 μm)	1	13.6	7.31	1.71	0.178	0.195						
	2	13.5	7.39	1.62	0.174	0.209						
	avg.	13.6	7.35	1.67	0.176	0.202	77.3	9.5	41.8	67.3	36.4	0.87
M1-part 2 (65 μm)	1	13.1	-	-	0.183	-						
	2	13.0	-	-	0.179	-						
	avg.	13.1	-	-	0.181	-	72.4	-	-	-	-	-
M1-part 3 (65 μm)	1	13.3	6.75	1.47	0.173	0.150						
	2	13.1	6.86	1.42	0.189	0.141						
	avg.	13.2	6.81	1.45	0.181	0.146	72.9	8.0	37.6	90.4	46.6	1.24
M2 (60 μm)	1	13.2	6.73	1.41	0.178	0.193						
	2	13.2	6.75	1.42	0.181	0.196						
	avg.	13.2	6.74	1.42	0.180	0.195	73.3	7.9	37.4	67.7	34.6	0.92
M3 (65 μm)	1	12.6	7.29	1.61	0.173	0.198						
	2	12.7	6.81	1.73	0.176	0.206						
	avg.	12.7	7.05	1.67	0.175	0.202	72.6	9.5	40.3	62.9	34.9	0.87



Table I.9 Reproducibility data for PC/pNA (1%)/zeolite 4A (20%) MMM.

Membrane Number	Run Number	Permeability (Barrer)				Selectivity					
		H <sub>2</sub>	CO <sub>2</sub>	O <sub>2</sub>	N <sub>2</sub>	CH <sub>4</sub>	H <sub>2</sub> /N <sub>2</sub>	O <sub>2</sub> /N <sub>2</sub>	CO <sub>2</sub> /N <sub>2</sub>	CO <sub>2</sub> /CH <sub>4</sub>	N <sub>2</sub> /CH <sub>4</sub>
M1 (60 μm)	1	10.6	4.55	0.99	0.145	0.083					
	2	10.9	4.67	1.12	0.136	0.094					
	avg.	10.8	4.61	1.06	0.141	0.089	76.6	7.5	32.7	121.3	51.8
M2 (55 μm)	1	11.1	-	-	0.149	-					
	2	10.3	-	-	0.129	-					
	avg.	10.7	-	-	0.139	-	-	-	-	-	-

Table I.10 Reproducibility data for PC/pNA (1%)/zeolite 4A (30%) MMM.

Membrane Number	Run Number	Permeability (Barrer)				Selectivity					
		H <sub>2</sub>	CO <sub>2</sub>	O <sub>2</sub>	N <sub>2</sub>	CH <sub>4</sub>	H <sub>2</sub> /N <sub>2</sub>	O <sub>2</sub> /N <sub>2</sub>	CO <sub>2</sub> /N <sub>2</sub>	CO <sub>2</sub> /CH <sub>4</sub>	N <sub>2</sub> /CH <sub>4</sub>
M1 (60 μm)	1	8.7	3.48	0.77	0.134	0.079					
	2	8.7	3.79	0.84	0.143	0.083					
	avg.	8.7	3.64	0.81	0.139	0.081	62.6	5.8	26.2	107.4	44.9
M2 (65 μm)	1	8.9	-	-	0.132	-					
	2	8.1	-	-	0.140	-					
	avg.	8.5	-	-	0.136	-	-	-	-	-	-

Table I.1.11 Reproducibility data for PC/pNA (2%)/zeolite 4A (5%) MMM.

Membrane Number	Run Number	Permeability (Barrer)				Selectivity					
		H <sub>2</sub>	CO <sub>2</sub>	O <sub>2</sub>	N <sub>2</sub>	CH <sub>4</sub>	H <sub>2</sub> /N <sub>2</sub>	O <sub>2</sub> /N <sub>2</sub>	CO <sub>2</sub> /N <sub>2</sub>	CO <sub>2</sub> /CH <sub>4</sub>	N <sub>2</sub> /CH <sub>4</sub>
M1-part 1 (45 μm)	1	10.6	4.82	1.44	0.155	0.129					
	2	9.8	5.51	1.26	0.173	0.134					
	avg.	10.6	5.17	1.35	0.164	0.129	64.6	8.2	31.5	82.2	40.1
M1-part2 (40 μm)	1	10.2	-	-	-	-					
	2	10.8	-	-	-	-					
	avg.	10.5	-	-	-	-	-	-	-	-	-

Table I.1.12 Reproducibility data for PC/pNA (2%)/zeolite 4A (10%) MMM.

Membrane Number	Run Number	Permeability (Barrer)				Selectivity					
		H <sub>2</sub>	CO <sub>2</sub>	O <sub>2</sub>	N <sub>2</sub>	CH <sub>4</sub>	H <sub>2</sub> /N <sub>2</sub>	O <sub>2</sub> /N <sub>2</sub>	CO <sub>2</sub> /N <sub>2</sub>	CO <sub>2</sub> /CH <sub>4</sub>	N <sub>2</sub> /CH <sub>4</sub>
M1 (55 μm)	1	9.5	4.13	1.01	0.187	0.116					
	2	9.6	4.28	1.21	0.172	0.129					
	avg.	9.6	4.21	1.11	0.180	0.123	53.3	6.2	23.4	78.0	34.2
M2 (50 μm)	1	10.2	-	1.03	0.173	-					
	2	8.9	-	1.16	0.179	-					
	avg.	9.6	-	1.10	0.176	-	54.5	6.3	-	-	-



Table I.13 Reproducibility data for PC/pNA (2%)/zeolite 4A (20%) MMM.

Membrane Number	Run Number	Permeability (Barrer)				Selectivity				
		H <sub>2</sub>	CO <sub>2</sub>	O <sub>2</sub>	CH <sub>4</sub>	H <sub>2</sub> /N <sub>2</sub>	O <sub>2</sub> /N <sub>2</sub>	CO <sub>2</sub> /N <sub>2</sub>	CO <sub>2</sub> /CH <sub>4</sub>	N <sub>2</sub> /CH <sub>4</sub>
M1 (45 μm)	1	10.4	3.79	1.11	0.139	0.072				
	2	10.0	3.99	1.08	0.145	0.076				
	avg.	10.2	3.89	1.10	0.142	0.074	71.8	7.7	27.4	137.8
M2 (50 μm)	1	10.7	3.85	1.04	0.147	0.078				
	2	10.7	4.22	1.10	0.143	0.083				
	avg.	10.7	4.04	1.07	0.145	0.081	73.8	7.4	27.9	132.1

Table I.14 Reproducibility data for PC/pNA (2%)/zeolite 4A (30%) MMM.

Membrane Number	Run Number	Permeability (Barrer)				Selectivity				
		H <sub>2</sub>	CO <sub>2</sub>	O <sub>2</sub>	CH <sub>4</sub>	H <sub>2</sub> /N <sub>2</sub>	O <sub>2</sub> /N <sub>2</sub>	CO <sub>2</sub> /N <sub>2</sub>	CO <sub>2</sub> /CH <sub>4</sub>	N <sub>2</sub> /CH <sub>4</sub>
M1 (60 μm)	1	9.2	4.30	0.94	0.136	0.109				
	2	8.9	4.35	0.94	0.130	0.088				
	avg.	9.1	4.33	0.94	0.133	0.099	68.4	7.1	32.6	91.9
M2 (65 μm)	1	8.7	4.34	0.98	0.123	0.103				
	2	8.9	4.52	0.97	0.128	0.115				
	avg.	8.8	4.43	0.98	0.126	0.109	69.8	7.8	35.2	80.7

Table I.15 Reproducibility data for PC/pNA (5%)/zeolite 4A (5%) MMM.

Membrane Number	Run Number	Permeability (Barrer)					Selectivity					
		H <sub>2</sub>	CO <sub>2</sub>	O <sub>2</sub>	N <sub>2</sub>	CH <sub>4</sub>	H <sub>2</sub> /N <sub>2</sub>	O <sub>2</sub> /N <sub>2</sub>	CO <sub>2</sub> /N <sub>2</sub>	H <sub>2</sub> /CH <sub>4</sub>	CO <sub>2</sub> /CH <sub>4</sub>	N <sub>2</sub> /CH <sub>4</sub>
M1 (55 μm)	1	10.3	3.99	1.02	0.154	0.113						
	2	8.9	4.28	0.95	0.147	0.129						
	avg.	9.6	4.14	0.99	0.151	0.121	63.6	6.6	27.4	79.3	34.2	1.25
M2 (45 μm)	1	9.1	-	0.99	-	-						
	2	9.1	-	0.98	-	-						
	avg.	9.1	-	0.99	-	-	-	-	-	-	-	-

Table I.16 Reproducibility data for PC/pNA (5%)/zeolite 4A (10%) MMM.

Membrane Number	Run Number	Permeability (Barrer)					Selectivity					
		H <sub>2</sub>	CO <sub>2</sub>	O <sub>2</sub>	N <sub>2</sub>	CH <sub>4</sub>	H <sub>2</sub> /N <sub>2</sub>	O <sub>2</sub> /N <sub>2</sub>	CO <sub>2</sub> /N <sub>2</sub>	H <sub>2</sub> /CH <sub>4</sub>	CO <sub>2</sub> /CH <sub>4</sub>	N <sub>2</sub> /CH <sub>4</sub>
M1 (45 μm)	1	8.2	-	0.91	0.139	-						
	2	8.7	-	0.93	0.146	-						
	avg.	8.4	-	0.92	0.143	-	59.0	6.4	-	-	-	-
M2 (50 μm)	1	8.8	3.62	0.93	0.144	0.111						
	2	8.9	4.02	0.98	0.150	0.121						
	avg.	8.8	3.82	0.96	0.147	0.116	59.9	6.5	26.0	75.9	32.9	1.27

Table I.17 Reproducibility data for PC/pNA (5%)/zeolite 4A (20%) MMM.

Membrane Number	Run Number	Permeability (Barrer)				Selectivity						
		H <sub>2</sub>	CO <sub>2</sub>	O <sub>2</sub>	N <sub>2</sub>	CH <sub>4</sub>	H <sub>2</sub> /N <sub>2</sub>	O <sub>2</sub> /N <sub>2</sub>	CO <sub>2</sub> /CH <sub>4</sub>	H <sub>2</sub> /CH <sub>4</sub>	CO <sub>2</sub> /CH <sub>4</sub>	N <sub>2</sub> /CH <sub>4</sub>
M1 (60 μm)	1	8.0	3.93	0.86	0.123	0.098						
	2	7.7	4.10	0.92	0.117	0.115						
	avg.	7.9	4.02	0.89	0.120	0.107	65.8	7.4	33.5	73.8	37.6	1.12
M2 (65 μm)	1	8.4	4.18	0.94	0.127	0.118						
	2	8.1	4.21	0.95	0.131	0.110						
	avg.	8.3	4.20	0.95	0.129	0.114	64.3	7.4	32.6	72.8	36.8	1.13

Table I.18 Reproducibility data for PC/pNA (5%)/zeolite 4A (30%) MMM.

Membrane Number	Run Number	Permeability (Barrer)				Selectivity						
		H <sub>2</sub>	CO <sub>2</sub>	O <sub>2</sub>	N <sub>2</sub>	CH <sub>4</sub>	H <sub>2</sub> /N <sub>2</sub>	O <sub>2</sub> /N <sub>2</sub>	CO <sub>2</sub> /CH <sub>4</sub>	H <sub>2</sub> /CH <sub>4</sub>	CO <sub>2</sub> /CH <sub>4</sub>	N <sub>2</sub> /CH <sub>4</sub>
M1 (70 μm)	1	8.2	3.09	0.79	0.122	0.077						
	2	8.2	3.22	0.87	0.111	0.082						
	avg.	8.2	3.16	0.83	0.117	0.080	70.1	7.1	27.0	102.5	39.5	1.46
M2 (65 μm)	1	7.9	3.13	0.72	0.109	0.068						
	2	7.7	2.99	0.78	0.110	0.074						
	avg.	7.8	3.06	0.75	0.110	0.071	70.9	6.8	27.8	109.9	43.1	1.55
M3 (75 μm)	1	8.4	3.42	0.82	0.116	0.068						
	2	8.5	3.50	0.79	0.121	0.071						
	avg.	8.5	3.46	0.81	0.119	0.070	71.4	6.8	29.1	121.4	49.4	1.70

## **APPENDIX J**

### **SEPARATION SELECTIVITY DATA CALCULATED FROM SEMI-EMPIRICAL CURVE FITTING METHOD**

The permeate side concentrations and separation selectivity data calculated from the semi-empirical curve fitting method described in Section 6.3 were compared with the experimental data in Table J.1. The data is for CO<sub>2</sub>/CH<sub>4</sub> binary gas mixture separation through PC/zeolite 4A (20%) MMMs.

Table J.1 Comparison of calculated and experimental data for permeate side compositions and separation selectivities of CO<sub>2</sub>/CH<sub>4</sub> binary gas mixture through PC/zeolite 4A (20%) MMMs.

Calculated Data*					Experimental Data			
(semi-empirical curve fitting method)					(measured by gas chromatography)			
x(CO <sub>2</sub> )	x(CH <sub>4</sub> )	y(CO <sub>2</sub> )	y(CH <sub>4</sub> )	CO <sub>2</sub> /CH <sub>4</sub>	x(CO <sub>2</sub> )	y(CO <sub>2</sub> )	y(CH <sub>4</sub> )	CO <sub>2</sub> /CH <sub>4</sub>
0	100	0.0	100.0	31.2	0.0	0.0	100.0	31.9
5	95	61.3	38.7	30.1	6.4	68.0	32.1	31.8
10	90	76.8	23.2	29.7	11.8	81.3	18.5	29.8
15	85	83.8	16.2	29.4	13.3	88.0	17.9	29.4
20	80	87.8	12.2	28.9	20.7	91.8	12.3	27.9
25	75	90.5	9.5	28.4	23.1	89.5	10.3	28.9
30	70	92.3	7.7	27.9	31.3	95.8	8.3	24.9
35	65	93.6	6.4	27.3	38.7	94.2	5.5	27.6
40	60	94.7	5.3	26.7	51.8	96.9	4.2	22.2
45	55	95.5	4.5	26.0	52.2	96.4	3.7	24.2
50	50	96.2	3.8	25.1	60.3	98.9	2.1	20.9
55	45	96.7	3.3	24.2	76.3	98.2	1.7	18.6
60	40	97.2	2.8	23.1	80.8	98.9	1.2	20.3
65	35	97.6	2.4	21.9	100.0	100.0	0.0	-
70	30	97.9	2.1	20.4				
75	25	98.2	1.8	18.6				
80	20	98.5	1.5	16.5				
85	15	98.7	1.3	13.8				
90	10	99.0	1.0	10.5				
95	5	99.1	0.9	6.1				
100	0	99.3	0.7	-				

\* x and y indicate feed side and permeate side compositions of gas components, respectively.

## APPENDIX K

### REPRODUCIBILITY EXPERIMENTS FOR BINARY GAS PERMEABILITY MEASUREMENTS

#### K.1 Reproducibility Data for CO<sub>2</sub>/CH<sub>4</sub> Separation through pure PC Membrane

Table K.1.1 Reproducibility data for CO<sub>2</sub>/CH<sub>4</sub> mixture permeabilities through pure PC membrane.

% CO <sub>2</sub> in feed	Membrane # 1 (55 μm)			% CO <sub>2</sub> in feed	Membrane # 2 (60 μm)		
	Permeability (Barrer)				Permeability (Barrer)		
	1st run	2nd run	avg		1st run	2nd run	avg
100.0	9.26	-	9.26	100.0	8.99	9.05	9.02
95.7	7.98	7.63	7.81	-	-	-	-
89.1	7.71	7.50	7.61	-	-	-	-
78.9	6.03	5.82	5.93	81.1	7.53	-	7.53
74.5	5.68	-	5.68	76.0	6.85	6.45	6.65
60.1	5.30	4.84	5.07	60.6	4.98	5.36	5.17
49.7	4.09	4.15	4.12	50.5	3.92	4.29	4.11
39.7	3.34	3.19	3.27	40.6	2.97	2.98	2.98
25.2	2.02	-	2.02	24.7	1.93	2.06	2.00
15.3	1.33	1.19	1.26	15.3	1.09	1.17	1.13
-	-	-	-	10.5	0.805	0.819	0.812
-	-	-	-	6.0	0.510	0.606	0.558
0.0	0.360	-	0.360	0.0	0.315	0.326	0.321

Table K.1.2 Reproducibility data for CO<sub>2</sub>/CH<sub>4</sub> selectivities of pure PC membrane.

% CO <sub>2</sub> in feed	Membrane # 1 (55 μm)			% CO <sub>2</sub> in feed	Membrane # 2 (60 μm)		
	Selectivity				Selectivity		
	1st	2nd	avg		1st	2nd	avg
100*	25.6	-	25.6	100*	28.5	27.8	28.2
95.7	25.1	-	25.1	-	-	-	-
89.1	23.1	24.9	24.0	-	-	-	-
78.9	18.0	18.2	18.1	81.1	26.8	-	26.8
74.5	26.5	-	26.5	76.0	28.0	30.2	29.1
60.1	28.1	28.6	28.4	60.6	30.1	28	29.1
49.7	30.0	28.3	29.2	50.5	29.6	30.7	30.2
39.7	29.7	28.6	29.2	40.6	28.4	29.6	29.0
25.2	24.0	-	24.0	24.7	25.7	25.4	25.6
15.3	21.2	20.5	20.9	15.3	20.0	20.4	20.2
-	-	-	-	10.5	20.1	18.5	19.3
-	-	-	-	6.0	24.6	21.7	23.2
0.0	-	-	-	0.0	-	-	-

\* selectivities given at 100% CO<sub>2</sub> indicate the ideal selectivities.

## K.2 Reproducibility Data for CO<sub>2</sub>/CH<sub>4</sub> Separation through PC/pNA (2%) Blend Membrane

Table K.2.1 Reproducibility data for CO<sub>2</sub>/CH<sub>4</sub> mixture permeabilities and selectivities of PC/pNA (2%) blend membrane.

% CO <sub>2</sub> in feed	Membrane # 1 (75 μm)					
	Permeability (Barrer)			Selectivity		
	1st run	2nd run	avg	1st run	2nd run	avg
100*	4.10	3.92	4.01	47.7	49.0	48.4
78.9	3.48	3.38	3.43	51.4	47.4	49.4
61.8	2.32	2.41	2.37	51.6	47.5	49.6
53.2	2.08	2.05	2.07	49.4	45.9	47.7
28.3	1.51	1.56	1.54	52.8	54.4	53.6
21.5	1.34	1.31	1.33	53.6	53.4	53.5
12.1	1.19	1.17	1.18	54.9	55.2	55.1
0.0	0.086	0.080	0.083	-	-	-

\* selectivities given at 100% CO<sub>2</sub> indicate the ideal selectivities.

### K.3 Reproducibility Data for CO<sub>2</sub>/CH<sub>4</sub> Separation through PC/zeolite 4A MMMs

Table K.3.1 Reproducibility data for CO<sub>2</sub>/CH<sub>4</sub> mixture permeabilities through PC/zeolite 4A (20%) MMM.

<b>Membrane # 1</b>							
<b>% CO<sub>2</sub> in feed</b>	<b>Part # 1 (65 μm)</b>			<b>% CO<sub>2</sub> in feed</b>	<b>Part # 2 (70 μm)</b>		
	Permeability (Barrer)				Permeability (Barrer)		
	1st run	2nd run	avg		1st run	2nd run	avg
100.0	7.74	7.96	7.85	100.0	7.97	8.03	8.00
79.3	6.81	6.93	6.87	89.6	7.42	-	7.42
52.7	3.69	3.73	3.71	80.8	6.86	7.05	6.96
31.1	2.47	2.58	2.53	61.9	5.28	5.43	5.36
10.9	0.943	-	0.943	51.8	4.07	3.94	4.01
0.0	0.242	0.247	0.245	31.2	2.66	2.63	2.65
				20.8	1.51	1.55	1.53
				10.6	0.867	0.893	0.880
				0.0	0.248	0.255	0.252

<b>Membrane # 2</b>							
<b>% CO<sub>2</sub> in feed</b>	<b>Part # 1 (65 μm)</b>			<b>% CO<sub>2</sub> in feed</b>	<b>Part # 2 (60 μm)</b>		
	Permeability (Barrer)				Permeability (Barrer)		
	1st run	2nd run	avg		1st run	2nd run	avg
100.0	8.16	8.31	8.24	100.0	8.44	8.58	8.51
96.4	8.08	8.19	8.14	76.3	6.13	-	6.13
91.3	7.76	7.92	7.84	52.2	4.05	4.17	4.11
80.8	6.55	6.89	6.72	38.7	3.42	3.63	3.53
60.3	4.53	4.91	4.72	23.1	1.68	1.79	1.74
51.8	3.77	3.91	3.84	11.8	0.823	0.856	0.840
31.3	2.66	2.72	2.69	0.0	0.276	0.283	0.280
20.7	1.77	1.84	1.81				
13.3	0.885	0.913	0.899				
6.4	0.450	0.457	0.454				
0.0	0.253	0.263	0.258				



Table K.3.2 Reproducibility data for CO<sub>2</sub>/CH<sub>4</sub> selectivities of PC/zeolite 4A (20%) MMM.

<b>Membrane # 1</b>							
<b>% CO<sub>2</sub> in feed</b>	<b>Part # 1 (65 μm)</b>			<b>% CO<sub>2</sub> in feed</b>	<b>Part # 2 (70 μm)</b>		
	Selectivity				Selectivity		
	1st run	2nd run	avg		1st run	2nd run	avg
100*	32.0	32.2	32.1	100*	31.7	31.7	31.7
79.3	24.4	24.3	24.4	89.6	19.6	-	19.6
52.7	26.8	26.4	26.6	80.8	18.5	16.6	17.6
31.1	27.3	25.9	26.6	61.9	23.2	24.2	23.7
10.9	23.2	-	-	51.8	21.1	21.1	21.1
0.0	-	-	-	31.2	22.3	22.6	22.5
				20.8	22.6	24.1	23.4
				10.6	21.7	22.0	21.9
				0.0	-	-	-

<b>Membrane # 2</b>							
<b>% CO<sub>2</sub> in feed</b>	<b>Part # 1 (65 μm)</b>			<b>% CO<sub>2</sub> in feed</b>	<b>Part # 2 (60 μm)</b>		
	Selectivity				Selectivity		
	1st run	2nd run	avg		1st run	2nd run	avg
100*	32.3	31.6	32.0	100*	30.4	30.4	30.4
96.4	19.6	19.6	19.6	76.3	18.6	-	18.6
91.3	19.5	17.9	18.7	52.2	25.2	23.2	24.2
80.8	19.4	21.1	20.3	38.7	27.7	27.5	27.6
60.3	20.9	20.8	20.9	23.1	29.8	28.2	28.9
51.8	22.4	21.9	22.2	11.8	30.3	29.2	29.8
31.3	24.3	25.4	24.9	0.0	-	-	-
20.7	28.5	27.3	27.9				
13.3	28.4	30.3	29.4				
6.4	31.8	31.8	31.8				
0.0	-	-	-				

\* selectivities given at 100% CO<sub>2</sub> indicate the ideal selectivities.

Table K.3.3 Reproducibility data for CO<sub>2</sub>/CH<sub>4</sub> mixture permeabilities through PC/zeolite 4A (30%) MMM.

% CO <sub>2</sub> in feed	Membrane # 1 (70 μm)			% CO <sub>2</sub> in feed	Membrane # 2 (70 μm)		
	Permeability (Barrer)				Permeability (Barrer)		
	1st run	2nd run	avg		1st run	2nd run	avg
100.0	6.64	6.96	6.80	100.0	6.98	7.20	7.09
89.8	6.11	6.03	6.07	74.6	5.28	5.42	5.35
79.4	5.43	5.50	5.47	51.4	3.42	3.57	3.50
60.6	4.02	4.11	4.07	38.7	2.99	3.16	3.08
52.2	3.31	3.36	3.34	20.9	1.41	1.57	1.49
31.0	1.86	1.91	1.89	0.0	0.198	0.202	0.200
10.7	0.660	0.723	0.692				
0.0	0.185	0.188	0.187				

Table K.3.4 Reproducibility data for CO<sub>2</sub>/CH<sub>4</sub> selectivities through PC/zeolite 4A (30%) MMM.

% CO <sub>2</sub> in feed	Membrane # 1 (70 μm)			% CO <sub>2</sub> in feed	Membrane # 2 (70 μm)		
	Selectivity				Selectivity		
	1st run	2nd run	avg		1st run	2nd run	avg
100*	35.9	37.0	36.5	100*	35.3	35.6	35.5
89.8	18.4	16.5	17.5	74.6	18.7	18.2	18.5
79.4	19.1	19.3	19.2	51.4	24.5	25.6	25.1
60.6	25.2	27.4	26.3	38.7	26.2	28.9	27.6
52.2	27.1	27.4	27.3	20.9	33.6	31.2	32.4
31.0	32.5	31.7	32.1	0.0	-	-	-
10.7	35.5	34.0	34.8				
0.0	-	-	-				

\* selectivities given at 100% CO<sub>2</sub> indicate the ideal selectivities.

#### K.4 Reproducibility Data for CO<sub>2</sub>/CH<sub>4</sub> Separation through PC/pNA/zeolite 4A MMMs

Table K.4.1 Reproducibility data for CO<sub>2</sub>/CH<sub>4</sub> mixture permeabilities and selectivities of PC/pNA (2%)/zeolite 4A (20%) MMM.

% CO <sub>2</sub> in feed	Membrane # 1 (65 μm)					
	Permeability (Barrer)			Selectivity		
	1st run	2nd run	avg	1st run	2nd run	avg
100*	3.96	4.18	4.07	48.5	-	48.5
73.7	1.15	1.31	1.23	17.6	16.4	17.0
61.6	0.702	0.791	0.747	18.7	17.4	18.1
51.0	0.482	0.512	0.497	22.4	21.4	21.9
41.8	0.391	0.409	0.400	23.9	20.9	22.4
36.3	0.325	0.303	0.314	36.8	34.0	35.4
30.8	0.281	0.296	0.289	32.0	34.2	33.1
21.9	0.190	0.204	0.197	38.5	41.7	40.1
10.4	0.099	0.110	0.105	41.1	39.1	40.1
0.0	0.080	0.088	0.084	-	-	-

\* selectivities given at 100% CO<sub>2</sub> indicate the ideal selectivities.

Table K.4.2 Reproducibility data for CO<sub>2</sub>/CH<sub>4</sub> mixture permeabilities and selectivities of PC/pNA (2%)/zeolite 4A (30%) MMM.

% CO <sub>2</sub> in feed	Membrane # 1 (75 μm)					
	Permeability (Barrer)			Selectivity		
	1st run	2nd run	avg	1st run	2nd run	avg
100*	5.08	5.17	5.13	41.0	-	41.0
74.8	3.98	-	3.98	17.2	-	17.2
61.9	3.33	3.12	3.23	18.7	17.9	18.3
50.4	2.32	2.44	2.38	19.2	21.9	20.6
41.2	1.59	-	1.59	22.3	-	22.3
31.9	1.12	1.23	1.18	29.6	30.9	30.3
21.4	0.787	0.813	0.80	34.9	36.2	35.6
11.5	0.403	0.431	0.42	36.4	38.1	37.3
0.0	0.120	0.431	0.28	-	-	-

\* selectivities given at 100% CO<sub>2</sub> indicate the ideal selectivities.

### K.5 Reproducibility Data for H<sub>2</sub>/CH<sub>4</sub> Separation through PC/zeolite 4A and PC/pNA/zeolite 4A MMMs

Table K.5.1 Reproducibility data for H<sub>2</sub>/CH<sub>4</sub> mixture permeabilities and selectivities of PC/zeolite 4A (20%) MMM.

% H <sub>2</sub> in feed	Membrane # 1 (65 μm)					
	Permeability (Barrer)			Selectivity		
	1st run	2nd run	avg	1st run	2nd run	avg
100*	14.9	15.2	15.1	61.4	-	61.4
84.3	11.6	12.0	11.8	59.8	61.7	60.8
51.8	7.58	7.81	7.70	37.5	38.2	37.9
17.8	2.16	2.23	2.20	26.7	25.5	26.1
0.0	0.242	0.247	0.24	-	-	-

\* selectivities given at 100% CO<sub>2</sub> indicate the ideal selectivities.

Table K.5.2 Reproducibility data for H<sub>2</sub>/CH<sub>4</sub> mixture permeabilities and selectivities of PC/pNA (2%)/zeolite 4A (20%) MMM.

% H <sub>2</sub> in feed	Membrane # 1 (65 μm)					
	Permeability (Barrer)			Selectivity		
	1st run	2nd run	avg	1st run	2nd run	avg
100*	11.6	12.0	11.8	140.5	-	140.5
84.3	8.57	9.52	9.05	96.7	91.7	94.2
51.3	6.22	6.74	6.48	45.3	49.8	47.6
16.8	2.04	2.12	2.08	24.3	23.9	24.1
0	0.080	0.088	0.084	-	-	-

\* selectivities given at 100% CO<sub>2</sub> indicate the ideal selectivities.

### K.6 Reproducibility Data for CO<sub>2</sub>/N<sub>2</sub> Separation through PC/zeolite 4A and PC/pNA/zeolite 4A MMMs

Table K.6.1 Reproducibility data for CO<sub>2</sub>/N<sub>2</sub> mixture permeabilities and selectivities of PC/zeolite 4A (20%) MMM.

% CO <sub>2</sub> in feed	Membrane # 1 (65 μm)					
	Permeability (Barrer)			Selectivity		
	1st run	2nd run	avg	1st run	2nd run	avg
100*	8.16	8.31	8.24	31.6	-	31.6
84.1	5.87	6.05	5.96	17.4	14.2	15.8
52.6	3.21	3.44	3.33	22.0	24.3	23.2
21.0	0.892	0.905	0.899	28.8	30.3	29.6
0	0.255	0.267	0.261	-	-	-

\* selectivities given at 100% CO<sub>2</sub> indicate the ideal selectivities.

Table K.6.2 Reproducibility data for CO<sub>2</sub>/N<sub>2</sub> mixture permeabilities and selectivities of PC/pNA (2%)/zeolite 4A (20%) MMM.

% CO <sub>2</sub> in feed	Membrane # 1 (65 μm)					
	Permeability (Barrer)			Selectivity		
	1st run	2nd run	avg	1st run	2nd run	avg
100*	3.96	4.18	4.07	30.8	-	30.8
82.7	2.75	2.84	2.80	14.4	12.4	13.4
52.5	1.79	1.89	1.84	21.2	19.8	20.5
15.7	0.795	0.805	0.800	25.0	26.7	25.9
0	0.129	0.135	0.132	-	-	-

\* selectivities given at 100% CO<sub>2</sub> indicate the ideal selectivities.

## CURRICULUM VITAE

### PERSONAL INFORMATION

Surname, Name: Şen, Değer

Nationality: Turkish (TC)

Date and Place of Birth: 20 December 1978, Ankara

Marital Status: Single

Phone: +90 312 210 43 89

Fax: +90 312 210 26 00

email: degersen@metu.edu.tr

### EDUCATION

- **Ph.D.** (Chemical Engineering) C.GPA: 3.86/4.00  
**[September 2003 – February 2008]**  
Middle East Technical University, Department of Chemical Engineering,  
Ankara, Turkey  
**Dissertation title:** Polycarbonate Based Zeolite 4A Filled Mixed Matrix  
Membranes: Preparation, Characterization and Gas Separation  
Performances  
**Supervised by:** Prof. Dr. Levent Yılmaz & Assist. Prof. Dr. Halil Kalıpçılar
- **M.Sc** (Chemical Engineering) C.GPA: 3.93/4.00  
**[September 2001 – September 2003 ]**  
Middle East Technical University, Department of Chemical Engineering,  
Ankara, Turkey  
**Dissertation title:** Effect of Compatibilizers on The Gas Separation  
Performance of Polycarbonate Membranes  
**Supervised by:** Prof.Dr. Levent Yılmaz & Assist. Prof. Dr. Halil Kalıpçılar

- **B.Sc** (Chemical Engineering) C.GPA: 3.57/4.00  
**[September 1996 – June 2001]**  
Gazi University, Department of Chemical Engineering, Ankara, Turkey

### **PROFESSIONAL EXPERIENCE**

- **Teaching Assistant** (Chemical Engineering)  
**[October 2002 - ]**  
Middle East Technical University, Department of Chemical Engineering,  
Ankara, Turkey.  
(Assistanship to undergraduate and graduate courses namely, Engineering  
Thermodynamics, Process control and Chemical Engineering Laboratory).
- **Training Experience** (Chemical Engineering)  
**[July 2000 – August 2000]**  
BAGFAŞ Sulfuric Acid and Fertilizer Factory, Bandırma, Turkey.
- **Training Experience** (Chemical Engineering)  
**[August 1999 – September 1999]**  
PETKİM Petrochemical Complex, Aliağa, İzmir, Turkey

### **COMPUTER/LANGUAGE SKILLS**

- Programming Language: Fortran, Matlab.
- Commercial Software Package: Microsoft Office (Word, Excel, PowerPoint),  
Front Page, Sigma Plot.
- Proficient in written and spoken English.

### **SCHOLARSHIPS AND AWARDS**

- Middle East Technical University, Department of Chemical Engineering,  
Hasan Orbey Research Award in Graduate Degree, 2002.
- The Scientific and Technological Research Council of Turkey, Scholarship in  
Graduate Degree, 2002-2003.

- Gazi University, Faculty of Engineering and Architecture, Department of Chemical Engineering, First rank award in faculty, 2001.
- Gazi University, Faculty of Engineering and Architecture, Department of Chemical Engineering, High Honour Degree, 1996-2001.

#### **JOURNAL ARTICLES COVERED BY SCIENCE CITATION INDEX**

- D. Şen, H. Kalıpçılar, L. Yılmaz, "Gas Separation Performance of Polycarbonate Membranes Modified With Multifunctional Low Molecular-Weight Additives", Separation Science and Technology, 41 (2006) 1813-1828.
- D. Şen, H. Kalıpçılar, L. Yılmaz, "Development of Polycarbonate Based Zeolite 4A Filled Mixed Matrix Gas Separation Membranes", Journal of Membrane Science 303 (2007) 194-203.
- D. Şen, H. Kalıpçılar, L. Yılmaz, "Binary Gas Separation Performances of Polycarbonate Based Zeolite 4A Filled Mixed Matrix Membranes", in preparation.

#### **INTERNATIONAL CONFERENCES ATTENDED AND ABSTRACTS PUBLISHED IN THE PROCEEDINGS**

- D.Şen, H.Kalıpçılar, L.Yılmaz, "Effect of compatibilizers on the gas separation performance of polycarbonate membranes", Euromembrane 2004, Book of abstracts, Gas and vapor separation session, 187, Hamburg, Germany, 2004.
- D. Şen, H. Kalıpçılar, L. Yılmaz, "Effect of compatibilizers on the development of polymer-zeolite mixed matrix gas separation membranes", ANVOC 2005, Proceedings, 130-136, İstanbul, Turkey, 2005.
- L. Yılmaz, D. Şen, "Past developments and future directions in development of glassy polymer/filler mixed matrix membranes", ANVOC 2005, Proceedings, 99-106, İstanbul, Turkey, 2005.



- D. Şen, "Effect of compatibilizers on the development of polymer-zeolite mixed matrix gas separation membranes", Network Young Membranes 7th Meeting, Book of Abstracts, Gas separation: Preparation and Characterization session, 30-32, Enschede, The Netherlands, 2005.
- D. Şen, H. Kalıpçılar, L. Yılmaz, "Development of Zeolite Filled Polycarbonate Mixed Matrix Gas Separation Membranes", Desalination, 200 (2006) 222-224.
- D. Şen, H. Kalıpçılar, L. Yılmaz, "Preparation and characterization of the polycarbonate based composite gas separation membranes", MRS Spring 2007 Meeting, San Francisco, CA, USA, 2007.

#### **NATIONAL CONFERENCES ATTENDED AND ABSTRACTS PUBLISHED IN THE PROCEEDINGS**

- D. Şen, H. Kalıpçılar, L. Yılmaz, "Uyumlaştırıcıların Polikarbonat Membranların Gaz Ayırım Performansına Etkisi", 6<sup>th</sup> National Chemical Engineering Conference, Bildiri Özetleri Kitabı, Taşınım Olayları ve Ayırım İşlemleri, TOA-49, Ege University, Faculty of Engineering, Chemical Engineering, Bornova, İzmir, Turkey, 2004.
- L. Yılmaz, H. Kalıpçılar, D. Şen, Polikarbonat-Uyumlaştırıcı Gaz Ayırım Membranlarının Karakterizasyonu, 18<sup>th</sup> National Chemistry Conference, Kimya 2004 Bildiri Özetleri, Polimer Kimyası, PK1057, Kafkas University, Faculty of Arts and Science, Department of Chemistry, Kars, Turkey, 2004.
- D. Şen, H. Kalıpçılar, L. Yılmaz, "Polikarbonat-Zeolit Karışık Matrisli Gaz Ayırım Membranlarının Performansı ve Karakterizasyonu", 7th National Chemical Engineering Conference", Book of Abstracts, TOA16, 549-550, Anadolu University, Faculty of Engineering and Architecture, Department of Chemical Engineering, Eskişehir, Turkey, September 5-8, 2006.

## PROJECTS ATTENDED

- L. Yılmaz, D. Şen, "Karışık Matrisli Gaz Ayırım Membranlarına Uyumlaştırıcıların Etkisi, BAP-2002-03-04-05, ODTÜ, Ankara, 2002.
- L. Yılmaz, D. Şen, "Karışık Matrisli Gaz Ayırım Membranlarının Geliştirilmesi", BAP-2004-07-02-00-93, ODTÜ, Ankara, 2004.
- L. Yılmaz, D. Şen, "Yeni Geliştirilen Yöntemlerle Camsı Polimer-Zeolit Gaz Ayırım Membranlarının Geliştirilmesi", BAP-2005-03-04-05, ODTÜ, Ankara, 2005.
- L. Yılmaz, D. Şen, "Polimer-Zeolite Karışık Matrisli Gaz Ayırım Membranlarının Performansı ve Karakterizasyonu", BAP-2006-07-02-00-01, ODTÜ, Ankara, 2006.
- H. Kalıpçılar, L. Yılmaz, D. Şen, "Polimer-Zeolit Gaz Ayırım Membranlarının Performansına Uyumlaştırıcıların Etkisi", TÜBİTAK, 104T329, Ankara, 2007.
- B. Tantekin-Ersolmaz, L. Yılmaz, F. Seniha Güner, H. Kalıpçılar, Ç. Atalay-Oral, D. Şen "Zeolit Katkılı Polimerik Kompozit Membranlarla Doğal Gazın Saflaştırılması", TÜBİTAK, 106M179, İTÜ-ODTÜ (continuing).